博士論文

Identification of N_2O-generating microorganisms in upland field after nitrogen fertilization

（窒素施肥畑圃場における一酸化二窒素ガス生成微生物の特定）

応用生命化学専攻
平成 23 年度博士課程入学
氏　　名　　魏　　巍
指導教員名　　妹尾　啓史

Identification of N_2O-generating microorganisms in upland field after nitrogen fertilization

by

Wei Wei

Department of Applied Biological Chemistry
Graduate School of Agricultural and Life Sciences
The University of Tokyo

Table of contents

Chapter 1

General introduction

1.1 Introduction

Nitrous oxide (N_2O) is a colorless, non-flammable and non-toxic gas. As one of the increasing atmospheric trace gases, N_2O is commonly known as a powerful greenhouse gas (GHG). Although N_2O accounts for only approximate 0.03 per cent of total GHG emissions (IPCC, 2007), it generates a 298-fold stronger effect on global warming than carbon dioxide (CO_2) (IPCC, 2007). N_2O can be photolyzed into nitric oxide (NO) in the stratosphere (Crutzen *et al.* 1970), which contributes to acid rain and involve in stratospheric ozone depletion (Ravishankara et al., 2009). Simultaneously, N_2O has an atmospheric lifetime of 114 years, which is longer than 30 years of CO_2 (IPCC, 2007). Therefore, N_2O has long drawn substantial attention in field of environmental science.

Soil, the largest source of N_2O emission, accounts for about 62% of the global N_2O emission (Thomson et al., 2012), to which cropland soils contribute mainly (Skiba and Smith, 2000; IPCC, 2007; Smith, 2008; Davidson, 2009). N_2O emissions from cropland soil are greatly stimulated after N fertilization (Mosier and Kroeze, 2000), because N input enhances the microbial N_2O-generating activities in soils (Sánchez-Martín et al., 2008). N_2O is known to be produced by soil microorganisms via nitrification and denitrification pathways (Fig. 1-1). Nitrification is commonly defined as the biological oxidation of ammonium (NH_4^+) to nitrate (NO_3^-) with nitrite (NO_2^-) as an intermediate, and N_2O is produced as a by-product during NH_4^+ oxidation to NO_2^- (Goreau et al., 1980). Denitrification is the stepwise microbial reduction of NO_3^- or NO_2^- to gaseous nitric oxide (NO), N_2O, or nitrogen gas (N_2), and N_2O is produced as an intermediate or end product. However, denitrification pathway plays a dual role on the soil N_2O emission and N_2O sink; because N_2O can be reduced to N_2 as the end product of denitrification. Rice paddy soil, where denitrification is active in general, acts such N_2O sink (Ishii et al., 2011a) and the major end product of denitrification in paddy soils is usually N_2 rather than N_2O (Minami, 1997; Ishii et al., 2011b). In contrast, upland crop cultivation always induces larger N_2O than that of paddy rice cultivation during the cropping season in the same field soil (Xiong et al., 2002; Nishimura et al., 2005; Zhao et al., 2011). Therefore, we suggest that upland field soil acts as a mainly N_2O source more than paddy soil.

This chapter (1) provides an introduction to the characteristics of N_2O emission in upland field soil induced by N fertilization, (2) describes the N_2O-generating microorganisms via nitrification and denitrification, and environmental factors controlling such N_2O emission, (3) summarizes the limitation of the current studies and future prospect, and (4) gives the main objectives of this thesis.

1.2 N_2O emission in upland field soil after N fertilization

N fertilizers, the hotspot of N_2O emission in cropland soil, include chemical fertilizers (synthetic ammoniacal fertilizers, e.g. urea, ammonium nitrate, ammonium sulfate) and organic fertilizers (e.g. animal manures, compost, and plant residues). These different types of fertilizer can influence the behavior of N_2O emissions.

N fertilizers are usually incorporated into the plowed layer as the basal fertilizers before the seed sowing. In general, N_2O emission in upland field soil induced by application with basal chemical fertilizers is often slower than that induced by application with organic fertilizers (Li et al., 2002; Hayakawa et al., 2009), although ammoniacal fertilizers are known as quick-release N fertilizers. The organic nitrogen in organic fertilizers has to be firstly mineralized to NH_4^+ or NO_3^-, which are the direct substance for the microbial nitrification or denitrification. Such mineralization can be completed rapidly by soil microorganisms because of the significant increasing of microbial population size induced by the organic carbon, which also contribute to the N_2O emission rate in the nitrification or denitrification process. In addition, the accumulated amount of total N_2O emissions is similar between the upland field soil applied with chemical and organic fertilizers in the same level of N fertilizers during the cropping season, although the maximum rate of N_2O emission from upland field soil induced by organic fertilizers is always higher than that by chemical fertilizers in the same field. Akiyama et al. (2003) found the maximum rate of N_2O emissions induced by swine manure (400μg N_2O-N·$m^{-2}h^{-1}$) was larger than that receiving urea fertilizers (90μg N_2O-N m^{-2} h^{-1}), but the accumulated N_2O in chemical fertilized field (46.8mg N_2O-N m^{-2}) indistinctly higher than that of organic fertilized field (28.8mg N_2O-N m^{-2}). Meng et al. (2005) reported a maximum rate of N_2O emissions induced by organic manure (305μg N_2O-N m^{-2} h^{-1}) was three-fold larger than that receiving chemical fertilizers

(urea as the N fertilizer), but the accumulated N_2O in chemical fertilized field (503g N_2O-N ha^{-1}) indistinctly higher than that of organic fertilized field (434g N_2O-N ha^{-1}). Thus, the different types of N fertilizer with the same N content can conduct distinct N_2O emissions rate in an upland field, but produce indistinct accumulated amount of total N_2O emissions during the crop cultivation period.

Additional fertilizers are conventionally applied to maintain sufficient soil nutrients for crop growth in top-dressing form. N_2O emission can be observed after the additional application of organic or chemical fertilizers. In an upland field of aquic Inceptisol, urea as the basal and additional N fertilizers was applied (6 g N m^{-2} and 9 g N m^{-2}, respectively). The peak of N_2O emission rate (250μg N_2O-N m^{-2} h^{-1}) measured after additional fertilizer application was two-fold higher than that of basal application, and the accumulated amount of N_2O emission derived from the additional chemical fertilizers was significantly higher than that from basal application (Meng et al., 2005). Thus, the application with additional fertilizers plays an equally important role with that of basal fertilizers on the N_2O emission in upland fields.

N fertilization, regardless of the types of fertilizers (organic and inorganic N fertilizers) or the types of fertilization practices (basal and additional application), can induce substantial N_2O emission in upland field soil. Simultaneously, the behavior of N_2O emissions can be influenced by these different types of fertilizer and fertilization practices.

1.3 N_2O-generating microorganisms in upland field soil after N fertilization

The availability of nitrogen (N) fertilizers is crucial determinants of globally sustainable crop yields. As a side environmental effect, N_2O emission from upland field soil induced by such N fertilization have drawn substantial attention in scientific fields, and the related microorganisms are receiving an increasing concern from microbiologist, ecologists and geochemists. Substantial studies for N_2O producing microorganisms in upland field soil are performed following the development of the various analytical techniques and research strategies.

1.3.1 Culture-based studies on N_2O-generating microorganisms in upland field soil

Substantial microbiological studies on N_2O emission focus on the physiological characteristics of

culture-based N_2O producing bacteria, archaea and fungi via nitrification and denitrification from various environment, e.g. terrestrial, aquatic environment and even marine environment (Goreau et al., 1980; Poth and Focht, 1985; Shoun et al., 1992; Shaw et al., 2006; Ma et al., 2008). These strains have been used in investigations of the mechanisms of nitrifying and denitrifying microorganisms that regulate N_2O emission. Takeda et al. (2012) isolated 92 bacterial strains belonging to three species *Leptothrix* sp., *Paenibacillus* sp., and *Streptomyces* sp. from a maize field with Andisol soil. These cultivable N_2O producing strains were not effective denitrifiers but weak N_2O emitters, and more active within a weakly acidic region (pH 4.5-5.0), which indicating the low soil pH, as the drive factor can increase the ratio N_2O/N_2 in the tested maize field. Bakken et al. (2012) suggested that the clarification of mechanisms at the cellular level which control the $N_2O/(N_2+N_2O)$ product ratio of denitrification can provide a clue to the understanding of N_2O emission from soils. Thus, the studies on the isolated strains from upland field soil can provide us available information to understand the physiological characters of N_2O emitters, which contribute to the clarification of the characteristic of N_2O emission in upland field soil. However, the specific study of microbial isolates in upland field soils is a little. In contrast, microbial isolates having N_2O-producing activity are always collected from rice paddy soil, peat soil and domestic wastewater, where are known as active denitrification condition (Takaya et al., 2003; Yanai, et al., 2007; Ashida et al., 2011; Nishizawa et al., 2012). Expecially, Ashida et al. (2011) isolated diverse denitrifying bacterial strains from a paddy field with gray lowland soil using functional single cell method, and most isolates having active ability to produce N_2O. This isolation strategy provides an available and efficient reference to the isolation of N_2O-producing microbes in upland field soil, which contributed to the future exploration of the mechanism of N_2O emitters and their regularity of N_2O emission in the upland field soil.

1.3.2 PCR-based molecular studies on N_2O-generating microorganisms in upland field soil

Following the development of PCR-based molecular microbial ecological techniques, the studies on microbial community involved in N_2O emission in environment become a concern. However, the N_2O producing ability varies at the species level of microorganisms (Yanai, et al., 2007; Ashida et al.,

2011; Nishizawa et al., 2012), indicating the difficulty of identifying N_2O producing microorganisms based on their taxonomic position. This situation demands the use of functional PCR primers that target the gene of crucial enzyme in N cycling to study the ecological behavior of N_2O producing microorganisms in the environment.

The denitrification process as described previously consists of four reactions catalyzed by nitrate reductase (Nar), nitrite reductase (Nir), nitric oxide reductase (Nor) and nitrous oxide reductase (Nos) (Fig. 1-1). The genes that encode these denitrification enzymes were often targeted to identify the phylogenetic diversity of the denitrifiers. The *napA* or *narG* genes, encoding the periplasmic Nar and large catalytic subunit of Nar, respectively, can also be responsible for dissimilatory reducers of NO_3^- to NH_3 (Philippot et al., 2002). Thus, *napA* or *narG* genes were not been widely used to characterise denitrifying bacterial communities (Philippot et al., 2002). Like the *napA* and *narG* genes, few studies have targeted *norB* genes, encoding the bacterial Nor, as a marker for denitrifying bacteria in soils, because the *norB* (*qnorB*-type) genes are present in a variety of non-denitrifying organisms and may be involved in the detoxification of exogenous NO (Richardson, 2000). Simultaneously, the studies of fungal $P450_{nor}$ genes encoding the fungal nitric oxide reductase have been limited to the culture-based strains (Kaya et al., 2004). In contrast, *nirK/S* and *nosZ* genes, encoding the microbial Nir and Nos, were widely used for to characterize denitrifiers involved in N_2O emission and sink, respectively, in soils. The reduction of nitrite to NO is a key step in denitrification process, which is catalyzed by two structurally different but functionally equivalent nitrite reductases, copper-containing reductase (NirK) and cytochrome cd1-containing reductase (NirS). The reduction of N_2O to N_2 is another key step in the denitrification process, involving the N_2O sink, which is catalyzed by copper-containing nitrous oxide reductase (NosZ). Many attempts have been made to design and modify the primers required for PCR amplification of *nirK*, *nirS* and *nosZ* (Braker et al., 1998; Hallin et al., 1999; Michotey et al., 2000; Braker et al., 2000; Throbäck et al., 2004). These approaches were conducted based on the *nirK*, *nirS* and *nosZ* sequences available from cultivable denitrifying bacterial strains, most of which belong to the class *Alpha-*, *Beta-* and *Gamma-proteobacteria* (Heylen 2006; Smith et al., 2007; Ishii et al., 2011;

Palmer et al., 2012). Philippot et al. (2011) suggested that a higher proportion of *nirK* and *nirS* abundance compared to *nosZ* abundance was related to a higher denitrification product ratios $N_2O/(N_2O+N_2)$ and N_2O emission, which explaining site-specific differences in N_2O emissions in some soils. Harter et al. (2014) reported that a higher proportion of *nosZ* abundance compared to *nirK* and *nirS* abundance was related to a low N_2O emission in a vineyard applied with nitrate fertilizers and biochar.

The nitrification process described previously consists of two reactions catalyzed by ammonia monooxygenase (AMO)/hydroxylamine oxidoreductase (HAO) (these two enzymes cooperatively oxidize NH_4^+ to NO_3^-) and nitrite oxidoreductase (Nxr) (Fig. 1-1). N_2O is produced during the oxidation process of NH_4^+ to NO_2^-, which is conducted by the ammonia oxidizing bacteria (AOB) and archaea (AOA). The ammonia monooxygenase gene (*amoA*) of AOA and AOB were usually utilized to indirectly assess N_2O emission derived from nitrification in some environment, e.g. grassland soil and ocean, where nitrification is active. Di et al. (2010) affirmed that nitrification was the source of N_2O emission in a grassland soil based on the increasing soil NO_3^- concentration and *amoA* abundance of ammonium oxidizing microbes. In addition, the AOB *amoA* abundance increased by 3.2 to 10.4 fold and transcript increased by 177 fold more than that of AOA *amoA*, which indicated that nitrification and N_2O emissions were driven by AOB rather than AOA in this nitrogen rich grassland soil. Löscher et al. (2012) suggested that the abundance and expression of AOA *amoA* genes and N_2O co-occurred throughout the water column in the eastern tropical North Atlantic (ETNA). Moreover, selective inhibition of archaea in seawater incubations from the ETNA decreased the N_2O production significantly, which strongly supported archaeal nitrification was the main source of N_2O emission in ETNA. According to above description, the abundance and expression quantification of *amoA* genes can be used to assess the N_2O produced via nitrification as a by-product, when nitrification was the absolute dominant source of N_2O emission. However, the N_2O emission in upland soil is known to be produced conjointly via nitrification and denitrification, and even mainly via denitrification (Maag and Vinther, 1996; Toyoda et al., 2011; Signor et al., 2013). In this case, the quantification of *amoA* genes

should be combined with some others analytic method, which can distinguish the contribution of nitrification and denitrification on the N_2O emission, e.g. acetylene inhibition analysis and isotopomer analysis (Tiedie, 1988; Maeda et al., 2010).

1.3.3 Gas measurement based studies on N_2O-generating microorganisms in upland field soil

Acetylene inhibition the acetylene inhibition method is the most commonly used method to study denitrification rates and denitrification enzyme activities in various environments, which has been widely used for more than 40 years (Balderston et al., 1976). However, substantial limitations of acetylene inhibition are found, such as the acetylene at concentrations of 10 kPa is a potential C source for microbial activity (Hatch et al., 1990), incomplete inhibition of reduction of N_2O to N_2 (Qin et al., 2011), or inhibition of NO_3^- production through nitrification (Seitzinger et al., 1993). The inhibition of denitrification is tightly coupled to nitrification (Rysgaard et al., 1993), because the partial pressure of acetylene for nitrification inhibition (usually at 0.1 to 10 Pa) is lower than that when denitrification rates are determined by the use of the acetylene inhibition method (usually at 10kPa). Based on the sensitivity of nitrification inhibition, acetylene inhibition can be used as a nitrification inhibitor to study nitrification rates in soil. The ammonium mono-oxygenase (AMO) was totally inhibited at such low partial pressure (0.1 to 10 Pa) of acetylene (Berg et al., 1982; Freney et al., 2000) by forming a reactive epoxide which then irreversibly inactivates the AMO enzyme (Hyman and Wood, 1985). Therefore, acetylene inhibition is a potential method to assess the nitrification rate more than that of denitrification rate.

Isotopomer analysis isotopomer analysis, a technique for determining intramolecular ^{15}N site preference in asymmetric molecules of N_2O, was developed recently (Toyoda et al., 1999). Three distribution states of stable isotope ^{15}N in linear N_2O molecule is observed, including $^{15}N^{\alpha}\cdot^{15}N^{\beta}\cdot O$, $^{15}N^{\alpha}\cdot^{14}N^{\beta}\cdot O$, and $^{14}N^{\alpha}\cdot^{15}N^{\beta}\cdot O$. The latter two types of molecules, abundantly in the environment, can be individually measured. The intramolecular distribution of ^{15}N is expressed as the site preference (*SP*, $SP=\delta^{15}N^{\alpha}-\delta^{15}N^{\beta}$), and this *SP* value enabled us to identify the source and sinks of N_2O in the environment (Toyoda et al., 1999; Toyoda et al., 2002). However, this isotopomer analysis for N_2O

source and sinks requires references *SP* value of individual production pathways from pure cultures of nitrifiers and denitrifiers. Thus, substantial *SP* value of N_2O produced during hydroxylamine oxidation by ammonia oxidizers and nitrite reduction during nitrifier denitrification, and nitrate and nitrite reduction by denitrifiers were collected (Toyoda et al., 2005; Sutka et al., 2006; Sutka et al., 2008; Ostrom et al., 2007). Based on these reference *SP*, Toyoda et al. (2011) affirmed that relative contributions from nitrification and denitrification to gross N_2O production in Andisol Komatsuna field were depended on fertilizer. The contribution of nitrification to N_2O production was dominant (40%-70%) in the field applied of ammonium sulfate fertilizer, and the contribution of denitrification to N_2O production was dominant (50%-90%) in the same soils amended with poultry manure. However, because the estimated ranges of $\delta^{15}N_{bulk}$ of N_2O produced by nitrification and fungal denitrification often overlaps, and reference $SP_{nitrifier}$ and SP_{fungi} were always similar (Sutka et al., 2008), the conclusion of this study considered only nitrification instead of both nitrification and fungal denitrification.

Substrate-induced respiration (SIR) inhibition fungal denitrification might play an indispensable role on N_2O emission in some soils. Shoun et al. (2012) notes that acidification of environments, e.g. excessive use of ammonia fertilizer, promoted fungal activity resulting in further increases in N_2O emissions. Thus, an available method to distinguish fungal denitrification from bacterial N_2O source can be of great assistance. Laughlin and Stevens (2002) firstly modified and utilized the substrate-induced respiration (SIR) inhibition method (Anderson and Domsch, 1975) to assess the relative contributions of fungal and bacterial activity to N_2O emission in a grassland soil, of which cycloheximide as a fungal inhibitor and streptomycin sulfate as a bacterial inhibitor. Yanai et al. (2007) assessed a greater contribution of fungi (81%) than bacteria (31%) to the N_2O emission in a maize field. Thus, the modified SIR inhibition method is such an available method to quantify the proportion of fungal and bacterial N_2O emission.

Thus, these various analytical techniques and research strategies may provide us substantial detail information of N_2O producing microorganisms in upland field soil, which attribute to the

understanding of the microorganisms responsible for N_2O emission in upland field soil induced by N fertilization.

1.4 Environmental factors controlling N_2O emission rate in upland field soil

N_2O emission in upland field soil is induced by microbial nitrification and denitrification, both of which are influenced by various environmental factors, e.g. soil mineral N concentration, soil organic C concentration, soil temperature, soil O_2 supply, water content and soil pH (Fig. 1-2). Soil mineral N and organic C concentration are known as the main factors that control N_2O emission, induced by soil management practices of N fertilization (Saari et al., 2009; Thomson et al., 2012; Saggar et al., 2103). Simultaneously, soil temperature, moisture, O_2 supply and pH induced by climate condition (e.g. daily temperature and daily precipitation) play an important role on controlling N_2O emission. Thus, many attempts have been made to explain the rate of N_2O emission based on the effect of environmental factors on soil microorganisms.

1.4.1 Soil mineral N concentration

Soil NH_4^+ is derived from the mineralization of organic nitrogen in organic fertilizers and release of chemical fertilizers and NH_4^+ further transforms to NO_3^- via microbial nitrification process, and soil NO_3^- is the initial substrate of microbial denitrification process. Higher nitrification rates provide more soil NO_3^- for denitrification. Coupled nitrification-denitrification is the microbial production of NO_3^- by aerobic nitrification followed by the anaerobic reduction of the same NO_3^- by microbial denitrification. Thus, although Groffman (1994) suggested that the relationship between NH_4^+ and NO_3^- concentrations and N_2O emission rates is complex, substantial studies assessed N_2O emission rates based on the soil NH_4^+-N to NO_3^--N. Meng et al., (2005) observed low N_2O emission in a wheat field with the high NO_3^--N and low NH_4^+-N contents after the basal urea fertilization, and suggest that the strong nitrification of the tested soil efficiently converted NO_3^--N to NH_4^+-N and the overall low N_2O emission rates were not due to a deficiency of inorganic N, but rather to the weak denitrification potential.

1.4.2 Soil organic C supply

Application of piggery manures has been shown to enhance N_2O emissions by increasing soil C supply (Bhandral et al., 2007). The amendment of soils with organic fertilizers, e.g. animal manures, compost and plant residues, containing readily organic C supply as an energy source for can increase the population size of the soil microorganisms and enhance their metabolic activity, such as N_2O emission via nitrification and denitrification. For example, application of piggery manures has been shown to enhance N_2O emissions by increasing soil organic C supply (Bhandral et al., 2007). The accessibility of available organic C to microorganisms is an important controlling factor for denitrification in field conditions (Saggar et al., 2012), which can influence the ratio of N_2O:N_2 (Smith and Tiedje, 1979; Arah and Smith, 1990; Dendooven et al., 1998). Simultaneously, available organic C in organic fertilizers is a suitable electron donor in denitrification, which may increase the denitrification activity, e.g. N_2O emission, in upland soil. In addition, dissolved organic C (DOC) is a fast type of C supply (Myrold and Tiedje, 1985), and the low molecular weight DOC fractions rather than total DOC concentrations is an important factor controlling N_2O emission in upland soils (Beauchamp et al., 1980; Drury et al., 2008; Saari et al., 2009). Despite the importance of soil NH_4^+ and NO_3^- concentration and available C to the nitrification and denitrification, these two N transformation processes are also influenced by others environmental factors, such as soil temperature, moisture, aeration and pH.

1.4.3 Soil temperature

Soil temperature is of great importance for N_2O emission, because the soil temperature affects the activity of microbial nitrification and denitrification in upland field soil (Signor et al., 2013). Moreover, soil temperature also strongly influences the diffusion of N_2O to the atmosphere (Davidson & Swank, 1986). Liu et al. (2011) reported that N_2O emissions exponentially increase with increasing soil temperatures in a wider range (0-50ºC) in upland field soil. This explains the existence of a close relationship among seasonal variation of N_2O flux and soil and air temperatures (Dobbie et al., 1999; Wolf & Brumme 2002; Zhang et al., 2008). Although these studies shown significant and positive effects of temperature on N_2O emissions, this effect is mainly based on experiments on a daily or

seasonal basis. N_2O emission can be observed in colder ecosystems (Röver et al.,1998), and even under freezing cropland field applied with organic manure or urea (Phillips 2007). Thus, the effect of temperature on N_2O emission might be considered only in a limited range of temperature in upland field soil.

1.4.4 Soil O_2 supply

Soil O_2 supply is an important controlling factor for N_2O emission in upland field soil, because nitrification and denitrification pathways leading to N_2O emissions from soil are dependent upon the availability of O_2 (Skiba *et al.* 1993, Ma *et al.* 2007). Nitrification is strictly aerobic, because the oxidation of NH_4^+ and NO_2^- are strongly diminished in low O_2 conditions (Khalil et al. 2004). Prokaryotic denitrification is a strictly anaerobic reaction, O_2 availability is one of the most important factors inhibiting this process in upland soil (Knowles, 1982; Lloyd, 1993). Gillam et al. (2008) determined the controlling factor of N_2O emission in an upland field soil applied with nitrate fertilizers, and found decreasing soil aeration by increasing the soil moisture increased cumulative N_2O emissions and cumulative denitrification. However, Brentrup et al. (2000) reported that N_2 not N_2O is the main nitrogen gas emitted from an upland field soil applied with organic fertilizer, when the soil aeration is lower. Although denitrification is known as an anaerobic process, it can occur in the topsoil of corn fields with high O_2 concentration (Parkin, 1987), because substantial intra-aggregates as the anaerobic sites are common in upland soils (Khalil et al. 2004). Soil aeration has a close relationship with soil moisture or soil water filled poor space (WFPS) (Bergsma *et al.* 2002, Bollman and Conrad 1998), because soil moisture or soil WFPS are influenced directly by precipitation, an indicator for the risk of anaerobic conditions in upland field soils. Soil moisture has the positive relation to the N_2O emission (Baggs et al. 2000), but the N_2O production decreases under very high moisture contents (Brentrup et al. 2000). Moreover, soil WFPS has significant correlations with N_2O emission via nitrification and denitrification are found by many studies. Ruser et al. (2006) reported that denitrification is the main source of N_2O in an upland field soil fertilized nitrate when WFPS was higher than 70%, but nitrification is the main process when the WFPS decreases to 60%.

1.4.5 Soil pH

Soil pH is another key regulator of the microbiological processes that affect N_2O production. Soil pH can affect the N_2O emission through the activity inhibition of the nitrifying and denitrifying bacteria (Tiedje, 1988), because the reduction of N_2O to N_2 is more sensitive to acidic conditions than the reduction of NO_3^- to N_2O, by which the ratio N_2O/N_2 strongly increases at decreasing pH (Firestone et al., 1980). This conclusion is further supported by several laboratory and field experiments (Koskinen and Keeney, 1982; Nägele and Conrad, 1990; Struwe and Kjøller, 1994; Venterea 2007; Zaman and Nguyen, 2010; Liu et al., 2010). Thus, the continuing acidification of upland soils through excessive application with N fertilizers could drastically enhance N_2O emissions (Thomson et al. 2012). Signor et al. (2013) further summarized that if denitrification is the main source of N_2O, higher pH values decrease the N_2O emissions in soil, but if nitrification is the main process of N_2O production, then an increase in the soil pH stimulates the N_2O production. However, some inconsistent relationships are also found between N_2O emission and pH in some upland fields (Goodroad et al., 1984; Bandibas et al., 1994).

In conclusion, soil mineral N and organic C supply induced by management practices are the primary conditions for N_2O emission in upland field after the fertilization, which can provide sufficient N substrate and energy to soil microorganisms for producing N_2O via different pathways, nitrification and denitrification. Soil physicochemical parameters, e.g. temperatures, O_2 supply, moisture and pH induced by climate conditions are the variable conditions for N_2O emission in upland field, which may control the type and interaction of pathways for N_2O emission.

1.5 Limitations in current study and future prospect

Before the PCR-based research of the functional microbial community, scientists often explored the N_2O emission rate in the upland field soil through the analytic comparison of various environmental factors as described previously. A default emission factor (EF) (e.g. default IPCC EF of 0.1%) is often used to estimate the soil N_2O emission, which is determined based on various environmental factors, e.g. climate, soil condition and type of fertilizer (Lesschen et al., 2011).

However, some inconsistent phenomenon and conclusions are always found, when we utilized the only environmental factors to explain the N_2O emission, because these factors may induce different N_2O emission rates and patterns replying the different decisive N_2O emitters and their pathways. For example, the soil O_2 supply is prerequisite for bacterial nitrifiers via nitrification but inhibited factor for bacterial denitrifier via denitrification (Knowles, 1982; Skiba et al. 1993; Lloyd, 1993; Khalil et al. 2004). Thus, environmental factors should be associated with the investigation of soil N_2O-generating microorganisms to exactly describe the N_2O emission in upland field soil, and such strategy has been performed in some recent studies. Takeda et al. (2012) affirmed the low soil pH level drove the N_2O emission in a maize upland field, because the isolated bacterial denitrifiers as the N_2O emitter were more active within a acidic region (pH 4.5-5.0). Toyoda et al. (2011) assessed the characterization and production and consumption processes of N_2O emitted from upland field soils through the isotopomer ratio analysis, and revealed that the relative contributions from nitrification and denitrification to gross N_2O production in upland field depended on soil bulk density and fertilizer types.

However, a crucial limitation of current research for the functional gene of microorganisms involved in N_2O production, the coverage deficiency of currently used functional markers, has been exposed. Sanford et al. (2012) and Jones et al. (2013) affirmed two distinct clusters of the *nosZ* gene coding the N_2OR through a comprehensive phylogenetic analysis of genomes retrieved from public databases. Microorganisms having *nosZ* gene in the new found cluster (Cluster II), failed to be amplified by currently used primers, is unaccounted yet abundant in environments. The same situation might occur in *nirK* and *nirS* phylogenies. Recent developments in the genome analysis of cultured and uncultured strains have revealed that bacteria belonging to various phyla (e.g. Proteobacteria, Nitrospirae, Actinobacteria, Bacteroidetes, Spirochaetes and Chloroflexi) and even archaea and fungi possess nitrite reductase (Cantera et al., 2007; Nolan et al, 2009; Bartossek et al., 2010; Moir 2011; Shoun et al., 2013; Nishizawa et al., 2013;). However, these new reported *nirK* and *nirS* sequences were not considered in the design and modification of the current *nirK* and *nirS* primers, which amplified the sequences from only Proteobacteria phylum. These finding strongly suggests the

possibility that previous studies that used conventional *nirK* and *nirS* and *nosZ* primers have underestimated the abundance, diversity and functional importance of denitrifying microorganisms involved in N_2O emission and sink in environments. Thus, a methodology to detect these important yet unaccounted denitrification-related genes should be developed to lead us to more comprehensive and precise estimations of the N_2O-generating microorganisms in upland field soils.

In addition, in isotopomer ratios analysis, the overlap of estimated isotopomer ratios of N_2O ($\delta^{15}N_{bulk}$ and *SP*) produced by nitrification and fungal denitrification is limiting the utilization of isotopomer analysis in some soils, e.g. upland field soil applied of excessive ammonia fertilizer, where nitrification and fungal denitrification process were potential N_2O source (Toyoda et al., 2011). Thus, isotopomer ratios analysis should be associated with some additional identification method for distinguishing the nitrification and fungal denitrification, and previous described acetylene inhibition and SIR inhibition method are able to be such additional identification method. Simultaneously, developing a methodology to detect fungal denitrification-related genes as described previously should be such a precise identification method.

Finally, subsequent questions require to be emphasized following the feasibility of more comprehensive and precise estimations of the denitrifiers in upland field soils, such as whether these diverse unaccounted denitrifiers are responsible for N_2O emission in upland field soils? Whether these diverse unaccounted denitrifiers are specifically responsible for N_2O emission induced by different fertilizer types and application practices? Whether these diverse unaccounted denitrifiers induce N_2O emission with different rate and how do the environmental factors control such N_2O emission rate? The clarification of these questions attributes us to understand the microorganisms and their pathway responsible for the N_2O emission in upland field soils induced by different N fertilization, which may provide substantial information for the minimization of N_2O emissions from the upland field soils.

1.6 Objective

The overall objective of this thesis was to determine the N_2O-generating microorganisms and related controlling environmental factors in the upland field soil after the basal and additional

application with organic or chemical fertilizer, based on the results from the observation of N_2O flux and environmental factors, the analysis of isotopomer ratio, and SIR inhibition and acetylene inhibition of N_2O, and abundance and expression of soil microbial genes associated with N_2O emission. For these purposes, five main studies will be performed in this thesis as following:

The first study (Chapter 2) is to design and validate the functional primers targeting the comprehensive prokaryotic nitrite reductase gene *nirK* and *nirS*, and determine the diversity, abundance and functional importance of these *nirK* and *nirS* in different terrestrial environments, especially in upland soil, using newly designed primers.

The second study (Chapter 3) is to design and validate functional primers targeting the fungal *nirK*, and determine the abundance of fungal *nirK* in different terrestrial environments using newly designed primers.

The third study (Chapter 4) is to determine N_2O-generating microorganisms and the related environmental controlling factors for such N_2O in a gray lowland field after basal and additional application with organic or chemical fertilizers in 2011, according to a comprehensive analysis based on the environmental factors, isotopomer ratio analysis of N_2O, and abundance and expression of soil microbial genes (prokaryotic 16S rRNA, fungal 18S rRNA, prokaryotic *nirK*, *nirS* and *nosZ*, fungal *nirK*, AOA *amoA* and AOB *amoA*).

The forth study (Chapter 5) is further focus on the temporal change of N_2O-generating microorganisms after only basal N fertilization in the same upland field soil applied 5-fold higher fertilizers but without cultivation in 2012, according to a combined analysis based on the environmental factors, substrate-induced respiration (SIR) and acetylene inhibition analysis of N_2O, and abundance and expression dynamics of soil microbial genes as described previously.

The final study (Chapter 6) is focus on the fungal N_2O emission after the additional organic fertilization in an Andisol radish field, based on the analysis of isolation and physiology of N_2O producing fungi, fungal 18S rRNA and ITS based DGGE analysis and clone library of the fungal *nirK*.

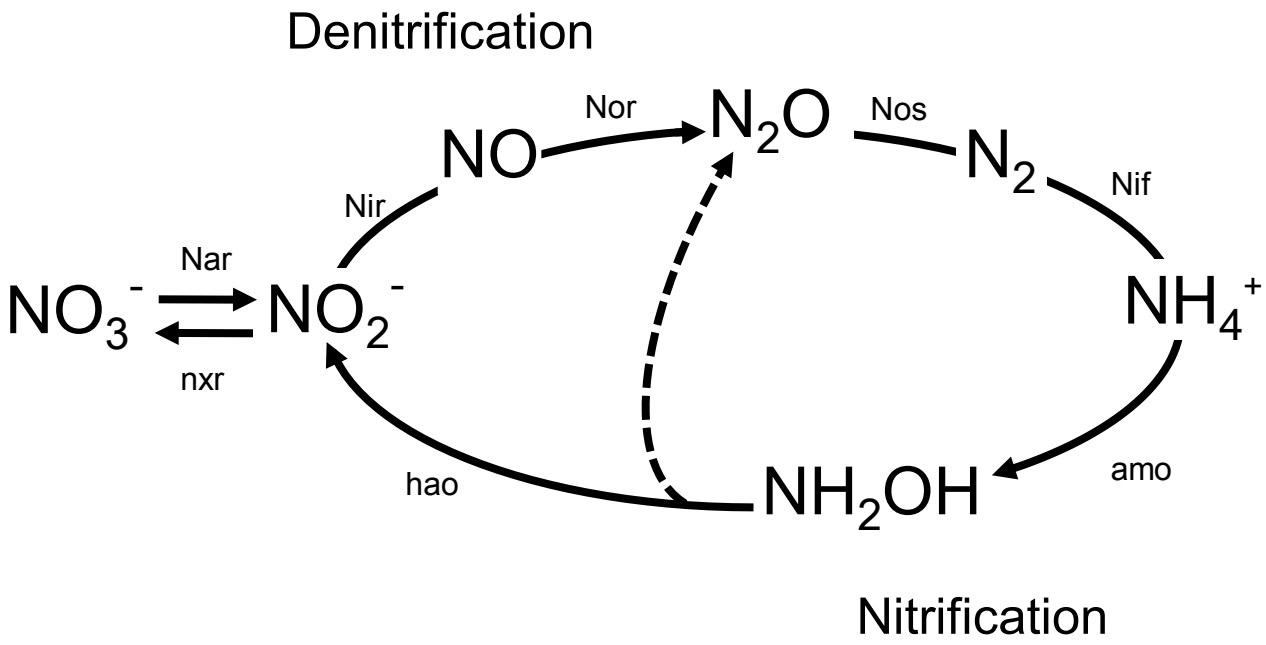

Fig. 1-1. The major biological pathways of N_2O emission in denitrification and nitrification. Genes encoding the associated enzymes are showed, including nitrate reductases (nas), nitrite reductases (nir), nitric oxide reductase (norB) and nitrous oxide reductase (nosZ) in denitrification, and ammonium monooxygenase (amo), hydroxylamine oxidoreductase (hao) and nitrite oxidoreductase (nxr) in nitrification.

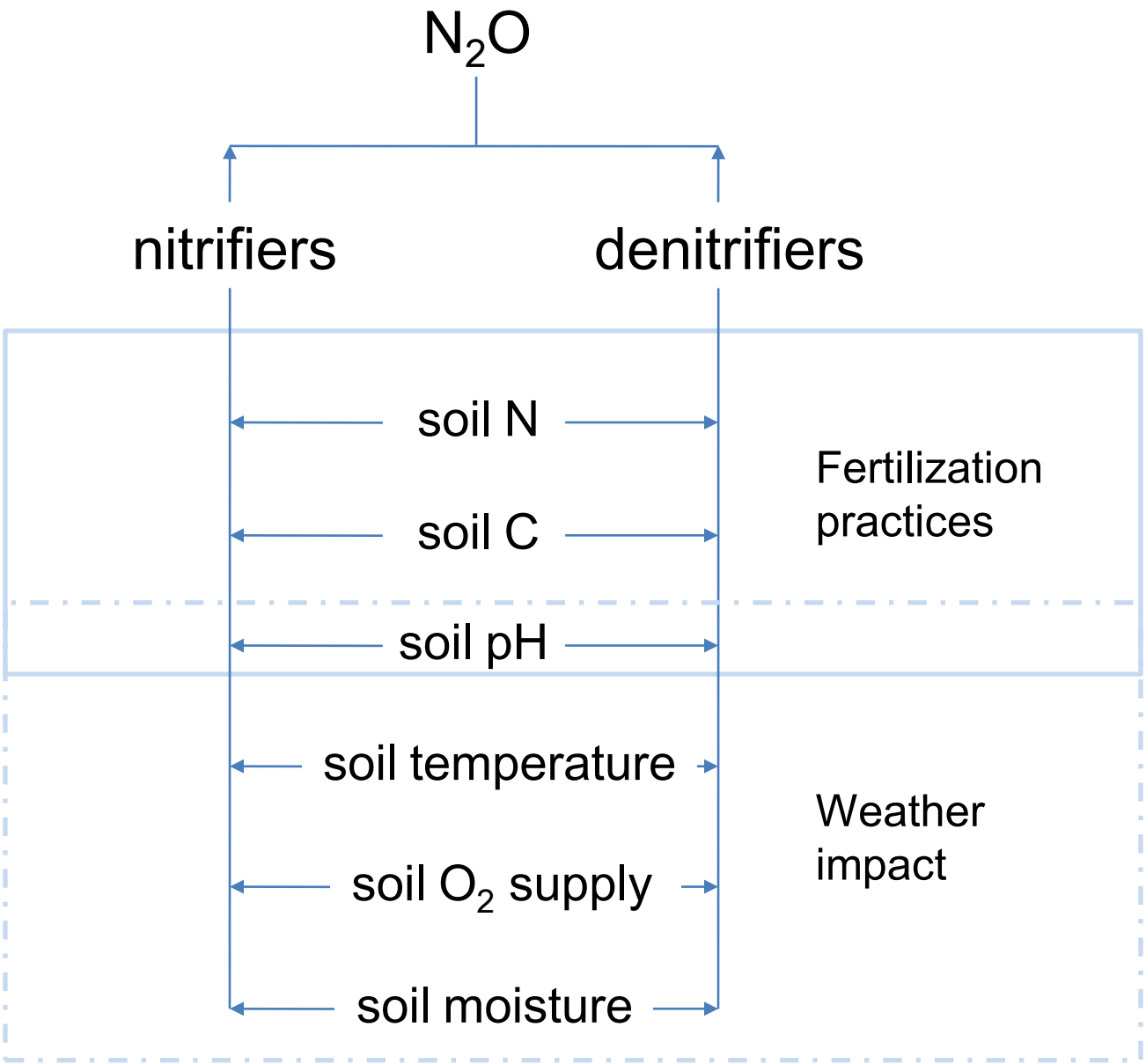

Fig. 1-2. The major environmental factors controlling the N_2O-generating nitrifiers and denitrifiers

Chapter 2

Greater diversity and abundance of prokaryotic denitrifiers in upland field soil than previously realized

2.1 Introduction

Denitrification is a microbial dissimilatory process in which nitrate and nitrite are reduced stepwise to gaseous compounds, such as nitric oxide (NO), nitrous oxide (N_2O) and dinitrogen (N_2) (Zumft, 1997; Knowles, 1982). Denitrification causes nitrogen (N) loss in natural ecosystems, agricultural fields and N removal in wastewater treatments (Tiedje, 1988; Conrad, 1996; Bouwman et al., 2002; Martin et al., 1999) and can also assist with the anaerobic degradation of organic pollutants (Leahy and Olsen, 1997). One of the end products of denitrification, N_2O, is a potent greenhouse gas and ozone depleting substance (Davidson, 2009; Ravishankara 2009). Therefore, denitrification has long drawn substantial attention in scientific and industrial fields. The ability to denitrify is a facultative trait, which is spread among a taxonomically wide variety of microorganisms; denitrification rates in the environment can be regulated by the physiological properties of denitrifiers, as well as by environmental factors, such as oxygen supply (Philippot, 2009; Morales1 et al., 2010).

The reduction of nitrite to NO is a key step in the denitrification process in which dissolved N is converted to gaseous N. This step is catalyzed by two structurally different but functionally equivalent nitrite reductases, copper-containing reductase (NirK) and cytochrome cd1-containing reductase (NirS) (Hochstein and Tomlinson, 1988; Sakurai and Kataoka, 2007; Francesca, et al., 2001). A taxonomically diverse microorganism has the ability to denitrify (Tiedje, 1994), and an incongruent phylogeny is present between the *nir* and 16S rRNA genes. This situation demands the use of functional polymerase chain reaction (PCR) primers that target the *nirK* and *nirS* to study the ecological behavior of denitrifying microorganisms in the environment (Zumft, 1997; Knowles, 1982; Tiedje, 1988).

Many attempts have been made to design and modify the primers required for PCR amplification of *nirK* and *nirS* (Braker et al., 1998; Hallin et al., 1999; Michotey et al., 2000; Throbäck et al., 2004; Braker, et al., 2000). These approaches were conducted based on the *nirK* and *nirS* sequences available from cultivable denitrifying bacterial strains, most of which belong to the class *Alpha-*, *Beta-* and *Gamma-proteobacteria* (Braker, et al., 2000; Heylen, et al., 2006; Smith et al., 2007; Palmer et al., 2012; Ishii et al., 2011). However, recent developments in the genome analysis of cultured and uncultured strains has revealed that bacteria belonging to, for example, the phyla Nitrospirae, Actinobacteria, Bacteroidetes, Spirochaetes, Chloroflexi and even archaea possess *nirK* or *nirS* (Cantera and Stein, 2007; Nishizawa, et al., 2013; Nolan, et al., 2009; Moir, 2011; Bartossek et al., 2010). These *nirK* and *nirS* sequences were not considered in the design and modification of the current *nirK* and *nirS* primers. This finding strongly suggests the possibility that previous studies that used conventional *nirK* and *nirS* primers have underestimated the diversity, abundance and functional importance of denitrifying microorganisms in the environment.

Consequently, the objective of this study was to unveil the previously unaccounted for diversity, abundance and functional importance of denitrifying microorganisms in the environment. To achieve this objective, we (1) performed a phylogenetic analysis of the sequence diversity of currently available *nirK* and *nirS* sequences in the public genome database, (2) designed multiple primer sets, which cover the full diversity of *nirK* and *nirS* sequences, (3) examined the diversity, abundance and distribution of *nirK* and *nirS* in various terrestrial environments using the newly designed primers and (4) assessed the abundance and diversity and functional importance of the N_2O producing denitrifiers with the previously unaccounted for *nirK* or *nirS* in upland field soil.

2.2 Materials and Methods

2.2.1 Selection, alignment and analysis of the sequences of NirK and NirS genes

The full-length nucleotide sequences of *nirK* and *nirS* were obtained from the Kyoto Encyclopedia of Genes and Genomes Repository (http://www.genome.jp/kegg), the National Center for Biotechnology Information (NCBI) Microbial Genomes (http://www.ncbi.nlm.nih.gov/genomes) and the Functional Gene Repository (http://fungene.cme.msu.edu/index.spr). The *nirK* and *nirS* sequences were aligned by amino acids using ClustalW2 (Larkin, et al., 2007). The homologs of the copper center type 1 domain in *nir*K, which contained a type 1 copper ligand (i.e., two His and one Met) and a type 2 copper ligand (i.e., two His) were retained for analysis (Fig. 2-1). The homologs of the cytochrome d1 domain in *nirS,* which bound and reduced the nitrite substrate, were retained for analysis (Fig. 2-2)**.** The phylogenetic trees based on the amino acid sequences and generated with the maximum likelihood algorithm were generated using MEGA 5 (Tamura, et al., 2011) and node support was determined using 500 bootstrap replicates.

2.2.2 Primer design for the detection of diverse NirK and NirS genes

We designed forward primers for *nirK***,** which can anneal with the sequences around the conserved methionine from the type 1 copper ligand, and reverse primers, which can anneal with sequences that contain conserved histidine from the type 2 copper ligand (Fig. 2-1). We also designed forward primers for *nirS,* which can anneal with sequences around conserved glycine**,** and reverse primers, which can anneal with the sequences that contain two consecutive conserved glycines (Fig. 2-2). Several sets of degenerate primers specific to the *nirK* and *nirS* sequences in each cluster were designed using the COnsensus-DEgenerate Hybrid Oligonucleotide Primers

(CODEHOP) algorithm (Rose, et al., 1998). The degenerate primers of each *nirK* and *nirS* cluster consisted of a 3` degenerate core region with an 11bp length across four highly conserved amino acid codons and a 5` consensus non-degenerate clamp region with an 11-14bp length (Fig. 2-1, 2-2, 2-3, Table 2-1). In the *nirK* phylogeny, a clade from the archaeal family, Halobacteriaceae, was assembled into Cluster II (Fig. 2-4) because the amino acid sequences of the core and clamp region were similar compared with different clades in Cluster II. In the *nirS* phylogeny, four sequences derived from the four recently reported genomes of Bacteroidetes, candidate division NC10, Planctomycetes and Epsilon-proteobacteria, were assembled into Cluster I (Fig. 2-4) because the amino acid sequences of the core and clamp regions were similar compared with a different clade of the Proteobacterial *nir*S in Cluster I (Fig. 2-2). In particular, the sequence of widely used conventional primers that had been designed to amplify the *nirK* and *nirS* in Cluster I showed mismatches with the sequences described in Tables 2-2. Therefore, we designed new primers for the *nirK* and *nirS* in Cluster I. The 3` end amino acid of the newly designed forward primer for *nirK* in Cluster I was a highly conserved proline, which was different from the non-conserved end amino acid (i.e., lysine or arginine) of the conventional primer F1aCu (Fig. 2-1a) (Hallin and Lindgren, 1999). The 3` end amino acid of the newly designed reverse primer for *nirK* in Cluster I was a highly conserved histidine, which was different with the non-conserved end amino acid (i.e., serine, asparagine or threonine) of the widely used primer R3Cu (Fig. 2-1b) (Hallin and Lindgren, 1999). The 3` end amino acid of the newly designed reverse primer for *nirS* in Cluster I was a highly conserved leucine, which was different from the non-conserved end amino acid (i.e., isoleucine, valine or leucine) of the conventional primer R3cd (Throbäck et al., 2004) (Fig. 2-2b).

2.2.3 Validation of the designed primers using the denitrifying strains

Eighteen bacterial strains obtained from the culture collection of the Japan Collection of Microorganisms (JCM, Tsukuba, Ibaraki, Japan) or the Biological Resource Center (NBRC, Kisarazu, Chiba, Japan) were used to validate the coverage and specificity of all designed primer candidates (Table 2-2). The strains were expected to belong to each cluster in the phylogenetic trees of *nirK* and *nirS* (Fig. 2-4) based on their 16S rRNA-based taxonomy. In addition, forty-four strains of denitrifying bacteria which had been isolated from rice field soil (Eutric Fluvisol) in Niigata, Japan (Nishizawa, et al., 2012; Nishizawa, et al., 2013; Ashida, et al., 2010) were used (Table 2-2). The denitrification abilities of all bacterial strains were analyzed using ^{15}N-labelled $NaNO_3$ (99.5 atom%-^{15}N, SI Sciences, Japan) and a gas chromatography-mass spectrometry (GC-MS) system (GCMS-QP2010Plus, Shimadzu, Kyoto, Japan) as previously described (Isobe, et al., 2011). Genomic DNA was extracted from the single colonies as previously described (Ashida, et al., 2010). Genomic DNA from a non-denitrifying bacterium, *Geobacillus kaustophilus*, which does not possess the *nirK* or *nirS*, was used as a negative control.

PCR conditions were optimized for *nirK* and *nirS* in each cluster that used the strains. All reactions were performed using the BIOTaq HS DNA polymerase system (Bioline, London, UK), with a final concentration of 4 mM $MgCl_2$, 0.2 mM dNTP Mix, 0.5 $\mu g \cdot \mu l^{-1}$ bovine serum albumin, 0.2 µM for each primer and 25-50 ng of genomic DNA. In addition, DMSO was used in the PCR amplification of *nirK* in Cluster III with a final concentration of 5% (v/v) because of the high guanine-cytosine (GC) content of the sequences of Actinobacteria. Thermal cycling conditions were initially set to 10 min at 95 °C for the denaturation step, followed by 30 cycles of 95 °C for 30 s, different annealing temperatures for 30 s (Table 2-1), a 72 °C extension for 30 s and a final extension at 72 °C for 10 min. The amplicon size was determined by electrophoresis using 2%

agarose in 1× Tris-acetate-EDTA buffer. The PCR products were further purified using a Gel and PCR clean-up system (Promega Corporation, USA) according to the manufacturer's instructions. The purified PCR products were cloned into pGEM-T Easy vector (Promega Corporation, USA) and transformed into *E. coli* JM109 high efficiency competent cells. Cloned insert DNA was amplified by PCR with the vector primers V2772F (5`-GTAAAACGACGGCCAGT-3`) and V172R (5`-GGAAACAGCTATGACCATG-3`). The final PCR products were then sequenced by Takara Bio Inc. (Otsu, Japan). According to the obtained *nirK* or *nirS* sequence, each denitrifier isolate was determined to belong to any cluster of *nirK* or *nirS* except for *nirS* Cluster III. Based on the results of the PCR amplification, the best primers were selected, and their sequences and conditions for conventional PCR and qPCR were optimized as shown in Table S1. The primers can amplify a 430-468 bp fragment of *nirK* or a 410-420 bp fragment of *nirS*.

2.2.4 Diversity of NirK and NirS genes in various environments

Clone library analyses were performed using the environmental samples to determine the diversity of the *nirK* and *nirS* sequences in various environments. We used cropland soil (Gray Lowland Soil, Eutric Fluvisol) (Ashida, et al., 2010), rice paddy soil (Gray Lowland Soil, Eutric Fluvisol) (Itoh, et al., 2013), forest soils (Brown Forest soil) (Urakawa, et al., 2014) and lake sediment (Abe et al., 2000) as described in Table 2-3. All soil samples were collected in triplicate at 5-10 cm depth from each experimental site, and lake sediment was sampled in triplicate at 10 cm depth from the sediment surface using an Ekman sampler. Environmental DNA was extracted using an ISOIL kit (Nippon Gene, Toyama, Japan). The PCR conditions were the same as previously described except that the $MgCl_2$ concentration was reduced to 2.0 mM. PCR product purification, cloning and sequencing were performed in the same way as previously described.

Three hundred fifty-two sequences of *nirK* and 228 sequences of *nirS* were obtained after the removal of poor-quality reads (i.e., low-quality base calling and frame shift errors) and potential chimeric sequences. The sequences from each library were then clustered into operational taxonomic units (OTUs) with 3% differences using the Mothur program (Schloss, et al., 2009). The final set of 195 sequences for *nirK* and 102 sequences for *nirS* were aligned by translating them to amino acid sequences as previously described, and the amino acid sequences from the selected microbial genomes and denitrifying cultured collections were used as a reference alignment.

2.2.5 Abundance and distribution of NirK and NirS genes in various environments

The abundance of *nirK, nirS* and 16S rRNA genes in the environmental samples was determined by quantitative PCR (qPCR). Various environmental samples from terrestrial habitats were used, including a cropland soil (Andosol) applied with organic fertilizer (Wei, et al., 2014), a cropland soil (Gray Lowland Soil, Eutric Fluvisol) applied with organic or urea fertilizer (Isobe, et al., 2011), paddy soils from flooded and non-flooded seasons (Gray Lowland Soil, Eutric Fluvisol) (Itoh, et al., 2013), two natural forest soils (Brown Forest soil and Andosol) (Urakawa, et al., 2014; Sheila , et al., 2008), a planted forest soil (Brown Forest soil) (Oda et al., 2009) and a lake sediment (Abe et al., 2000).

Environmental DNA was extracted as previously described. The qPCR was conducted using a StepOne real-time PCR system (Applied Biosystems, Warrington, UK) and a KOD SYBR qPCR Mix kit, which was suitable for the degenerate primers that had long sequences and high Tm values. The quantification of the 16S rRNA gene was performed with the primers 357F/520R as previously described (Itoh, et al., 2013). The quantification of *nirK* and *nirS* in each cluster was performed with the designed primers. We also utilized the widely used conventional primers

F1aCu/R3Cu (Hallin and Lindgren, 1999) for *nirK* in Cluster I and cd3aF/R3cd (Throbäck et al., 2004, Michotey et al., 2000) for *nirS* in Cluster I for comparison. qPCR was performed in 20 ml reactions that included 10 µl of KOD SYBR qPCR Mix (ToYoBo, Osaka, Japan), 0.4 µl of 50×ROX reference dye, 0.2 µM of primers and 10 ng of environmental DNA. The thermal cycling conditions consisted of an initial denaturation step of 98 °C for 2 min, followed by 40 cycles of 98 °C for 10 s, different annealing temperatures for 10 s (Table S1) and 68°C for 30 s. However, PCR with F1aCu/R3Cu using KOD SYBR qPCR Mix showed nonspecific amplification based on the melt curve analysis and electrophoresis (data not shown) despite attempting the process with a high annealing temperature or a two-step PCR. Instead, we used *Power* SYBR Green PCR Master Mix (Applied Biosystems, Warrington, UK) to avoid the nonspecific amplification. The reaction mixture consisted of 10 µl of *Power* SYBR Green PCR Master Mix (Applied Biosystems, Warrington, UK), 0.5 $\mu g \cdot \mu l^{-1}$ of bovine serum albumin, 0.2 µM of primers and 10 ng of environmental DNA. The thermal cycling conditions consisted of an initial denaturation step of 95 °C for 10 min, followed by 40 cycles of 95 °C for 30 s, 58°C for 30 s and 72 °C for 30 s.

The standard curves in the qPCR analyses of the 16S rRNA, *nirK* and *nirS* genes were generated using linearized plasmids that contained the following: the cloned 16S rRNA gene from *Pseudomonas stutzeri* JCM-5965; *nirK* from *Ochrobactrum anthropi* JCM21032 in Cluster I, which can be amplified by the designed primers nirKC1F and nirKC1R, as well as by the widely used primers F1aCu/R3Cu; *nirK* from *Azospirillum lipoferum* NBRC-1022290 in Cluster II; *nirK* from *Actinosynnema mirum* NBRC-10460 in Cluster III; *nirK* from *Nitrobacter winogradskyi* NBRC-14297 in Cluster IV; *nirS* from *Denitratisoma oestradiolicum* JCM12830 in Cluster I, which can be amplified by the designed primers nirSC1F and nirSC1R, as well as the widely used

conventional primers cd3aF andR3cd; and *nirS* from *Methylomonas koyamae* NBRC-105905 in Cluster II. The absence of the PCR inhibitors in soil DNA was confirmed by mixing a known amount of standard DNA with environmental DNA in a qPCR reaction. The amplification efficiencies, R^2 of the standard curve and Tm value of the melting curve in the qPCR assay for the 16S rRNA gene, *nirK* in Clusters I-IV, and *nirS* in Clusters I and II were estimated as shown in Table S1.

2.2.6 Response of NirK and NirS genes under denitrification-induced conditions

The expression of *nirK* and *nirS* in soil were analyzed using the soil microcosm under denitrification-induced conditions. We used the Gray Lowland Soil (Eutric Fluvisol) of cropland in Niigata, Japan. This soil is the same as the soil from which forty-four bacterial strains have previously been isolated (6-8, Table 2-2). Forty grams of the non-fertilized soil were placed in 80-ml glass bottles, mixed with 0.5 g of granular organic fertilizers and incubated for 20 days as previously described (Wei et al., 2014). The soil without fertilizer was also incubated as a control. The N_2O flux was measured every 2 days, and the highest N_2O emission rate was observed on the 8th day. The soil RNA and DNA were extracted on the 8th day using an RNA PowerSoil Total RNA Isolation Kit and DNA Elution Accessory Kit (MO BIO Laboratories, Carlsbad, USA). Total RNA and DNA were extracted from 1.2 g of soil according to the manufacturer's protocol. The concentration of the extracted RNA and DNA were determined using the Qubit 2.0 Fluorometer (Life Technologies). Digestion of the residual DNA in RNA solution was performed using the Ambion TURBO DNA-free Kit (Life Technologies). RNA was transcribed into complementary DNA using the High Capacity cDNA Reverse Transcription Kit (Applied Biosystems, Warrington, UK). The absence of residual DNA was confirmed in the PCR without reverse transcription. The

DNA and cDNA of *nirK* and *nirS* in soils were quantified with the designed primers as previously described. The 16S rRNA gene was also quantified as previously described. Clone library analyses of *nirK* and *nirS* in the soil on the 8th day after fertilization were simultaneously performed as previously described.

2.2.7 Nucleotide sequence accession numbers

The nucleotide sequences of partial *nirK* from the environmental samples in this study have been deposited in the DDBJ/EMBL/GenBank databases with accession numbers AB936839 to AB937093. The nucleotide sequences of partial *nirS* from the environmental samples in this study have been deposited in the DDBJ/EMBL/GenBank databases with accession numbers AB937560 to AB937661. The nucleotide sequences of partial *nirK* and *nirS* from the denitrifying isolates have been deposited in the databases with accession numbers AB937662 to AB937717.

2.3 Results and Discussion

2.3.1 Phylogeny of NirK and NirS genes

Ninety-seven full-length *nirK* sequences that belong to the bacterial phyla Actinobacteria, Bacteroidetes, Chloroflexi, Nitrospirae, Proteobacteria and Spirochaetes and the archaeal phyla Euryarchaeota were obtained from a public database after selecting a representative sequence with high similarity (>99% of amino-acid sequence) from one species. We constructed a phylogenetic tree based on the sequences for the electron entry site (including type I copper center; 480-560bp) in NirK. All widely used conventional primer sets, such as F1aCu/R3Cu and nirK2F/nirK5R, were also designed to amplify the sequence for this site (17, 18). The tree was divided into 4 clusters (i.e., Clusters I-IV) with high bootstrap support (>70%) (Fig. 2-4a; see Fig. 2-3a for species names). We determined that the sequences that can be amplified with the conventional primers, including F1aCu/R3Cu and nirK2F/nirK5R, are located in Cluster I, which contains *nirK* from the class *Alpha-*, *Beta-* and *Gamma-proteobacteria*, but not in Clusters II-IV (Figs. 2-1 and 2-3a). Cluster II contains *nirK* from the class *Alpha-*, *Beta-*, *Gamma*, *Delta-* and *Epsilon-proteobacteria* and the phyla Bacteroidetes, Chloroflexi and Spirochaetes. The *nirK* from the halophilic archaeal family, Halobacteriaceae, formed a distinct clade, but it had similar sequences in the primer region to all bacterial phyla in Cluster II (Fig. 2-1). Cluster III consisted entirely of the *nirK* from the phylum Actinobacteria. Cluster IV consisted entirely of *nirK* from nitrifiers, including the genera *Nitrospira*, *Nitrosococcus*, *Nitrosomonas* and *Nitrobacter*; however, additional *nirK* sequences from other nitrifiers were also assembled in Clusters I and II (Fig. 2-1), which was in agreement with the previous study of Cantera et al. (2007).

Seventy-five full-length *nirS* sequences that belong to the bacterial phyla Bacteroidetes,

NC10, Planctomycetes and Proteobacteria were obtained with the same approach as the *nirK* sequences. We constructed the phylogenetic tree based on the sequences of the catalytic site (including cytochrome heme d1; 530-570bp) in NirS. All widely used conventional primers, such as cd3aF/R3cd and nirS2F/nirS4R, were also designed to amplify the sequence of this site (17, 20). The tree was divided into 3 clusters (i.e., Clusters I-III) with high bootstrap support (>87%) (Fig. 2-4b; see Fig. 2-3b for species names). We determined that the sequences that can be amplified with conventional primers, including cd3aF/R3cdand nirS2F/nirS4R, are located in Cluster I, but not in Clusters II and III (Figs. 2-2 and 2-3b). Cluster I contained the *nirS* gene from the class *Alpha-*, *Beta-* and *Gamma-proteobacteria* and also the class *Epsilon-proteobacteria* and the phyla Bacteroidetes, Planctomycetes and NC10. Cluster II consisted entirely of the *nirS* from methane-oxidizing bacteria, including the genera *Methylobacter*, *Methylomonas* and *Methylomicrobium*. Cluster III consisted entirely of the Epsilon-proteobacterial *nirS* from deep-sea sediments in hydrothermal fields, including the genera *Nitratifractor*, *Sulfurovum* and *Sulfurimonas*. These phylogenetic analyses indicate that *nirK* and *nirS* are distributed among taxonomically diverse microorganisms, and a considerable proportion (i.e., primarily *nirK* in Clusters II, III and IV and *nirS* in Clusters II and III, Fig. 1) cannot be detected by the widely used conventional primers; thus, they represent the previously unaccounted for *nirK* and *nirS* sequences.

2.3.2 New primer design and its validation using denitrifying strains

We designed 7 sets of primers that can potentially amplify *nirK* or *nirS* located in each of the clusters shown in Fig. 1 (nirKC1F/nirKC1R, nirKC2F/nirKC2R, nirKC3F/nirKC3R and nirKC4F/nirKC4R for Clusters I-IV in the phylogenetic tree of *nirK* and nirSC1F/nirSC1R,

nirSC2F/nirSC2R and nirSC3F/nirSC3R for Clusters I-III in the phylogenetic tree of *nirS*, Table 2-1). The amplified position and expected amplified fragment size (ca. 430-468bp for *nirK* and 410-420bp for *nirS*) were approximately the same as the widely used conventional primers (e.g., F1aCu/R3Cu or nirK2F/nirK5R for *nirK* and cd3aF/R3cd for *nirS*). This finding enables the comparative analysis of the *nir* sequences obtained via the newly designed primers with the massive store of *nir* sequences previously obtained using the conventional primers.

Eighteen strains of denitrifying bacteria obtained from the culture collection, which were expected to belong to each cluster in the phylogenetic trees (Fig. 2-4) according to their 16S rRNA-based taxonomy, were used to validate the coverage and specificity of the newly designed primer sets (Table 2-2). In addition, our denitrifying bacterial isolates from rice paddy soils were used (Table 2-2). All primer sets successfully generated single amplified fragments with the expected size from the genomic DNA of the denitrifying bacteria. A sequence analysis of the amplified fragments confirmed that each primer set amplified the *nirK* or *nirS* belonging to each target cluster. No amplification product was generated from non-denitrifying bacteria (Table 2-2). For comparison, the amplification of *nirK* and *nirS* from the denitrifier strains using the most widely used conventional primers (F1aCu/R3Cu for *nirK* and cd3aF/R3cd for *nirS*) was tested. These primers amplified the *nirK* and *nirS* in Cluster I, but failed to amplify them in the other Clusters. Non-specific amplifications were also observed (Table 2-2). These results indicate the superior coverage and specificity of the newly designed primer sets compared with the conventional primers.

2.3.3 Diversity of NirK and NirS genes in various environments

To examine the diversity of *nirK* and *nirS* in the environment, including previously

unaccounted for *nirK* and *nirS*, we performed a DNA-based clone library analysis using the newly designed primers. The *nirK* clones in Clusters I-IV and the *nirS* clones in Clusters I and II were obtained from all environmental samples examined, i.e., cropland, rice paddy, forest soils and lake sediment (Figs. 2-5 and 2-6) (Table 2-3). The *nirS* clones in Cluster III, which contained the entire *nirS* sequence from deep-sea sediments in hydrothermal fields (Takai, et al., 2006), was not obtained from these environmental samples.

A comparative sequence analysis of the obtained environmental clones with the *nir* sequences of known denitrifier strains in the public database was conducted. The *nirK* sequences of all clones in Cluster I showed the highest similarities (>70% of amino acid sequence) with those of the denitrifiers that belong to class *Alpha-*, *Beta-* and *Gamma-proteobacteria*. The *nirK* sequences of 90, 13 and 5 clones of a total of 112 clones in Cluster II exhibited the highest similarities (64-99%, 68-87% and 72-76%, respectively) with those of the denitrifiers that belong to the phyla Proteobacteria, Bacteroidetes and Spirochaetes, respectively. The other 4 clone sequences did not exhibit similarities with those of the known denitrifier strains or genomes. The *nirK* sequences from 34 of a total of 103 clones in Cluster III showed the highest similarity (60-90%) with those of the phylum Actinobacteria. The remaining clones did not show substantial similarity (<50%) with those of any of the known Actinobacterial strains or genomes. Moreover, 26 sequences formed an unexpected clade distant to Cluster III. However, these sequences were amplified with the primers for Cluster III; thus, we included this clade in Cluster III (Fig. 2-5). The *nirK* sequences of all 31 clones in Cluster IV showed the highest similarities (60-90%) to those from the nitrifying genera, including *Nitrobacter*, *Nitrosomonas*, *Nitrosococcus* and *Nitrospira*.

The *nirS* sequences from 96 of 99 clones in Cluster I showed the highest similarities (71-95%) with those of the denitrifiers that belong to class *Alpha*-, *Beta*- and *Gamma-proteobacteria*. The other 3 clone sequences showed the highest similarity (77-80%) to those from the phylum Chloroflexi. The *nirS* sequences of all 65 clones in Cluster II showed the highest similarities (82-99%) with those from the methane oxidizing genera *Methylomicrobium*, *Methylobacter* and *Methylomonas* (Fig. 2-6).

Previous studies that utilized the conventional primer sets have analyzed the *nirK* and *nirS* sequences of the denitrifiers that primarily belong to *Alpha-, Beta- and Gamma-proteobacteria* from various environmental samples. However, our results strongly suggest that more diverse denitrifiers carrying previously unaccounted for *nirK* and *nirS* sequences, which potentially belong not only to class *Alpha-, Beta- and Gamma-proteobacteria* but also to other phyla (e.g., Actinobacteria, Bacteroidetes, Chloroflexi and Spirochaetes), are distributed in terrestrial environments and have been missed by the conventional primers.

2.3.4 Abundance of NirK and NirS genes in various environments

We performed a quantitative PCR study using the newly designed primers to examine the abundance and distribution of *nirK* and *nirS* sequences, including previously unaccounted for sequences, in various terrestrial environmental samples: cropland soils with different soil types or fertilizations, rice paddy soils in water-flooding and non-flooding seasons, natural and planted forest soils and lake sediment. For comparison, *nirK* and *nirS* in Cluster I were quantified using the widely used conventional primers F1aCu/R3Cu for *nirK* and cd3aF/R3cd for *nirS*. The abundance of the *nirK* and *nirS* in each cluster was normalized by the abundance of the 16S rRNA gene to standardize the unit.

First, we determined that the *nirK* sequence in Clusters I-IV and the *nirS* sequence in Clusters I-II were present in abundance in all environmental samples (Fig. 2-7). The *nirS* sequence in Cluster III, which contained only *Epsilon-proteobacteria nirS* sequences from hydrothermal regions, was not detected in the tested samples. Previous studies also showed that the abundance of *Epsilon-proteobacteria* was quite low in soils and sediments, as examined by their 16S rRNA and *nos*Z genes (Roesch, et al., 2007; Jones, et al., 2013). Many studies have used the conventional primer sets F1aCu/R3Cu and cd3aF/R3cd for the quantification of *nir* in environments despite the possibility of nonspecific amplification previously described. The abundances of *nirK* and *nirS* in Cluster I that were quantified by the newly designed primers were similar to or higher than those quantified by the conventional primers, with the exception of *nirK* in Cropland-3. The total abundances of *nirK* in Clusters I-IV and *nirS* in Clusters I-II quantified with the newly designed primers were approximately 2 to 6 times larger compared with the primers F1aCu/R3Cu and cd3aF/R3cd (Table 2-4). This result clearly indicates that the abundance of denitrifiers in these environments had been severely underestimated.

The distribution of *nirK* and *nirS* differed in the environmental samples (Fig. 2-7). For example, cropland soils (Fluvisols) that received organic fertilization (Cropland-2) had more *nirK* in Clusters I and II but less *nirS* in Clusters I and II compared with cropland soils (Fluvisols) that received urea fertilization (Cropland-3). Water flooding increased *nirK* and *nirS* in paddy soils (Rice paddy-1 and 2). In addition, the abundance of *nirS* in Cluster II, which contains *nirS* sequences only from methane oxidizers, was high in rice paddy soils (10-17% of total *nir* gene) but low in cropland, forest soil and lake sediment (1-3% of total *nir* gene), which indicated a higher abundance or contribution to the denitrification of methane oxidizers in rice paddy soil.

The total abundance of *nirK* fragments (Clusters I, II, III and IV) was highest in cropland soils (Fluvisols), whereas the total abundance of *nirS* fragments (Clusters I and II) was highest in flooded paddy soils (Fluvisols). Notably, the total abundance of *nirK* fragments was much larger compared with that of the *nirS* fragments in the cropland and forest soils and lake sediment but comparable in the rice paddy soils where denitrification is active in general. Iron and copper availability in soil might account for the different distributional patterns of *nirK* and *nirS* in various environments. A high abundance of *nirS* compared with *nirK* in paddy field soils may be attributed to the high availability of soluble iron (Yamazaki et al., 1995; Einsle et al., 2002). Soluble iron is used for the production of NirS but is generally limited because of the insolubility of iron under aerobic conditions above pH 4 (Kraemer 2004). However, soluble iron can be seasonally available in paddy field soils because soils become completely anaerobic in the water flooding season. By contrast, Enwall et al. (2010) noted that copper availability might be a strong driving factor that shapes the abundance of *nirK* or *nirK*/*nirS* because NirK is a multicopper protein (Enwall et al., 2010). Alternatively, microorganisms that possess *nirS* may adapt to the conditions specific to paddy fields, such as the temporally broad dynamics of aerobic/anaerobic conditions, because denitrifiers generally have an alternative life strategy other than denitrification.

2.3.5 Functional importance of microorganisms with the previously unaccounted for NirK and NirS genes in upland soil

We examined the functional importance of denitrification by microorganisms with the previously unaccounted for *nirK* and *nirS* through a combination of RNA-based and culture-based analyses. To achieve this, we used a soil microcosm system. The soil was incubated

in a vial bottle after the application of N fertilizer to induce denitrification. Control soil without fertilizer application was also prepared. N_2O emission as a result of denitrification peaked at 8 days after the fertilizer application (Fig. 2-8) when the DNA and RNA transcripts of *nirK* and *nirS* in both soils were quantified using the newly designed primers (Table 2-5). Their abundance was normalized based on the 16S rRNA gene abundance. The *nirK* in Clusters I-III and the *nirS* in Clusters I-II were abundant in both soils (Table 2-6). The abundance of the *nirK* in Clusters I-II was larger in the denitrification-induced soil compared with the control soil, which indicates an increase in the proportion of these *nirK*-carrying populations in the total microbial community. In addition, the *nirK* transcript in Clusters I-III and the *nirS* transcript in Cluster I were detected in both soils and the abundance of these transcripts were higher in the denitrification-induced soil compared with the control soil (Table 2-6). These results indicated that the microorganisms with *nirK* in Clusters I-III and *nirS* in Cluster I are functionally important in denitrification in the tested soil. In particular, microorganisms with *nirK* in Clusters I-II could form the most active and rapidly growing denitrifying populations in the tested soil because the abundance at the RNA and DNA levels increased tremendously in the denitrification-induced condition. However, we did not detect the gene transcript of *nirK* in Cluster IV or *nirS* in Cluster II despite the presence of the genes in both soils. This finding indicates that nitrifiers having *nirK* that are located in Cluster IV and methane oxidizers were not involved in the denitrification in the tested soil.

We previously isolated denitrifying bacteria using a single-cell isolation method (Ashida, et al., 2010) from the same soil that was used in this soil microcosm study (Nishizawa, et al., 2012). Because the isolates were isolated under conditions in which the activity and growth of denitrifiers were enhanced, the isolates had been considered to be dominant and active denitrifying

populations in the soil. Of the 44 denitrifying isolates, 24 isolates carried the previously unaccounted for *nir*, which can be detected using the newly designed primers, but cannot be detected with the conventional primers (Table 2-2). We attempted to clarify the denitrification ability of the microorganisms that were thought to be active in denitrification and growth in the tested soils and to estimate their taxonomic position via an analysis of the sequence similarity of *nirK* and *nirS* between samples from the soil microcosm study (Table 2-3) and the isolates. The *nir* sequences of 45 of 111 soil clones that belong to Clusters I-III for *nirK* and Cluster I for *nirS* showed high similarity compared with the isolates with denitrification ability (Figs. 2-9 and 2-10). This result reinforces our findings regarding the functional importance of microorganisms that have *nirK* and *nirS* amplified with the newly designed primers for denitrification in environments. Additionally, the *nir* sequences from 26 out of 45 clones showed highly similarity (i.e., >80% of amino acid sequence) with the previously unaccounted for *nir* sequences of the denitrifying isolates; these sequences included *Enterobacter* sp. and *Sinorhizobium* sp. in Cluster I of *nirK*, *Ralstonia* sp., *Curvibacter* sp., *Wautersia* sp. and *Yersinia* sp. in Cluster II of *nirK*, *Streptomyces* sp. and *Micromonospora* sp. in Cluster III of *nirK* and *Dechloromonas* sp. in Cluster I of *nirS* (Table 2-2; Figs. 2-9 and 2-10). All of these denitrifying isolates, which have the previously unaccounted for *nir* sequences, demonstrated a strong ability to produce N_2O as the end-product of denitrification (i.e., the ratio of N_2O production rate to N_2O and N_2 production rate > 80%). The corresponding isolates were not identified for many soil clones most likely because of the limited number of isolates. However, the results of the combined RNA-based and culture-based analyses strongly suggest that microorganisms having the previously unaccounted for *nir* sequences were functionally important in denitrification, in particular N_2O production, in the tested cropland soils.

2.4 Conclusion

We demonstrated the possibility that previous studies that utilized widely used conventional *nirK* and *nirS* primer sets had underestimated the diversity, abundance and functional importance of denitrifying microorganisms in various environments. We obtained many denitrifying isolates in our previous studies through single cell isolation methods (Ashida, et al., 2010; Nishizawa, et al., 2012); however, we could not amplify the *nir* of many of these isolated strains using conventional primers, as shown in this study. In the present study, we designed multiple primer sets, which can cover the full diversity of *nir*, and verified the possibility of its presence in many terrestrial environments. We found that more diverse denitrifying microorganisms than previously realized are present in abundance (i.e., 2 to 6 times) in all tested terrestrial environments. We also revealed that microorganisms that have the previously unaccounted for *nir* could be substantially involved in denitrification, especially N_2O emission, in the soil microcosm experiment.

Recent studies have demonstrated that denitrification in environments can be closely associated with the abundance and physiology of the denitrifying microorganisms (Philippot, et al., 2009; Moralesl et al., 2010). A more recent study has attempted to estimate the biogeochemical N cycles in environments from the dynamics of the relevant gene abundances with mathematical modeling (Reed et al., 2014). Because most studies that used environmental DNA/RNA utilize PCR, the lack of suitable primers is expected to cause key misunderstandings of the microbial ecosystem functions. The knowledge and methodology obtained and developed in this study will lead us to more precise estimations of the N_2O-generating microorganisms via denitrification in various environments, especially in upland field.

Table 2-1. Sequences of the primers for *nirK* and *nirS* in each cluster and the 16S rRNA gene and the optimal PCR conditions.

Primers	Sequence *	Cluster	Conventional PCR	Real-time QPCR		
			Annealing temperature (°C)/time (second)	Annealing temperature (°C)	Tm (°C)	R^2/Efficiency (%)
nirKC1F/ nirKC1R	ATGGCGCCATCatggtnytncc/ TCGAAGGCCTCGatnarrttrtg	I	54/30	54	88.4	0.999/86
nirKC2F/nirKC2R	TGCACATCGCCAACggnatgtwygg/ GGCGCGGAAGATGshrtgrtcnac[a]	II	56/30	56	89.0	0.992/97
nirKC3F/nirKC3R	CATCGGCAACGGCatgyayggngc/ CGACCATGGCCGTGGswnacraangg	III	58/30	58	92.5	0.991/91
nirKC4F/nirKC4R	TACGGTGTGATCatcrtsgatcc/ GCATCACGCATGgaatgatysac	IV	60/30	60	87.4	0.996/84
F1aCu/R3Cu	(16)	I	57/35	58	88.0	0.998/87
nirSC1F/ nirSC1R	ATCGTCAACGTCaargaracvgg/ TTCGGGTGCGTCttsabgaasag	I	56/30	56	90.2	0.999/80
nirSC2F/ nirSC2R	TGGAGAACGCCggncargtntgg/ GATGATGTCCACGgcnacrtangg	II	56/30	56	86.8	0.993/73
nirSC3F/ nirSC3R	TTCGCCCTGaargayggngg/ AGGTGCCCACGaanarnccncc	III	—†	—	—	—
cd3aF/R3cd	(17, 18)	I	57/30	57	90.4	0.996/95
357F/520R	(11)	16S rRNA	58/30	58	83.2	0.999/91

* the sequences with capital and lowercase letters denote the clamp and core region of the primer, respectively.

† not detected in the test strains and environmental samples.

Table 2-2. Amplification of the *nirK* and *nirS* sequences in each cluster of the denitrifying strains obtained from the culture collections and cropland soils.

Strains	Cluster	Amplicon by primer sets *									Demitrification activity ‡	Closest relative genome		
		nirKC1F/ nirKC1R	nirKC2F/ nirKC2R	nirKC3F/ nirKC3R	nirKC4F/ nirKC4R	F1aCu/ R3Cu	nirSC1F/ nirSC1R	nirSC2F/ nirSC2R	nirSC3F/ nirSC3R	cd3aF/ R3cd		Affiliations	Accession number	Similarity
Culture collections:														
Caulobacter segnis NBRC-15250	*nirK*-II	−	++	−	−	−	−	−	−	−	D	*C. segnis* ATCC 21756	CP002008	99%
Azospirillum lipoferum NBRC-102290	*nirK*-II	−	++	−	−	−	−	−	−	−	A	*A. lipoferum* 4B	FQ311871	90%
Azospirillum brasilense JCM-1224	*nirK*-II	−	+++	−	−	−	−	−	−	−	A	*A. brasilense* Sp245	HE577330	94%
Neisseria denitrificans JCM-21446	*nirK*-II	−	+++	−	−	700 †	−	−	−	−	B	*N. lactamica* 020-06	FN995097	90%
Pseudoalteromonas haloplanktis NBRC-100993	*nirK*-II	−	+	−	−	−	−	−	−	−	B	*P. haloplanktis* TAC125	CR954246	100%
Pseudoxanthomonas suwonensis NBRC-106385	*nirK*-II	−	++	−	−	300, 1400	−	−	−	−	D	*P. suwonensis* 11-1	CP002446	97%
Stenotrophomonas nitritireducens JCM-13311	*nirK*-II	−	+++	−	−	−	−	−	−	−	D	*P. suwonensis* 11-1	CP002446	89%
Haloarcula hispanica NBRC-102182	*nirK*-II	−	++	−	−	−	−	−	−	−	D	*H. hispanica* ATCC 33960	CP002921	100%
Actinoplanes missouriensis NBRC-13243	*nirK*-III	−	−	++	−	−	−	−	−	−	D	*A. missouriensis* 431	AP012319	99%
Actinosynnema mirum NBRC-14064	*nirK*-III	−	−	+++	−	−	−	−	−	−	D	*A. mirum* DSM 43827	CP001630	99%
Nitrobacter winogradskyi NBRC-14297	*nirK*-IV	−	−	−	++	1500	−	−	−	−	D	*N. winogradskyi* Nb-255	CP000115	96%
Ochrobactrum anthropi JCM-21032	*nirK*-I	++	−	−	−	+	−	−	−	−	A	*O. anthropi* ATCC 49188	CP000759	99%
Alcaligenes faecalis JCM-20522	*nirK*-I	++	−	−	−	++, 1500	−	−	−	−	B	*A. faecalis* ATCC 8750	AF114786	99%
Pseudomonas stutzeri JCM-5965	*nirS*-I	−	−	−	−	−	+++	−	−	+++	B	*P. stutzeri* ATCC 17588	CP002881	99%
Denitratisoma oestradiolicum JCM-12830	*nirS*-I	−	−	−	−	−	+++	−	−	+++	A	*R. gelatinosus* IL144	NC017075	88%
Cupriavidus metallidurans JCM-21315	*nirS*-I	−	−	−	−	1000, 1200	++	−	−	++, 1400	A	*C. metallidurans* CH34	CP000352	98%
Methylomonas koyamae NBRC-105905	*nirS*-II	−	−	−	−	−	−	+++	−	−	A	*M. methanica* MC09	CP002738	92%
Geobacillus kaustophilus JCM-12893	−	−	−	−	−	700, 1500	−	−	−	−	−	−	−	−
Bacterial isolates:														

Streptomyces sp. UNPA38	*nirK*-III	−	−	+++	−	−	−	−	−	−	D	−[§]	−	−
Micromonospora sp. UNPA97	*nirK*-III	−	−	+	−	−	−	−	−	−	D	−	−	−
Agromonas sp. NC2H-3-107	*nirK*-I	+++	−	−	−	−	−	−	−	−	D	*Bradyrhizobium sp*. S23321	AP012279	96%
Bradyrhizobium sp. UNPA215	*nirS*-I	−	−	−	−	−	++	−	−	+	D	−	−	−
Bradyrhizobium sp. UNPF333	*nirS*-I	−	−	−	−	−	++	−	−	++	C	−	−	−
Bradyrhizobium sp. UNPF42	*nirK*-I	++	−	−	−	++	−	−	−	−	A	*Bradyrhizobium* sp. BTAi1	CP000494	89%
Bradyrhizobium sp. UNPA324	*nirK*-I	+	−	−	−	+	+	−	−	−	D	*Bradyrhizobium* sp. BTAi1	CP000494	92%
Ensifer sp. NC3H-6bA	*nirK*-II	−	++	−	−	1200[§]	−	−	−	−	A	*O. anthropi* ATCC 49188	CP000758	88%
Ensifer sp. NC3H-75	*nirK*-I	+++	−	−	−	−	−	−	−	−	D	*S. fredii* HH103	HE616890	80%
Sinorhizobium sp. NC2L-3-23	*nirK*-I	+++	−	−	−	−	−	−	−	−	D	*S. fredii* HH103	HE616890	82%
Sinorhizobium sp. NC2L-3-2-34	*nirK*-I	++	−	−	−	−	−	−	−	−	D	*Rhizobium etli* CFN 42	CP000138	84%
Sinorhizobium sp. NH30B	*nirK*-I	+++	−	−	−	−	−	−	−	−	D	*S. fredii* HH103	HE616890	82%
*Magnetospirillum*sp.NC3H-69bA	*nirS*-I	−	−	−	−	−	+++	−	−	−	D	*M. gryphiswaldense* MSR-1	HG794546	90%
Achromobacter sp. OF-24	*nirK*-I	+	−	−	−	+	−	−	−	−	D	*A. cycloclastes* ATCC 21921	AAD26537	97%
*Cupriavidus*sp. NC3H-55a	*nirS*-I	−	−	−	−	900	++	−	−	++	D	*C. necator* N-1	CP002878	97%
*Cupriavidus*sp. NC3H-55b	*nirS*-I	−	−	−	−	1500	+	−	−	++	C	*C. necator* N-1	CP002878	97%
*Cupriavidus*sp. NC3H-76b	*nirS*-I	−	−	−	−	−	+++	−	−	+++	D	*C. taiwanensis* LMG19424	CU633750	87%
*Cupriavidus*sp. NC3H-95a	*nirS*-I	−	−	−	−	1200	+++	−	−	+++	C	*C. taiwanensis* LMG19424	CU633750	87%
Ralstonia sp. UNPF2a	*nirK*-II	−	+++	−	−	−	−	−	−	−	D	*R. pickettii* 12D	CP001645	97%
Ralstonia sp. UNPF19a	*nirK*-II	−	+++	−	−	−	−	−	−	−	D	*R. pickettii* 12D	CP001645	97%
Ralstonia sp. UNPF45	*nirK*-II	−	+++	−	−	−	−	−	−	−	D	*R. pickettii* 12D	CP001645	95%
*Wautersia*sp. NH26B	*nirK*-II	−	++	−	−	−	−	−	−	−	D	−	−	−
Wautersia sp. NC2H-3-95	*nirK*-I	−	−	−	−	600	+++	−	−	+++	D	*R. eutropha* JMP134	CP000091	93%
Acidovorax sp. NC3L-63c	*nirK*-II	−	++	−	−	1200	−	−	−	−	A	−	−	−
Curvibacter sp. UNPF65	*nirK*-I/	−	+++	−	−	−	++	−	−	++	D	*R. solanacearum* CFBP2957	FP885907	85%
	nirS-I											*Dechlorosoma suillum* PS	CP003153	81%
Rhodoferax sp. NC3L-59aB	*nirK*-II	−	+	−	−	−	−	−	−	−	A	−	−	−
Rhodoferax sp. NC3L-68a	*nirK*-II	−	+	−	−	−	−	−	−	−	A	−	−	−

Rhodoferax sp. NC3L-63bB	*nirK*-II	−	++	−	−	−	−	−	−	−	A	−	−	−
*Duganella*sp. NC3L-7a	*nirS*-I	−	−	−	−	−	+	−	−	++	D	*Leptothrix cholodnii* SP-6	(CP001013)	80%
Janthinobacterium sp. NC3L-11b	*nirK*-II	−	+++	−	−	1500	−	−	−	−	D	−	−	−
Ideonalla sp. UNPF83	*nirS*-I	−	−	−	−	−	++,700	−	−	+,700	D	*Rubrivivax gelatinosus* IL144	(NC017075)	83%
	nirK-II/	−	+++	−	−	−	+	−	−	−	C	−	−	−
Ideonella sp. NC3L-43b	*nirS*-I													
												Rubrivivax gelatinosus IL144	(NC017075)	83%
Pseudogulbenkiania sp. UNPF3a	*nirS*-I	−	−	−	−	−	+++	−	−	+++	D	*Pseudogulbenkiania* sp.NH8B	(AP012224)	96%
*Vogesella*sp.NS47	*nirS*-I	−	−	−	−	−	++	−	−	+	−	*Pseudogulbenkiania* sp.NH8B	(AP012224)	94%
Azoarcus sp. UNPF34a	*nirS*-I	−	−	−	−	−	+	−	−	−	D	*Azoarcus* sp. KH32C	(AP012304)	99%
*Azospira*sp. NC3H-14	*nirS*-I	−	−	−	−	700	++	−	−	+++	A	*Rubrivivax gelatinosus* IL144	(NC017075)	79%
Dechloromonas sp. UNPF85	*nirS*-I	−	−	−	−	−	+	−	−	−	D	*D. aromatica* RCB	(CP000089)	89%
Dechloromonas sp. NC3L-11a	*nirS*-I	−	−	−	−	−	+	−	−	−	A	*D. aromatica* RCB	(CP000089)	88%
Zoogloea sp. UNPF11a	*nirS*-I	−	−	−	−	−	++	−	−	++	D	*Rubrivivax gelatinosus* IL144	(NC017075)	80%
*Zoogloea*sp. UNPF89	*nirS*-I	−	−	−	−	−	++	−	−	++	D	*Rubrivivax gelatinosus* IL144	(NC017075)	81%
Zoogloea sp. UNPF86	*nirS*-I	−	−	−	−	−	++	−	−	++	D	*Rubrivivax gelatinosus* IL144	(NC017075)	80%
Zoogloea sp. UNPF36	*nirS*-I	−	−	−	−	−	++	−	−	++	D	*Rubrivivax gelatinosus* IL144	(NC017075)	81%
Yersinia sp. NC3L-70	*nirK*-II	−	++	−	−	1500	−	−	−	−	D	−	−	−
Enterobacter sp. NC3H-6aB-1	*nirK*-I	++	−	−	−	+,900	−	−	−	−	D	−	−	−

* The concentration of PCR amplification product: +, 0-20 ng/μl; ++, 20-50 ng/μl; +++, >50 ng/μl.

† Numbers indicate approximate sizes of non-specific amplification product.

‡Denitrification activity was normalized with the ratio of N_2O to N_2O+N_2. The capital letter represents the ratio value: A, 0-20%; B, 20-40%; C, 40-80%; D, 80-100%.†

§No significant similarity of genome or partial reference sequences found in database.

Table 2-3. Amplification and clones of *nirK* and *nirS* in each cluster of environmental samples.

Habitat type [*]	*nirK* and *nirS* Cluster		Amplicon [†]	No. of sequences	No. of OTUs (3% cut)	Reference
Cropland soil	*nirK*	Cluster I	+++	47	15	(11)
		Cluster II	+++	44	20	
		Cluster III	+++	43	30	
		Cluster IV	++	23	2	
	nirS	Cluster I	+++	31	21	
		Cluster II	+	12	8	
		Cluster III	—	—	—	
Rice paddy soil	*nirK*	Cluster I	++	18	14	(11)
		Cluster II	+++	24	20	
		Cluster III	++	21	16	
		Cluster IV	—	—	—	
	nirS	Cluster I	+++	28	24	
		Cluster II	++	29	16	
		Cluster III	—	—	—	
Forest soil	*nirK*	Cluster I	++	18	13	(12)
		Cluster II	+++	20	17	
		Cluster III	+++	20	17	
		Cluster IV	—	—	—	
	nirS	Cluster I	+	15	3	
		Cluster II	—	—	—	
		Cluster III	—	—	—	
Lake sediment	*nirK*	Cluster I	++	23	8	(15)
		Cluster II	+++	24	15	
		Cluster III	++	19	6	
		Cluster IV	+	8	2	
	nirS	Cluster I	+++	25	20	
		Cluster II	+	24	10	
		Cluster III	—	—	—	
Cropland soil (soil microcosm)	*nirK*	Cluster I	+++	19	15	(11)
		Cluster II	+++	24	14	
		Cluster III	+++	20	15	
		Cluster IV	+	5	1	
	nirS	Cluster I	+++	48	20	
		Cluster II	+	16	9	
		Cluster III	—	—	—	

[*] Cropland soil, gray lowland soil applied with organic fertilizers; rice paddy, a flooded paddy soil; forest soil, a natural forest soil

[†] The concentration of PCR amplification product: +, 0-20 ng/μl; ++, 20-50 ng/μl; +++, >50 ng/μl.

Table 2-4. Abundance of 16S rRNA and *nirK* and *nirS* genes in each cluster expressed as the number of gene copies per gram of soil in environmental samples from different terrestrial habitat types.

Site name *	Reference	Replicates	16S rRNA	*nirK* Cluster I	*nirK* Cluster II	*nirK* Cluster III	*nirK* Cluster IV	*nirK* Cluster I (F1aCu/R3Cu)	*nirS* cluster I	*nirS* cluster II	*nirS* cluster I (cd3aF/R3cd)
Cropland-1	(10)	3	$5.7\pm1.2\times10^{9}$	$6.1\pm0.3\times10^{7}$	$1.4\pm0.1\times10^{7}$	$1.2\pm0.9\times10^{7}$	$2.1\pm0.3\times10^{5}$	$4.7\pm1.9\times10^{7}$	$1.0\pm0.1\times10^{7}$	$2.9\pm0.6\times10^{6}$	$4.2\pm0.3\times10^{6}$
Cropland-2	In this study	3	$4.7\pm1.0\times10^{9}$	$1.4\pm0.1\times10^{8}$	$1.0\pm0.1\times10^{8}$	$4.0\pm0.2\times10^{7}$	$4.0\pm0.4\times10^{5}$	$1.4\pm0.2\times10^{8}$	$2.7\pm0.1\times10^{7}$	$9.0\pm1.1\times10^{6}$	$1.1\pm0.2\times10^{7}$
Cropland-3	In this study	3	$4.1\pm0.9\times10^{9}$	$4.5\pm0.2\times10^{7}$	$4.3\pm0.1\times10^{7}$	$5.6\pm0.2\times10^{7}$	$6.3\pm0.4\times10^{5}$	$8.7\pm0.1\times10^{7}$	$3.7\pm0.0\times10^{7}$	$1.6\pm0.1\times10^{7}$	$3.1\pm1.7\times10^{7}$
Rice paddy-1	(11)	3	$3.5\pm0.4\times10^{9}$	$2.6\pm0.0\times10^{7}$	$2.0\pm0.0\times10^{7}$	$2.6\pm0.1\times10^{7}$	$2.7\pm0.0\times10^{5}$	$1.2\pm0.1\times10^{7}$	$4.0\pm0.1\times10^{7}$	$2.2\pm0.4\times10^{7}$	$4.3\pm2.7\times10^{7}$
Rice paddy-2	(11)	3	$8.3\pm0.4\times10^{8}$	$4.8\pm0.4\times10^{6}$	$4.5\pm0.1\times10^{6}$	$5.0\pm0.5\times10^{6}$	$6.2\pm0.7\times10^{5}$	$2.5\pm1.5\times10^{6}$	$6.1\pm0.1\times10^{6}$	$2.3\pm0.1\times10^{6}$	$6.5\pm0.4\times10^{6}$
Forest-1	(12)	3	$2.0\pm1.4\times10^{9}$	$1.4\pm0.1\times10^{7}$	$4.8\pm0.1\times10^{6}$	$1.0\pm0.3\times10^{7}$	$2.1\pm0.2\times10^{5}$	$6.5\pm0.9\times10^{6}$	$2.0\pm0.1\times10^{6}$	$1.1\pm0.1\times10^{6}$	$7.0\pm0.0\times10^{5}$
Forest-2	(13)	3	$2.2\pm1.0\times10^{9}$	$1.8\pm0.1\times10^{7}$	$1.6\pm0.3\times10^{7}$	$1.5\pm0.1\times10^{7}$	$2.3\pm0.1\times10^{5}$	$1.1\pm0.1\times10^{7}$	$6.6\pm0.4\times10^{6}$	$7.0\pm0.5\times10^{5}$	$3.9\pm0.5\times10^{6}$
Forest-3	(14)	3	$2.0\pm0.4\times10^{9}$	$1.5\pm0.1\times10^{7}$	$6.6\pm0.5\times10^{6}$	$1.6\pm0.1\times10^{7}$	$2.1\pm0.3\times10^{5}$	$6.5\pm1.3\times10^{6}$	$1.4\pm0.1\times10^{6}$	$1.1\pm0.1\times10^{6}$	$2.7\pm0.2\times10^{5}$
Lake sediment	(15)	2	$1.2\pm0.2\times10^{9}$	$0.9\pm0.2\times10^{7}$	$1.4\pm0.6\times10^{7}$	$1.3\pm0.5\times10^{7}$	$3.4\pm1.9\times10^{6}$	$0.7\pm0.1\times10^{7}$	$1.6\pm0.2\times10^{6}$	$1.7\pm0.2\times10^{6}$	$1.2\pm0.1\times10^{6}$

* Cropland-1 denotes an Andosol soil treated with organic fertilizer; Cropland-2 and 3 denote a Gray Lowland soil treated with organic and urea fertilizer, respectively; Rice paddy-1 and 2 denote a Gray Lowland soil of flooded and non-flooded paddy fields, respectively; Forest-1 and 3 denote Brown Forest soil and Andosol soil from a natural forest, respectively; Forest-2 denotes Brown Forest soil from a planted forest.

Table 2-5. Abundance of 16S rRNA, *nirK* and *nirS* genes in each cluster and their transcripts in the soil microcosm expressed as the number of copies per gram of soil.

Treatments [*]		16S rRNA	*nirK* in Cluster I	*nirK* in Cluster II	*nirK* in Cluster III	*nirK* in Cluster IV	*nirS* in Cluster I	*nirS* in Cluster II
DNA based	NF-8	$2.41\pm0.10 \times 10^9$	$1.22\pm0.06 \times 10^7$	$1.73\pm0.05 \times 10^7$	$5.28\pm0.93 \times 10^7$	$6.50\pm0.38 \times 10^4$	$4.49\pm0.13 \times 10^7$	$1.20\pm0.22 \times 10^7$
	OF-8	$9.75\pm1.03 \times 10^9$	$5.49\pm0.63 \times 10^8$	$5.14\pm0.94 \times 10^8$	$1.25\pm0.09 \times 10^8$	$1.34\pm0.15 \times 10^5$	$1.31\pm0.12 \times 10^8$	$2.68\pm0.60 \times 10^7$
RNA based	NF-8	$2.01\pm0.18 \times 10^9$	$4.43\pm2.42 \times 10^4$	$7.59\pm1.49 \times 10^4$	$1.13\pm0.63 \times 10^4$	— [†]	—	—
	OF-8	$3.23\pm0.26 \times 10^{10}$	$1.02\pm0.30\times 10^6$	$4.81\pm1.43 \times 10^6$	$2.02\pm0.75 \times 10^5$	—	$9.38\pm1.28 \times 10^4$	—

[*] NF-8 and OF-8 denote the control and organic fertilized soil on the 8th day of N_2O flux in soil microcosm, which corresponds with the curve in Fig. 2-8.

[†] not detected

Table 2-6. The relative abundance of the nitrite reductase gene and transcript responsible for N_2O emission in a soil microcosm

	Treatments[*]	*nirK* in Cluster I[†]	*nirK* in Cluster II	*nirK* in Cluster III	*nirK* in Cluster IV	Total *nirK*	*nirS* in Cluster I	*nirS* in Cluster II	Total *nirS*	Total Nitrite reductase gene
Gene	NF-8	0.506	0.717	2.191	0.027	3.441	1.863	0.498	2.36	5.802
	OF-8	5.631	5.272	1.282	0.014	12.199	1.344	0.275	1.619	13.818
Transcript	NF-8	0.002	0.003	0.001	—[‡]	0.006	—	—	—	0.006
	OF-8	0.010	0.049	0.002	—	0.062	0.001	—	0.001	0.063

[*] NF-8 and OF-8 represent the control and organic fertilized soil on the 8th day of N_2O flux in the soil microcosm, which corresponds to the curve in Fig. 2-8.

[†]Relative abundance of the nitrite reductase gene or transcript copies calculated as a percentage of the total bacterial 16S rRNA gene copies (for the mean and standard deviation of replicates by treatment see Table 2-5). [‡] Not detected.

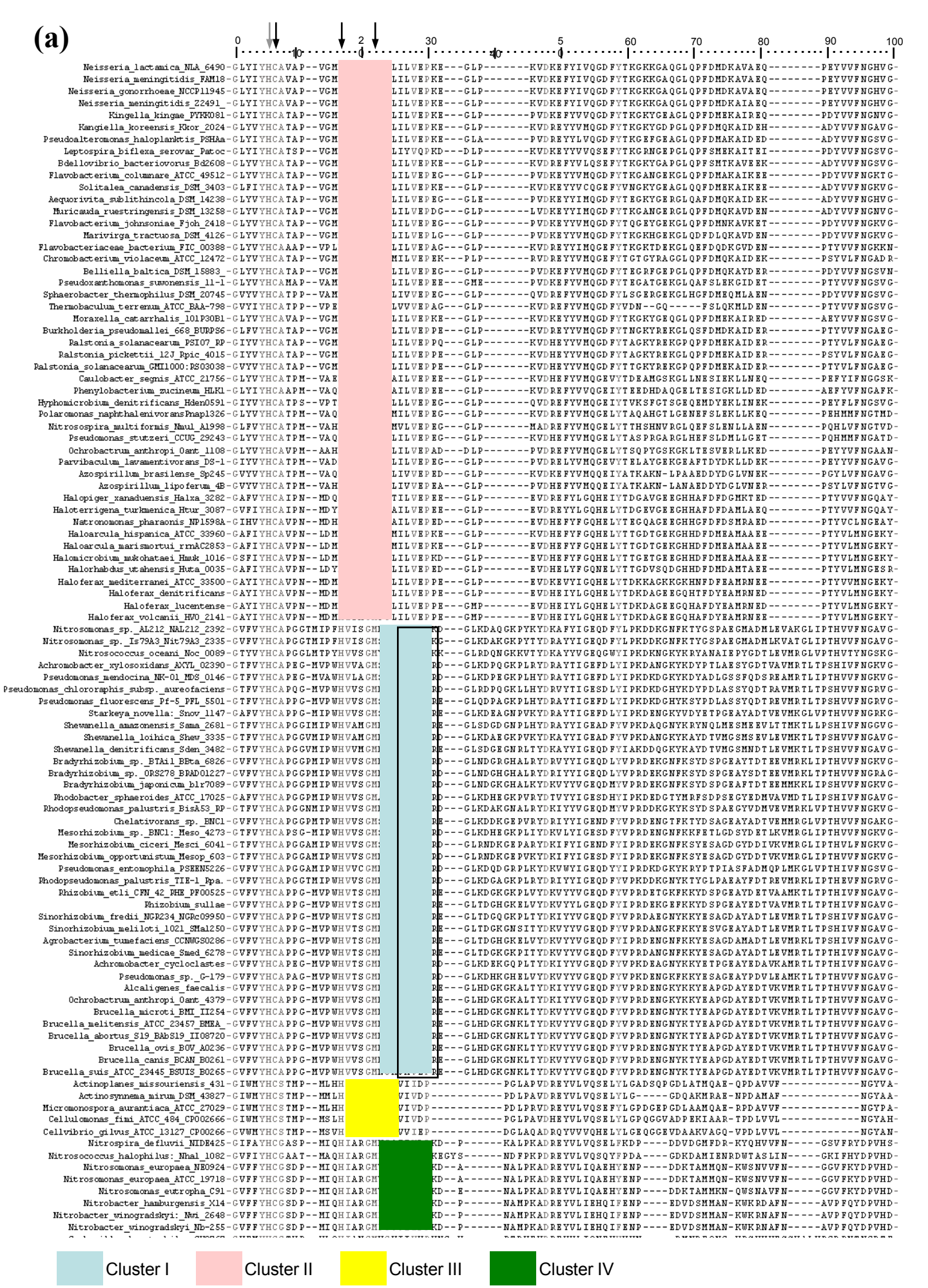

Fig. 2-1 be continued

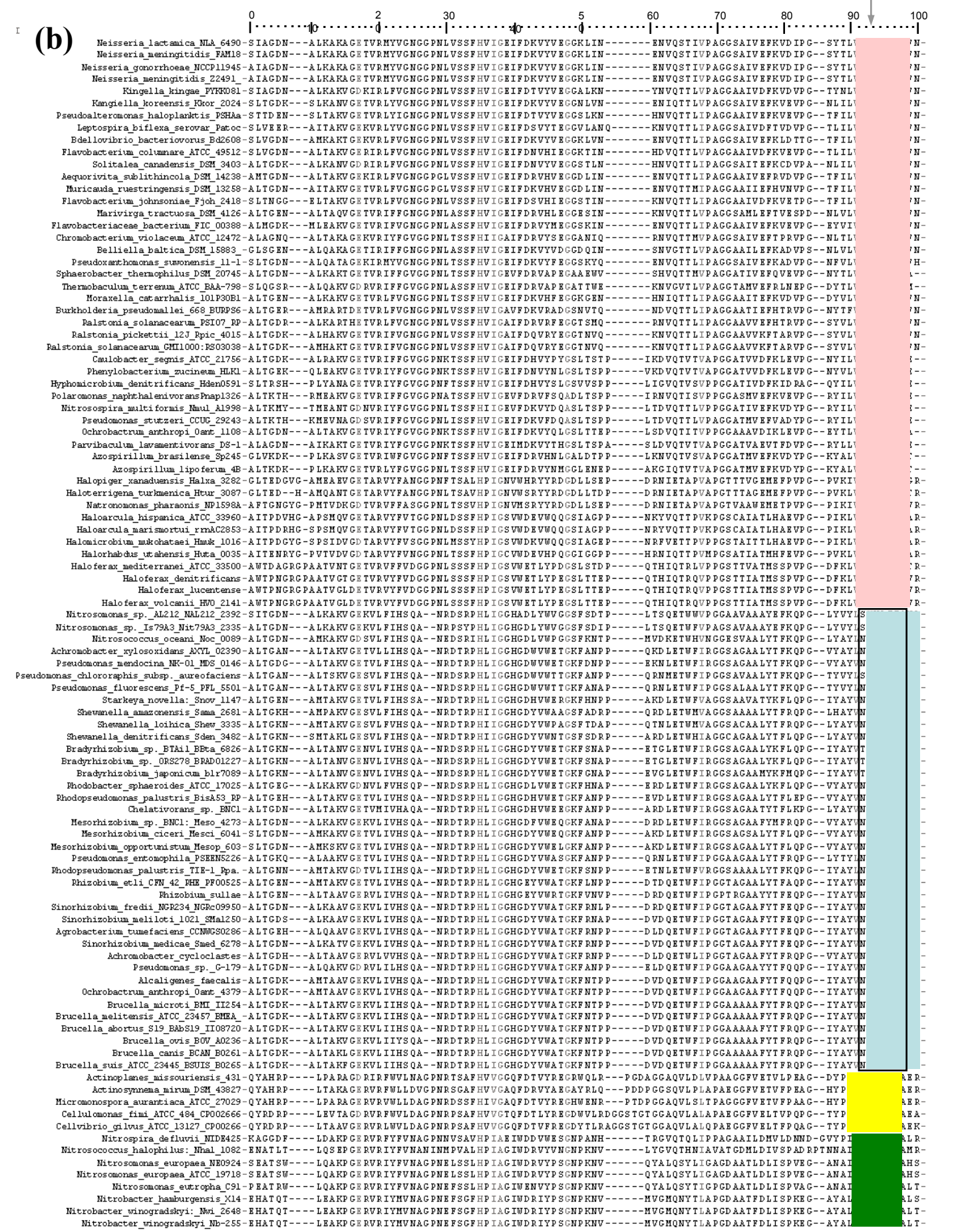

Fig. 2-1 The core and clamp position of the forward (a) and reverse (b) primers in the amino acid sequence alignment of nirK from 97 reference. The amino acid codons with different colored backgrounds denote the primer-designed region of each cluster, and the black frames denote the region of the currently used primer F1aCu/R3Cu. The black and gray arrows in (a) and (b) denote type I and type II copper ligands of NirK.

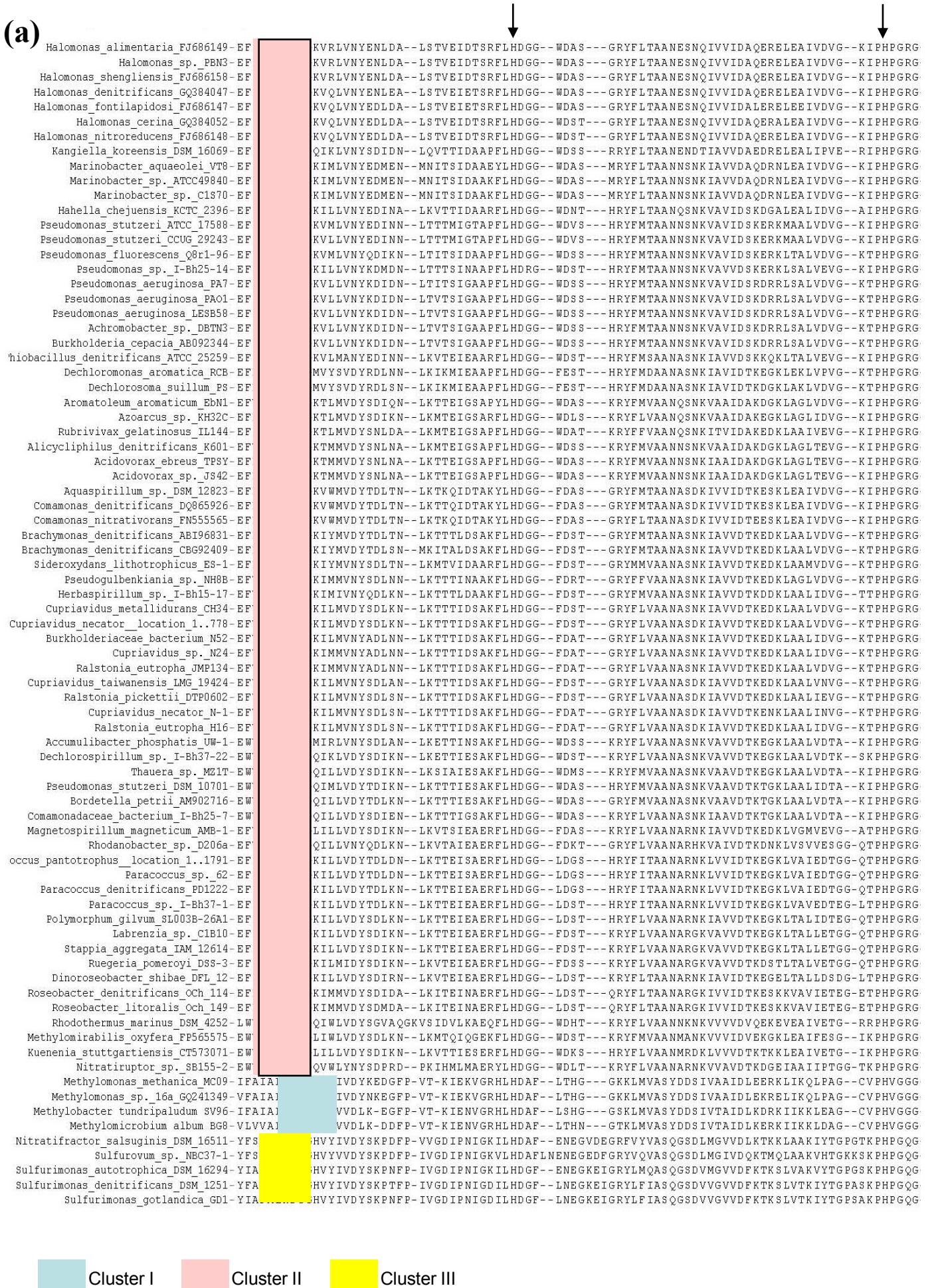

Fig. 2-2 be continued

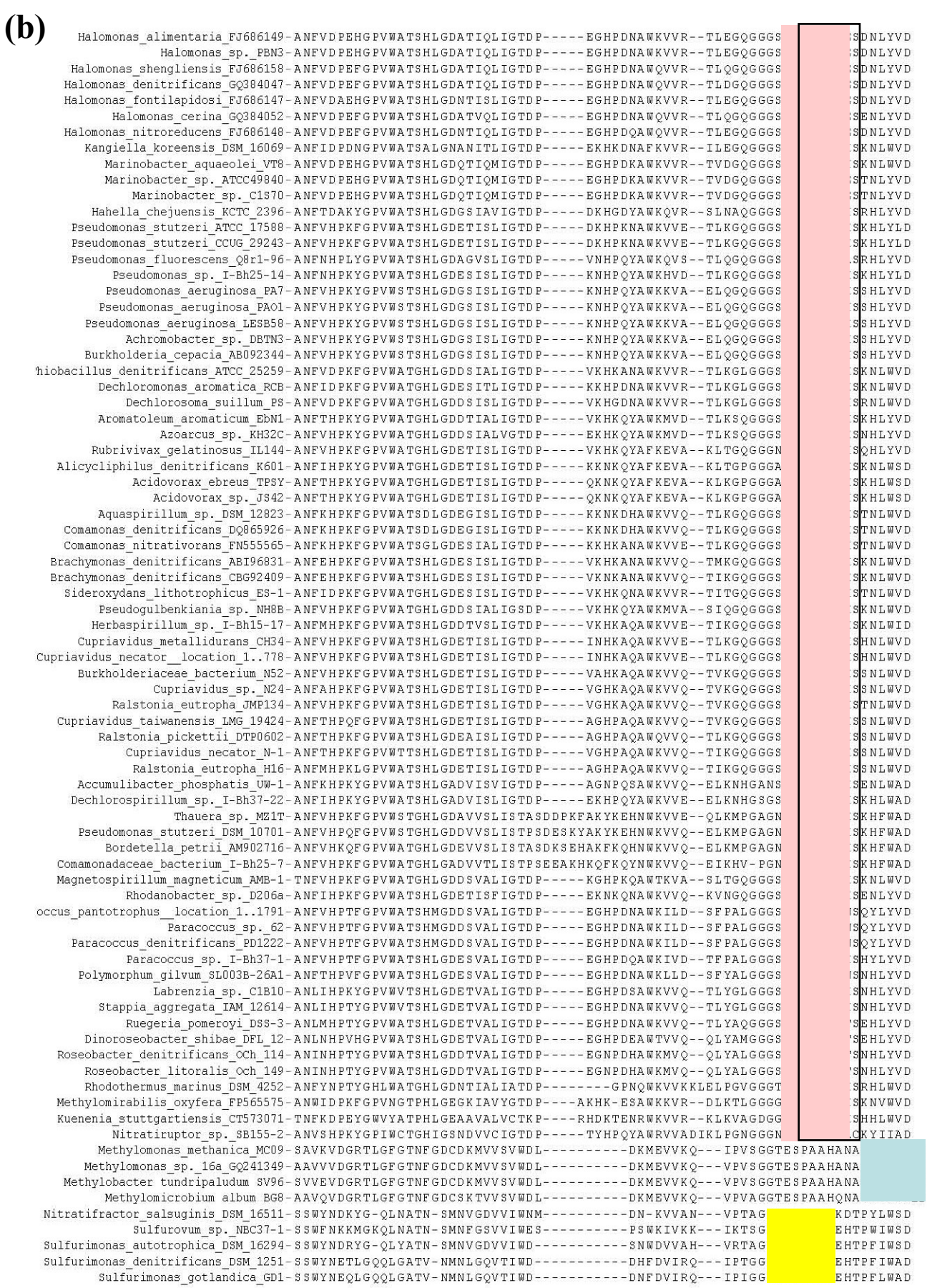

Fig. 2-2 The core and clamp position of the forward (a) and reverse (b) primers in the amino acid sequence alignment of *nirS* from 75 reference genomes. The amino acid codons with different colored backgrounds denote the primer-designed region of each cluster, and the black frames denote the region of the currently used cd3aF/R3cd. The black arrows in (a) denote active sites of the *nirS* gene.

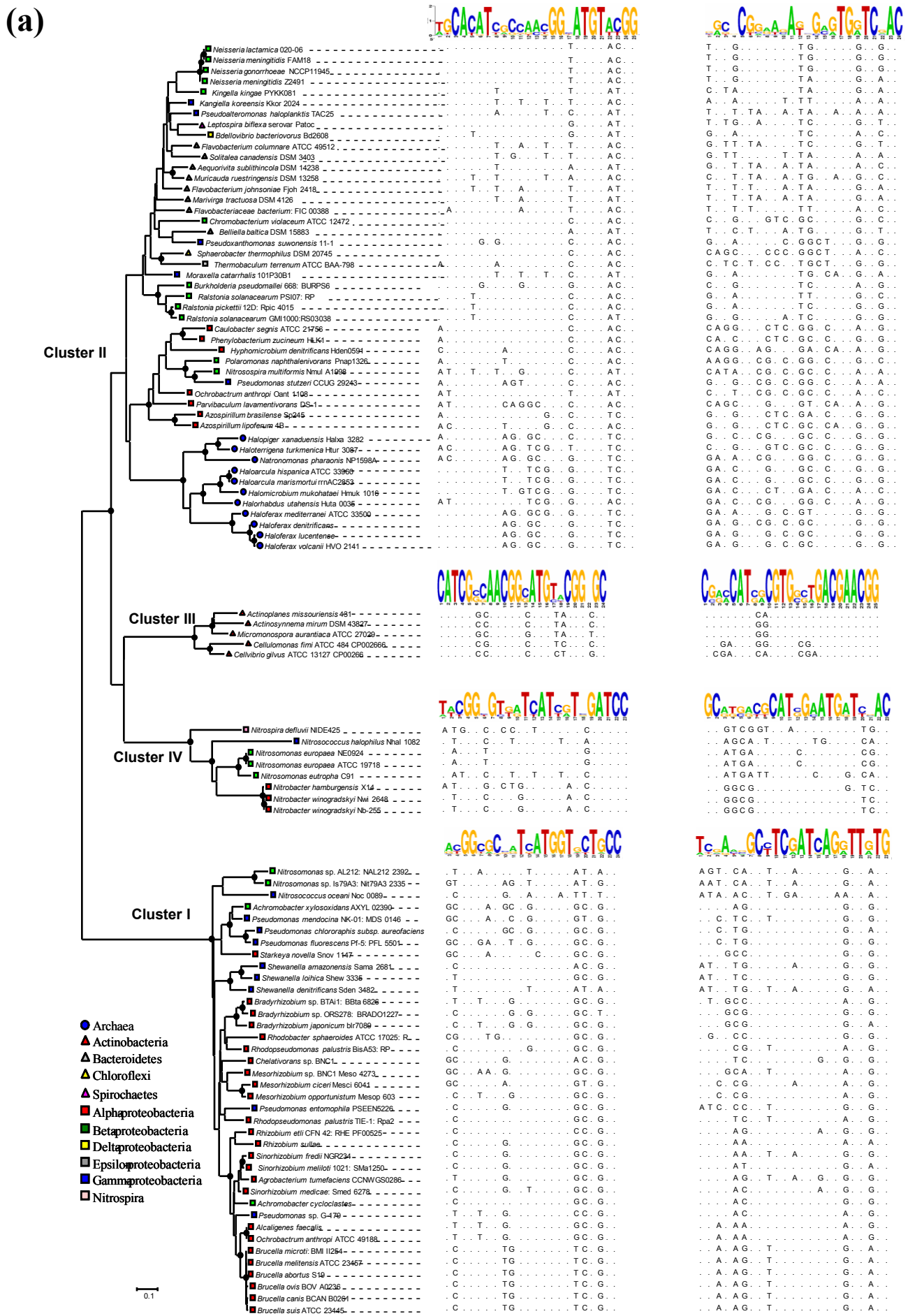

Fig. 2-3 be continued

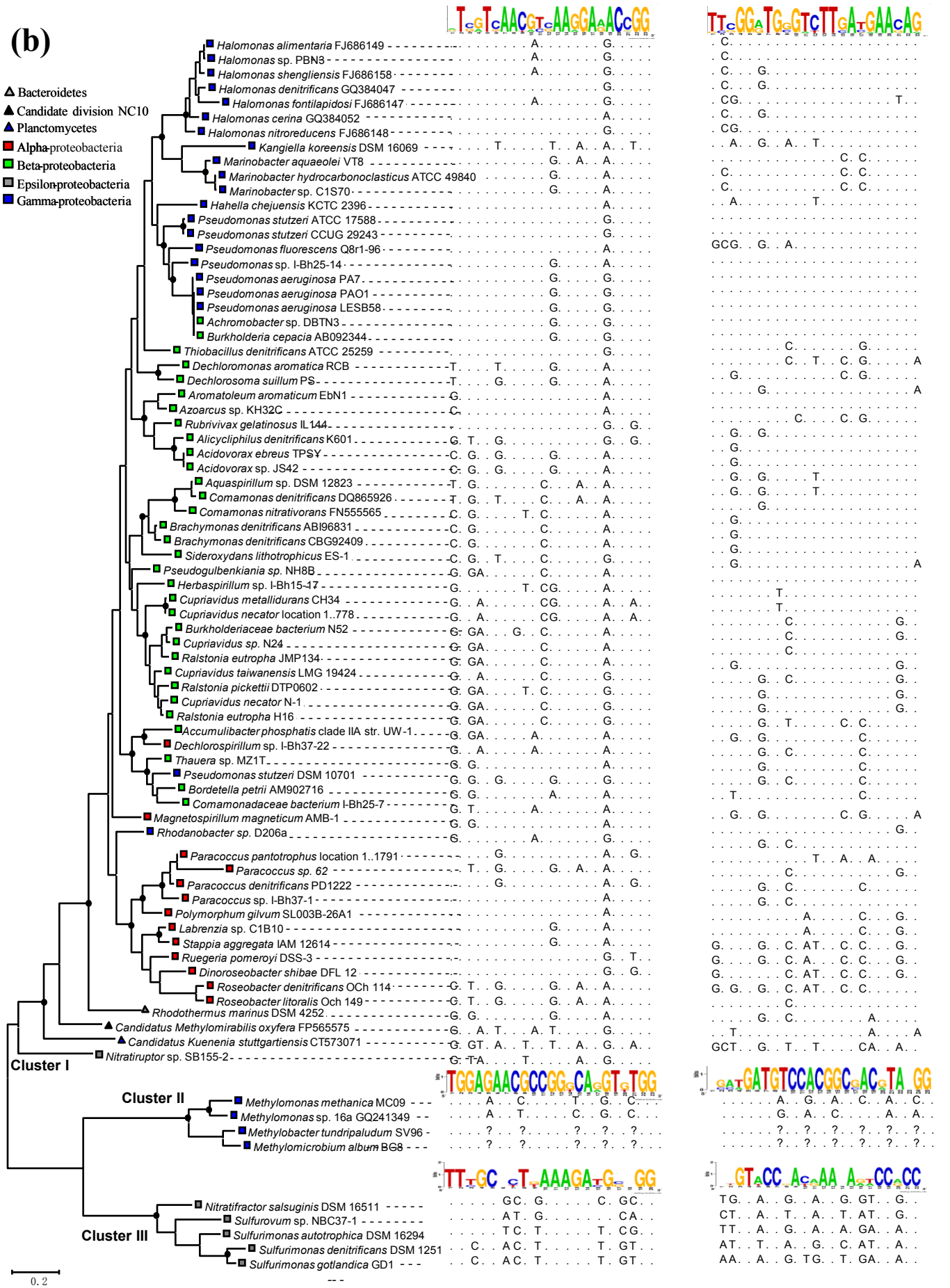

Fig. 2-3 Maximum likelihood phylogeny of amino acid sequences of the nirK copper center type I (a) and nirS cytochrome d1 heme (b). The sequences at the forward and reverse primer sites are shown as seq-logo in the upper right and corresponding sequences below. Bootstrap values (500 replicates) greater than 70% are denoted by dots above the branches, and the branch lengths correspond to sequence differences indicated by the scale bar. Symbols on tree tips indicate the taxonomic affiliations of reference sequences.

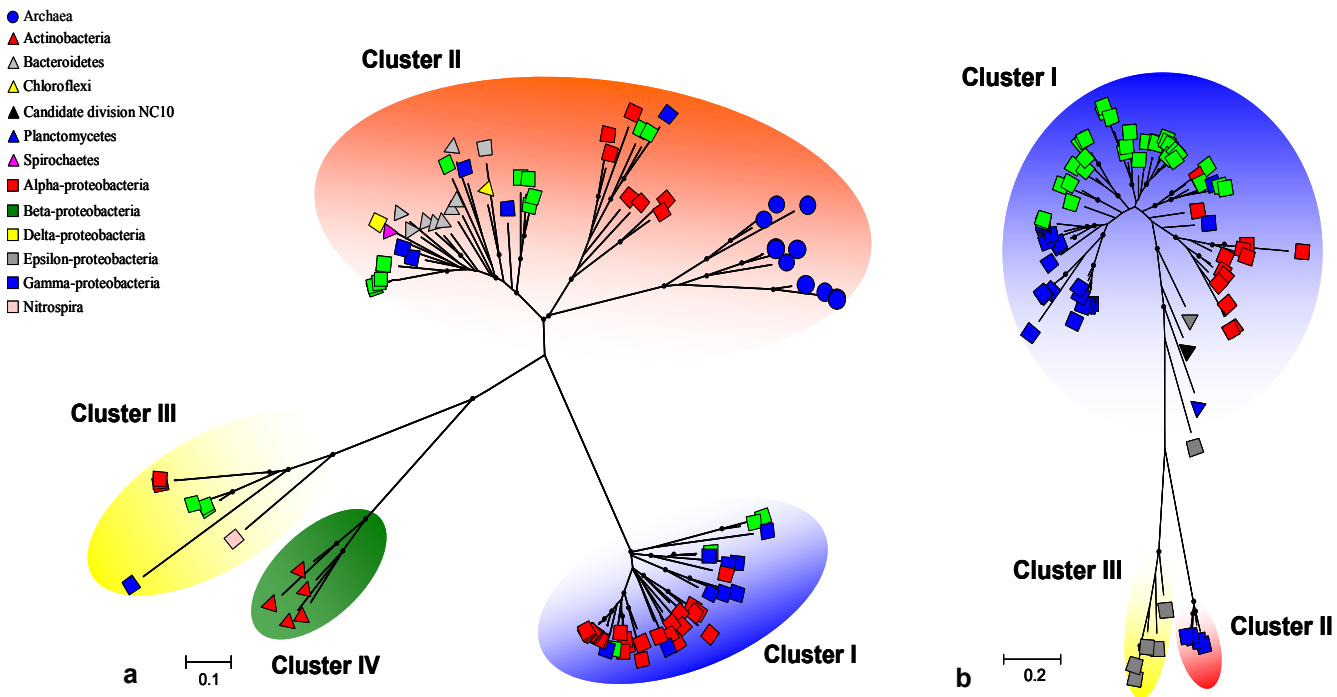

Fig. 2-4 Unrooted maximum likelihood phylogeny of partial *nirK* (a) and *nirS* (b) amino acid sequences obtained from genomes. The *nirK* type 1 copper center and *nirS* cytochrome d1 heme were detected for each cluster. Bootstrap values (500 replicates) greater than 70% are denoted by dots above the branches, and the branch lengths correspond to sequence differences, which are indicated by the scale bar. Symbols on tree tips indicate the taxonomic affiliations of reference sequences.

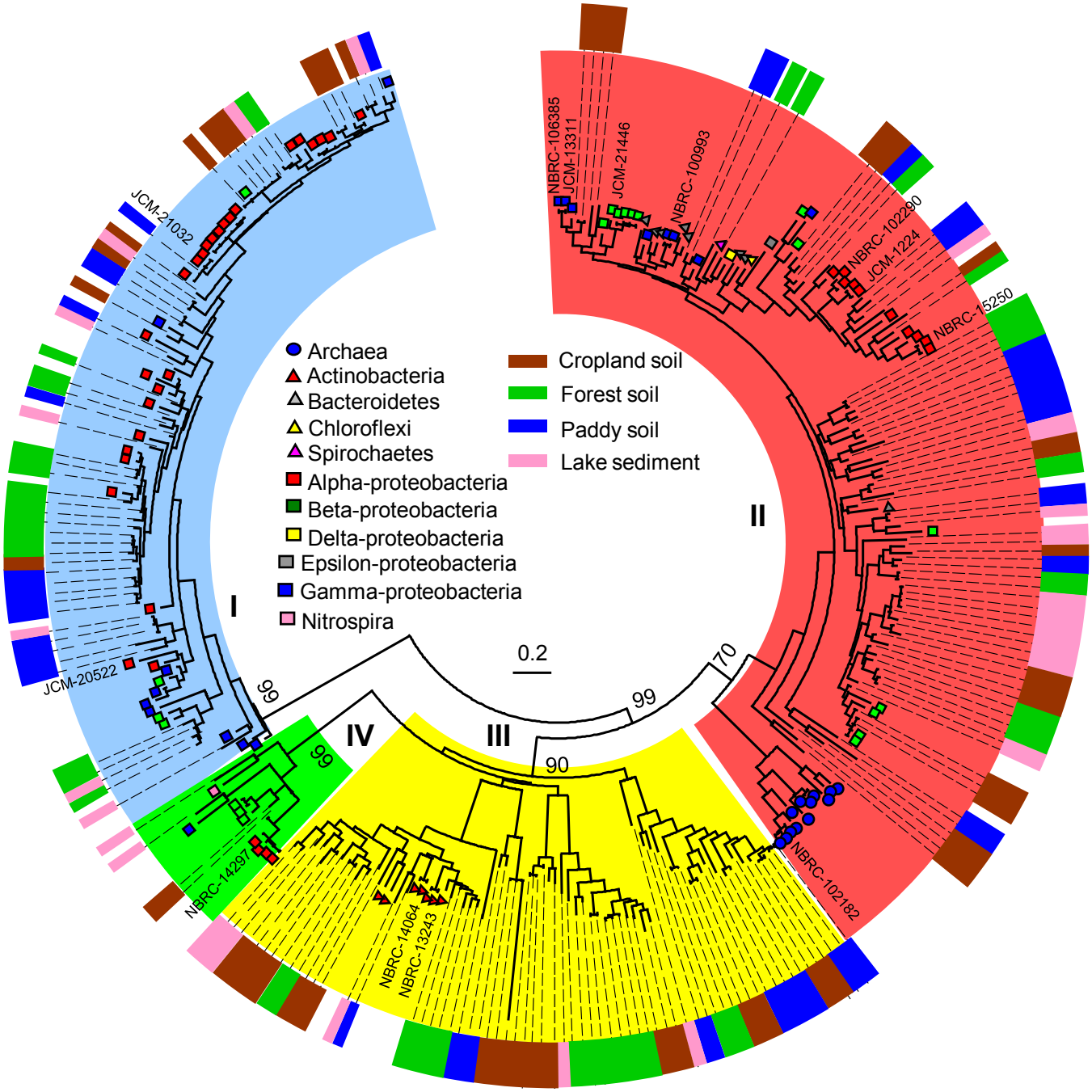

Fig. 2-5 Maximum likelihood phylogeny of the 4 clusters of *nirK* amino acid sequences obtained from the environmental samples listed in Table 2-3 and the reference sequences from the genomes and denitrifying strains listed in Table 2-2. Bootstrap values (500 replicates) of each cluster are denoted above the branches. Non-coded and coded symbols on tree tips indicate the taxonomic affiliations of the reference sequences from genomes and denitrifying strains, respectively. The outer color strip shows the source of environmental clones. The branch lengths correspond to sequence differences, which are indicated by the scale bar.

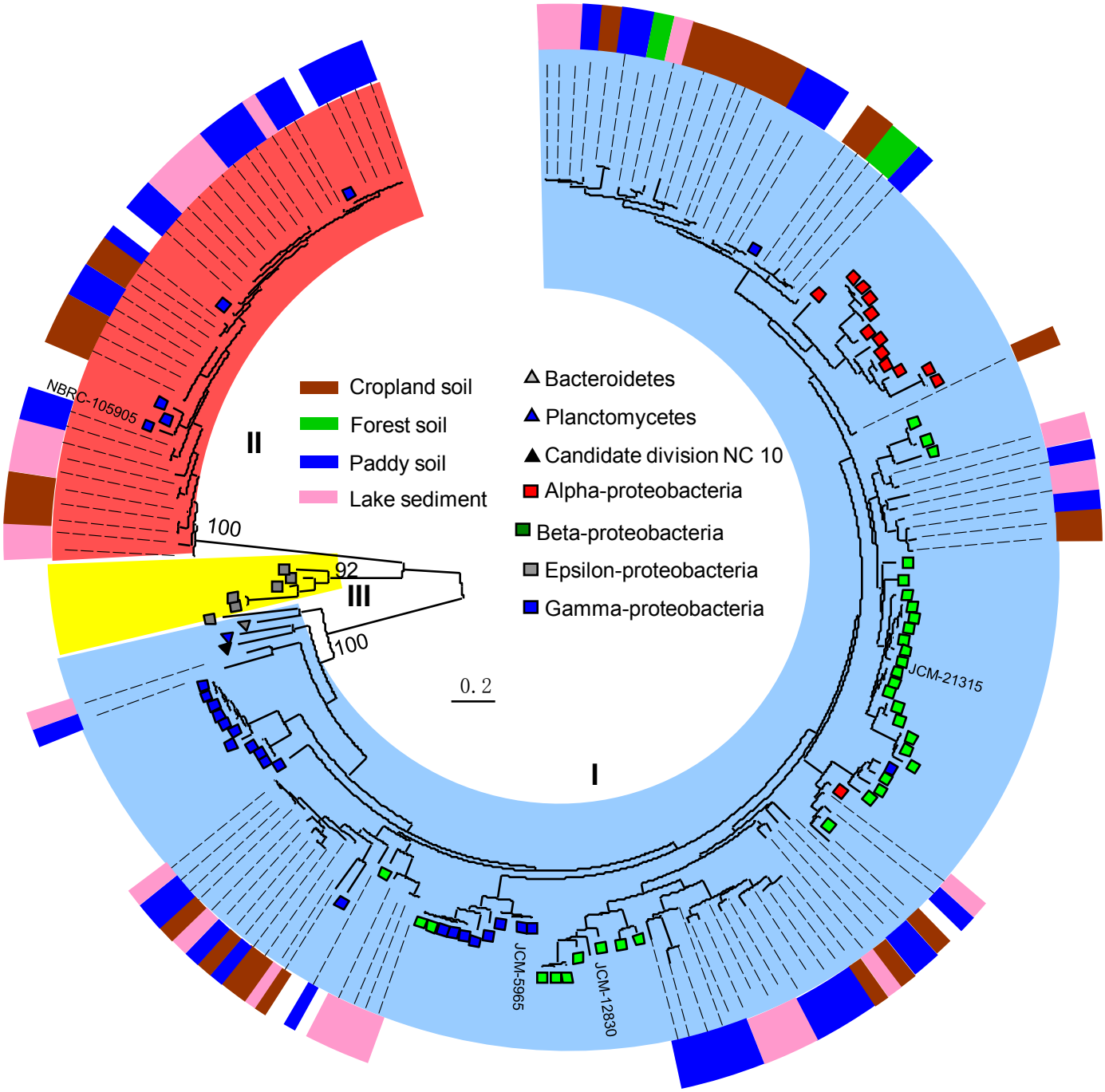

Fig. 2-6 Maximum likelihood phylogeny of the 3 clusters of *nirS* amino acid sequences obtained from the environmental samples listed in Table 2-3 and the reference sequences from the genomes and denitrifying strains listed in Table 2-2. Bootstrap values (500 replicates) of each cluster are denoted above the branches. Non-coded and coded symbols on tree tips indicate the taxonomic affiliations of the reference sequences from genomes and denitrifying strains, respectively. The outer color strip shows the source of environmental clones. The branch lengths correspond to sequence differences, which are indicated by the scale bar.

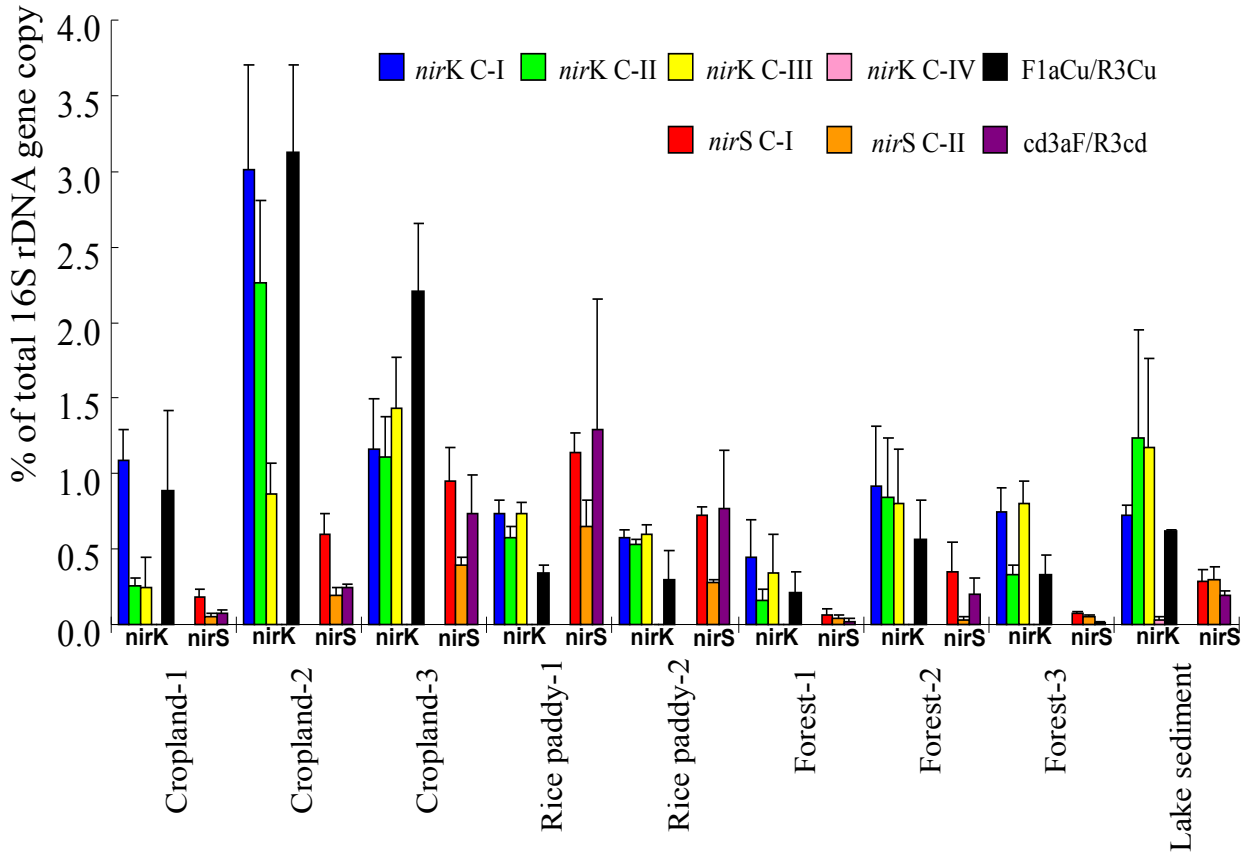

Fig. 2-7 Relative abundance of each *nirK* and *nirS* cluster of gene copies from the different environmental samples listed in Supplementary Table 2-4, calculated as a proportion of the total number of bacterial 16S rRNA gene copies (for the mean and standard deviation of replicates by site, see Tables 2-4). Relative abundance of *nirK* cluster IV and *nirS* cluster I genes detected by the widely used primer sets F1aCu/R3Cu and cd3aF/R3cd are shown as a reference.

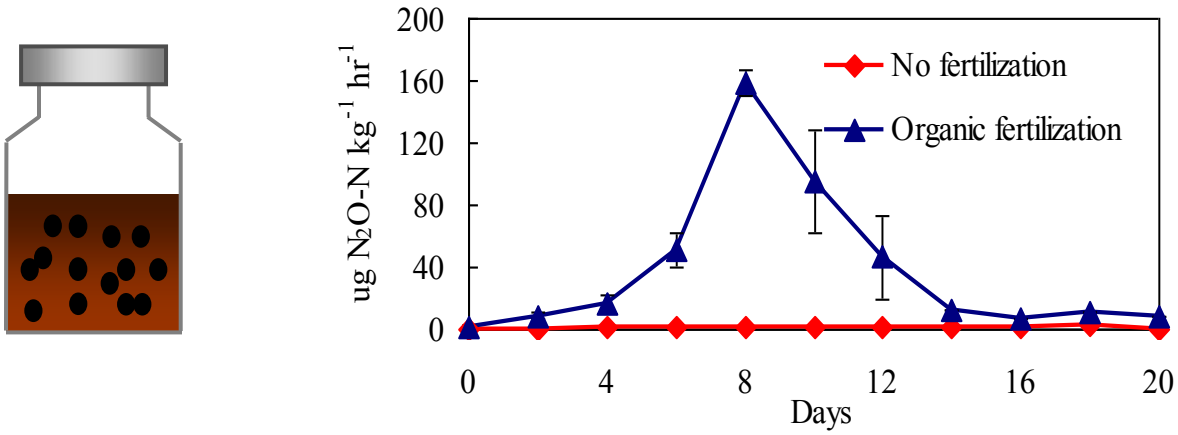

Fig. 2-8 N_2O fluxes in the soil microcosm. The error bars represent standard deviations (n=3).

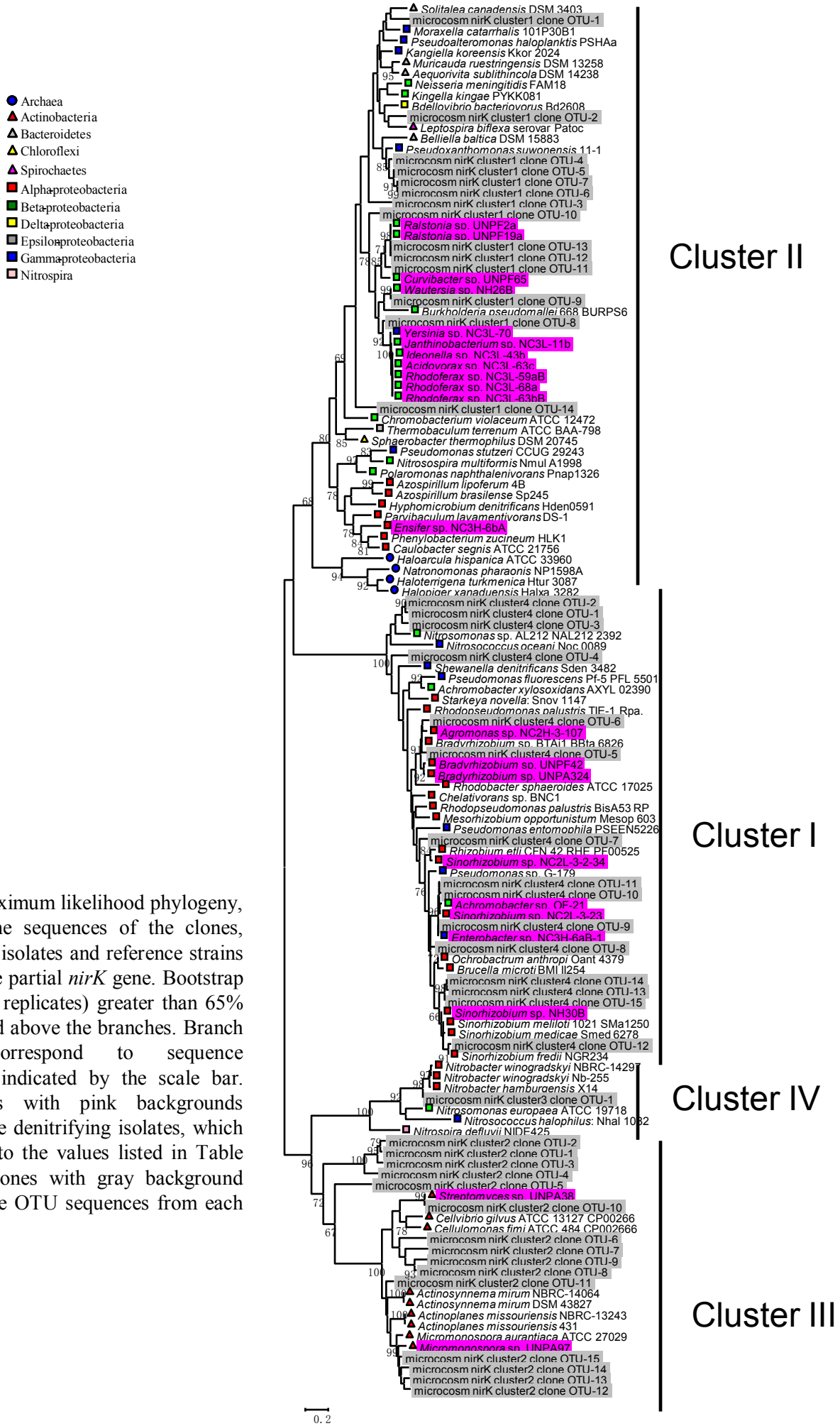

Fig. 2-9 Maximum likelihood phylogeny, including the sequences of the clones, denitrifying isolates and reference strains based on the partial *nirK* gene. Bootstrap values (500 replicates) greater than 65% are indicated above the branches. Branch lengths correspond to sequence differences indicated by the scale bar. The strains with pink backgrounds exhibited the denitrifying isolates, which correspond to the values listed in Table 2-2. The clones with gray background exhibited the OTU sequences from each cluster.

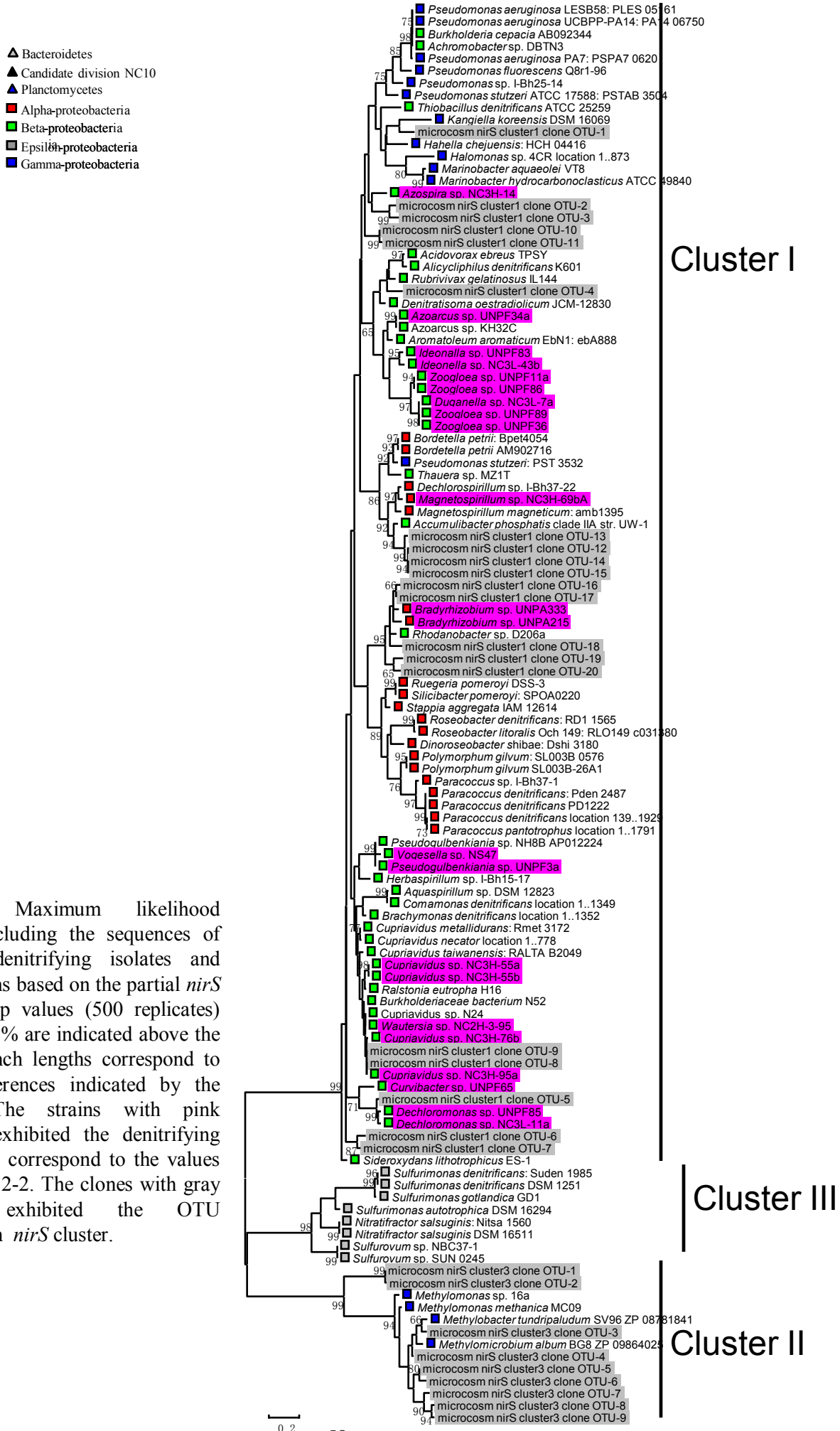

Fig. 2-10 Maximum likelihood phylogeny, including the sequences of the clones, denitrifying isolates and reference strains based on the partial *nirS* gene. Bootstrap values (500 replicates) greater than 65% are indicated above the branches. Branch lengths correspond to sequence differences indicated by the scale bar. The strains with pink backgrounds exhibited the denitrifying isolates, which correspond to the values listed in Table 2-2. The clones with gray background exhibited the OTU sequences from *nirS* cluster.

Chapter 3

Unaccounted diversity and abundance of fungal denitrifiers in upland field soil

3.1 Introduction

Nitrous oxide (N_2O) is a potent greenhouse gas (IPCC, 2007) and is involved in stratospheric ozone depletion (Ravishankara et al., 2009). It is produced through the microbial denitrification process, in which nitrate and nitrite are reduced to gaseous N_2O (Isobe and Ohte, 2014). Fungal denitrification in terrestrials has recently received considerable attention as an N_2O production process. In fact, some previously studies in grassland and forest soils used antibiotic assay and isolated denitrifying fungi to demonstrate the dominance of fungal denitrification (Laughlin and Stevens, 2002; Blagodatskaya et al., 2010). Many fungal species produce N_2O as the end product of the denitrification (Shoun et al., 1992); however, the diversity and ecological behavior of denitrifying fungi in soil, unlike denitrifying bacteria, remains unknown, probably because of the lack of a methodology to detect fungal denitrification-related genes. In addition, the ability to denitrify varies at the species level (Shoun et al., 1992; Yanai et al., 2007), indicating the difficulty of identifying denitrifying fungi based on their taxonomic position. Previous studies revealed that *Fusarium oxysporum* and *Cylindrocarpon tonkinese*, the most thoroughly characterized denitrifying fungi (Nakanishi et al., 2010), use copper-containing nitrite reductase (NirK) to reduce nitrite to nitric oxide, bearing a close resemblance to its bacterial counterpart (Kobayashi and Shoun 1995; Kim et al., 2010). Fungal *nirK* show the similar sequences with prokaryotic *nirK* in Cluster II as described in Chapter 2. Additionally, fungal cytochrome cd1-type nitrite reductase remains undiscovered. Thus, developing a methodology to specifically detect fungal *nirK* should lead to the precise identification of denitrifying fungi and elucidation of their ecological behavior.

Consequently, the objectives of this chapter are to design suitable PCR primers to detect

fungal *nirK* and use these primers to investigate the diversity of fungal *nirK* and identify the denitrifying fungi in upland soil, and assess the abundance of fungal denitrifier in different environments.

3.2 Materials and Methods

3.2.1 Selection, alignment and analysis of the sequences of fungal NirK genes

We searched the full-length *nirK* fungal sequences from the public databases, NCBI Microbial Genomes (http://www.ncbi.nlm.nih.gov/genomes) and Functional Gene Repository (http://fungene.cme.msu.edu/index.spr) and obtained 15 sequences belonging to Ascomycota. We also obtained the representative sequences of *nirK* from diverse bacterial phyla and Euryarchaeota from the database. The phylogenetic trees based on the amino acid sequences and generated with the maximum likelihood algorithm were generated using MEGA 5, and node support was determined using 500 bootstrap replicates (Fig. 3-1).

3.2.2 Primer design for the detection of fungal NirK genes

NirK is a two-domain enzyme including two copper centers, types 1 and 2 (Sakurai and Kataoka, 2007). We designed the primer sets nirKfF (5′-TACGGGCTCATGtaygtnsarcc-3′) and nirKfR (5′-AGGAATCCCACAscnccyttntc-3′) based on homologs of the copper center type 1 domain (Fig. 3-2). Because widely used primers for bacterial *nirK* (such as primer set F1aCu/R3Cu and nirK2F/nirK5R, Braker et al., 1998; Hallin and Lindgren, 1999) also target this region, we can compare fungal *nirK* sequences with the massive store of bacterial *nirK* sequences. Several sets of primers specific to fungal *nirK* sequences were designed based on the CODEHOP algorithm (Rose et al., 1998). We designed the forward primers to anneal with four conserved amino acid codons (tyrosine, valine, glutamine, and proline) and reverse primers to anneal with four conserved amino acid codons (aspartic acid, lysine, glycine, and alanine; Fig 3-2a). Most of these codons were not conserved in prokaryotic *nirK* (Fig 3-2b).

3.2.3 Primer validation using N_2O producing fungal and bacterial isolates

We validated the specificity and sensitivity of the designed primer sets using fungal and prokaryotic strains. We used seventeen denitrifying and three nondenitrifying fungal strains isolated from an Andisol upland field soil located at the Niigata Agricultural Research Institute (N37°26′, E138°52′, Nagaoka, Niigata, Japan). The fungal strains were isolated from the field soils applied with granular organic fertilizer. The applied granular organic fertilizers were separated from the soil, and then fungal strains were isolated from the collected organic fertilizer (COF) and residual soil (RS), respectively. The more detail information for this process will be described in the Chapter 6. We also used ten prokaryotic strains (nine bacteria and one archaea) obtained from the culture collections (Japan Collection of Microorganisms, Koyadai, Japan or the Biological Resource Center (NBRC), Kazusakamatari, Japan; Table 3-1 and Fig. 3-1).

The abilities of the fungal isolates to produce N_2O and N_2 were analyzed. Isolated strains were pre-incubated for 4 days in liquid basal medium containing 1% glucose, 0.2% peptone, and mineral salts (Shoun et al., 1991). The pH was adjusted to 7.5 as described in Shoun et al. (1992). Subsequently, 1-ml aliquots were inoculated into 4 ml of fresh basal medium (pH 7.5) in 25-ml glass serum vials. The medium contained 3.5 mM ^{15}N-labelled $NaNO_2$ (98 atom%-^{15}N, Cambridge Isotope Laboratories, USA). After inoculation, the vials were tightly sealed with rubber stoppers. The vials were sealed without gas replacement under initially aerobic conditions, which allowed improved initial growth of the fungal mycelia (Bollag and Tung, 1972). The isolates were grown at 27 °C for 1 week on a rotary shaker (150 rpm) in the both condition. The $^{15}N_2O$ and $^{15}N_2$ concentrations in the headspace were determined using a GC-MS system (GCMS-QP2010 Plus, Shimadzu, Kyoto, Japan) equipped with a CP-PoraPLOT Q-HT column (25 m × 0.32 mm; Agilent, Japan) or a CP Molsieve 5 Å column (30 m × 0.32 mm; Agilent, Japan) as described by Isobe et al.

(2011). The $^{15}N_2O$ and $^{15}N_2$ concentrations dissolved in the media were calculated as described by Tiedje (1994). The biomass of the fungal strains was determined as described by Bollag and Tung (1972).

Genomic DNA was extracted as described previously (Wei et al., 2014), and PCR was performed with the designed primers. PCR reaction condition was optimized by amplifying all fungal isolates and performed using BIOTaq HS DNA polymerase system (Bioline, London, UK), with an final concentration of 4mM $MgCl_2$, 0.2mM dNTP Mix, 0.5 $mg \cdot ml^{-1}$ bovine serum albumin, 0.2 μM for each primer and 50 ng of genomic DNA. Thermal cycling conditions were an initial 10 min denaturing step at 95 °C, followed by 30 cycles of 95 °C for 30 s, 54 °C for 30 s, 72 °C extension for 30 s and a final extension at 72 °C for 10 min.

3.2.4 Abundance and distribution of fungal NirK genes in environments

The abundance of the fungal *nirK* and 18S rRNA gene in environmental samples were determined by the quantitative PCR (qPCR). Various environmental samples from terrestrials were used including a cropland soil (Andosol) applied with organic fertilizer as described in Chapter 2, including an cropland soil (Grey Lowland Soil, Eutric Fluvisol) applied with organic or urea fertilizer, a flooded and non-flooded paddy soils (Grey Lowland Soil, Eutric Fluvisol), two natural forest soils (Brown Forest soil and Andosol) and a planted forest soil (Brown Forest soil) and a lake sediment.

Environmental DNA was extracted as described in Chapter 2. The quantification of the 18S rRNA gene was performed with the primers as described above. The quantification of the fungal *nirK* were performed with the designed primers. The qPCR was performed in 20 ml reactions that included 10 μl of KOD SYBR qPCR Mix (ToYoBo, Osaka, Japan), 0.4 μl of 50×ROX reference

dye, 0.2 μM of primers and 10 ng of the environmental DNA. The reaction was performed in 20 ml reactions that included of 10 μl KOD SYBR qPCR Mix, 0.4μl 50×ROX reference dye, 0.2 μM for primers and 10 ng of genomic DNA. Thermal cycling conditions consisted of an initial denaturing step of 98 °C 2 min, followed by 40 cycles of 98 °C 10s, 54°C 10 s (58°C for 18S rRNA sequences), 68 °C 30 s. Standard curves for qPCR of fungal nirK and 18S rRNA sequences were generated from linearized plasmids, containing cloned fungal *nir*K and 18S rRNA genes from *Fusarium oxysporum* isolate COF-2. The presence of PCR inhibitors in soil DNA for each cluster was estimated by mixing a known amount of standard DNA with environmental DNA before qPCR reaction. The efficiencies for fungal *nir*K and 18S rRNA gene amplifications were estimated at 87% and 85%, with a R^2 of >0.999 for each gene.

3.2.5 Nucleotide sequence accession numbers

The nucleotide sequences of partial fungal *nirK* from the environmental samples and denitrifying fungal isolates in this study have been deposited in the DDBJ/EMBL/GenBank databases with accession numbers AB938217 to AB938239.

3.3 Results and Discussion

3.3.1 Prokaryotic and fungal *nirK* phylogeny

Fifteen full-length *nirK* s sequences belonging to Ascomycota and representative sequences of *nirK* from diverse bacterial phyla and Euryarchaeota described in Chapter 2 were obtained from the public database after selecting the representative sequence within the highly similarity (>99% of amino-acid sequence) from one species. Then, we generated the phylogenetic tree of *nirK* (Fig. 3-1), and found that fungal *nirK* formed a monophyletic cluster distinct from the prokaryotic *nirK* with 100% bootstrap support.

3.3.2 New primer design and its validation using denitrifying strains

We designed several primer sets which can potentially amplify the fungal *nirK* located in the clusters shown in Fig. 3-1. Several sets of degenerate primers specific to fungal *nir*K sequences were designed based on CODEHOP algorithm (Rose et al., 1998). We designed the forward primers which can anneal with four conserved amino acid codons (tyrosine, valine, glutamine and proline) as the degenerate core region, and reverse primers which can anneal with four conserved amino acid codons (asparatic acid, lysine, glycine and alanine) as the degenerate core region (Fig. 3-2). Both degenerate core region of forward and revise primer region were distinct from all homologues of prokaryotic nirK gene Fig. 3-2), which effectively guaranteed the specificity of fungal *nirK* primers (Fig. 3-2).

We validated the specificity and sensitivity of the designed primer sets using fungal and prokaryotic strains. PCR using the designed primers amplified the *nirK* fragment (ca. 480 bp) from the twelve denitrifying fungal strains tested, belonging to Ascomycota (Table 3-1), but did not amplify the fragment from nondenitrifying fungal strains or all prokaryotic strains tested and

denitrifying *F. equiseti* of Ascomycota or *Actinomucor elegans* and *Rhizomucor* sp. of Zygomycota. PCR using the widely-used bacterial nirK primers, F1aCu/R3Cu, did not amplify the fragment with the expected size. Thus, the designed primers could successfully amplify the diverse fungal *nirK* of Ascomycota, the most dominant fungal group in soil (Wei et al., 2014), except *F. equiseti*, with sufficient selectivity and specificity. These results indicate the superior coverage and specificity of the newly designed primer for fungal *nirK*.

3.3.3 Fungal *nirK* and 18S rRNA phylogenies

We analyzed *nirK* and 18S rRNA phylogenies of the fungal species isolated from upland soil described previously. We constructed the phylogenetic tree of the amplified *nirK* and the corresponding 18S rRNA gene (Fig. 3-3). The tree also includes the database-retrieved *nirK* and 18S rRNA gene of fungi (Fig. 3-1). The *nirK* and 18S rRNA gene-based phylogenies can be congruent at the order level of Ascomycota, whereas bacterial *nirK* and 16S rRNA gene-based phylogenies are known to be incongruent (Jones et al., 2010). This suggests that we can estimate the taxonomic position of denitrifying fungi based on their *nirK* phylogeny.

3.3.4 Abundance of fungal NirK genes in various environments

We performed a quantitative PCR study using the newly designed primers to examine the abundance and distribution of fungal *nirK* sequences in various terrestrial environmental samples: cropland soils with different soil types or fertilizations, rice paddy soils in water-flooding and non-flooding seasons, natural and planted forest soils and lake sediment. The abundance of the fungal *nirK* was normalized by the abundance of the fungal 18S rRNA gene to standardize the unit.

The distribution of fungal *nirK* differed in the environmental samples (Fig. 3-3). For example,

cropland soils (Fluvisols) that received chemical fertilization (Cropland-3) had more fungal *nirK* compared with cropland soils (Fluvisols) that received organic fertilization (Cropland-2). Water flooding decreased fungal *nirK* in paddy soils (Rice paddy-1 and 2). In addition, the abundance of fungal *nirK* was high in cropland and low in rice paddy soils, forest soil and lake sediment; but the relative abundance was low in cropland and high in rice paddy soils, forest soil and lake sediment. These results indicated that fungi having the nirK gene were dominant the fungal community in some environments, e.g. the upland soil applied chemical N fertilizers, the paddy soil after the water-flooding, forest soil or lake sediment.

3.4 Conclusion

In this Chapter, to overcome the lack of a methodology to detect fungal denitrification-related genes, we designed a suitable primer set to detect fungal *nirK* and showed that the *nirK* of the most dominant denitrifying fungal group in soil (Ascomycota) can be sufficiently detected. The methodology developed here allows to precisely identify denitrifying fungi and to elucidate the importance of fungal N_2O emission in upland field. Thus, the combination of the methodologies developed in Chapter 2 and Chapter 3 can make us obtain more comprehensive and precise information of prokaryotic and fungal denitrifiers, the potential N_2O emitters, in upland filed.

Table 3-1. Primer validation using denitrifying fungal isolates and prokaryotic strains

Strain number	Taxonomic assignment	N_2O production[a]	PCR products using primers[b]	
			nirKfF/nirKfR	F1aCu/R3Cu
Fungi				
COF-2	*Fusarium oxysporum*	+++	+++	–[c]
COF-3	*Actinomucor elegans*	++	–	–
COF-5	*Fusarium equiseti*	++	–	–
COF-6	*Fusarium solani*	–	–	–
COF-7	*Rhizomucor* sp.	+++	–	300, 700[d]
COF-8	*Fusarium equiseti*	++	–	–
COF-10	*Fusarium oxysporum*	+++	+++	–
COF-11	*Fusarium oxysporum*	+++	+++	–
COF-12	*Fusarium equiseti*	++	–	–
COF-13	*Fusarium oxysporum*	++	++	–
COF-16	*Bionectria ochroleuca*	–	–	–
COF-17	*Fusarium oxysporum*	–	–	–
COF-19	*Fusarium solani*	+++	++	400
COF-20	*Fusarium solani*	++	++	–
RS-1	*Aspergillus niger*	+	+	–
RS-3	*Bionectria ochroleuca*	+++	+++	–
RS-5	*Fusarium oxysporum*	+++	+++	–
RS-6	*Penicillium purpurogenum*	++	++	–
RS-8	*Fusarium avenaceum*	+	+	–
RS-9	*Fusarium oxysporum*	++	+++	–
Bacteria				
ATCC-21756	*Caulobacter segnis*	+	–	
ATCC-49188	*Ochrobactrum anthropi*	+	–	+++
NCIB-8687	*Alcaligenes faecalis*	+	–	++
NBRC-13243	*Actinoplanes missouriensis*	++	–	700, 1200
DSM-43827	*Actinosynnema mirum*	+	–	–
CCUG-29243	*Pseudomonas stutzeri*	+	–	300, 900
NBRC-100993	*Pseudoalteromonas haloplanktis*	+	–	–
NBRC-106385	*Pseudoxanthomonas suwonensis*	+++	–	900
Archaea				
ATCC-33500	*Haloarcula hispanica*	++	–	–

[a]N_2O production: +, 0–10 μg/day/g-biomass; ++, 10–100 μg/day/g-biomass; +++, >100 μg/day/g-biomass

[b]The concentration of PCR products: +, 0–20 ng/μl; ++, 20–50 ng/μl, +++, >50 ng/μl.

[c]Not amplified.

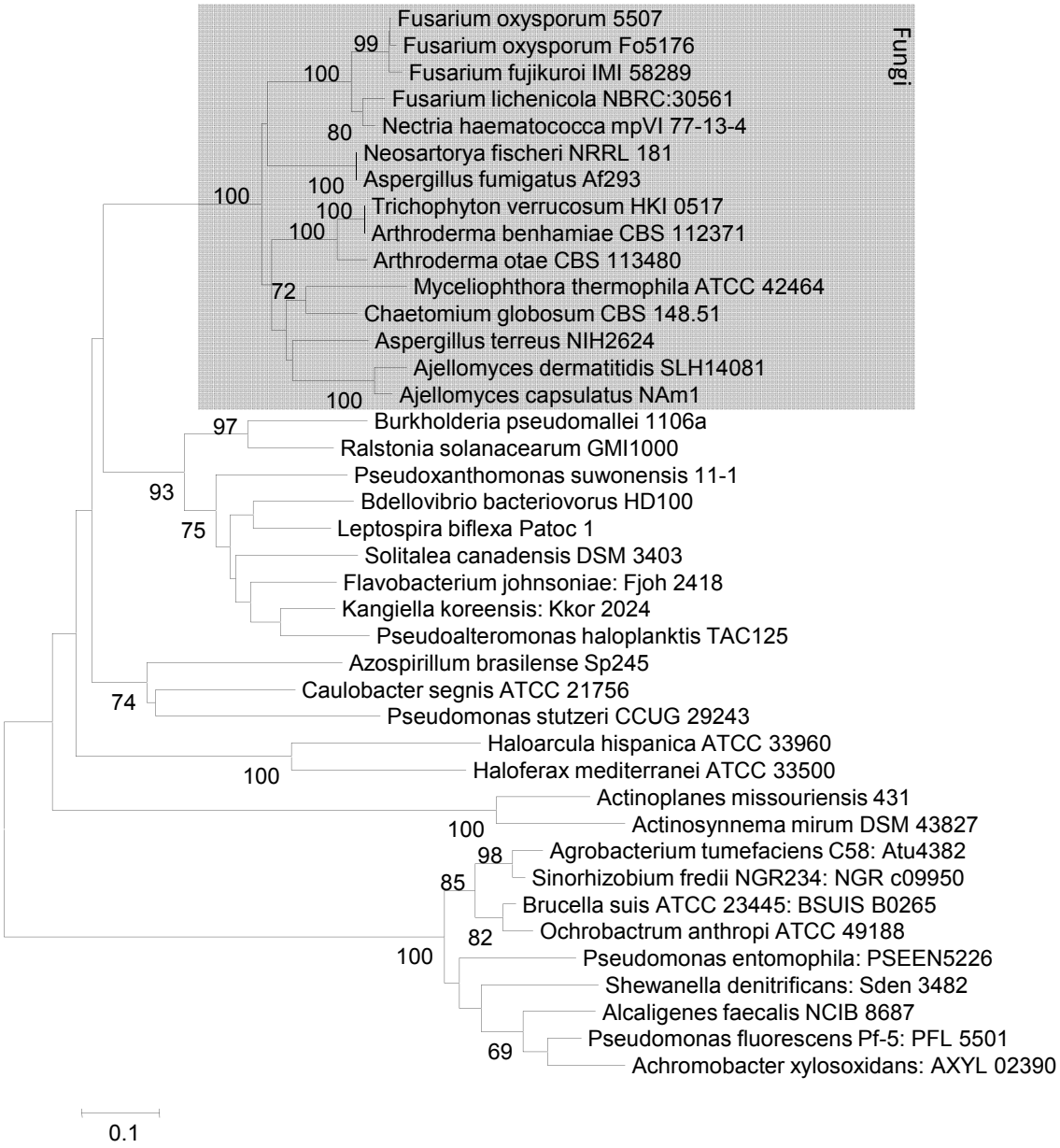

Fig. 3-1 Tree of maximum likelihood phylogeny of database-retrieved full-length NirK amino acid sequences of fungi, bacteria, and archaea. Bootstrap values (500 replicates) greater than 70% are denoted by dots above the branches and branch lengths correspond to sequence differences, which are indicated by a scale bar. Sequences from fungi are in bold within the gray box.

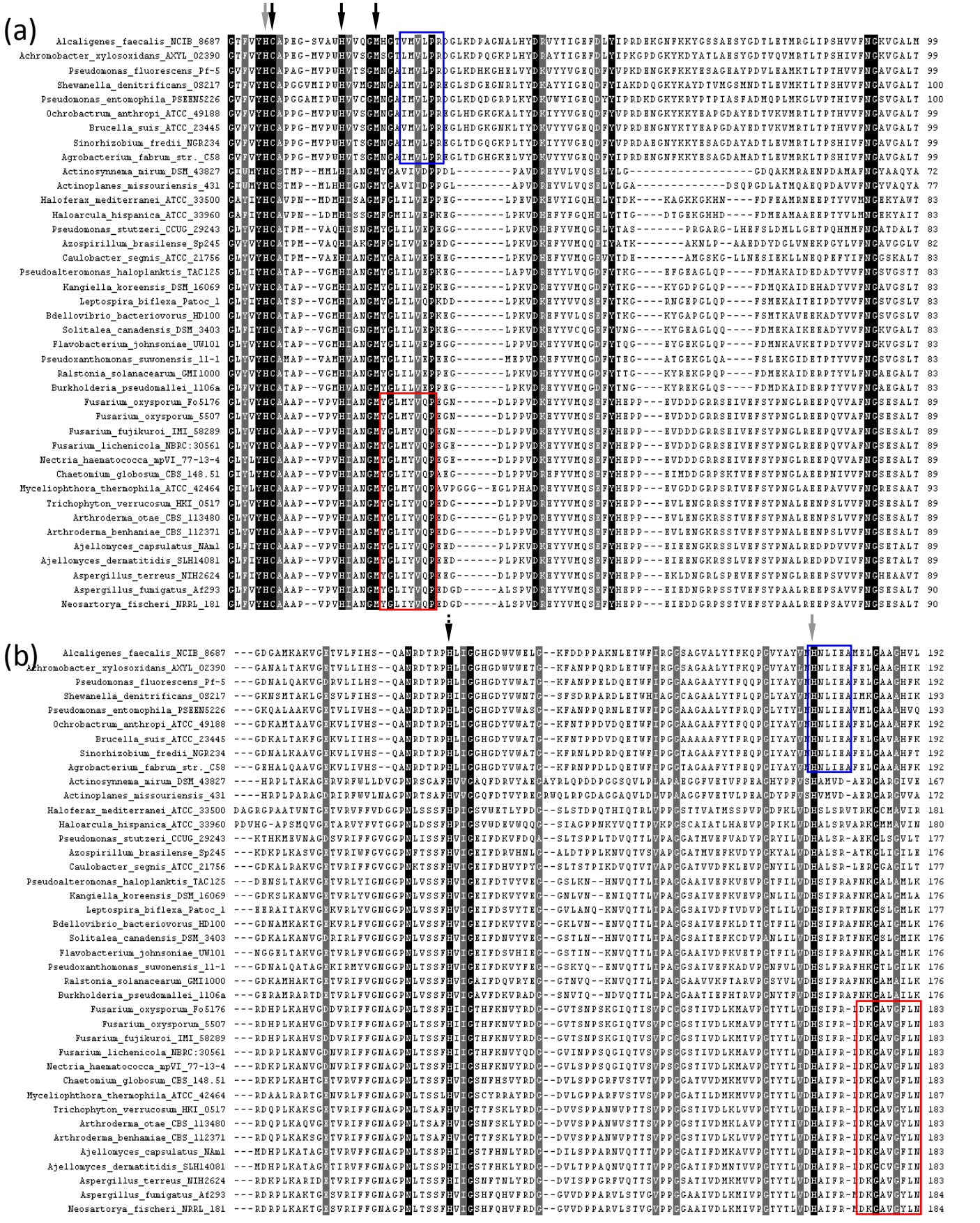

Fig. 3-2 The core and clamp position of the forward (a) and reverse (b) primers in the amino acid sequence alignment of the *nirK* copper center type 1 domain from the reference genomes of 10 prokaryotic *nirK* sequences and 11 fungal *nirK* sequences. The amino acid codons within the red frame indicate the primer-designed regions of fungal *nirK*, and those within the blue frame indicate the region of currently used primer F1aCu/R3Cu. The black and gray arrows indicate type I and type II copper ligands of *nirK*, respectively, and the dotted arrows indicate the active-site residue His240 of *nirK*.

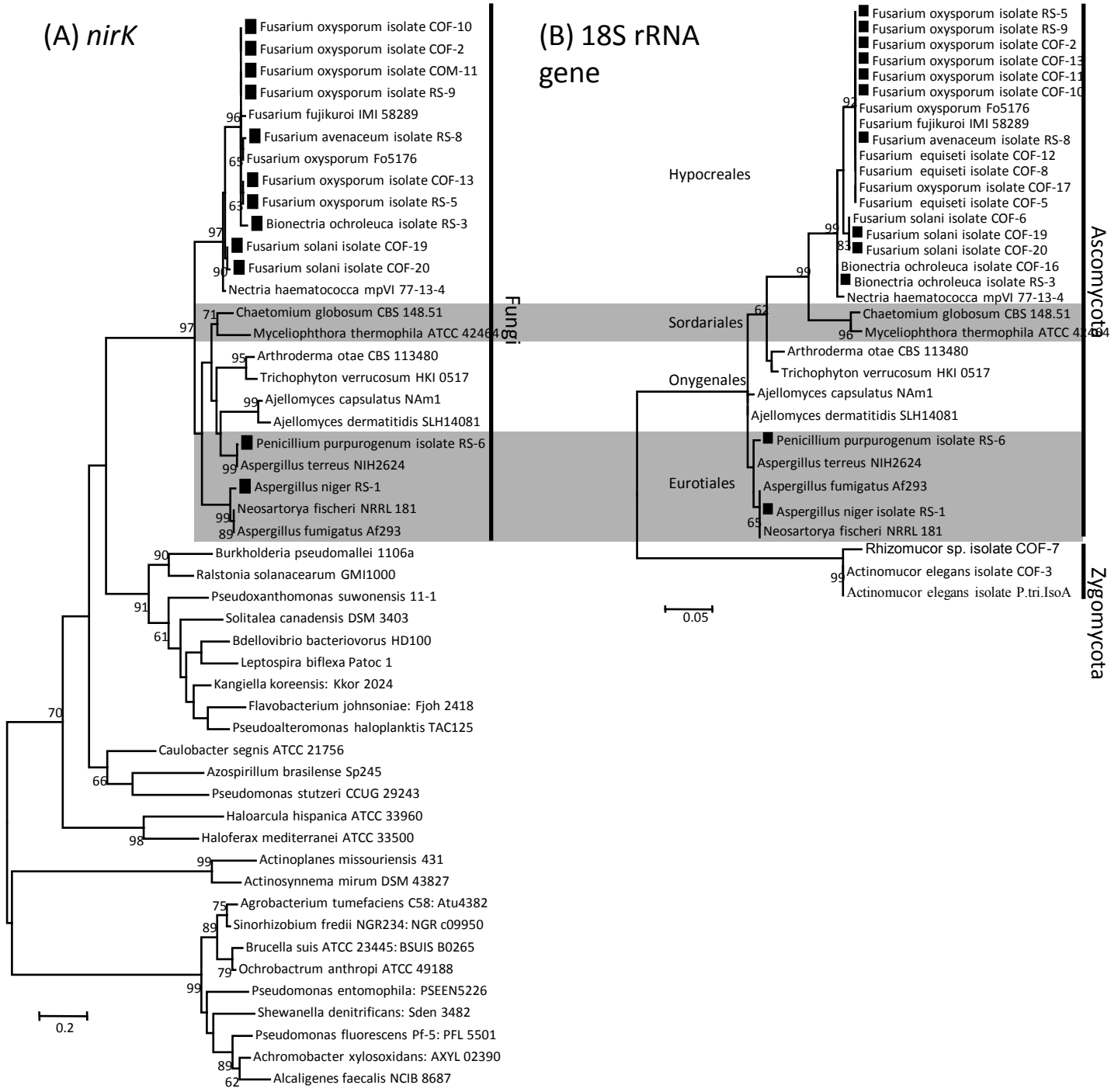

Fig. 3-3 Tree of maximum likelihood phylogeny of the (A) *nirK* and (B) the 18S rRNA gene of fungal isolates obtained from COF, RS, and the database search. The *nirK* phylogenetic tree includes prokaryotic *nirK*. The 18S rRNA gene and *nirK* of the fungal isolates are highlighted in gray. The numbers in parentheses represent the numbers of fungal *nirK* clones in the operational taxonomic units. The bootstrap values (>70%) from 500 replicates are indicated next to the branches.

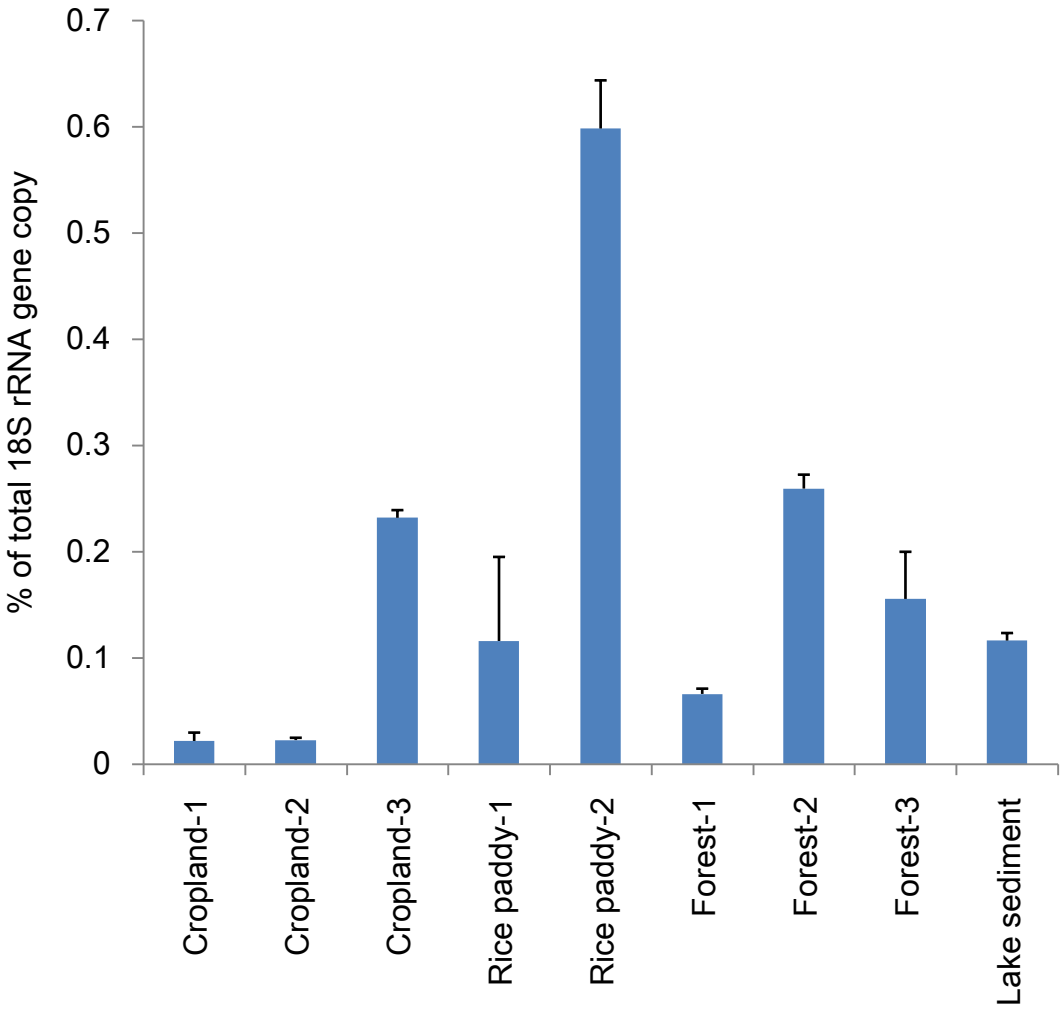

Fig. 3-4 Relative abundance of fungal *nirK* gene copies from the different environmental samples calculated as a proportion of the total number of fungal 18S rRNA gene.

Chapter 4

Microbial N_2O emission in upland field soil after N fertilization

4.1 Introduction

N_2O is a potent greenhouse trace gas (IPCC, 2007), which generates a 298-fold stronger effect on global warming than carbon dioxide (CO_2). N_2O is also involved in stratospheric ozone depletion (Ravishankara et al., 2009). Upland field soil mainly contribute to the total N_2O emissions from soil environments (Skiba and Smith, 2000; Smith, 2008; Davidson, 2009), because substantial N_2O emissions are greatly stimulated by organic or chemical N fertilization (Mosier and Kroeze, 2000), and N input enhances the microbial N_2O-producing activities in soils (Sánchez-Martín et al., 2008).

To maintain sufficient soil nutrients for crop growth, organic or chemical N fertilizers are usually applied several times in upland field soil, including incorporation into the plowed layer as the basal fertilizers and top-dressing application on the soil surface as the additional fertilizers. N_2O emission can be observed after the basal and additional fertilization, but the N_2O emission rate was always different (Li et al., 2002; Akiyama et al., 2003; Meng et al., 2005; Hayakawa et al., 2009). N_2O is known to be produced by soil microorganisms via nitrification and denitrification pathway, which might cause such different emission regularity. Thus, the clarification of the contribution of nitrification and denitrification to N_2O emission is the crucial determinants to understand the regularity of N_2O emission induced by the basal and additional application with organic or chemical fertilizers.

The development of comprehensive detection for prokaryotic and fungal nitrite reductase gene in Chapter 2 and 3 contribute to clarifying the sources of N_2O emission derived from denitrification. In addition, Sanford et al. (2012) and Jones et al. (2013) affirmed a newly found cluster of *nosZ* gene coding the N_2OR and designed specific primer set for them through a

comprehensive phylogenetic analysis of genomes retrieved from public databases, which contribute to clarifying the total N_2O sink by denitrification in soils. The knowledge and methodology of nitrite reductase and nitrous oxide reductase obtained in above-mentioned studies will lead us to a more comprehensive understanding of N_2O source and sink by denitrifying microorganisms in upland field soil. The ammonia monooxygenase (*amoA*) gene of AOA and AOB were usually utilized to assess the ecology of nitrifying microorganisms in environments, where nitrification is active and dominant source of N_2O emission (Di et al., 2010; Löscher et al., 2012). Isotopomer analysis, a recent developed technique for determining intramolecular ^{15}N site preference (*SP*) in asymmetric molecules of N_2O, can enable us to identify the source and sinks of N_2O in upland field soil. Therefore, a combined analysis with isotopomer ratio analysis of N_2O, and abundance and expression of soil microbial genes associated with N_2O emission attributed to precise understanding of N_2O emission regularity in upland field soil.

The objective of this Chapter is to describe the microorganisms and their pathways responsible for N_2O emission and the environmental factors affecting such N_2O in the upland field soil after the basal and additional application with organic or chemical fertilizer. To achieve this objective, we (1) measured the environmental parameters involved in N_2O emission, (2) determined the contribution of prokaryotic nitrifiers and denitrifiers and fungal denitrifiers to N_2O emission using the isotopomer ratio analysis, and (3) quantified the abundance of microbial genes and transcripts associated with N_2O emission.

4.2Materials and Methods

4.2.1 Study site and field management

The study field is located at the Niigata Agricultural Research Institute (N37°26′, E138°52′, Nagaoka, Niigata, Japan) (Fig. 4-1). The soil is a grey lowland soil (Eutric Fluvisol), which is widespread in Japan. The field experiment was arranged in a randomized block design with three replicate plots per treatment. Each block was 12.5m^2 (2.5 m × 5 m) and comprised three 5 m × 2.5 m plots: one applied with organic fertilizer (OF) and one applied with chemical fertilizer (CF) and one without fertilizer (NF) application as the control. A commercially available granulated organic fertilizer was used as organic fertilizer, which is a mixture of food manufacturing residues such as rice bran, fish meal, rapeseed meal, feather meal, oil palm ash and poultry litter ash (Total N: 6%, P_2O_5: 6%, K_2O: 6%). A commercially available urea, P_2O_5 and K_2O were used as chemical fertilizer. A basal fertilization of organic fertilizer and chemical fertilizer at 28 g N m^{-2} were performed on Jun. 6 in 2011 by incorporating the fertilizer into the plowed layer. Then corn was cultivated in all the plots from Jun. 6 after the fertilization to Aug. 13. Supplemental top-dressings of granular organic fertilizer at 10 g N m^{-2} were performed on Jul. 2. The total precipitation and mean daily air temperature during the cultivation period were 667.5 mm and 25.1 °C, respectively.

4.2.2 Measurements of N_2O flux and soil geochemical parameters during the cultivation period

N_2O flux in the field was measured for eight times during the cultivation period using the chamber method (Jun. 6, 13, 16, 20, 27 and Jul. 2, 13 and 26). Chambers were set at three locations in each plot. Gas samples (500 ml) were taken from the chambers into plastic bags at 0, 15, and 30 min after closure. The N_2O concentration in the samples was measured using a gas

chromatograph equipped with an electron capture detector (GC-ECD; GC-14B, Shimadzu, Kyoto, Japan). The N_2O flux was calculated from the increase in the N_2O concentration of the sample. Soil samples were collected at 5-10 cm depth at three locations in each plot on Jun. 13, 20, 27 and Jul. 13 and 26. The half of soil samples was used to measure the ammonium (NH_4^+), nitrite (NO_2^-) and nitrate (NO_3^-) concentrations in the soils, and the other half was stored at -80°C for molecular analysis. Ten-gram soil samples were extracted with 100 ml of 2 M KCl solution. The NH_4^+, $NO_2^-$and NO_3^- concentrations in the extract were measured colorimetrically (Akiyama and Tsuruta, 2003). The moisture and pH value was determined according to protocols of the International Organization for Standardization.

4.2.3 Analysis of N_2O Isotopomer Ratios

The gas samples in plastic bags for N_2O measurement was also used for isotopomer analysis. All gas samples were transferred immediately into an evacuated glass bottle (1L) equipped with two stopcocks. Ambient air was collected into another glass bottle at 2 m above ground near the experimental field. The N_2O isotopomer ratios were measured using a gas chromatograph-isotope ratio mass spectrometer (GC-IRMS MAT 252, Thermo Fisher Scientific K.K., Yokohama, Japan) system described elsewhere (Toyoda et al., 2005).

Site-specific nitrogen isotope analysis in N_2O was performed using ion detectors, which was modified for mass analysis of fragment N_2O ions (NO^+) containing N atoms in the central positions of N_2O molecules. The oxygen and bulk nitrogen (N^{bulk}) isotope ratios were determined from molecular ions as described previously (Toyoda and Yoshida, 1999). Pure N_2O (purity > 99.999%; Syowa Denko K.K., Japan) was calibrated under international standards and used for isotopomer ratios as a working standard. The ^{15}N site preference (*SP*) was defined as an illustrative

parameter of the intramolecular distribution of ^{15}N.

4.2.4 Abundance and expression of bacterial and archaeal 16S rRNA and fungal 18S rRNA gene during the N_2O emission period

The soil RNA and DNA were extracted using an RNA PowerSoil Total RNA Isolation Kit and DNA Elution Accessory Kit (MO BIO Laboratories, Carlsbad, USA). Total RNA and DNA were extracted from 1.2 g of soil according to the manufacturer's protocol. The concentration of the extracted RNA and DNA were determined using the Qubit 2.0 Fluorometer (Life Technologies). The digestion of the residual DNA in RNA solution was performed using the Ambion TURBO DNA-free Kit (Life Technologies). RNA was transcribed into complementary DNA using the High Capacity cDNA Reverse Transcription Kit (Applied Biosystems, Warrington, UK). The absence of the residual DNA was confirmed in the PCR without reverse transcription. DNA and cDNA of the bacterial and archaeal 16S rRNA and fungal 18S rRNA in soils were determined by the quantitative PCR (qPCR).

The qPCR was conducted by using a StepOne real-time PCR system (Applied Biosystems, Warrington, UK). The quantification of the bacterial 16S rRNA gene, archaeal 16S rRNA gene and fungal 18S rRNA gene were performed with the primers 357F/520R, Arch364aF/A934R and NS1/Fung. The qPCR was performed in 20 ml reactions that included 10 µl of KOD SYBR qPCR Mix (ToYoBo, Osaka, Japan), 0.4 µl of 50×ROX reference dye, 0.2 µM of primers and 10 ng of the environmental DNA. Thermal cycling conditions consisted of an initial denaturing step of 98 °C for 2 min, followed by 40 cycles of 98 °C for 10s, 58°C for 10s (archaeal 16S rRNA gene for 60°C and fungal 18S rRNA gene for 56°C), 68°C for 30s.

The standard curves in the qPCR analyses of bacterial 16S rRNA gene, archaeal 16S rRNA

gene and fungal 18S rRNA gene were generated by using the linearized plasmids, containing the cloned bacterial 16S rRNA gene of *Pseudomonas stutzeri* JCM-5965, archaeal 16S rRNA gene of an environmental clone and fungal 18S rRNA gene of isolats *Fusarium oxysporum* COF-2. The absence of the PCR inhibitors in soil DNA was confirmed by mixing a known amount of standard DNA with environmental DNA in qPCR reaction. The amplification efficiencies, R^2 of the standard curve and Tm value of the melting curve in the qPCR assay for each gene were estimated as shown in Table 4-1.

4.2.5 Abundance and expression of N-cycling functional marker genes during the N_2O emission period

The quantification of the *nirK* and *nirS* were performed with the newly designed primers, and that of the AOA *amoA* and AOB *amoA* were performed with CrenamoA23f/ CrenamoA616r (Nicol et al., 2008) and amoA1F/amoA2R (Rotthauwe et al., 1997). Their qPCR was performed in 20 ml reactions as described above. The annealing temperature of each primer was described in Table 2-1. However, qPCR for *nosZ*-1 and *nosZ*-2 with nosZF/nosZR and nosZ-II-F/nosZ-II-R, respectively, using KOD SYBR qPCR Mix showed no amplification, because of the inhibition of inosine base in the sequences of two pairs of primers on the qPCR system with KOD SYBR qPCR Mix. Instead, we used *Power* SYBR Green PCR Master Mix (Applied Biosystems, Warrington, UK) to avoid this situation. The reaction mixture consisted of the 10μl of *Power* SYBR Green PCR Master Mix (Applied Biosystems, Warrington, UK), 0.5 $\mu g \cdot \mu l^{-1}$ of bovine serum albumin, 1 μM of primers and 10 ng of environmental DNA. Thermal cycling conditions consisted of an initial denaturing step of 95 °C for 10 min, followed by 40 cycles of 95 °C for 15 s, 56°C (52°C for *nosZ*-2) for 40 s, 72 °C for 45 s.

The standard curves in the qPCR analyses of *nirK* and *nirS* gene were performed as described in Chapter 1. The standard curves of the AOA and AOB *amoA*, *nosZ* in Cluster-I and II were generated by using the linearized plasmids, containing the cloned AOA *amoA* gene of an environmental clone, AOB *amoA* gene of *Nitrosospira multiformis* ATCC 25196, *nosZ* in Cluster-I gene of *Azospirillum brasilense* JCM-1224 and *nosZ* in Cluster-II gene of *Curvibacter* sp. UNPF65, respectively. The absence of the PCR inhibitors in soil DNA was confirmed by mixing a known amount of standard DNA with environmental DNA in qPCR reaction. The amplification efficiencies, R^2 of the standard curve and Tm value of the melting curve in the qPCR assay for each gene were estimated as shown in Table 4-1.

4.2.6 Statistical analysis

The statistical analysis was performed for each time point of sampling and for each measured geochemical parameter and gene copy number values. Using a univariate analysis of variance (ANOVA) with the least significant difference *post hoc* test ($P<0.05$), all geochemical and molecular parameter values from the control (field with no fertilizer) were individually compared with the field applied with organic and chemical fertilizers in order to reveal differences between the control and fertilized fields that were statistically significant. These statistical analyses were performed using the R software package (version 3.0, R Development Core Team). Linear dependences between geochemical and molecular variables were described by correlations with Pearson's product-moment correlation coefficient (r) and P-values.

4.3 Result

4.3.1 N_2O emission rate following the rainfall during the cultivation period

Two N_2O flux peaks were observed in plots applied with organic fertilizer (OF) or chemical fertilizer (CF) during crop cultivation, which were occurred after the basal or additional fertilization, respectively (Fig. 4-2b). No obvious N_2O flux peak was observed in non-fertilized plots.

In OF plots, the first peak occurred on 20 Jun. (2 weeks after basal fertilization), and the second peak occurred on 13 Jul. (1 weeks after the additional fertilization) (Fig. 4-2b). The first peak value of 900μg N_2O-N $m^{-2}h^{-1}$ was observed after a moderate rain and related increase in soil water-filled pore space (WFPS) (Fig. 4-2a). The second peak (277μg N_2O-N $m^{-2}h^{-1}$) was observed after a heavy rain. The total amount of emitted N_2O derived from the basal fertilization in OF plots (from 6 Jun. to 2 Jul.) was 213.4 mg N_2O-N m^{-2}, and the amount derived from the additional top-dressings (from 2 Jul. to 26 Jul.) was 87.1 mg N_2O-N m^{-2} (Fig. 3-1).

In CF plots, the first peak occurred on 27 Jun. (3 weeks after basal fertilization), and the second peak occurred on 13 Jul. (1 weeks after the first additional fertilization) (Fig. 4-2b). The first peak was the largest (872 μg N_2O-N $m^{-2}h^{-1}$), which was observed after a rainstorm and the related increase in soil water-filled pore space (WFPS) (Fig. 4-2a). The second peak (149 μg N_2O-N $m^{-2}h^{-1}$) was observed after a heavy rain, the same period with that in OF plots. The total amount of emitted N_2O derived from the basal fertilization in CF plots (from 6 Jun. to 2 Jul.) was 220.8 mg N_2O-N m^{-2}, and the amount derived from the additional top-dressings (from 2 Jul. to 26 Jul.) was 49.2 mg N_2O-N m^{-2} (Fig. 3-1). In addition, according to the linear dependences among N_2O emission rate and physicochemical variables in the CF plots during the whole observation

period, we found that N_2O emission had a positive correlations with the soil WFPS (R^2=0.549, P=0.081) (Table 4-3).

4.3.2 Soil N concentration and pH during the N_2O flux period

After the basal fertilization, the soil NH_4^+ concentrations in OF and CF plots decreased rapidly from 61.0±40.2 mg N kg^{-1} (OF) and 106.4±23.5 mg N kg^{-1} (CF) to the nearly background levels before the additional fertilization (Fig. 4-3). Compared with the ammonia concentrations, soil NO_3^- concentrations increased and reached 56.1±38.6 mg N kg^{-1} (OF) and 100.1±24.5 mg N kg^{-1} (CF) after the basal fertilization, and then decreased and reached the nearly background levels before the first additional fertilization (Fig. 4-3). The pH values in OF plots were close to neutral which is similar with that in non-fertilized field, except that (pH=6.39) on 20 Jun. In contrast, pH values in chemical fertilized field (pH 5.79-6.42) were always lower than that of non-fertilized and organic fertilized field (Fig. 4-3). In addition, according to the linear dependences among N_2O emission rate and physicochemical variables in the OF plots during the whole observation period, we found that N_2O emission had significant positive correlations with the soil NO_3^- concentration (R^2=0.909, P=0.000) and negative correlations with soil pH (R^2= -0.744, P=0.009) (Table 4-2).

4.3.3 Isotope/Isotopomer ratios of N_2O

The production and consumption process of the N_2O was analyzed via isotopomer ratio analysis (bulk nitrogen, $\delta^{15}N_{bulk}$; oxygen isotope ratios, $\delta^{18}O$; intramolecular ^{15}N site preference, *SP*). The observed ranges of $\delta^{15}N_{bulk}$, $\delta^{18}O$, and *SP* of N_2O in three treatments were -45‰ to -4‰, 20‰ to 49‰, and -7‰ to 45‰, respectively (Fig. 4-4).

The N_2O isotopomer ratios in OF and CF plots on Jul. 19 during the second peak of N_2O emission were significantly higher than those on Jun. 20 and Jun. 27 during the first peak of N_2O

emission (Fig. 4-4) ($P<0.05$), which strongly suggested that the production and/or consumption process of N_2O in upland field after the additional fertilization were distinctive among those after the basal fertilization managements. The isotopomer ratio of N_2O during the peak period of N_2O flux in OF (Jun. 20) and CF (Jun. 27) plots were close to the ratio corresponding to denitrification more than that of nitrification (Fig. 4-4). In addition, the *SP* values of N_2O in OF and CF plots after the additional fertilization were always more than 36 (Fig. 4-4).

4.3.4 Abundance and expression of prokaryotic 16S rRNA and fungal 18S rRNA gene

The total gene abundance of prokaryotic (bacteria and archaea) and fungal population were determined by quantification of their 16S rRNA and 18S rRNA gene copy numbers. As shown in Fig. 4-5, the gene copy numbers of bacterial and archaeal 16S rRNA and fungal 18S rRNA in OF, CF and NF plots fluctuated slightly during the cultivated period ($P>0.05$). Except that gene copy numbers of bacterial 16S rRNA in OF and CF plots were always significantly higher ($P<0.05$) than that in NF plot (Fig. 4-5a), both archaeal 16S rRNA and fungal 18S rRNA gene copies in OF and CF were similar with those in NF over the whole observation period (Fig. 4-5c, e).

However, the corresponding transcript abundance of bacterial and archaeal and fungal population by RNA-based quantification shown obvious fluctuant dynamic in OF and CF plot (Fig. 4-5b, d and f). In OF plots, the transcript abundance of bacterial and archaeal 16S rRNA and fungal 18S rRNA were always significantly higher than those in NF over the whole observation period ($P<0.05$) (Fig. 4-5b, d and f). The abundance of bacterial 16S rRNA transcript in OF was 2.0×10^{11} copies g^{-1} soil during the first peak (Jun. 20) of N_2O emission after the basal fertilization, and remained until the end of observation (Fig. 4-5b). The abundance of archaeal 16S rRNA transcript in OF was 1.1×10^{9} copies g^{-1} soil during the first peak of N_2O emission, and then slowly

decreased and reached the nearly background levels (Fig. 4-5d). The abundance of fungal 18S rRNA transcript increased and reached 1.0×10^8 copies g^{-1} soil during the first peak of N_2O emission, and then continued to increased and reached 1.0×10^8 copies g^{-1} soil during the second peak (15 Jul.) of N_2O emission after the additional fertilization (Fig. 4-5f).

In CF plots, the abundance of bacterial 16S rRNA transcript was indistinctly higher than that in NF plots during the first (27 Jun.) and second (15 Jul.) peak of N_2O emission ($P>0.05$) (Fig. 4-5b). The abundance of archaeal 16S rRNA transcript in CF was significantly higher than those in NF plots at the first and second peak of N_2O emission ($P<0.05$) (Fig. 4-5d). The abundance of archaeal 16S rRNA transcript increased and reached 5.5×10^8 copies g^{-1} soil during the first peak of N_2O emission (27 Jun.), and then continued to increased and peaked at 7.2×10^8 copies g^{-1} soil during the second peak of N_2O emission after the additional fertilization (Fig. 4-5d). The abundance of fungal 18S rRNA transcript in CF was significantly higher than those in NF plots at the first and second peak of N_2O emission ($P<0.05$) (Fig. 4-5f). The abundance of fungal 18S rRNA transcript increased and peaked at 1.4×10^8 copies g^{-1} soil during the first peak of N_2O emission (27 Jun.) after the basal fertilization, and then remained the high abundance until the second peak of N_2O emission (1.2×10^8 copies g^{-1} soil, Fig. 4-5f).

4.3.5 Abundance and expression of nitrite reductase gene

The population abundance and functional importance of microorganisms capable of reducing nitrite was determined by quantification of the gene and transcript copy numbers of *nirK* and *nirS* using the newly designed primers.

For 5 different types of *nirK* gene (4 clusters of prokaryotic *nirK* and fungal *nirK*) and 2 different types of *nirS* gene (2 clusters of prokaryotic *nirS*) in both OF and CF plots, except the

gene abundances of prokaryotic *nirK* in Cluster I (Fig. 4-6a) and fungal *nirK* (Fig. 4-7a) in OF plots were significantly higher than those in NF plots during the first and second peak of N_2O emission ($P<0.05$), all *nir* gene abundance in both OF and CF plots were similar ($P>0.05$) or lower than those in NF plot over the whole observation period ($P>0.05$) (Fig. 4-6a, c, e and g; Fig. 4-7a). These results indicated that the population abundance of prokaryotic denitrifiers having Cluster I *nirK* gene and fungal denitrifiers were increased after the basal and additional organic fertilization, and the population abundance of prokaryotic and fungal denitrifiers were not impacted distinctly by the basal or additional chemical fertilization.

For 5 different types of *nirK* transcript (4 clusters of prokaryotic *nirK* and fungal *nirK*) and 2 different types of *nirS* transcript (2 clusters of prokaryotic *nirS*) in OF plots, the transcript abundances of prokaryotic *nirK* in Cluster I (7.1×10^3 copies g^{-1} soil) and II (1.4×10^4 copies g^{-1} soil) and fungal *nirK* (1.1×10^3 copies g^{-1} soil) were significantly higher than those in NF plots during the first peak of N_2O emission ($P<0.05$) (Fig. 4-6b, d; Fig. 4-7b), and the abundance of prokaryotic *nirK* transcript in Cluster II was highest. Only the transcript abundances of fungal *nirK* (1.1×10^3 copies g^{-1} soil) were significantly higher than those in NF plots during the second peak of N_2O emission ($P<0.05$) (Fig. 3-6b). The transcript abundance of *nirK* in Cluster III and IV and *nirS* in Cluster I and II in OF plots were similar ($P>0.05$) or lower than those in NF plot over the whole observation period (Fig. 4-6f, h; Fig. 4-8b, d). According to the linear dependences among N_2O emission rate and soil physicochemical and microbial variables in the OF plots during the whole observation period, we found that N_2O emission had significant correlations with the transcript abundance of prokaryotic *nirK* in Cluster I ($R^2=0.663$, $P=0.026$) and Cluster II ($R^2=0.625$, $P=0.040$) and fungal *nirK* ($R^2=0.590$, $P=0.056$) (Table 4-2).

For 5 different types of *nirK* transcript (4 clusters of prokaryotic *nirK* and fungal *nirK*) and 2 different types of *nirS* transcript (2 clusters of prokaryotic *nirS*) in CF plots, the abundances of prokaryotic *nirK* transcript in Cluster I (2.9×10^3 copies g^{-1} soil), fungal *nirK* transcript (1.4×10^3 copies g^{-1} soil) and prokaryotic *nirS* transcript in Cluster II (9.1×10^3 copies g^{-1} soil) were significantly higher than those in NF plots ($P<0.05$) during the first peak of N_2O emission (Fig. 4-7b; Fig. 4-8d), and only the transcript abundances of fungal *nirK* (1.4×10^3 copies g^{-1} soil) was significantly higher than those in NF plots ($P<0.05$) during the second peak of N_2O emission (Fig. 4-7b). According to the linear dependences among N_2O emission rate and soil physicochemical and microbial variables in the CF plots during the whole observation period, we found that the N_2O emission in CF plots during the whole observation had significant correlations with the abundance of fungal *nirK* transcript ($R^2=0.619$, $P=0.042$) (Table 4-3).

4.3.6 Abundance and expression of ammonium oxidizing gene

The population abundance and functional importance of microorganisms capable of oxidizing ammonium was determined by quantification of the gene and transcript copy numbers of AOA and AOB *amoA*.

The gene abundance of AOA *amoA* and AOB *amoA* in OF and CF plots were always higher than those in NF plots over the whole observation period (Fig. 4-9a, c). Except the gene abundance of AOA *amoA* during the first peak of N_2O emission in OF plots was indistinctly higher that in NF plots ($P>0.05$) (Fig. 4-9a), all of the gene abundances of AOA and AOB *amoA* in OF and CF plots were significantly higher than those in NF plots during the first or second peak of N_2O emission ($P<0.05$) (Fig. 4-9a, c). These results indicated that the population abundance of ammonium oxidizing microorganisms could be stimulated and increased after the organic or chemical

fertilization.

The transcript abundances of AOA *amoA* and AOB *amoA* in OF plots were always higher than those in NF plots, especially the abundances during the first and second peak of N_2O emission were significantly higher than that in NF plots ($P<0.05$) (Fig. 4-9b). The transcript abundance of AOA *amoA* was always one order of magnitude higher than that of AOB *amoA* transcript (Fig. 4-9b). According to the linear dependences among N_2O emission rate and soil physicochemical and microbial variables in the OF plots during the whole observation period, we found that N_2O emission had significant correlations with the abundance of AOA and AOB *amoA* transcript ($R^2=0.641$, $P=0.034$; $R^2=0.869$, $P=0.001$), and soil NO_3^- and NH_4^+ concentration had significant correlations with the abundance of AOB *amoA* transcript ($R^2=0.902$, $P=0.000$; $R^2=0.624$, $P=0.040$) (Table 3-2).

The transcript abundances of AOA *amoA* in CF plots was always significantly higher than that in NF plots ($P<0.05$), but the transcript abundances of AOB *amoA* in CF plots only during the second peak of N_2O emission was significantly higher than that in NF plots ($P<0.05$). According to the linear dependences among N_2O emission rate and soil physicochemical and molecular variables in the CF plots during the whole observation period, we found that N_2O emission had a significant correlation with the transcript abundance of AOA *amoA* ($R^2=0.550$, $P=0.008$), and soil pH value had a significant negative correlation with the transcript abundance of AOA *amoA* ($R^2=-0.782$, $P=0.005$) (Table 3-3).

4.3.7 Abundance and expression of nitrous oxide reductase gene

The population abundance and functional importance of microorganisms capable of reducing nitrous oxide was determined by quantification of the gene and transcript copy numbers of *nosZ* in

Cluster I and II.

The gene abundance of *nosZ* in Cluster I and II in OF and CF plots were always significantly higher than those in NF plots over the whole observation period ($P<0.05$) (Fig. 4-10a, c). The gene abundance of *nosZ* in Cluster I in the OF and CF plots during the first peak of N_2O emission were similar (1.0×10^8 and 9.7×10^7 copies g^{-1} soil, Fig. 4-10a). Then the gene abundance in the OF plots increased and reached 1.4×10^8 copies g^{-1} soil on Jul. 13 during the second peak of N_2O emission, but the gene abundance in the CF plots stay the same level with that during the first peak (Fig. 4-10a). The gene abundance of *nosZ* in Cluster II in CF plots (1.3×10^7 copies g^{-1} soil) was significantly higher than that in OF plots (5.2×10^6 copies g^{-1} soil, $P<0.05$) during the first peak of N_2O emission (Fig. 4-10c). Then the gene abundance of *nosZ* in Cluster II in CF plots decreased and reached 9.8×10^6 copies g^{-1} soil during the second peak of N_2O emission, and that in OF plots increased and reached 9.8×10^6 copies g^{-1} soil (Fig. 4-10c). These results indicated that the population abundance of microorganism having *nosZ* gene in Cluster I and II were affected slightly by the application with organic or chemical fertilizers, except that by the additional application with organic fertilizers.

The transcript abundance of *nosZ* in Cluster I in OF plots (1.7×10^4 copies g^{-1} soil) were significantly higher than those in NF plots during the first peak of N_2O emission, and decreased and reached the nearly background levels during the second peak of N_2O emission (Fig. 4-10b). The abundance of *nosZ* transcript in Cluster I in CF plots was always similar with that in NF plots during the first and second peak of N_2O emission ($P>0.05$) (Fig. 4-10b). The abundance of *nosZ* transcript in Cluster II was not detected over the whole observation period (Fig. 4-10d). According to the linear dependences among all molecular variables in the OF plots during the whole

observation period, we found that the gene abundance of *nosZ* in Cluster I and II had significant correlation with the gene abundance of *nirK* in Cluster I and II and fungal *nirK*, and the transcript abundance of *nosZ* in Cluster I had significant correlation with the transcript abundance of *nirK* in Cluster I and II and fungal *nirK* (Table 3-2).

4.4 Discussion

4.4.1 Potential environmental factors controlling N_2O emission rate

The rapid decreasing of soil NH_4^+ concentrations and increasing of soil NO_3^- concentrations in OF and CF plots after the basal fertilization showed an active conversion process of soil N from NH_4^+ to NO_3^-, which indicated nitrification was a potential source of N_2O emission because N_2O is a by-product during the NH_4 oxidation, the first step of nitrification. Simultaneously, the subsequent decreasing of high concentration of NO_3^- in OF and CF plots indicated denitrification was another source of N_2O emission because N_2O is a mediate or end product during the NO_3^- reduction.

Rainfall as one of the important controlling factor on the N_2O emission in agricultural soil had been focused for a long time, because the substantial N_2O emission was always observed after the rainfall. According to the field observation in this study, we found there were two increasing stages of WFPS (first stage, from 12 Jun. to 22 Jun.; second stage, from 23 Jun. to 30 Jun.) following the respective moderate rainfall and rainstorm before the additional fertilization. The N_2O emission after basal fertilization in OF plots peaked during the first increasing stages of WFPS, and the N_2O emission in CF plots peaked during the second increasing stages of WFPS. Simultaneously, the WFPS after the additional fertilization decreased and was similar with that the first increasing stages as above-mentioned, when the second peak of N_2O emission in OF plots was higher than that in CF plot. These results indicated that the increasing WFPS caused by rainfall was a potential cofactor of N fertilization for the N_2O emission in upland field soil, and N_2O emission induced by chemical fertilizers might need higher level of WFPS than N_2O emission induced by organic fertilizers. Nitrification usually occurred in soil where was dry and at low

WFPS (Abbasi and Adams, 2000), because of the O_2 supply was necessary for nitrification and soil aeration could decrease at high WFPS situation after the rainfall. Thus, we thought that the nitrification was not the main source for N2O emission after the additional chemical fertilization, although Toyoda et al. (2010) affirmed that the contribution of nitrification to N_2O emission was relatively high in upland field soil with gray lowland soil applied of synthetic ammonium fertilizers (urea).

The pH value was known as an important controlling factor for the N_2O emission, because soil hydroxylamine (NH_2OH) and nitrite (NO_2^-), the direct substrate of N_2O production in microbial nitrification and denitrification pathway respectively, can be decomposed into N_2O chemically under the controlling of soil pH value (Bremner 1997). In addition, the nitrous oxide reductase (N_2OR), the only one enzyme known that coverts N_2O to N_2, can be inhibited by low soil pH value (Thomson et al. 2011). In our field, pH value in OF plots was always similar with that in NF plots (Fig. 4-3) ($P>0.05$), but the pH value in CF plots was always lower than that in NF plots. These results indicated that pH level in our cultivated field might be a promoted factor for N_2O emission after the chemical fertilization because of the limitation of N_2O sink.

4.4.2 Isotope/Isotopomer ratios in N_2O

N_2O produced by nitrification (hydroxylamine oxidation) and denitrification (nitrite reduction) was known to have different *SP* values according to some previously reported isotopomeric N_2O signatures produced by nitrifying or denitrifying bacteria and fungi (Toyoda et al., 2005; Sutka et al., 2006; Sutka et al., 2008; Ostrom et al., 2007), especially denitrifying fungi have the highest *SP* values more than 36 (Sutka et al., 2008). In this study, the *SP* values of N_2O in OF and CF plots after the additional fertilization were always more than 36 (Fig. 4-4), which strongly indicated that

the N_2O emission after the additional organic or chemical fertilization might derive dominantly from the fungal denitrification.

The result shown in Fig. 4-4 indicated that the N_2O emission induced by the basal organic or chemical fertilization might be mainly derived from the denitrification more than that from nitrification.

4.4.3 Abundance and expression of prokaryotic 16S rRNA and fungal 18S rRNA gene

The results of abundance of bacterial and archaeal 16S rRNA and fungal 18S rRNA gene indicated that the abundance dynamic of the microbial population in our cultivated fields was stable during the cultivation period after organic or chemical fertilization, and only the abundance of bacterial population had been stimulated to increase obviously by the application of organic or chemical fertilizers. Simultaneously, the results of expression indicated that the bacterial and archaeal and fungal community behaved active metabolic state during the peak period of N_2O emission induced by organic fertilization, and the archaeal and fungal community behaved active metabolic state during the peak period of N_2O emission induced by chemical fertilization.

4.4.4 Abundance and expression of denitrifier's nitrite reducing gene

The prokaryotes having the *nirK* in Cluster I and II and fungi having *nirK* were active during the period of large N_2O emission after the basal organic fertilization, which indicated that diverse denitrifiers were responsible for N_2O emission induced by the basal organic fertilization in the cultivated upland field soil. However, only the fungi having *nirK* were active during the N_2O emission period after the surface additional organic fertilization, which indicated that arbitrary fungal denitrifiers were responsible for the N_2O emission induced by the additional surface organic fertilization in the cultivated upland field soil, an agreed conclusion with that of isotopomer

analysis described previously. Soil oxygen availability might account for the different distributional patterns of denitrifiers in the cultivated upland field soil after the basal and additional fertilization. Oxygen-free condition might be used to activate bacterial denitrification, which is different from fungal denitrification (Shoun et al., 2012). Thus, diverse bacterial denitrifier could be active in the plowed layer incorporated by organic fertilizers. The additional fertilizers were performed on the soil surface contained many oxidative sites, and such an aerobic environment is inhospitable for the bacterial denitrifiers. In contrast to bacterial anaerobic denitrification, fungal denitrification generally requires a minimal oxygen supply as suggested in several studies (Zhou et al., 2002; Shoun et al., 2012), which might lead the active fungal denitrification in the cultivated upland field soil after the additional surface organic fertilization.

The prokaryotic denitrifiers having *nirK* in Cluster I, *nirS* in Cluster II and fungal denitrifiers were active during the large N_2O emission period after the basal chemical fertilization, which indicated that denitrifiers having *nirK* in Cluster I and fungal denitrifiers were not sensitive to the types of basal fertilizers, and prokaryotic denitrifiers having *nirK* in Cluster II and *nirS* in Cluster II were specifically responsible for the basal organic or chemical fertilizers, respectively. Only the fungi having *nirK* were active during the N_2O emission period after the surface additional chemical fertilization, which indicated that fungal denitrifiers may adapt to the conditions specific to cultivated upland field soil after the additional surface chemical fertilization, such as the previous described aerobic conditions and low soil pH level. Rousk et al. discussed that a five-fold decrease in bacterial growth and a five-fold increase in fungal growth from pH 8.3 to pH 4.5, which resulted in an approximately 30-fold increase in soil fungal importance in lower pH (Rousk et al., 2009). It indicated that the low pH level in cultivated field after the chemical fertilization

(Fig. 4-3) might inhibit and decrease the growth of most bacterial denitrifiers and have no effect or even increase the growth of fungal denitrifiers. Simultaneously, in contrast to the other bacterial denitrifiers, methane-oxidizing bacteria might adapt to a wide range of pH, because methane in soils can be oxidized at pH value of 2.5 to 8.0 (Borne et al., 1990; Dunfield et al., 1993; Chisteroserdova et al., 1994; Bender et al., 1995). Thus, the bacterial denitrifiers having *nirS* in Cluster II and fungal denitrifiers could endure the low pH in the CF plots and produce the N_2O via denitrification after the basal fertilization.

In addition, the high transcript abundance of fungal *nirK* in both OF and CF plots after the additional fertilization and their high correlation with N_2O emission reinforced the result of N_2O isotopomer ratios regarding the N_2O emission in OF and CF plots after the additional fertilization might derive from the fungal denitrification. Simultaneously, the active fungal *nirK* over the whole observation period strongly suggested that fungi having *nirK* was always responsible for the N_2O emission in the cultivated field after the N fertilization, independently of the application with organic or chemical fertilizers and basal or additional fertilization measures.

4.4.5 Abundance and expression of nitrifier's ammonium oxidizing gene

The prokaryote having *amoA* gene were active during the N_2O emission period after the basal and additional N fertilization, which indicated that AOA and AOB might be responsible for the partial N_2O emission induced by organic or chemical fertilizers through nitrification in our upland field soil. Simultaneously, the significantly higher abundance of AOA *amoA* gene and transcript than those of AOB in both OF and CF plots strongly indicated that AOA mainly contributed to the partial N_2O emission derived from nitrification process in our upland field soil after the N fertilization. It has been suggested that the population abundance of AOA might be

increased by several soil chemical parameters, e.g. low pH value (Nicol *et al.*, 2008) and plant roots exudates (Herrmann *et al.*, 2008). Soil pH is known to be an important driver for the ammonia oxidizing community. Nicol *et al.* (2008) reported that an increasing abundance of AOA population in an acidic cropland soil. This study supported our observation that soil low pH value induced by chemical fertilization might increase the AOA population abundance. Hallam *et al.* (2006) reported that the AOA might be able to utilize organic material as a carbon source and be capable of mixotrophic or heterotrophic growth, but be disadvantaged when competing for carbon source in soil with high carbon content (Wessén et al., 2010). Thus, Herrmann *et al.* suggested that exudates from plant roots might be easily available by the AOA. This could give an explanation for the dominating of the population size and function importance of AOA in our cultivated upland field soil, and also imply that the dominance of the population size and function importance of the AOB over that of the AOA might occur in our field when an excessive organic carbon was applied.

4.4.6 Abundance and expression of denitrifier's nitrous oxide reducing gene

The microorganisms having *nosZ* in Cluster I were active during the N_2O emission period after the basal organic fertilization in our cultivated field, which indicated that the denitrifiers capable of reducing nitrous oxide might sink the N_2O produced by microorganisms via denitrification and nitrification, and this reduction was induced by the application with organic fertilizers. However, the microorganisms having *nosZ* in Cluster I were not active during the N_2O emission period after the basal chemical fertilization, and same as that after additional organic or chemical fertilization, which indicated that microbial N_2O reduction was inhibited in the upland field after the basal chemical fertilization and the additional organic or chemical fertilization. We

found that the transcript abundances of prokaryotic denitrifiers having *nirK* in Cluster I and II responsible for N_2O emission in our cultivated field as described previously were also decreased in the field after the basal chemical fertilization and additional organic or chemical fertilization, and there were high correlation between the transcript abundance of *nirK* in Cluster I and II and *nosZ* in Cluster I. These strongly indicated that microorganism having the *nosZ* in Cluster I might possess the similar habit of growth and physiological characters with those having *nirK* in Cluster I and II, which could also affected by soil oxygen availability and pH as described previously.

4.5 Conclusion

In upland field soil with corn cultivation, substantial N_2O emission was induced by basal and additional organic or chemical fertilization. However, the microorganisms and their pathways responsible for N_2O emission were distinct because of the different environmental factors induced by weather condition and fertilization management with different fertilizer types and application practices. From the results obtained in this chapter, the following N_2O emission regularity in upland field soil is proposed, (i) after the basal organic fertilization, N_2O was produced rapidly following a sharp increasing of WFPS and induced mainly by denitrification more than nitrification. In such denitrification, the prokaryotes having the *nirK* in Cluster I and II and the fungi having the *nirK* as the N_2O emitters and those having the *nosZ*-I gene as the N_2O reducers played active role. For the N_2O induced by nitrification, the archaea having *amoA* contributed more than bacteria having *amoA*. (ii) After the basal chemical fertilization, N_2O was also produced mainly by denitrification more than nitrification following a sharp increasing of WFPS, but emitted more slowly than that after the basal organic fertilization. The prokaryotes having the *nirK* in Cluster I and *nirS* in Cluster II and fungi having the *nirK*, as the N_2O emitters, played active role in denitrification and no microorganism as the N_2O reducers because of the low soil pH. Archaea having the *amoA* as the acidophilic N_2O emitters contributed to the N_2O induced by nitrification process. (iii) After the surface additional organic or chemical fertilization, N_2O was produced more slightly than that after the basal fertilization and induced mainly by denitrification. Because of the O_2 availability, fungal denitrifiers play a dominant active role in N_2O emission and prokaryotes were inactive as the N_2O emitters and reducers.

Table 4-1. The primers and optimal qPCR conditions for bacterial *nosZ* and *amoA* and the bacterial and archaeal 16S rRNA and fungal 18S rRNA gene .

Primers	Target	Real-time QPCR		
		Annealing temperature (°C)	Tm (°C)	R^2/Efficiency (%)
nosZF/ nosZR	*nosZ*-1	56	88.4	0.997/81
nosZ-II-F/ nosZ-II-R	*nosZ*-2	50	87.4	0.998/79
CrenamoA23f/ CrenamoA616r	AOA amoA	56	82.3	0.991/98
amoA1F/amoA2R	AOB amoA	60	87.8	0.992/86
NS1/Fung	18S rRNA	56	82.3	0.994/85
Arch364aF/A934R	16S rRNA	61	87.3	0.997/91
357F/520R	16S rRNA	58	83.2	0.999/91

Table 4-2. Linear dependences among N_2O emission rate and physicochemical and microbial variables in upland field soil after the organic fertilization

Factor	N2O	daily temperature	daily precipitation	WFPS	pH	NO3-N	NH4-N	NO2-N	16S gene	16S trans	nirK C-I gene	nirK C-I trans	nirK C-II gene	nirK C-II trans	nirK C-III gene	nirK C-III trans	nirK C-IV gene	nirK C-IV trans	nirS C-I gene	nirS C-I trans	nirS C-II gene	nirS C-II trans	18S gene	18S transcript	fungal gene	fungal trans	nosZ-1 gene	nosZ-1 trans	nosZ-2 gene	Arc 16S gene	Arc 16S transcript	AOA amoA gene	AOA amoA trans	AOB amoA gene	AOB amoA trans
N2O		0.869	0.391	0.954	**0.009**	**0.000**	0.451	0.820	0.125	0.077	0.053	**0.026**	0.472	**0.040**	0.545	0.222	0.563	0.133	0.772	0.257	0.118	0.532	0.595	0.159	0.002	**0.056**	0.124	**0.039**	0.239	0.554	0.005	0.194	**0.034**	0.345	**0.001**
daily temperature	-0.057		0.358	0.996	0.940	0.682	0.350	0.006	0.957	0.852	0.612	0.400	0.835	0.265	0.092	0.888	0.420	0.487	0.787	0.171	0.055	0.410	0.081	0.524	0.692	0.619	0.692	0.545	0.497	0.493	0.744	0.866	0.883	0.191	0.866
daily precipitation	-0.288	0.307		0.215	0.759	0.818	0.457	0.934	0.997	0.997	0.714	0.757	0.733	0.754	0.402	0.521	0.334	0.797	0.370	0.444	0.410	0.829	0.786	0.712	0.754	0.647	0.997	0.173	0.616	0.223	0.401	0.174	0.786	0.161	0.938
WFPS	0.020	0.002	-0.407		0.526	0.703	0.206	0.198	0.778	0.775	0.775	0.806	0.189	0.774	0.195	0.828	0.687	0.462	0.898	0.504	0.449	0.687	0.700	0.943	0.955	0.819	0.669	0.399	0.619	0.523	0.420	0.692	0.502	0.952	0.857
pH	**-0.744**	-0.026	-0.105	0.215		0.001	0.546	0.562	0.473	0.325	0.125	0.370	0.269	0.505	0.691	0.581	0.556	0.207	0.423	0.659	0.345	0.889	0.749	0.319	0.093	0.158	0.369	0.716	0.418	0.644	0.183	0.393	0.259	0.271	0.027
NO3-N	**0.909**	-0.140	-0.079	-0.130	-0.865		0.132	0.365	0.132	0.090	0.034	0.022	0.194	0.042	0.491	0.254	0.735	0.250	0.864	0.390	0.087	0.547	0.422	0.144	0.012	0.054	0.147	0.276	0.185	0.650	0.029	0.369	0.061	0.255	0.000
NH4-N	0.254	-0.312	0.251	-0.414	-0.205	0.484		0.101	0.019	0.083	0.062	0.003	0.008	0.005	0.103	0.065	0.195	0.365	0.276	0.106	0.025	0.190	0.002	0.093	0.179	0.082	0.059	0.705	0.034	0.190	0.387	0.666	0.201	0.192	0.040
NO2-N	0.078	-0.766	-0.028	-0.420	-0.197	0.303	0.520		0.678	0.798	0.633	0.369	0.187	0.320	0.333	0.868	0.391	0.773	0.960	0.605	0.113	0.120	0.056	0.906	0.915	0.679	0.737	0.952	0.764	0.919	0.791	0.723	0.890	0.726	0.535
16S gene	0.492	0.018	-0.001	-0.097	-0.242	0.483	0.688	0.142		0.000	0.001	0.001	0.005	0.003	0.061	0.000	0.083	0.874	0.099	0.073	0.038	0.010	0.038	0.000	0.001	0.002	0.000	0.028	0.000	0.089	0.006	0.053	0.000	0.006	0.005
16S trans	0.555	0.064	0.002	0.098	-0.328	0.534	0.545	0.088	0.954		0.000	0.003	0.024	0.011	0.193	0.004	0.085	0.645	0.167	0.091	0.109	0.008	0.114	0.000	0.000	0.001	0.000	0.017	0.000	0.156	0.001	0.072	0.000	0.001	0.002
nirK C-I gene	0.596	0.172	0.125	-0.098	-0.492	0.640	0.579	0.163	0.873	0.903		0.015	0.008	0.044	0.154	0.054	0.137	0.305	0.459	0.447	0.286	0.049	0.117	0.000	0.000	0.000	0.000	0.087	0.000	0.702	0.011	0.285	0.001	0.001	0.002
nirK C-I trans	**0.663**	-0.283	-0.106	-0.084	-0.300	0.677	0.798	0.301	0.856	0.796	0.709		0.060	0.000	0.158	0.008	0.067	0.936	0.283	0.003	0.004	0.076	0.008	0.020	0.004	0.025	0.011	0.034	0.017	0.040	0.007	0.171	0.006	0.133	0.000
nirK C-II gene	0.243	-0.071	0.116	-0.428	-0.365	0.424	0.748	0.430	0.782	0.669	0.752	0.582		0.120	0.103	0.013	0.808	0.435	0.148	0.749	0.062	0.048	0.059	0.010	0.071	0.013	0.002	0.514	0.002	0.443	0.272	0.135	0.090	0.044	0.082
nirK C-II trans	**0.625**	-0.368	-0.107	-0.098	-0.226	0.619	0.778	0.331	0.798	0.728	0.614	0.987	0.497		0.230	0.017	0.063	0.876	0.367	0.001	0.003	0.081	0.006	0.053	0.011	0.063	0.030	0.031	0.048	0.037	0.012	0.227	0.017	0.238	0.002
nirK C-III gene	0.205	0.532	0.281	-0.423	-0.136	0.233	0.518	-0.323	0.581	0.424	0.460	0.456	0.518	0.395		0.052	0.126	0.364	0.178	0.668	0.447	0.862	0.644	0.125	0.157	0.201	0.076	0.940	0.045	0.257	0.704	0.332	0.371	0.099	0.203
nirK C-III trans	-0.400	0.048	0.217	0.074	0.187	-0.376	-0.574	-0.057	-0.876	-0.787	-0.595	-0.748	-0.718	-0.699	-0.599		0.421	0.210	0.017	0.077	0.006	0.041	0.158	0.012	0.016	0.105	0.006	0.075	0.012	0.004	0.031	0.001	0.013	0.104	0.041
nirK C-IV gene	-0.197	-0.271	-0.322	-0.138	-0.200	-0.116	-0.423	0.288	-0.545	-0.542	-0.478	-0.570	-0.083	-0.577	-0.490	0.271		0.554	0.681	0.059	0.930	0.564	0.196	0.097	0.147	0.115	0.152	0.257	0.092	0.401	0.241	0.796	0.109	0.073	0.168
nirK C-IV trans	0.482	0.235	0.088	0.248	-0.413	0.379	-0.303	-0.098	-0.055	0.157	0.341	-0.027	-0.263	-0.053	-0.304	0.410	-0.201		0.062	0.641	0.223	0.921	0.578	0.593	0.306	0.226	0.791	0.402	0.827	0.061	0.281	0.334	0.391	0.421	0.360
nirS C-I gene	-0.099	0.092	-0.300	0.044	0.270	-0.059	0.361	0.017	0.523	0.448	0.250	0.356	0.467	0.302	0.438	-0.699	-0.140	-0.579		0.259	0.288	0.140	0.370	0.194	0.426	0.681	0.220	0.748	0.153	0.009	0.488	0.161	0.255	0.483	0.603
nirS C-I trans	0.374	-0.444	-0.258	0.226	0.150	0.289	0.514	0.176	0.560	0.533	0.256	0.801	0.110	0.858	0.146	-0.554	-0.584	-0.159	0.373		0.029	0.158	0.037	0.310	0.154	0.529	0.322	0.044	0.381	0.005	0.043	0.360	0.080	0.715	0.088
nirS C-II gene	0.499	-0.591	-0.277	-0.255	-0.315	0.539	0.667	0.505	0.629	0.511	0.354	0.785	0.580	0.803	0.257	-0.769	-0.030	-0.400	0.352	0.654		0.087	0.050	0.272	0.107	0.391	0.137	0.115	0.249	0.021	0.079	0.030	0.148	0.744	0.046
nirS C-II trans	-0.212	0.277	0.074	0.137	0.048	-0.204	-0.427	-0.497	-0.737	-0.747	-0.605	-0.556	-0.606	-0.548	-0.060	0.622	0.196	0.034	-0.474	-0.456	-0.539		0.088	0.018	0.048	0.078	0.020	0.050	0.025	0.311	0.028	0.224	0.014	0.115	0.152
18S gene	0.180	-0.547	-0.093	-0.132	0.110	0.270	0.815	0.590	0.630	0.504	0.500	0.750	0.585	0.765	0.157	-0.457	-0.422	-0.189	0.300	0.632	0.602	-0.538		0.161	0.270	0.105	0.068	0.205	0.085	0.238	0.288	0.750	0.204	0.510	0.155
18S transcript	0.456	0.216	0.126	0.025	-0.332	0.471	0.530	0.040	0.930	0.968	0.948	0.686	0.738	0.595	0.491	-0.721	-0.525	0.182	0.424	0.337	0.363	-0.693	0.454		0.001	0.000	0.000	0.065	0.000	0.365	0.007	0.131	0.000	0.000	0.008
nirKF gene	0.811	0.135	-0.107	-0.020	-0.531	0.726	0.437	0.037	0.869	0.912	0.889	0.794	0.563	0.728	0.457	-0.704	-0.467	0.340	0.268	0.460	0.513	-0.607	0.365	0.866		0.001	0.001	0.008	0.002	0.300	0.000	0.078	0.000	0.011	0.000
nirKF trans	**0.590**	0.169	0.156	-0.078	-0.457	0.594	0.547	0.141	0.832	0.860	0.987	0.667	0.715	0.578	0.418	-0.515	-0.502	0.398	0.140	0.213	0.288	-0.553	0.515	0.920	0.847		0.000	0.082	0.000	0.915	0.021	0.378	0.002	0.001	0.005
nosZ-1 gene	0.493	0.135	0.001	-0.146	-0.301	0.468	0.585	0.115	0.951	0.908	0.935	0.731	0.817	0.652	0.555	-0.766	-0.462	0.091	0.403	0.330	0.478	-0.686	0.568	0.942	0.865	0.922		0.034	0.000	0.370	0.016	0.084	0.001	0.003	0.012
nosZ-1 trans	0.628	-0.205	-0.443	0.283	-0.124	0.360	0.129	0.021	0.657	0.698	0.539	0.640	0.221	0.649	0.026	-0.557	-0.374	0.281	0.110	0.616	0.503	-0.602	0.414	0.573	0.749	0.547	0.639		0.135	0.243	0.001	0.058	0.007	0.313	0.062
nosZ-2 gene	0.388	0.229	0.171	-0.169	-0.272	0.432	0.641	0.103	0.937	0.908	0.945	0.696	0.827	0.607	0.613	-0.722	-0.533	0.075	0.462	0.294	0.380	-0.668	0.543	0.967	0.816	0.921	0.968	0.481		0.410	0.040	0.204	0.002	0.000	0.015
Arc 16S gene	0.201	-0.232	-0.400	0.216	0.157	0.155	0.427	-0.035	0.536	0.458	0.131	0.625	0.259	0.632	0.374	-0.785	-0.282	-0.581	0.741	0.779	0.680	-0.337	0.388	0.303	0.344	0.037	0.300	0.385	0.277		0.171	0.036	0.181	0.811	0.261
Arc 16S transcript	0.782	-0.112	-0.282	0.271	-0.434	0.654	0.290	0.091	0.763	0.873	0.727	0.755	0.363	0.721	0.130	-0.648	-0.386	0.357	0.234	0.617	0.550	-0.656	0.352	0.754	0.910	0.682	0.701	0.865	0.625	0.444		0.056	0.000	0.067	0.001
AOA amoA gene	0.424	-0.058	-0.442	0.135	-0.287	0.301	0.147	-0.121	0.597	0.561	0.354	0.445	0.480	0.397	0.324	-0.843	0.089	-0.322	0.454	0.306	0.652	-0.399	0.109	0.485	0.553	0.296	0.543	0.586	0.416	0.636	0.590		0.077	0.390	0.204
AOA amoA trans	**0.641**	0.050	-0.093	0.227	-0.373	0.581	0.418	0.047	0.883	0.978	0.863	0.763	0.534	0.699	0.300	-0.716	-0.510	0.288	0.376	0.550	0.467	-0.710	0.415	0.920	0.927	0.818	0.835	0.759	0.819	0.436	0.943	0.554		0.004	0.001
AOB amoA gene	0.316	0.426	0.454	-0.021	-0.364	0.376	0.426	-0.120	0.768	0.838	0.866	0.482	0.615	0.389	0.523	-0.516	-0.561	0.271	0.237	0.125	0.112	-0.503	0.223	0.922	0.726	0.852	0.797	0.336	0.881	0.082	0.570	0.288	0.783		0.040
AOB amoA trans	**0.869**	-0.058	-0.027	-0.062	-0.661	0.902	0.624	0.210	0.781	0.819	0.828	0.881	0.547	0.825	0.416	-0.621	-0.447	0.306	0.177	0.538	0.612	-0.462	0.460	0.747	0.913	0.778	0.725	0.580	0.706	0.371	0.838	0.415	0.835	0.624	

Table 4-3. Linear dependences among N_2O emission rate and physicochemical and microbial variables in upland field soil after the chemical fertilization

Factor	N2O	daily temperature	daily precipitation	WFPS	pH	NO3-N	NH4-N	NO2-N	16S gene	16S trans	*nirK* C-I gene	nirK C-I trans	nirK C-II gene	nirK C-II trans	nirK C-III gene	nirK C-III trans	nirK C-IV gene	nirK C-IV trans	nirS C-I gene	nirS C-I trans	nirS C-II gene	nirS C-II trans	18S gene	18S transcript	nirK fungal gene	nirK fungal trans	nosZ-1 gene	nosZ-1 trans	nosZ-2 gene	Arc 16S gene	Arc transcript	16SAOA amoA gene	AOA amoA trans	AOB amoA gene	AOB amoA trans
N2O		0.497	0.320	**0.081**	0.352	0.401	0.987	0.819	0.027	0.063	0.800	0.506	0.462	0.194	0.414	0.123	0.324	0.228	0.490	0.462	0.247	0.123	0.971	0.004	0.262	**0.042**	0.046	0.854	0.067	0.016	0.053	0.020	**0.080**	0.308	0.824
daily temperature	-0.230		0.358	0.996	0.758	0.410	0.131	0.003	0.952	0.308	0.689	0.556	0.282	0.330	0.527	0.967	0.548	0.199	0.425	0.548	0.923	0.785	0.044	0.818	0.616	0.754	0.456	0.043	0.964	0.885	0.887	0.686	0.708	0.422	0.736
daily precipitation	-0.331	0.307		0.215	0.508	0.761	0.733	0.301	0.678	0.363	0.259	0.949	0.061	0.982	0.680	0.671	0.969	0.721	0.711	0.759	0.916	0.674	0.260	0.356	0.743	0.909	0.628	0.460	0.784	0.116	0.471	0.840	0.679	0.170	0.553
WFPS	**0.549**	0.002	-0.407		0.618	0.523	0.190	0.281	0.809	0.989	0.837	0.718	0.982	0.167	0.577	0.762	0.453	0.893	0.976	0.951	0.788	0.023	0.259	0.162	0.373	0.334	0.916	0.824	0.911	0.311	0.526	0.728	0.674	0.876	0.283
pH	-0.311	-0.105	-0.224	0.170		0.023	0.451	0.587	0.003	0.030	0.006	0.076	0.938	0.503	0.059	0.001	0.608	0.329	0.472	0.277	0.006	0.113	0.199	0.225	0.002	0.114	0.012	0.453	0.000	0.305	0.036	0.002	**0.005**	0.002	0.195
NO3-N	0.282	-0.277	-0.104	-0.216	-0.675		0.077	0.545	0.080	0.001	0.546	0.199	0.865	0.969	0.432	0.038	0.176	0.306	0.224	0.082	0.029	0.110	0.391	0.922	0.013	0.841	0.121	0.906	0.025	0.538	0.405	0.064	0.199	0.445	0.095
NH4-N	-0.006	-0.485	-0.117	-0.427	-0.254	0.555		0.278	0.252	0.046	0.891	0.006	0.934	0.004	0.080	0.113	0.656	0.151	0.636	0.007	0.032	0.321	0.995	0.857	0.311	0.999	0.086	0.243	0.249	0.417	0.740	0.322	0.541	0.576	0.001
NO2-N	-0.079	-0.808	-0.344	-0.357	0.185	0.205	0.359		0.682	0.561	0.583	0.985	0.145	0.337	0.237	0.720	0.326	0.889	0.869	0.971	0.661	0.436	0.084	0.489	0.803	0.413	0.905	0.072	0.717	0.428	0.780	0.653	0.546	0.150	0.747
16S gene	0.659	-0.021	-0.142	0.083	-0.810	0.550	0.378	-0.140		0.002	0.071	0.011	0.658	0.809	0.010	0.000	0.343	0.343	0.916	0.065	0.001	0.586	0.477	0.004	0.004	0.005	0.000	0.918	0.000	0.008	0.000	0.000	0.000	0.004	0.038
16S trans	0.577	-0.339	-0.304	-0.005	-0.651	0.854	0.611	0.197	0.817		0.471	0.031	0.810	0.774	0.155	0.005	0.100	0.387	0.688	0.011	0.002	0.352	0.741	0.141	0.008	0.297	0.004	0.453	0.001	0.086	0.030	0.015	0.014	0.205	0.013
nirK C-I gene	0.087	0.136	0.373	-0.071	-0.768	0.205	0.047	-0.187	0.564	0.243		0.079	0.551	0.681	0.165	0.128	0.901	0.512	0.584	0.428	0.058	0.254	0.988	0.345	0.083	0.035	0.058	0.734	0.049	0.845	0.097	0.100	0.036	0.003	0.657
nirK C-I trans	0.225	-0.200	-0.022	-0.123	-0.555	0.420	0.770	-0.006	0.726	0.648	0.552		0.638	0.084	0.003	0.014	0.458	0.198	0.820	0.001	0.000	0.445	0.900	0.244	0.083	0.067	0.001	0.404	0.015	0.125	0.079	0.058	0.028	0.027	0.003
nirK C-II gene	0.248	-0.356	-0.580	-0.008	0.027	-0.058	-0.029	0.470	0.151	0.083	-0.202	-0.160		0.636	0.797	0.464	0.040	0.913	0.630	0.204	0.468	0.887	0.762	0.330	0.662	0.672	0.576	0.958	0.858	0.251	0.439	0.461	0.737	0.514	0.951
nirK C-II trans	-0.424	-0.325	-0.008	-0.449	0.227	0.014	0.791	0.320	-0.083	0.098	-0.140	0.543	-0.161		0.358	0.980	0.995	0.796	0.564	0.080	0.438	0.488	0.531	0.369	0.744	0.683	0.723	0.078	0.716	0.868	0.621	0.508	0.674	0.827	0.035
nirK C-III gene	0.274	0.214	0.141	-0.190	-0.585	0.264	0.550	-0.389	0.737	0.460	0.450	0.804	-0.088	0.308		0.003	0.635	0.146	0.821	0.062	0.003	0.766	0.156	0.134	0.060	0.055	0.008	0.469	0.020	0.021	0.109	0.022	0.034	0.004	0.016
nirK C-III trans	-0.493	0.014	0.145	0.104	0.834	-0.628	-0.505	0.123	-0.931	-0.778	-0.488	-0.713	-0.247	-0.009	-0.802		0.673	0.181	0.684	0.118	0.002	0.375	0.207	0.049	0.008	0.058	0.000	0.578	0.000	0.008	0.011	0.000	0.001	0.013	0.017
nirK C-IV gene	-0.329	-0.204	-0.014	-0.253	0.174	-0.440	-0.152	0.327	-0.317	-0.521	0.043	-0.250	0.624	-0.002	-0.162	0.144		0.632	0.865	0.030	0.122	0.954	0.608	0.535	0.148	0.832	0.621	0.565	0.248	0.641	0.443	0.805	0.325	0.550	0.324
nirK C-IV trans	-0.396	0.420	-0.122	0.046	0.325	-0.340	-0.463	-0.048	-0.317	-0.290	-0.222	-0.420	-0.037	-0.089	-0.468	0.435	-0.163		0.003	0.452	0.259	0.407	0.786	0.888	0.551	0.765	0.145	0.414	0.331	0.313	0.845	0.041	0.884	0.325	0.738
nirS C-I gene	0.234	-0.268	0.126	-0.010	-0.243	0.399	0.161	0.057	0.036	0.137	0.186	0.078	-0.164	-0.196	0.077	-0.139	0.058	-0.809		0.813	0.666	0.630	0.864	0.459	0.545	0.494	0.725	0.200	0.695	0.990	0.329	0.283	0.603	0.871	0.518
nirS C-I trans	0.248	-0.204	-0.105	-0.021	-0.360	0.547	0.758	0.013	0.573	0.729	0.267	0.858	-0.415	0.549	0.578	-0.499	-0.650	-0.253	0.081		0.001	0.533	0.815	0.476	0.082	0.367	0.034	0.190	0.052	0.277	0.225	0.280	0.114	0.211	0.004
nirS C-II gene	-0.381	0.033	-0.036	0.092	0.765	-0.653	-0.646	0.149	-0.865	-0.817	-0.586	-0.908	0.245	-0.261	-0.797	0.829	0.495	0.373	-0.147	-0.858		0.307	0.534	0.149	0.003	0.074	0.001	0.770	0.000	0.093	0.028	0.013	0.003	0.006	0.004
nirS C-II trans	0.493	-0.093	-0.144	0.673	0.506	-0.509	-0.331	-0.262	-0.185	-0.311	-0.377	-0.257	0.049	-0.234	-0.102	0.297	0.020	-0.279	0.164	-0.211	0.339		0.499	0.434	0.115	0.721	0.686	0.735	0.401	0.413	0.615	0.930	0.427	0.611	0.144
18S gene	0.013	-0.616	-0.372	0.373	0.420	-0.288	-0.002	0.544	-0.240	-0.113	0.005	0.043	0.104	0.212	-0.459	0.413	0.174	0.093	-0.059	0.080	0.211	0.229		0.935	0.160	0.838	0.934	0.014	0.424	0.478	0.915	0.355	0.612	0.252	0.544
18S transcript	0.793	0.079	-0.309	0.453	-0.398	0.033	-0.062	-0.234	0.791	0.474	0.315	0.383	0.325	-0.300	0.481	-0.604	-0.210	-0.048	-0.250	0.241	-0.466	0.264	-0.028		0.215	0.000	0.013	0.974	0.018	0.004	0.000	0.034	0.002	0.071	0.408
nirKF gene	0.371	0.171	0.112	-0.299	-0.824	0.715	0.337	-0.085	0.788	0.747	0.545	0.545	-0.149	-0.112	0.583	-0.752	-0.467	-0.202	0.205	0.546	-0.804	-0.502	-0.455	0.406		0.230	0.023	0.545	0.001	0.262	0.045	0.035	0.009	0.027	0.076
nirKF trans	**0.619**	0.107	-0.039	0.322	-0.504	-0.069	0.001	-0.275	0.773	0.346	0.638	0.570	0.145	-0.140	0.591	-0.587	-0.073	-0.102	-0.231	0.302	-0.559	0.122	0.070	0.892	0.395		0.006	0.908	0.021	0.044	0.000	0.044	0.001	0.006	0.383
nosZ-1 gene	0.611	-0.251	-0.165	0.036	-0.725	0.495	0.541	0.041	0.947	0.788	0.586	0.846	0.190	0.121	0.750	-0.890	-0.168	-0.470	0.120	0.640	-0.867	-0.138	-0.028	0.716	0.675	0.767		0.738	0.000	0.015	0.002	0.001	0.001	0.010	0.026
nosZ-1 trans	-0.063	-0.617	-0.249	0.076	0.253	0.040	0.385	0.563	-0.035	0.253	-0.116	0.280	-0.018	0.553	-0.244	0.189	-0.195	0.274	-0.419	0.427	-0.100	-0.115	0.710	-0.011	-0.205	0.040	0.114		0.859	0.555	0.676	0.443	0.942	0.508	0.348
nosZ-2 gene	0.562	-0.015	-0.094	0.038	-0.875	0.668	0.380	-0.124	0.982	0.857	0.604	0.706	0.061	-0.124	0.686	-0.920	-0.381	-0.324	0.134	0.598	-0.891	-0.282	-0.269	0.695	0.863	0.682	0.914	-0.061		0.029	0.001	0.000	0.000	0.006	0.047
Arc 16S gene	0.704	0.049	-0.501	0.337	-0.341	0.209	0.273	-0.267	0.746	0.541	0.067	0.491	0.379	-0.057	0.683	-0.752	-0.159	-0.336	-0.005	0.360	-0.531	0.275	-0.239	0.792	0.370	0.616	0.706	-0.200	0.654		0.031	0.014	0.029	0.203	0.119
Arc 16S transcript	0.596	0.049	-0.244	0.215	-0.636	0.280	0.113	-0.096	0.893	0.651	0.525	0.551	0.261	-0.169	0.510	-0.730	-0.259	0.067	-0.325	0.399	-0.657	-0.171	-0.037	0.896	0.613	0.873	0.814	0.142	0.842	0.649		0.026	0.000	0.027	0.120
AOA amoA gene	0.685	-0.138	-0.069	0.119	-0.820	0.575	0.330	-0.153	0.888	0.706	0.522	0.586	0.249	-0.224	0.677	-0.915	-0.084	-0.623	0.356	0.358	-0.720	-0.030	-0.309	0.640	0.638	0.616	0.865	-0.258	0.882	0.715	0.665		0.007	0.011	0.211
AOA amoA trans	**0.550**	0.128	-0.141	0.143	**-0.782**	0.420	0.207	-0.205	0.952	0.714	0.634	0.657	0.115	-0.144	0.640	-0.833	-0.328	-0.050	-0.177	0.504	-0.797	-0.267	-0.172	0.821	0.742	0.840	0.864	0.025	0.931	0.656	0.965	0.756		0.005	0.067
AOB amoA gene	0.339	0.270	0.445	-0.054	-0.812	0.257	0.190	-0.465	0.782	0.415	0.795	0.662	-0.221	-0.075	0.790	-0.718	-0.203	-0.328	0.056	0.409	-0.763	-0.173	-0.378	0.564	0.659	0.765	0.735	-0.224	0.771	0.417	0.662	0.726	0.777		0.229
AOB amoA trans	0.076	-0.115	-0.201	-0.356	-0.423	0.528	0.840	0.110	0.630	0.715	0.151	0.810	0.021	0.638	0.703	-0.697	-0.329	-0.114	-0.219	0.783	-0.782	-0.471	-0.206	0.278	0.555	0.292	0.664	0.313	0.608	0.498	0.497	0.410	0.570	0.395	

(a)

(b)

Fig. 4-1 the upland field cultivated with corn in 2011. (a) the chamber positions in field sited before the sowing. (b) the corn growth in the different treatment plots

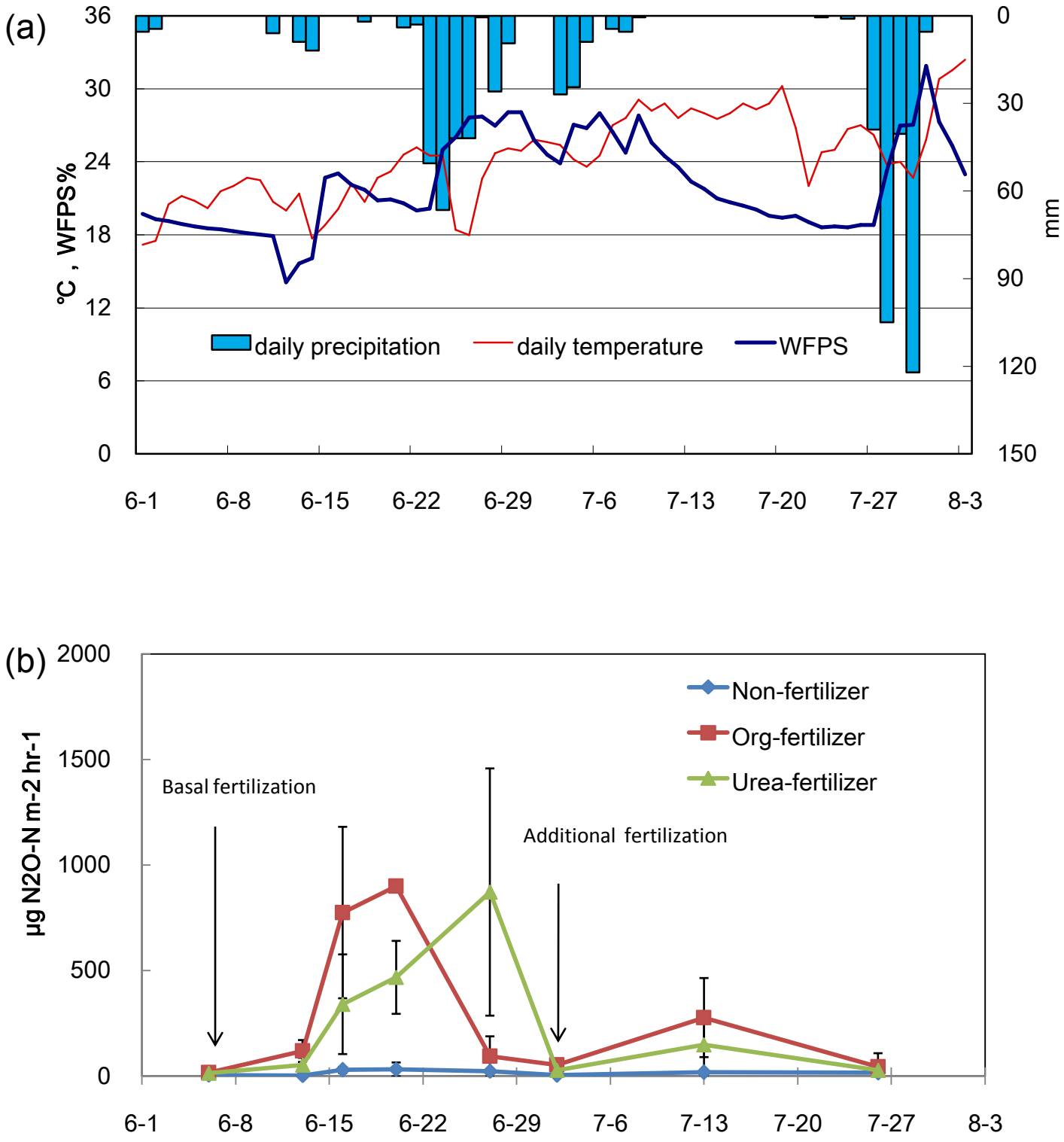

Fig. 4-2 Soil water-filled pore space (WFPS), daily precipitation and daily temperature and N_2O fluxes in an upland field during the cultivation period. The error bars represent the standard deviations (n=3). The arrows indicate the dates of basal and additional fertilizer applications

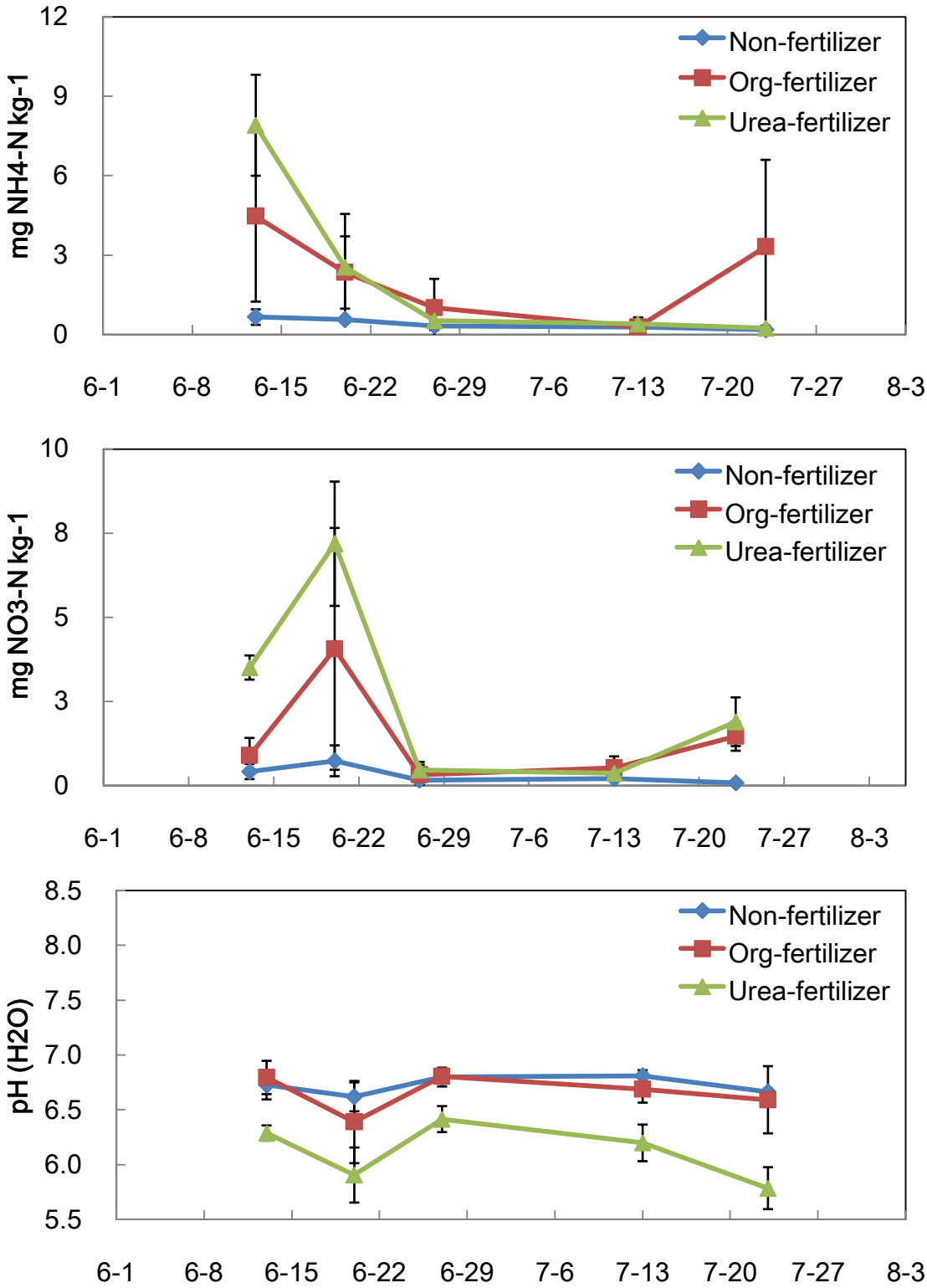

Fig. 4-3 Soil NH4+-N and NO3−-N concentrations and soil pH in upland field during the cultivation period. The error bars represent the standard deviations (n=3).

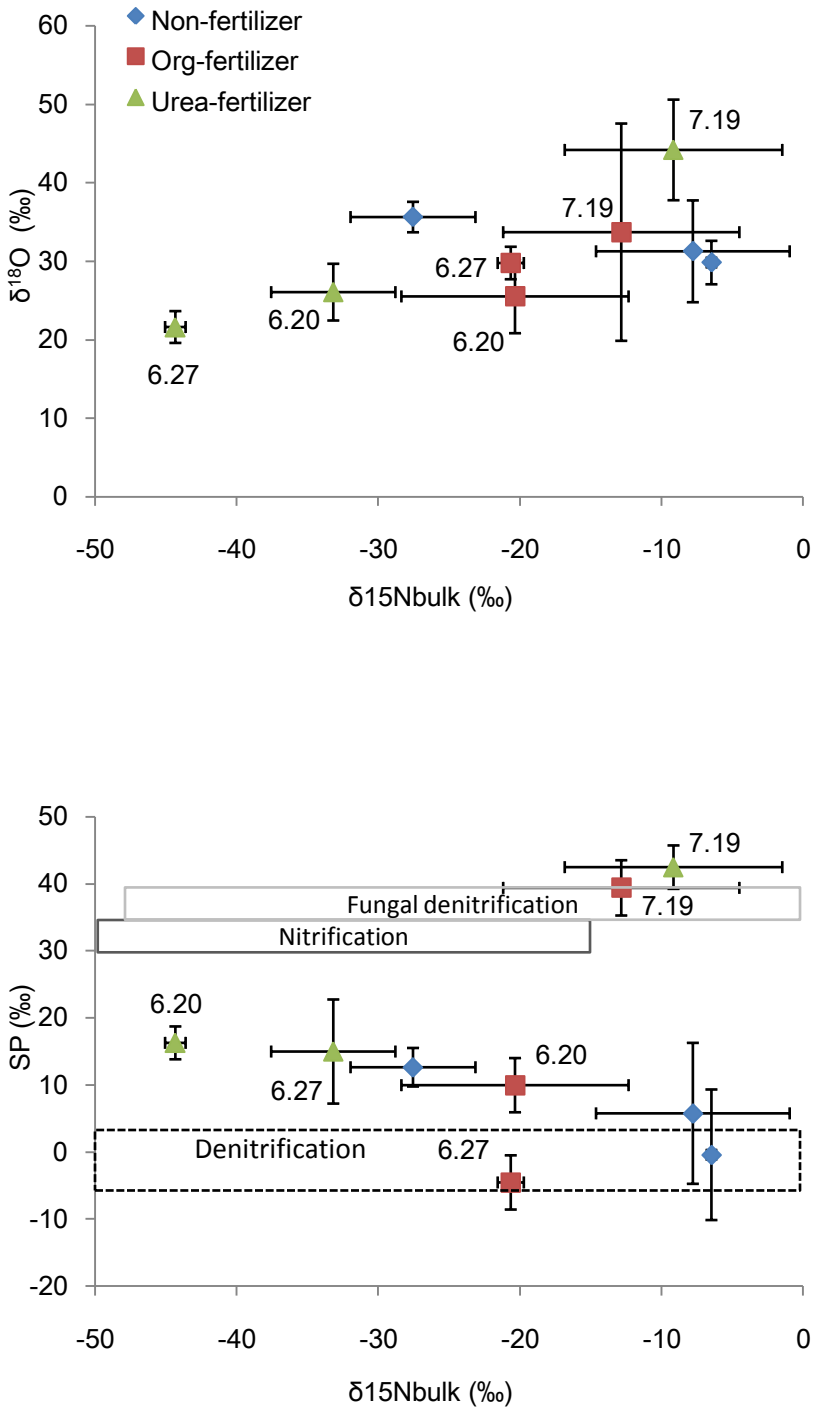

Fig. 4-4 Isotopomer ratio of N2O induced by basal and additional N fertilization. Non-fertilizer, applied with no fertilizer. Org-fertilizer, applied with granular organic fertilizer. Urea-fertilizer applied chemical urea fertilizer.

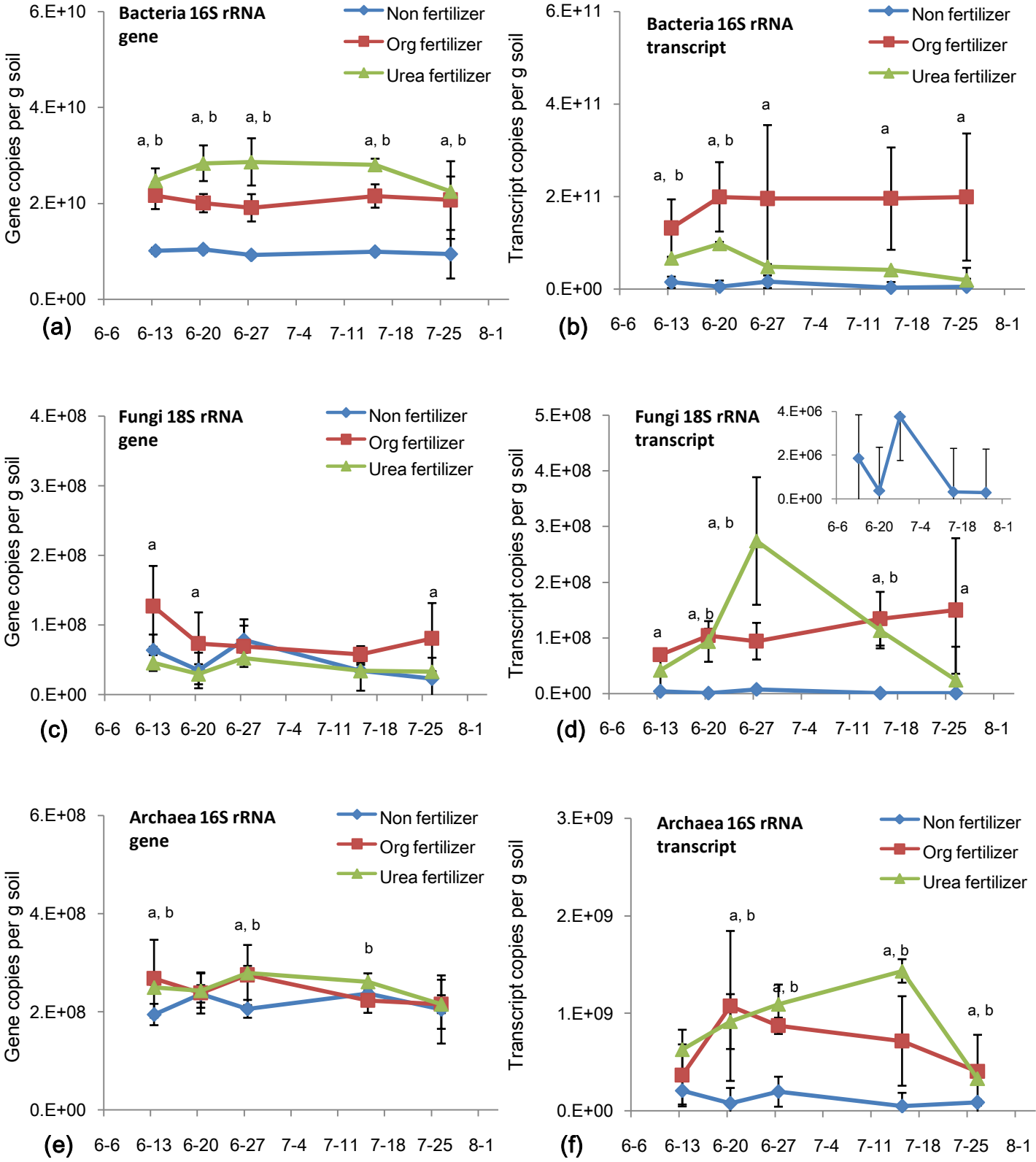

Fig. 4-5 The abundance and expression of bacterial and archaeal 16S rRNA and fungal 18S rRNA gene in upland field after the basal and additional N fertilization. Statistically significant differences (least significant difference, $p<0.05$) between the plots applied with non fertilizers and fertilizers at a certain time point are indicated by small letters above the individual data points (a, between the plots applied with organic fertilizers and no fertilizers; b, between the plots applied with chemical fertilizers and no fertilizers)

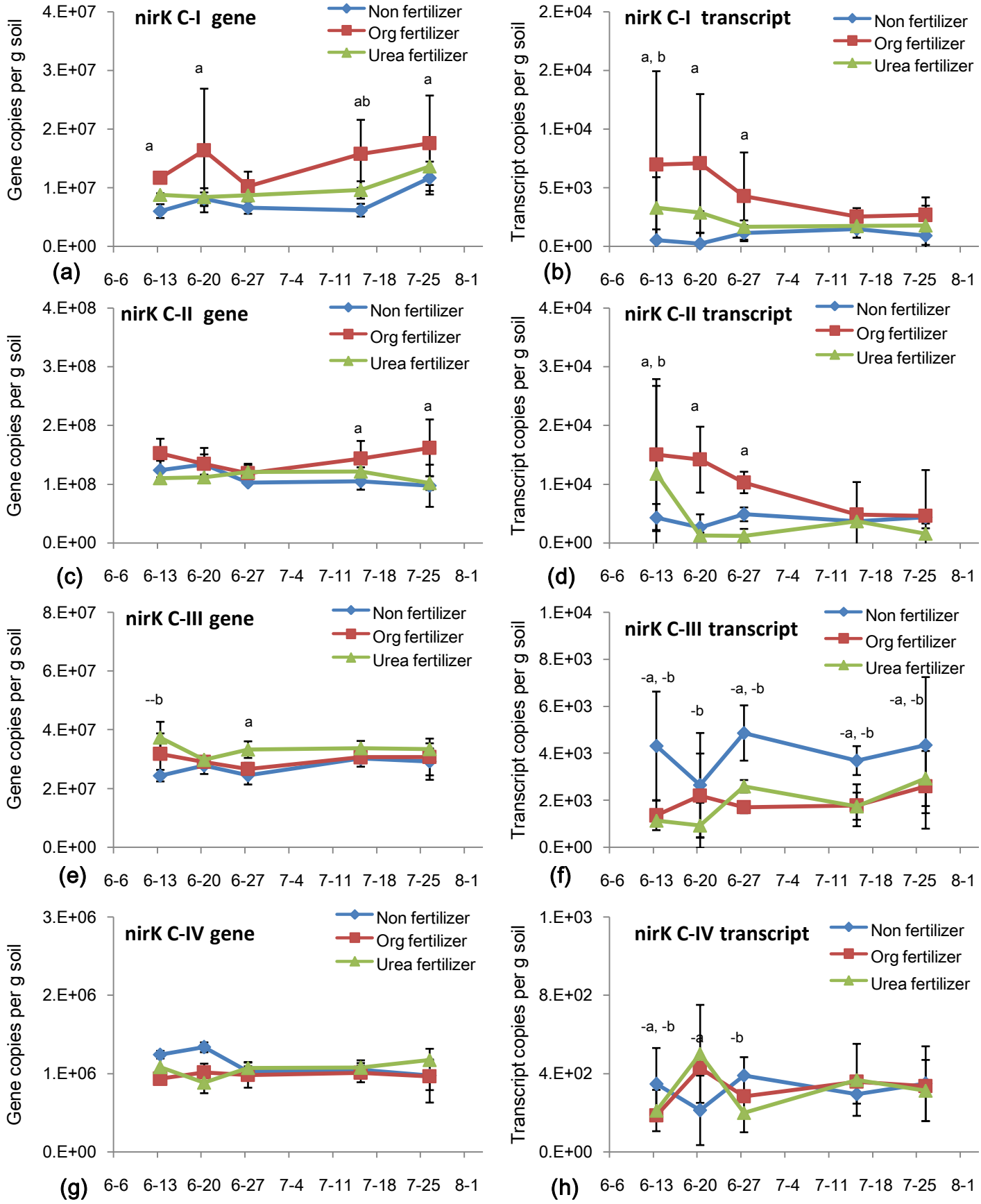

Fig. 4-6 The abundance and expression of prokaryotic nirK in Cluster I to IV in upland field after the basal and additional N fertilization. Statistically significant differences (LSD, $p<0.05$) between the plots applied with non fertilizers and are indicated by small letters above the individual data points (a, between the plots applied with organic fertilizers and no fertilizers; b, between the plots applied with chemical fertilizers and no fertilizers)

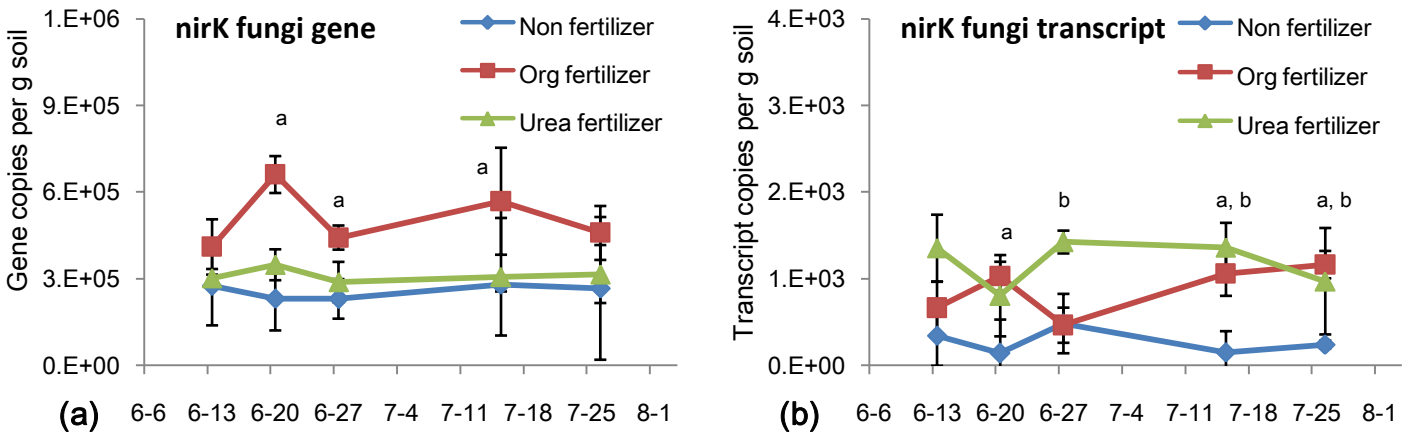

Fig. 4-7 The abundance and expression of fungal *nirK* in upland field after the basal and additional N fertilization. Statistically significant differences (least significant difference, $p<0.05$) between the plots applied with non fertilizers and fertilizers at a certain time point are indicated by small letters above the individual data points (a, between the plots applied with organic fertilizers and no fertilizers; b, between the plots applied with chemical fertilizers and no fertilizers)

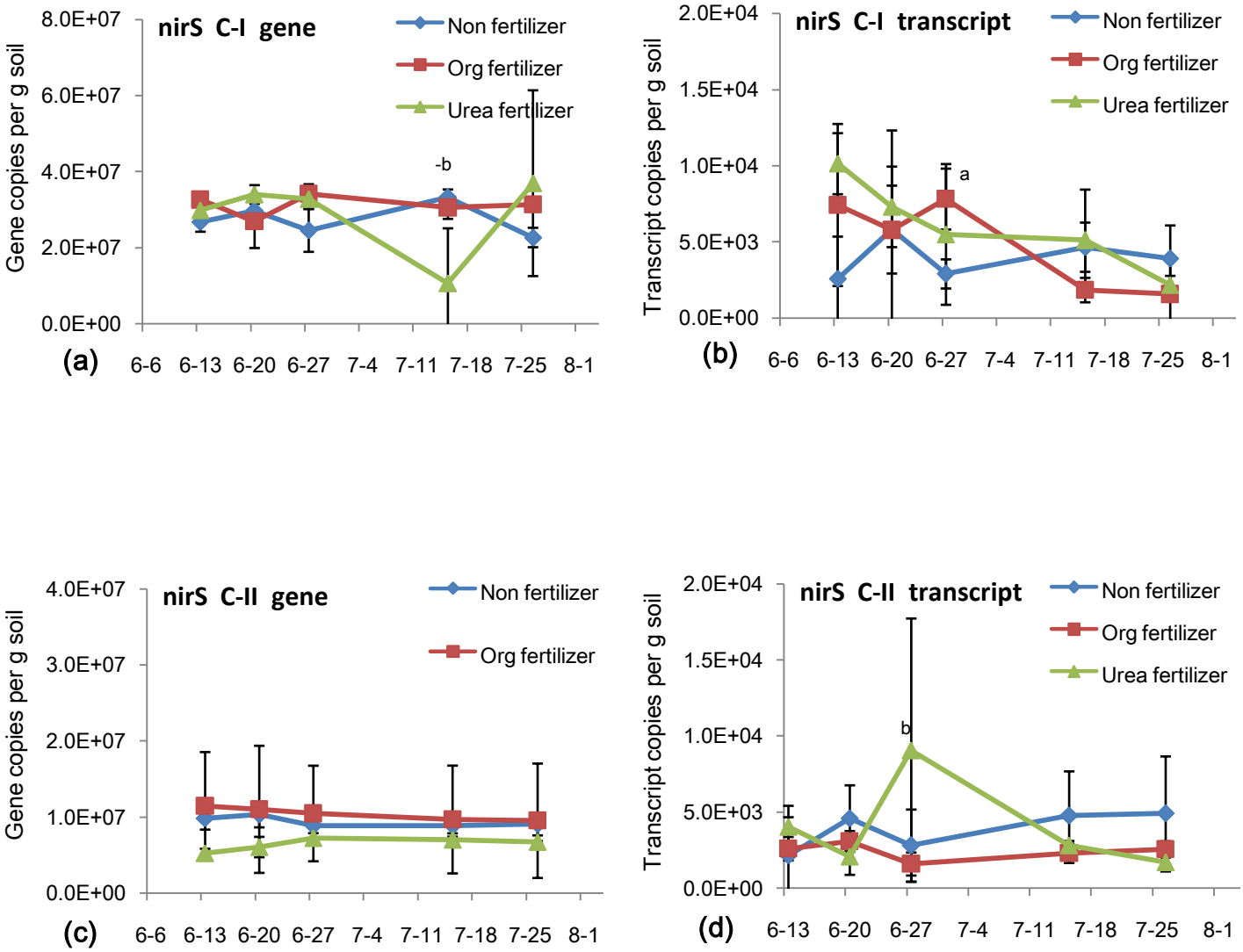

Fig. 4-8 The abundance and expression of prokaryotic *nirS* in Cluster I and I in upland field after the basal and additional N fertilization. Statistically significant differences (least significant difference, $p<0.05$) between the plots applied with non fertilizers and fertilizers at a certain time point are indicated by small letters above the individual data points (a, between the plots applied with organic fertilizers and no fertilizers; b, between the plots applied with chemical fertilizers and no fertilizers)

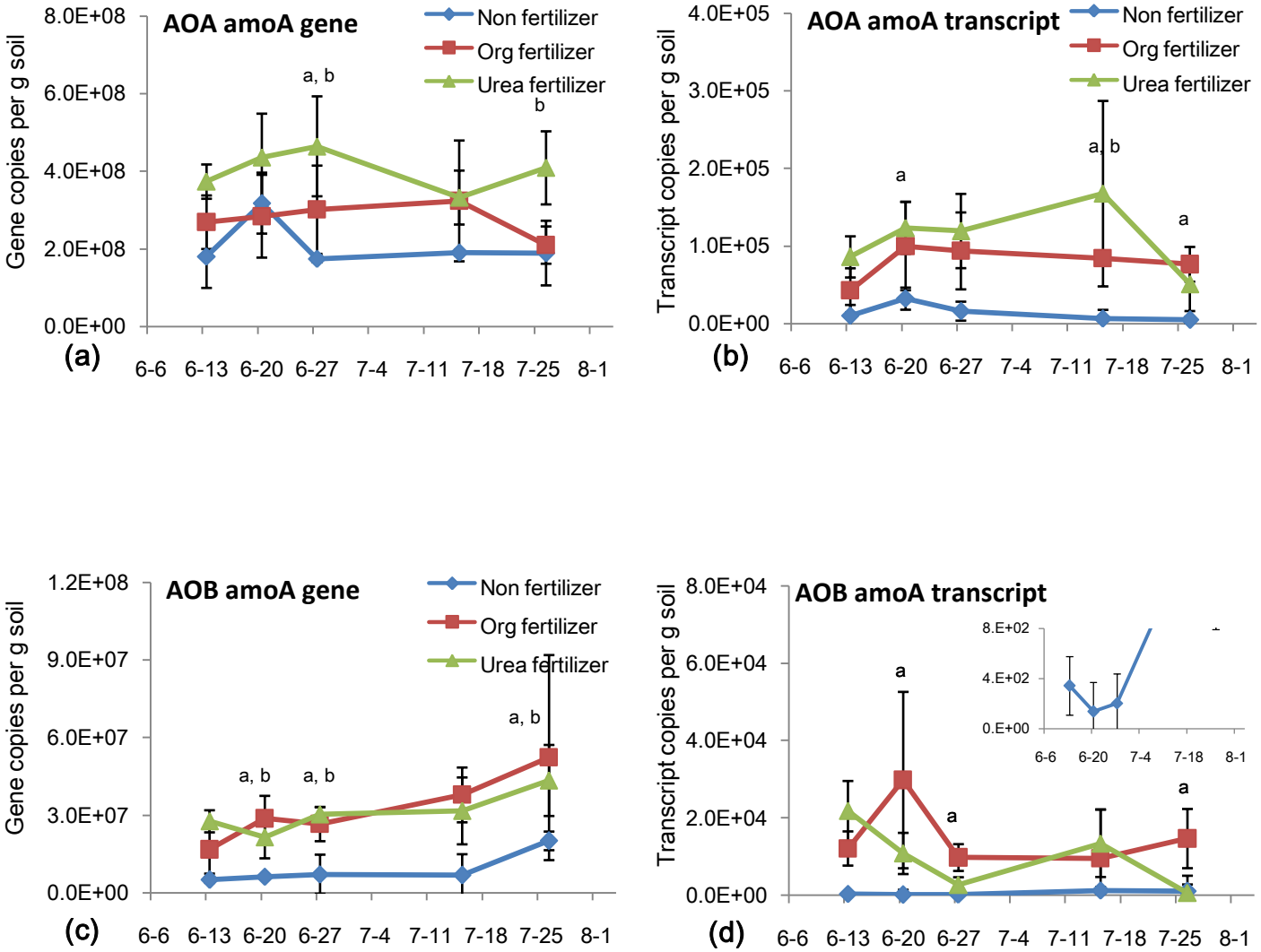

Fig. 4-9 The abundance and expression of bacterial and archaeal *amoA* gene in upland field after the basal and additional N fertilization. Statistically significant differences (least significant difference, $p<0.05$) between the plots applied with non fertilizers and fertilizers at a certain time point are indicated by small letters above the individual data points (a, between the plots applied with organic fertilizers and no fertilizers; b, between the plots applied with chemical fertilizers and no fertilizers)

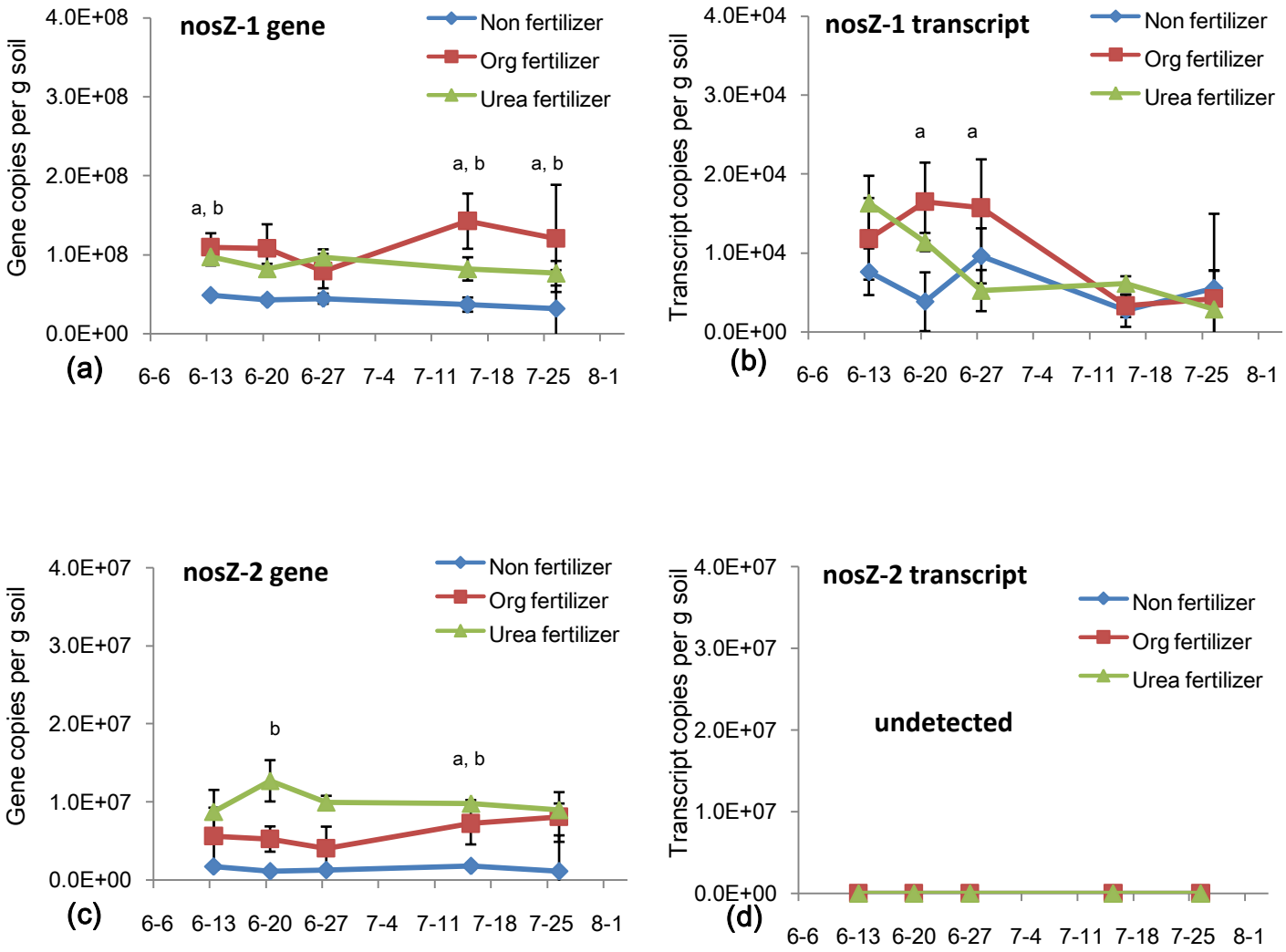

Fig. 4-10 The abundance and expression of prokaryotic *nosZ* gene in upland field after the basal and additional N fertilization. Statistically significant differences (least significant difference, $p<0.05$) between the plots applied with non fertilizers and fertilizers at a certain time point are indicated by small letters above the individual data points (a, between the plots applied with organic fertilizers and no fertilizers; b, between the plots applied with chemical fertilizers and no fertilizers)

Chapter 5

Temporal change of N_2O-generating microorganisms in upland field soil after basal N fertilization

5.1 Introduction

N_2O emissions induced by basal N fertilization are always concentrated in several weeks after the application with N fertilizer. The peak of N_2O emission usually occur during the first two weeks after the N fertilization, while such N_2O emissions disappear in one months after the application (Li et al., 2002; Hayakawa et al., 2009; Akiyama et al., 2003; Meng et al., 2005; Bergstrom et al. 2001, Liu et al. 2005, Liu et al. 2006, Schils et al. 2008) (Zhang & Han 2008). In contrast, N_2O emissions induced by additional N fertilization always lasted for a longer time than that by basal fertilization. Simultaneously, the concentrated N_2O emission after the basal fertilization performs larger contribution for total N_2O emission than that of additional fertilization. Such large and rapid N_2O emission induced by basal fertilization should have priority to mitigation for global and local N_2O budgets. Therefore, the clarification of microorganisms and their pathways responsible for N_2O emission and related controlling environmental factors induced by basal N fertilization will lead us to a more comprehensive understanding of the microbial N_2O emission in upland field soils, which attribute to perform strategies to mitigate the excessive N_2O emission arising from intensive N fertilization in upland field soil.

As described in Chapter 4, the N_2O emission induced by basal fertilization lasted two weeks (OF) or three weeks (CF), and the accumulated amount of N_2O emission was 2.5-fold or 4.5-fold larger than that by additional fertilization, respectively. However, three times of the interspaced quantification of microbial functional genes could only over a partial process of N_2O emission. If the highest activities of all N_2O emitters were not synchronous, a potential temporal variation of microorganisms and their pathways responsible for N_2O emission may exist, which lead us to misestimate the microbial N_2O emission process in upland field soils.

5.1 Introduction

It is well known that NO_3^- is used by both plants and denitrifiers and the competition for NO_3^- is therefore high in the rhizosphere during the growing season (Philippot et al., 2007; Thomson et al., 2012), and organic carbon compounds, which can be used as electron donor by denitrifiers (Isobe and Ohte, 2014), are released by plants roots in the surrounding soil (Philippot et al., 2007). Thus, the general smooth curves of the abundance and expression of all target genes, whether prokaryotic 16S rRNA, fungal 18S rRNA or functional gene associated with N_2O emission, indicated a potential effect of crops on the population size and function of denitrifiers in the upland field.

In addition, multiple analyses, e.g. substance induced respiration inhibition (SIR) method and acetylene inhibition method, were required to associate the isotopomer analysis used in Chapter 4, because the isotopomer analysis provided us an important but complicated result for the contribution of microbial nitrifiers and denitrifiers to N_2O emission.

Thus, the objective of this chapter is focus on the temporal change of N_2O-generating microorganisms and controlling environmental factors responsible for such N_2O emission in upland field induced by basal application with organic or chemical fertilizers. To achieve this objective, we (1) established experimental site with 5-fold higher N fertilizers than conventional application and no crop cultivation, (2) observed the N_2O emission and potential controlling environmental factors during the N_2O emission period, (3) determined the contribution of the nitrifiers and denitrifiers to N_2O emission based on the multiple analysis using SIR and acetylene inhibition analysis, (4) described the temporal variation of abundance and expression of microbial functional gene associated with N_2O emission in upland field soils.

5.2 Materials and Methods

5.2.1 Study site and field management

The study field is the same with the study in 2011 (Chapter 4), located at the Niigata Agricultural Research Institute (N37°26′, E138°52′, Nagaoka, Niigata, Japan), but without cultivation. The field experiment was arranged in a randomized block design with three replicate plots per treatment (Fig. 5-1). Each plot was 1.44m^2 (1.2 m × 1.2 m) and three treatments included one applied with organic fertilizer (OF) and one applied with chemical fertilizer (CF) and one without fertilizer (NF). A commercially available granulated organic fertilizer and a commercially available urea, P_2O_5 and K_2O, the same with those in 2011, were used as organic and chemical fertilizer, respectively. A basal fertilization of organic fertilizer and chemical fertilizer at 144 g N m^{-2} (5 fold higher than that in 2011) were performed in each plot on Jun. 4 in 2012 by incorporating the fertilizer into the plowed layer. The total precipitation and mean daily air temperature during the cultivation period were 390 mm and 24.9 °C, respectively.

5.2.2 Measurements of N_2O flux and soil sampling and geochemical parameters measurement

N_2O flux in the field was measured for ten times during the cultivation period using the chamber method (Jun. 4, 11, 18, 25 and Jul. 2, 9, 17, 23, 30 and Sep. 19). Chambers have fixed position in each plot. Gas samples (500 ml) and N_2O measurement were performed with the same procedure as described in Chapter 4. The N_2O flux was calculated from the increase in the N_2O concentration of the sample. Soil samples were collected at 5-10 cm, 15-20 cm, 25-30 cm and 35-40 cm depth surrounding the chamber in each plot after each time of gas sampling. Half of the soil sample was used to measure the soil physicochemical parameters, e.g. soil N concentration,

water content and soil pH, and the other half was stored at -80°C for molecular analysis. Ten-gram soil samples were extracted with 100 ml of 2 M KCl solution. All physicochemical parameters were measured with the same procedure as described in Chapter 4.

5.2.3 Substrate-induced respiration and acetylene inhibition analysis

The relative contributions of fungal and bacterial activity to N_2O emission were evaluated through the substrate-induced respiration (SIR) inhibition method (Anderson and Domsch 1975) using the soil samples collected from the organic and Urea fertilized plots on Jun. 18 and Jul. 9, when N_2O flux peaks were observed after basal fertilizations, respectively. Optimal inhibitor concentrations (5 mg g^{-1} soil of cycloheximide and 5 mg g^{-1} soil of chloramphenicol) were determined through preliminary experiments, in which glucose (5.0 mg g^{-1} soil) as a C source, cycloheximide (0, 2.0, 5.0, and 10.0 mg g^{-1} soil) as a fungal inhibitor and chloramphenicol (0, 2.0, 5.0, 8.0, and 12.0 mg g^{-1} soil) as a bacterial inhibitor were used according to Laughlin and Stevens (2002). The inhibitors and glucose were dissolved in 5 ml of distilled water and applied into the bottles with 40g soil samples as described above. The bottles containing soil, glucose, and antibiotic solutions were incubated at 27 °C under aerobic conditions for 2 hours on a rotary shaker (150 rpm). The bottles were then sealed and incubated for 4 hours under the same conditions, and gaseous N_2O and CO_2 concentrations were measured every 2 hours using a GC-TCD instrument (GC-14, Shimadzu, Kyoto, Japan).

The contributions of nitrifiers to N_2O emission were determined using 0.01% acetylene (C_2H_2) as a nitrification inhibitor (Schimel et al., 1984). The C_2H_2 was added in the headspace of the soil samples on the 8th and 34th incubation days after sealing the bottles. The bottles were incubated at 27 °C for 4 hours. Gaseous N_2O concentrations were measured every 2 hours using a GC-ECD

instrument (GC-2014, Shimadzu, Kyoto, Japan).

5.2.4 Abundance and expression dynamic of bacterial and archaeal 16S rRNA and fungal 18S rRNA gene

The soil RNA and DNA extraction, RNA transcription to cDNA and qPCR detection of the abundance and expression of bacterial 16S rRNA gene, archaeal 16S rRNA gene and fungal 18S rRNA gene were performed as described in Chapter 4.

5.2.5 Abundance and expression dynamic of N-cycling functional marker genes

The soil RNA and DNA extraction, RNA transcription to cDNA and qPCR detection of the abundance and expression of the *nirK* and *nirS*, AOA *amoA* and AOB *amoA*, and *nosZ*-1 and *nosZ*-2 were performed as described in Chapter 4.

5.2.6 Statistical analysis

The statistical analysis was performed for each time point of sampling and for each measured geochemical parameter and gene copy number values. Using a univariate analysis of variance (ANOVA) with the least significant difference *post hoc* test ($P<0.05$), all geochemical and molecular parameter values from the control (field with no fertilizer) were individually compared with the field applied with organic and chemical fertilizers in order to reveal differences between the control and fertilized fields that were statistically significant. These statistical analyses were performed using the R software package (version 3.0, R Development Core Team). Linear dependences between geochemical and molecular variables were described by correlations with Pearson's product-moment correlation coefficient (r) and P-values.

5.3 Results

5.3.1 N_2O emission rate and climate change during the observation period

That 5-fold higher N amount than conventional application level and no cultivation were performed in order to exaggerate N fertilizer effects and remove the effects of crop root on soil microorganisms (Fig. 5-1).

Two N_2O flux peaks were observed in plots applied with organic fertilizer (OF) during the observation period, and the first peak and second peak occurred two weeks (Jun. 18) and five weeks (Jul. 9) after the basal fertilization (Fig. 5-2b). Two N_2O flux peaks were observed in plots applied with chemical fertilizer (CF) synchronizing with that in OF plots, which also occurred on Jun. 18 and Jul. 9 after the basal fertilization (Fig. 5-2b). N_2O flux in NF plots was used as the background level, and no obvious N_2O flux peak was observed.

In OF plots, the first peak (Jun. 18) was 4347μg N_2O-N $m^{-2}h^{-1}$), which was observed after moderate rain and the related increase in soil water-filled pore space (WFPS) (Fig. 5-2a). The second peak (2993μg N_2O-N $m^{-2}h^{-1}$) was observed after rainstorm and more increasing WFPS than that during the first peak (Fig. 5-2a). The total amount of emitted N_2O derived from the basal fertilization in OF plots (from Jun. 3 to Sep. 19) was 2.58 g N_2O-N m^{-2} (Fig. 5-2b), which was approximately 12-fold higher than that in the plots applied with basal organic fertilizers in 2011 (described in Chapter 4).

In CF plots, the first peak (Jun. 18) of N_2O emission (742μg N $m^{-2}h^{-1}$) was significantly lower than that in OF plots ($P<0.05$), and the second peak of N_2O emission (4172μg N $m^{-2}h^{-1}$, Jul. 9) was higher than that of the second peak in OF plots after rainstorm and the related high soil WFPS (Fig. 5-a). The total amount of emitted N_2O derived from the basal fertilization in CF plots (from Jun. 3

to Sep. 19) was 2.57 g N m^{-2} (Fig. 5-2b), which was approximately 12-fold higher than that in the plots applied with basal chemical fertilizers in 2011 (described in Chapter 4).

According to the field observation in this chapter, we found there were also two increasing stages of WFPS like that in 2011 (Chapter 4). The first stage was from Jun. 3 to Jul. 2 and the second stage was from Jul. 2 to Jul. 10 following a moderate rainfall and a rainstorm, respectively. The first peak of N_2O emission in OF and CF plots occurred during the first increasing stages of WFPS. The second peak of N_2O emission in OF and CF plots occurred during the second increasing stage of WFPS (Fig. 5-2b).

5.3.2 Soil physicochemical parameters during the N_2O flux period

To determine the active soil layer for N_2O emission, we sampled soil from 4 depths, including the depth 5-10 cm, 15-20 cm, 25-30 cm and 35-40 cm. After the comparison among soil NH_4^+, NO_3^- and NO_2^- concentration in all three treatments, we found the highest concentration of all N chemical parameters and the largest fluctuation occurred at the depth of 5-10 cm (Figs. 5-3, 5-4 and 5-5). Therefore, the depth of 5-10 cm, the most active for nitrification and denitrification, might be the main soil layer for N_2O emission. We performed all investigation in this layer.

After the basal fertilization, the soil NH_4^+ concentrations in OF plots increased rapidly and peaked at 116.3±25.6 mg N kg^{-1} (Jun. 18), and then decreased slightly and reached background level on Jul. 9. (Fig. 5-6a). The soil NH_4^+ concentrations in CF plots increased rapidly from 20.6.0±14.4 mg N kg^{-1} (Jun. 4) to 170±8.6 mg N kg^{-1} (Jun. 7), and fluctuated slightly until Jul. 2 and then decreased and reached background level on Jul. 30. (Fig. 5-6a).

Compared with the NH_4^+ concentrations, soil NO_3^- concentrations remained at background level after basal fertilization until Jun. 11 in both OF and CF plots, and then increased and peaked

at 263±63 mg N kg^{-1} (OF) and 286±21 mg N kg^{-1} (CF) on Jul. 2 (Fig. 5-6b). A sharply decreasing to background level of NO_3^- concentration in both OF and CF was observed on Jul. 9, when a rainstorm occurred. After this unexpected decreasing, soil NO_3^- concentration in OF and CF plots recovered to 41±7 mg N kg^{-1} and 111±17 mg N kg^{-1}, respectively, and decreased to background level on Sep. 19 (Fig. 5-6b).

Soil NO_2^- concentrations in CF plots also remained at background level after basal fertilization until Jun. 11 like that of NO_2^- concentration, and increased and peaked at 15.8±6.3 mg N kg^{-1} on Jun. 18, and then decreased to background level on Jul. 9 (Fig. 5-6c). Soil NO_2^- concentrations in OF plots remained at background level after basal fertilization until Jun. 25 and increased and peaked at 1.5±0.2 mg N kg^{-1} on Jun. 2, and then decreased to background level on Jul. 9 (Fig. 5-6c).

The pH values in OF plots increased to 7.1±0.1 after basal fertilization and decreased to background level on Jun. 18 (Fig. 5-6d). Then pH values continued to decrease to the lowest (5.7±0.2) on Jul. 2 and remained until the end of observation. The pH values in CF plots increased to 7.8±0.2 on Jun. 18 after basal fertilization and decreased to the lowest (5.0±0.2) on Jul. 30 (Fig. 5-6d).

5.3.3 Substance-induced respiration inhibition and acetylene inhibition analysis

The relative contributions of fungal and bacterial activity to N_2O emission were evaluated through the substrate-induced respiration (SIR) inhibition analysis (Table 5-1). The addition of cycloheximide as a fungal inhibitor into the soil from OF plots on Jun. 18 and Jul. 9 (the first and second peak of N_2O emission) decreased the N_2O emission rate by 33% and 88%, respectively (Table 5-1). The addition of chloramphenicol as a bacterial inhibitor into the soil from OF plots on

Jun. 18 and Jul. 9 decreased the N_2O emission rate by 75% and 54%, respectively (Table 5-1). In contrast, the addition of cycloheximide as a fungal inhibitor into the soil from CF plots Jun. 18 and Jul. 9 decreased the N_2O emission rate by 19% and 27%, and the addition of chloramphenicol as a bacterial inhibitor decreased the N_2O emission rate by 72% and 74%, respectively (Table 5-1).

The relative contributions of nitrification to N_2O emission were evaluated through the acetylene inhibition analysis (Table 5-1). A nitrification inhibitor, 0.01% acetylene, decreased the rate by 9% and 3% of the soil from OF plots on Jun. 18 and Jul. 9, and decreased the rate by 14% and 33% of the soil from CF plots on Jun. 18 and Jul. 9 (Table 5-1).

5.3.4 Abundance and expression dynamic of bacterial and archaeal 16S rRNA and fungal 18S rRNA gene

The abundance dynamic of prokaryotic (bacteria and archaea) and fungal population were determined by quantification of their 16S rRNA and 18S rRNA gene copy numbers (Fig. 5-7). In OF plots, the gene copy numbers of archaeal 16S rRNA was always similar with those in NF plots during the whole observation period, but the gene copy numbers of bacterial 16S rRNA and fungal 18S rRNA increased sharply after the basal fertilization and peaked at 3.0×10^{10} copies g^{-1} soil (bacteria) and 1.1×10^{9} copies g^{-1} soil (fungi) on Jun. 18, when the first peak of N_2O occurred (Fig. 5-7a, c, e). In CF plots, the gene copy numbers of bacterial and archaeal 16S rRNA were always similar with those in NF plots ($P>0.05$), but the gene copy numbers of fungal 18S rRNA was always higher than that in NF plots during the whole observation period (Fig. 5-7a, c, e). the bacterial and fungal population size increased rapidly after basal organic fertilization, while the archaeal population size did not change. Simultaneously, archaeal and fungal population size increased slightly after the basal chemical fertilization, while the bacterial population size did not

changed.

The expression dynamic of prokaryotic (bacteria and archaea) and fungal population were determined by quantification of their 16S rRNA and 18S rRNA trascript copy numbers (Fig. 5-7b, d, f). In OF plots, the transcript abundance of bacterial and archaeal 16S rRNA and fungal 18S rRNA increased sharply after the basal fertilization and peaked at 2.9×10^{11} copies g^{-1} soil (bacteria) and 3.3×10^{9} copies g^{-1} soil (archaea) and 3.2×10^{9} copies g^{-1} soil (fungi) on Jun. 18, when the first peak of N_2O occurred (Fig. 5-7b, d, f). Then the transcript abundance of bacterial 16S rRNA and fungal 18S rRNA decreased but remained higher abundance than that of NF plots; the transcript abundance of archaeal 16S rRNA decreased and remained similar expression level with that in NF plots, except that of fungal 18S rRNA on Jul. 17 (Fig. 5-7b, d, f). In CF plots, the transcript copy numbers of bacterial 16S rRNA were always significantly higher than that in NF plots ($P<0.05$), and the transcript copy numbers of fungal 18S rRNA were always similar with those in NF plots ($P>0.05$), and the transcript copy numbers of archaeal 16S rRNA were always significantly lower than that in NF plots ($P<0.05$) (Fig. 5-7b, d, f). These results indicated that the bacterial and fungal community behaved active metabolic state after basal organic and chemical fertilization during the first and second peak of N_2O emission, especially after the organic fertilization. The archaeal community behaved active metabolic state only after the basal organic fertilization.

5.3.5 Abundance and expression dynamic of nitrite reductase gene

The abundance and expression dynamic of microorganisms capable of reducing nitrite was determined by quantification of the gene and transcript copy numbers of *nirK* and *nirS* using the newly designed primers like that in Chapter 4.

The abundance dynamic of 5 different types of *nirK* gene (4 clusters of prokaryotic *nirK* and

fungal *nirK*) and 2 different types of *nirS* gene (2 clusters of prokaryotic *nirS*) were assessed and shown in Figs. 5-8, 5-9 and 5-10. In OF plots, prokaryotic *nirK* in Cluster I, II and *nirS* in Cluster I, and fungal *nirK* rapidly increased after the basal fertilization and peaked at 9.8×10^7, 3.4×10^8, 2.5×10^7 and 4.1×10^5 copies g^{-1} soil on Jun. 18, when the first peak of N_2O emission occurred in OF plots, and then decreased to the background level (Figs. 5-8ac, 5-9a and 5-10a). Simultaneously, prokaryotic *nirK* in Cluster III, IV and *nirS* in Cluster II increased slowly after the basal fertilization and peaked at 2.7×10^7, 9.5×10^5 and 1.9×10^7 copies g^{-1} soil on Jun. 25, one week later than the first peak period of N_2O emission, and then decreased to the background level (Figs. 5-8eg, 5-9b and 5-10c). In CF plots, prokaryotic *nirK* in Cluster I, II, III and IV and *nirS* in Cluster I fluctuated slightly after the basal fertilization, which were always similar with that in NF plots (Figs. 5-8aceg and 5-10a). In contrast, prokaryotic *nirS* in Cluster II increased rapidly and peaked at 3.4×10^7 copies g^{-1} soil on Jun. 18 and 2.5×10^7 copies g^{-1} soil on Jul. 30, and decreased to the background level at the end of observation (Fig 5-10c). The fungal *nirK* increased suddenly and peaked at 1.2×10^6 copies g^{-1} soil on Jul. 30, and decreased to background level at the end of observation (Fig 5-9a).

The expression dynamic of 5 different types of *nirK* transcript (4 clusters of prokaryotic *nirK* and fungal *nirK*) and 2 different types of *nirS* transcript (2 clusters of prokaryotic *nirS*) were assessed and shown in Figs. 5-8, 5-9 and 5-10. In OF plots, the transcript abundance of prokaryotic *nirK* in Cluster I, II and IV rapidly increased after the basal fertilization and peaked at 4.3×10^4, 6.5×10^5 and 7.3×10^3 copies g^{-1} soil on Jun. 18, when the first peak of N_2O emission occurred in OF plots, and then decreased to the background level on Jul. 2 (Figs. 5-8bdh). The dynamic of prokaryotic *nirK* in Cluster III and *nirS* in Cluster II fluctuated drastically and peaked at 3.6×10^4

and 1.1×10^5 copies g^{-1} soil on Jun. 25 (Figs. 5-8f, 5-10d). The transcript abundance of fungal *nirK* increased and peaked at 8.1×10^3 copies g^{-1} soil on Jul. 2, and decreased yet remained higher abundance than that in NF plots (Fig. 5-9b). The transcript abundance of prokaryotic *nirS* in Cluster I was always lower than that in NF plots (Fig. 5-10b). According to the linear dependences among N_2O emission rate and soil physicochemical and microbial variables in the OF plots during the whole observation period, we found that N_2O emission had significant correlations with the transcript abundance of prokaryotic *nirK* in Cluster I (R^2=0.651, P=0.003) and Cluster II (R^2=0.618, P=0.005) and fungal *nirK* (R^2=0.467, P=0.039) (Table 5-2).

In CF plots, the transcript dynamic of prokaryotic *nirK* in Cluster I, II, III and IV and *nirS* in Cluster I fluctuated slightly during the whole observation (Figs. 5-8bdfh and 5-10b) and only the transcript abundance of *nirK* in Cluster I was significantly higher than that in NF plots during the peak period of N_2O emission (P<0.05). The dynamic of prokaryotic *nirS* in Cluster II fluctuated drastically during the whole observation and was significantly higher than that in NF plots during the peak period of N_2O emission (Fig. 5-10d). The transcript abundance of fungal *nirK* increased and peaked at 5.1×10^3 copies g^{-1} soil on Jul. 9, when the peak of N_2O emission occurred in CF plots, and decreased yet remained higher abundance than that in NF plots (Fig. 5-9b). According to the linear dependences among N_2O emission rate and soil physicochemical and microbial variables in the CF plots during the whole observation period, we found that the N_2O emission in CF plots during the whole observation had significant correlations with the abundance of prokaryotic *nirK* in Cluster I (R^2=0.793, P=0.000) fungal *nirK* transcript (R^2=0.624, P=0.004) (Table 5-3).

5.3.6 Abundance and expression dynamic of ammonium oxidizing gene

The abundance and expression dynamic of microorganisms capable of oxidizing ammonium

was determined by quantification of the gene and transcript copy numbers of AOA and AOB *amoA*.

The abundance dynamic of AOA *amoA* and AOB *amoA* were assessed and shown in Fig. 5-11. In OF plots, the abundance dynamic of AOA *amoA* and AOB *amoA* fluctuated drastically during the whole observation period (Fig. 5-11ac). The gene abundance of AOA *amoA* reached 3.4×10^8 and 3.5×10^8 copies g^{-1} soil during the first and second peak of N_2O emission, which is significantly higher than that in NF plots ($P<0.05$) (Fig. 5-11a). The gene abundance of AOB *amoA* increased sharply and peaked at 7.3×10^8 copies g^{-1} soil after the basal fertilization, and decreased yet remained higher abundance than that in NF plots (Fig. 5-11c). In CF plots, the gene abundance of AOA *amoA* remained the similar level with that in NF plots until Jun. 2 and decreased stepwise until the end of observation (Fig. 5-11a). In contrast, the gene abundance of AOB *amoA* increased and peaked at 3.1×10^8 copies g^{-1} soil on Jun. 2 and decreased to background level at the end of observation (Fig. 5-11c).

The expression dynamic of AOA *amoA* and AOB *amoA* were assessed and shown in Fig. 5-11. In OF plots, the expression dynamic of AOA *amoA* and AOB *amoA* fluctuated drastically during the whole observation period, and the transcript abundance of both AOA *amoA* and AOB *amoA* on Jun. 18 and Jul. 9 were significantly higher than that in NF plots ($P<0.05$) (Fig. 5-11bd). The expression level of AOB *amoA* was significantly higher than that of AOA *amoA* ($P<0.05$) (Fig. 5-11bd). According to the linear dependences among N_2O emission rate and biogeochemical variables in the OF plots during the whole observation period, we found that N_2O emission had significant correlations with the abundance of AOB *amoA* transcript ($R^2=0.869$, $P=0.025$) (Table 5-2).

In CF plots, the transcript abundance of AOA *amoA* remained the similar level with that in NF plots after the basal fertilization until Jul. 2, and increased and reached 3.2×10^5 copies g^{-1} soil on Jul. 7, when the peak of N_2O emission occurred (Fig. 5-11b). The transcript abundance of AOB *amoA* increased stepwise after the basal fertilization, and peaked at 1.6×10^7 on Jul. 7 and decreased to the background level at the end of observation (Fig. 5-11d). According to the linear dependences among N_2O emission rate and biogeochemical variables in the CF plots during the whole observation period, we found that N_2O emission had significant correlations with the abundance of AOB *amoA* transcript (R^2=0.902, P=0.000) (Table 5-3).

5.3.7 Abundance and expression dynamic of nitrous oxide reductase gene

The abundance and expression dynamic of microorganisms capable of reducing nitrous oxide was determined by quantification of the gene and transcript copy numbers of *nosZ* in Cluster I and II.

The abundance dynamic of *nosZ* in Cluster I and II were assessed and shown in Fig. 5-12. In OF plots, the gene abundance of *nosZ* in Cluster I increased and peaked at 2.1×10^8 copies g^{-1} soil on Jun. 18 after the basal fertilization and then decreased to the background level at the end of observation (Fig. 5-12a). The gene abundance of *nosZ* in Cluster II increased and peaked at 8.4×10^5 copies g^{-1} soil on Jun. 25 after the basal fertilization and then decreased to the background level at the end of observation (Fig. 5-12c). In CF plots, the gene abundance of *nosZ* in Cluster I was always similar to that in NF pots, but the gene abundance of *nosZ* in Cluster II fluctuated drastically, which increased and peaked at 6.0×10^5 and 2.0×10^5 copies g^{-1} soil on Jun. 25 and Jul. 9 (Fig. 5-12ac).

The expression dynamic of *nosZ* in Cluster I and II were assessed and shown in Fig. 5-12. In

OF plots, the expression dynamic of *nosZ* in Cluster I increased sharply after the basal fertilization and peaked at 4.6×10^5 copies g^{-1} soil on Jun. 18, and decreased to background level on Jul. 9 (Fig. 5-12b). In contrast, the expression dynamic of *nosZ* in Cluster I in CF plots fluctuated slightly and was always similar with that in NF plots (Fig. 5-12b). The transcript of *nosZ* in Cluster II was failed be detected in all three treatments (Fig. 5-12d). According to the linear dependences among all molecular variables in the OF plots during the whole observation period, we found that the transcript abundance of *nosZ* in Cluster I had significant correlation with the N_2O emission (R^2=0.701, P=0.001) and the transcript abundance of *nirK* in Cluster I (R^2=0.987, P=0.000) and Cluster II (R^2=0.974, P=0.000) (Table 5-2).

5.4 Discussion

5.4.1 Potential environmental factors controlling N_2O emission rate

When we increased the application amount of N fertilizer, we obtained an extended and fluctuant N_2O flux curve. We found the dynamic of N_2O emission fluctuated after basal organic or chemical fertilization, which might depend on the change of N_2O-generating microorganisms' growth and expression induced by environmental factors. The dynamic change of soil WFPS strongly support the observation and conclusion of the experiment in 2011, that the increasing WFPS caused by rainfall was a cofactor of N fertilization for the N_2O emission in cropland soil, and N_2O emission induced by chemical fertilizers might need higher level of WFPS than that by organic fertilizers. Soil NH_4^+ concentrations in OF plots decreased to the background level on Jul. 9, which indicated that the contribution of nitrification to N_2O emission in OF plots during the second peak might be inhibited and denitrification might be the main source of N_2O emission. A sharply decrease of soil pH was observed in both OF and CF during the second peak of N_2O emission, which indicated that soil pH might be a potential environmental factor for the N_2O emission during the second peak, and denitrifiers having prokaryotic *nirK* in Cluster I, *nirS* in Cluster II and fungal *nirK* might be responsible for the N_2O emission in such low soil pH as discussed in Chapter 4.

5.4.2 Contribution of nitrifiers and denitrifiers to N_2O emission

In the SIR inhibition assays, the inhibition rate of fungal and bacterial antibiotic in OF plots showed that the bacterial N_2O was dominated during the first peak of N_2O emission and fungal N_2O increased and dominated during the second peak of N_2O emission. These results indicated that bacteria could be responsible for N_2O emission rapidly after the basal organic fertilization, and

fungi could dominate the N_2O emission a period of time after the basal organic fertilization. In contrast, the inhibition rate of bacterial and fungal antibiotic in CF plots showed that the bacterial contributions to N_2O emission were higher than that of fungal contribution during the two peaks of N_2O emission after the basal chemical fertilization.

In the acetylene inhibition assays, the lower inhibition rate in OF plots during the two peaks of N_2O emission showed that the nitrification was not mainly responsible for N_2O emission induced by basal organic fertilization. Simultaneously, the higher inhibition rate in CF plots indicated that nitrification play a more active role on N_2O emission induced by chemical fertilization than that by organic fertilization.

According to the results of N_2O flux, soil physicochemical parameters, and SIR and acetylene inhibition assays, the contribution of microbial nitrification and denitrification to N_2O emission in upland fields induced by N fertilization is proposed as following, (i) prokaryotic denitrification mainly induced the N_2O emission rapidly in 2 weeks after the basal organic fertilization followed by fungal denitrification, and the contribution of prokaryotic nitrification was the least, (ii) fungal denitrification might dominantly induce the N_2O emission substituting prokaryotic denitrification in 4 weeks after the basal organic fertilization, and the contribution of prokaryotic nitrification was still the least, (iii) prokaryotic denitrification mainly induced the N_2O emission in 2 weeks after the basal chemical fertilization, and the contribution of fungal denitrification and prokaryotic nitrification was similar and next to prokaryotic denitrification, (iv) prokaryotic denitrification mainly induced the N_2O emission in 4 weeks after the basal chemical fertilization, but its dominance declined because of the increased contribution of prokaryotic nitrification and fungal denitrification, especially prokaryotic nitrification.

5.4.3 Abundance and function of nitrite reducing microorganisms

The extended N_2O flux process induced by the application with 5-fold higher amount of N fertilizers made us clarify the regularity of N_2O emission in more detail than that in 2011 (Chapter 4).

During the first peak of N_2O emission in OF plots, we found denitrifiers having the prokaryotic *nirK* in Cluster I, II, III and IV, and *nirS* in Cluster II and fungal *nirK* were responsible for the N_2O emission. Denitrifiers having the *nirK* in Cluster I and II were most active on Jun. 18, like that of the observation in 2011, and denitrifiers having the *nirK* in Cluster III and IV and *nirS* in Cluster II and fungal *nirK* were most active on Jun. 25, which were not detected from the field after the basal organic fertilization in 2011. These results indicated that the activity of denitrifiers responsible for N_2O emission induced by basal organic fertilization had the order according to the types of their nitrite reductase gene, and excessive interspaced measurements in 2011 might underestimate the abundance and diversity of active denitrifiers. During the second peak of N_2O emission in OF plots, only fungal denitrifiers were active, which indicated that the prokaryotic denitrifiers were responsible for rapid N_2O emission induced by basal organic fertilization and fungal denitrifiers were continuously responsible for this N_2O emission.

During the first peak of N_2O emission in CF plots, we obtained the same trend with that in OF plots as described above, although the expression level of these denitrifiers was lower than that in OF. Denitrifiers having the prokaryotic *nirK* in Cluster III and *nirS* in Cluster II and fungal *nirK* were most active on Jun. 25, one week later than that of denitrifiers having the *nirK* in Cluster I and II on Jun. 18. During the second peak of N_2O emission in CF plots, only

denitrifiers having the prokaryotic *nirK* in Cluster I and *nirS* in Cluster II and fungal *nirK* were active, the same result with that in field after the basal chemical fertilization in 2011, which depend on the low soil pH as described in Chapter 4.

In addition, fungi having the *nirK* gene remained high activity during the both peaks of N_2O emission induced by basal organic and chemical fertilization, which strongly supported the previous conclusion that fungal denitrifiers were always responsible for the N_2O emission in the upland field after the N fertilization, irrespective of the application with basal organic or chemical fertilizers.

5.4.4 Abundance and function of ammonium oxidizing microorganisms

The abundance and expression level of AOA and AOB *amoA* in both OF and CF plots in 2012 were entirely opposite with those in upland field in 2011 (Chapter 4). The abundance and expression of AOA *amoA* in all OF, CF and NF plots were always higher than that of AOB *amoA* by an order of magnitude in upland field in 2011. However, in 2012, although the abundance and expression of AOA *amoA* in NF plots were still higher than those of AOB *amoA*, the abundance and expression of AOA *amoA* in OF and CF plots were significantly lower than those of AOB *amoA*. As we described in Chapter 4, AOA favored the exudates from plant roots as the carbon source and was disadvantaged when competing for carbon source in soil with high carbon content (Hallam et al., 2006; Wessén et al., 2010). In the field study of this chapter, high organic carbon content in organic fertilizers and no crop cultivation in field might be the determining factors for the abundance and expression dominance of the AOB over that of the AOA occurring in the field in 2012.

In addition, based on the result of expression dynamics of AOA and AOB *amoA* in OF and

CF plots, AOB might be responsible for N_2O emission via nitrification during the all peaks of N_2O emission induced by basal organic and chemical fertilization. In contrast, AOA might play an active role on N_2O emission during the first peak of N_2O emission induced by basal organic fertilization, although it accounted for only a little proportion of total N_2O emission.

5.4.5 Abundance and function of nitrous oxides reducing microorganisms

In OF plots, we found denitrifiers having the *nosZ* in Cluster I were abundant during the first and second peaks of N_2O emission and active for N_2O sink during the first peak of N_2O emission (Fig. 5-x), which were extremely similar with the dynamic of denitrifiers having the *nirK* in Cluster I or II as described previously (Fig. 5-x). These results supported the previous conclusion that the nitrous oxide reductase (*nosZ* in Cluster I) shared the similar activation and inhibition conditions with some nitrite reductase (*nirK* in Cluster I or II). Thus, we purposed that (1) a close phylogenetic relationship might exist between the denitrifiers having the *nosZ* in Cluster I and *nirK* in Cluster I or II in our upland field, or (2) some denitrifiers having both the *nosZ* in Cluster I and *nirK* in Cluster I or II play an important role in denitrification in our upland field, both of which could lead to the congruent dynamic of abundance and expression between the *nirK* in Cluster I or II and *nosZ* in Cluster I in tested upland field after the basal organic fertilization.

In CF plots, the nitrous oxide reducing denitrifiers (*nosZ* in Cluster I) was inactive for N_2O sink during the first peak of N_2O emission, which was distinctly different with that in OF plots. The soil in CF and OF plots during the first peak of N_2O emission possessed the similar physicochemical controlling factors, i.e. high concentration of NH_4^+, NO_3^- and NO_2^-, neutral pH value and water content, except the organic carbon content induced by organic fertilizers. Organic carbon was reported as a handy electron donor in nitrate reduction process of

denitrification (Beauchamp et al., 1980; Bhandral et al., 2007; Drury et al., 2008; Saari et al., 2009; Saggar et al., 2012), which might be a potential factor to control the activity of the Nir and N_2OR enzyme of denitrifiers in upland soil after the basal N fertilization. In addition, the nitrous oxide reducing denitrifiers (*nosZ* in Cluster I) was inactive during the second peak of N_2O emission after the basal organic and chemical fertilization. Except the deficiency of soil organic carbon as the limited factor, the decrease of soil pH might be another controlling factor as described in Chapter 4. This result suggested that the continuing acidification of upland soils through excessive use of nitrogen fertilizers, as the soil situation during the second peak of N_2O emission in OF and CF plots in this study, enhance N_2O emissions drastically.

Thus, the level of organic carbon content and soil pH were the determining factors for the N_2O sink by nitrous oxide oxidizing denitrifiers in the tested upland field soil.

5.4.6 Temporal change of N_2O generating microorganisms

From the results obtained in this study, the temporal change of N_2O-generating microorganisms induced by basal N fertilization is proposed as follow, (i) after the basal organic fertilization, firstly emitted N_2O was produced mainly via denitrification more than nitrification. Bacterial denitrification, performed by denitrifiers having the prokaryotic *nirK* in Cluster I, II, III and IV and *nirS* in Cluster II, contributed more to N_2O emission than fungal denitrification. The limited N_2O emission via nitrification was mainly produced by AOB than AOA; (ii) after the firstly emitted N_2O induced by basal organic fertilization, N_2O was still produced mainly via denitrification more than nitrification, but fungal denitrifiers contributed more to N_2O emission than bacterial denitrification; (iii) after the basal chemical fertilization, firstly emitted N_2O was produced slightly and induced mainly via denitrification more than nitrification. Bacterial

denitrification, performed by denitrifiers having the prokaryotic *nirK* in Cluster I, II and III and *nirS* in Cluster II, contributed more to N_2O emission than fungal denitrification. The minor N_2O emission via nitrification was mainly produced by AOB; (iv) after the firstly emitted N_2O induced by basal chemical fertilization, N_2O was produced largely mainly via denitrification more than nitrification following a rainstorm, but fungal denitrifiers and bacterial denitrifiers and bacteria nitrifiers contributed equally to N_2O emission; (v) the denitrifiers having *nosZ* in Cluster I as the N_2O reducers play a crucial role in final amount of N_2O emission. The high expression of such denitrifiers only occurred during the first peak period of N_2O emission after the basal organic fertilization because of the sufficient organic carbon and low soil pH level, which lead to an equally released amount of N_2O during the first and second peak period of N_2O emission.

5.5 Conclusion

We performed a field experiment in upland field to determine the temporal variation of microbial N_2O emission in upland field induced by basal application with organic or chemical fertilizers, based on the exaggerated application of N fertilizer and the prolonged field-scale and lab-scale observation and investigation. The results based on such improvements showed that the temporal change of diverse N_2O-generating microorganisms and different environmental factors controlling such N_2O emission induced by basal N fertilization. After the basal organic or chemical fertilization, denitrification contributed mainly to N_2O emission more than nitrification. Under the potential influence of organic carbon supply, prokaryotes having *nirK* in Cluster I to III could be firstly activated by basal N fertilization and produced N_2O via denitrification rapidly at two weeks after the fertilization; then following the decrease of soil pH, the prokaryotes having *nirS* in Cluster II and fungal denitrifiers were most active and produced N_2O via denitrification at three weeks after the basal fertilization. Bacterial nitrifiers, rather than archaeal nitrifiers were mainly responsible for the N_2O produced via nitrification. In addition, under the influence of organic carbon supply and soil pH, denitrifiers having *nosZ* in Cluster I as the N_2O reducers play a role in N_2O sink only in upland field during the early phase after the basal organic fertilization.

Table 5-1 Fungal and bacterial antibiotic and nitrifiers inhibition rate for N_2O emission in field after N fertilization.

	Inhibition rate in OF plots (%)				Inhibition rate in CF plots (%)			
	Jun. 18		Jul. 9		Jun. 18		Jul. 9	
	N_2O	CO_2	N_2O	CO_2	N_2O	CO_2	N_2O	CO_2
F antibiotic	33±2	47±4	88±2	45±13	19±4	31±2	27±5	53±3
B antibiotic	75±1	63±3	54±12	63±1	72±7	66±1	74±2	57±3
F+B antibiotic	94±2	86±4	98±1	90±1	91±2	87±1	82±1	40±4
C_2H_2	9±4	—	3±7	—	14±7	—	33±19	—

Table 5-2. Linear dependences among N_2O emission rate and physicochemical and microbial variables in upland field after basal organic fertilization

Factor	N_2O	NO2-N	NH4-N	NO3-N	pH	water content	16S gene	16S trans	nirK C-I gene	nirK C-I trans	nirK C-II gene	nirK C-II trans	nirK C-III gene	nirK C-III trans	nirK C-IV gene	nirK C-IV trans	nirS C-I gene	nirS C-I trans	nirS C-II gene	nirS C-II trans	18S gene	18S transcript	nirKF gene	nirKF trans	nosZ-1 gene	nosZ-1 trans	nosZ-2 gene	Arc 16S gene	Arc transcript	16SAOA amoA gene	AOA amoA trans	AOB amoA gene	AOB amoA trans
N_2O		0.130	0.000	0.089	0.858	0.292	0.003	0.002	0.000	**0.003**	0.004	**0.005**	0.842	0.321	0.628	0.514	0.128	0.052	0.806	0.138	0.000	0.019	0.010	**0.039**	0.004	**0.001**	0.686	0.006	0.098	0.031	0.067	0.356	**0.025**
NO2-N	0.360		0.307	0.000	0.048	0.649	0.723	0.457	0.149	0.479	0.443	0.755	0.712	0.525	0.442	0.804	0.570	0.259	0.564	0.483	0.309	0.678	0.335	0.007	0.482	0.272	0.805	0.250	0.121	0.487	0.813	0.583	0.594
NH4-N	0.803	0.247		0.095	0.280	0.523	0.000	0.007	0.000	0.003	0.010	0.004	0.521	0.843	0.320	0.780	0.002	0.097	0.334	0.490	0.000	0.005	0.001	0.660	0.001	0.002	0.139	0.005	0.270	0.160	0.026	0.230	0.009
NO3-N	0.401	0.750	0.394		0.029	0.590	0.015	0.002	0.001	0.067	0.007	0.112	0.084	0.824	0.008	0.063	0.128	0.269	0.003	0.655	0.013	0.003	0.000	0.002	0.003	0.025	0.038	0.035	0.513	0.542	0.163	0.001	0.002
pH	-0.044	-0.460	0.262	-0.501		0.316	0.901	0.126	0.302	0.866	0.467	0.638	0.238	0.250	0.047	0.296	0.090	0.070	0.113	0.593	0.793	0.523	0.397	0.001	0.784	0.944	0.883	0.804	0.064	0.147	0.407	0.028	0.347
water content	0.255	0.112	0.156	0.132	0.243		0.376	0.669	0.509	0.592	0.286	0.583	0.752	0.145	0.631	0.957	0.671	0.473	0.429	0.123	0.492	0.553	0.863	0.241	0.507	0.503	0.821	0.305	0.993	0.835	0.113	0.901	0.752
16S gene	0.644	0.087	0.750	0.551	0.031	0.215		0.000	0.000	0.000	0.000	0.000	0.026	0.982	0.185	0.306	0.000	0.142	0.058	0.844	0.000	0.000	0.000	0.298	0.000	0.000	0.013	0.000	0.564	0.026	0.000	0.005	0.000
16S trans	0.653	0.181	0.595	0.671	-0.363	0.105	0.887		0.000	0.000	0.000	0.000	0.010	0.886	0.020	0.138	0.008	0.043	0.010	0.874	0.000	0.000	0.000	0.019	0.000	0.000	0.017	0.001	0.304	0.001	0.002	0.000	0.000
nirK C-I gene	0.786	0.344	0.795	0.691	-0.250	0.162	0.892	0.938		0.000	0.000	0.001	0.030	0.663	0.040	0.436	0.008	0.014	0.040	0.415	0.000	0.000	0.000	0.028	0.000	0.000	0.051	0.000	0.102	0.012	0.003	0.001	0.000
nirK C-I trans	**0.651**	0.173	0.647	0.429	0.041	0.132	0.872	0.737	0.755		0.000	0.000	0.571	0.901	0.720	0.700	0.010	0.193	0.685	0.731	0.000	0.000	0.000	0.546	0.000	**0.000**	0.212	0.000	0.440	0.053	0.000	0.259	0.000
nirK C-II gene	0.629	0.187	0.576	0.594	-0.178	0.258	0.918	0.899	0.869	0.891		0.000	0.042	0.729	0.433	0.407	0.013	0.218	0.189	0.597	0.000	0.000	0.000	0.122	0.000	0.000	0.079	0.000	0.361	0.023	0.000	0.010	0.000
nirK C-II trans	**0.618**	0.077	0.635	0.377	0.116	0.135	0.866	0.726	0.721	0.988	0.875		0.639	0.607	0.668	0.745	0.003	0.326	0.680	0.984	0.000	0.000	0.000	0.762	0.000	**0.000**	0.147	0.000	0.712	0.043	0.000	0.300	0.000
nirK C-III gene	0.049	-0.091	0.157	0.407	-0.284	0.078	0.509	0.578	0.498	0.139	0.470	0.115		0.430	0.001	0.000	0.149	0.552	0.001	0.745	0.192	0.003	0.023	0.272	0.014	0.571	0.036	0.096	0.505	0.276	0.116	0.000	0.002
nirK C-III trans	-0.241	-0.156	0.049	0.055	0.278	-0.348	0.006	-0.035	-0.107	0.031	-0.085	0.126	-0.192		0.724	0.425	0.034	0.120	0.281	0.000	0.953	0.874	0.421	0.105	0.873	0.853	0.018	0.100	0.008	0.396	0.985	0.905	0.831
nirK C-IV gene	0.119	0.187	0.241	0.591	-0.460	-0.118	0.318	0.528	0.475	-0.088	0.191	-0.105	0.698	0.087		0.000	0.176	0.218	0.000	0.422	0.410	0.040	0.016	0.034	0.129	0.852	0.009	0.769	0.691	0.192	0.774	0.000	0.024
nirK C-IV trans	-0.160	-0.061	-0.069	0.435	-0.253	-0.013	0.248	0.353	0.190	-0.095	0.202	-0.080	0.752	0.194	0.737		0.205	0.264	0.000	0.123	0.995	0.068	0.134	0.386	0.212	0.739	0.007	0.751	0.379	0.661	0.515	0.000	0.048
nirS C-I gene	0.362	-0.139	0.666	0.362	0.399	0.104	0.772	0.589	0.586	0.573	0.559	0.638	0.345	0.489	0.324	0.305		0.788	0.037	0.062	0.003	0.000	0.000	0.707	0.000	0.010	0.000	0.111	0.114	0.453	0.005	0.048	0.001
nirS C-I trans	-0.452	-0.273	-0.392	-0.267	0.425	0.175	-0.350	-0.468	-0.551	-0.313	-0.297	-0.238	-0.146	0.369	-0.296	0.270	-0.066		0.620	0.105	0.036	0.132	0.084	0.041	0.157	0.194	0.956	0.090	0.059	0.075	0.998	0.154	0.126
nirS C-II gene	0.060	0.141	0.235	0.642	-0.375	-0.193	0.442	0.577	0.474	0.100	0.315	0.101	0.720	0.261	0.911	0.825	0.482	-0.122		0.104	0.257	0.007	0.003	0.183	0.030	0.603	0.001	0.551	0.867	0.180	0.627	0.000	0.003
nirS C-II trans	-0.354	-0.171	-0.169	0.110	0.131	-0.367	-0.049	-0.039	-0.199	-0.084	-0.130	0.005	-0.080	0.909	0.196	0.366	0.436	0.384	0.385		0.528	0.891	0.601	0.337	0.915	0.767	0.010	0.052	0.000	0.359	0.737	0.571	0.793
18S gene	0.785	0.247	0.811	0.560	-0.065	0.168	0.929	0.883	0.944	0.914	0.917	0.898	0.313	-0.014	0.201	0.001	0.646	-0.484	0.273	-0.154		0.000	0.000	0.184	0.000	0.000	0.086	0.000	0.221	0.018	0.000	0.033	0.000
18S transcript	0.531	0.102	0.615	0.647	-0.156	0.145	0.954	0.940	0.888	0.783	0.912	0.776	0.643	0.039	0.476	0.427	0.729	-0.358	0.594	0.034	0.872		0.000	0.163	0.000	0.000	0.003	0.000	0.731	0.023	0.000	0.000	0.000
nirKF gene	0.577	0.234	0.708	0.725	-0.206	0.043	0.910	0.935	0.923	0.757	0.852	0.757	0.517	0.196	0.542	0.357	0.748	-0.407	0.645	0.128	0.895	0.945		0.139	0.000	0.000	0.002	0.002	0.586	0.017	0.002	0.000	0.000
nirKF trans	**0.476**	0.599	0.108	0.663	-0.718	0.283	0.252	0.532	0.503	0.148	0.368	0.075	0.265	-0.383	0.488	0.211	-0.092	-0.474	0.319	-0.233	0.318	0.334	0.352		0.248	0.359	0.752	0.281	0.127	0.200	0.901	0.021	0.110
nosZ-1 gene	0.622	0.172	0.722	0.636	-0.067	0.162	0.982	0.914	0.918	0.869	0.939	0.857	0.552	0.039	0.361	0.300	0.736	-0.338	0.497	-0.026	0.937	0.974	0.943	0.279		0.000	0.010	0.000	0.472	0.035	0.000	0.002	0.000
nosZ-1 trans	**0.701**	0.265	0.673	0.511	-0.017	0.164	0.867	0.769	0.799	**0.987**	0.912	**0.974**	0.139	0.046	-0.046	-0.082	0.574	-0.311	0.128	-0.073	0.937	0.789	0.790	0.223	0.877		0.187	0.000	0.423	0.060	0.000	0.207	0.000
nosZ-2 gene	0.099	-0.061	0.352	0.479	0.036	-0.056	0.559	0.542	0.453	0.300	0.413	0.346	0.483	0.538	0.583	0.596	0.771	-0.014	0.699	0.578	0.405	0.645	0.670	0.078	0.575	0.317		0.455	0.104	0.619	0.108	0.002	0.003
Arc 16S gene	0.611	0.277	0.616	0.485	-0.061	0.249	0.813	0.679	0.756	0.802	0.827	0.739	0.393	-0.389	0.072	0.078	0.378	-0.400	0.146	-0.452	0.798	0.765	0.656	0.261	0.814	0.787	0.182		0.140	0.123	0.000	0.106	0.000
Arc 16S transcript	-0.391	-0.368	-0.266	-0.160	0.432	-0.002	-0.141	-0.249	-0.387	-0.188	-0.222	-0.091	-0.163	0.586	-0.098	0.214	0.375	0.440	0.041	0.739	-0.295	-0.084	-0.134	-0.363	-0.176	-0.195	0.385	-0.352		0.110	0.908	0.611	0.572
AOA amoA gene	0.495	-0.170	0.336	0.149	-0.346	-0.051	0.510	0.682	0.566	0.451	0.519	0.468	0.264	-0.207	0.313	0.108	0.183	-0.419	0.321	-0.223	0.537	0.519	0.541	0.308	0.485	0.439	0.122	0.367	-0.378		0.192	0.067	0.023
AOA amoA trans	0.429	-0.058	0.508	0.333	0.202	0.376	0.860	0.674	0.646	0.866	0.893	0.875	0.373	-0.005	-0.071	0.159	0.613	-0.001	0.119	-0.083	0.782	0.802	0.671	0.031	0.849	0.845	0.381	0.790	-0.029	0.313		0.153	0.000
AOB amoA gene	0.225	0.134	0.289	0.684	-0.504	-0.031	0.614	0.796	0.689	0.273	0.573	0.251	0.838	0.029	0.875	0.735	0.458	-0.340	0.870	0.139	0.490	0.780	0.761	0.526	0.668	0.303	0.667	0.383	-0.125	0.429	0.341		0.000
AOB amoA trans	**0.869**	-0.058	-0.027	-0.062	-0.661	0.902	0.624	0.210	0.781	0.819	0.828	0.881	0.547	0.825	0.416	-0.621	-0.447	0.306	0.177	0.538	0.612	-0.462	0.460	0.747	0.913	0.778	0.725	0.580	0.706	0.371	0.838	0.415	0.835

Table 5-3. Linear dependences among N_2O emission rate and physicochemical and microbial variables in upland field after basal chemical fertilization

Factor	N_2O	NO2-N	NH4-N	NO3-N	pH	water content	16S gene	16S trans	nirKC-I gene	nirKC-I trans	nirKC-II gene	nirKC-II trans	nirKC-III gene	nirKC-III trans	nirKC-IV gene	nirKC-IV trans	nirSC-I gene	nirSC-I trans	nirSC-II gene	nirSC-II trans	18S gene	18S transcript	nirKF gene	nirKF trans	nosZ-1 gene	nosZ-1 trans	nosZ-2 gene	Arc 16S gene	Arc 16S transcript	AOA amoA gene	AOA amoA trans	AOB amoA	AOB amoA trans
N_2O		0.875	**0.070**	0.394	**0.054**	0.380	0.028	0.134	0.128	**0.000**	0.109	0.801	0.275	0.491	0.087	0.257	0.210	0.023	0.495	0.832	0.421	0.985	0.535	**0.004**	0.410	0.218	0.900	0.064	0.303	0.126	0.086	0.011	**0.000**
NO2-N	0.039		0.003	0.224	0.113	0.742	0.640	0.157	0.058	0.030	0.736	0.001	0.583	0.771	0.340	0.610	0.314	0.467	0.000	0.723	0.117	0.044	0.874	0.636	0.374	0.754	0.160	0.274	0.066	0.645	0.706	0.089	0.158
NH4-N	**0.425**	0.650		0.002	0.677	0.885	0.643	0.000	0.000	0.004	0.526	0.035	0.052	0.291	0.003	0.177	0.273	0.059	0.044	0.657	0.011	0.118	0.757	0.013	0.062	0.812	0.115	0.012	0.025	0.934	0.179	0.000	0.019
NO3-N	0.208	0.293	0.658		0.168	0.407	0.230	0.010	0.001	0.215	0.448	0.248	0.460	0.372	0.011	0.228	0.986	0.102	0.259	0.340	0.035	0.444	0.454	0.008	0.541	0.685	0.535	0.033	0.279	0.437	0.357	0.000	0.339
pH	**-0.449**	0.376	0.102	-0.330		0.234	0.000	0.503	0.993	0.564	0.020	0.122	0.559	0.691	0.455	0.099	0.000	0.018	0.565	0.664	0.137	0.274	0.162	0.132	0.715	0.837	0.227	0.162	0.197	0.000	0.054	0.175	0.275
water content	0.214	-0.081	-0.036	-0.202	0.287		0.069	0.225	0.640	0.922	0.074	0.462	0.698	0.428	0.545	0.437	0.402	0.465	0.297	0.606	0.035	0.662	0.154	0.104	0.366	0.870	0.354	0.178	0.570	0.072	0.053	0.980	0.605
16S gene	-0.504	0.115	-0.114	-0.289	0.788	0.426		0.082	0.852	0.232	0.001	0.741	0.798	0.971	0.745	0.202	0.000	0.008	0.384	0.738	0.093	0.343	0.058	0.577	0.598	0.990	0.490	0.016	0.244	0.000	0.020	0.214	0.229
16S trans	0.357	0.338	0.783	0.577	-0.164	-0.292	-0.40		0.022	0.033	0.123	0.283	0.185	0.474	0.072	0.082	0.807	0.046	0.039	0.903	0.004	0.454	0.101	0.066	0.505	0.923	0.081	0.002	0.490	0.265	0.178	0.009	0.136
nirK C-I gene	0.362	0.442	0.738	0.718	-0.002	0.115	0.046	0.521		0.016	0.769	0.045	0.409	0.135	0.001	0.672	0.299	0.619	0.182	0.321	0.165	0.030	0.725	0.001	0.915	0.373	0.092	0.155	0.005	0.452	0.805	0.000	0.035
nirK C-I trans	**0.793**	0.498	0.622	0.298	-0.141	-0.024	-0.28	0.491	0.545		0.308	0.024	0.378	0.119	0.032	0.332	0.852	0.158	0.011	0.615	0.101	0.353	0.249	0.027	0.536	0.046	0.159	0.028	0.041	0.519	0.179	0.005	0.000
nirK C-II gene	-0.380	0.083	-0.155	-0.185	0.528	0.419	0.692	-0.36	0.072	-0.247		0.918	0.135	0.538	0.662	0.004	0.171	0.001	0.548	0.610	0.041	0.541	0.229	0.478	0.336	0.500	0.803	0.004	0.853	0.001	0.000	0.409	0.264
nirK C-II trans	0.062	0.714	0.485	0.278	0.367	-0.180	0.081	0.260	0.465	0.515	-0.02		0.070	0.001	0.047	0.856	0.034	0.622	0.003	0.011	0.108	0.157	0.557	0.888	0.944	0.017	0.003	0.035	0.001	0.751	0.584	0.152	0.207
nirK C-III gene	-0.264	-0.134	-0.452	-0.180	-0.143	-0.095	0.063	-0.31	-0.20	-0.215	0.356	-0.42		0.016	0.103	0.139	0.090	0.299	0.931	0.012	0.105	0.548	0.390	0.265	0.008	0.841	0.097	0.035	0.009	0.538	0.117	0.232	0.449
nirK C-III trans	0.168	0.072	0.255	0.217	0.098	-0.193	0.009	0.175	0.356	0.370	-0.15	0.697	-0.54		0.033	0.811	0.033	0.305	0.869	0.000	0.085	0.719	0.817	0.698	0.961	0.008	0.002	0.017	0.002	0.992	0.343	0.275	0.285
nirK C-IV gene	0.404	0.232	0.638	0.568	0.183	0.148	0.080	0.422	0.702	0.494	-0.10	0.462	-0.38	0.490		0.987	0.026	0.507	0.290	0.024	0.751	0.435	0.727	0.015	0.408	0.458	0.161	0.103	0.011	0.230	0.416	0.002	0.061
nirK C-IV trans	-0.273	-0.125	-0.323	-0.290	0.390	0.190	0.307	-0.40	-0.10	-0.235	0.631	0.045	0.352	0.059	0.004		0.364	0.001	0.631	0.839	0.012	0.883	0.727	0.107	0.032	0.264	0.741	0.018	0.670	0.019	0.003	0.162	0.223
nirS C-I gene	-0.302	0.244	0.265	0.004	0.818	0.204	0.737	-0.06	0.252	-0.046	0.328	0.487	-0.39	0.491	0.510	0.221		0.073	0.917	0.013	0.674	0.227	0.112	0.642	0.386	0.542	0.043	0.839	0.005	0.000	0.487	0.961	0.607
nirS C-I trans	-0.520	-0.177	-0.441	-0.387	0.537	0.179	0.587	-0.46	-0.12	-0.337	0.701	0.121	0.251	0.249	-0.16	0.709	0.420		0.320	0.368	0.041	0.769	0.725	0.049	0.042	0.097	0.484	0.052	0.981	0.003	0.000	0.037	0.063
nirS C-II gene	0.167	0.785	0.467	0.273	0.141	-0.253	-0.21	0.476	0.320	0.571	-0.14	0.647	0.021	0.041	0.256	-0.11	-0.02	-0.24		0.628	0.310	0.263	0.015	0.879	0.551	0.188	0.190	0.118	0.435	0.598	0.658	0.216	0.122
nirS C-II trans	0.052	-0.087	0.109	0.232	0.107	-0.126	0.082	-0.03	0.240	0.123	-0.12	0.567	-0.56	0.906	0.515	0.050	0.560	0.219	-0.11		0.406	0.940	0.846	0.909	0.862	0.041	0.041	0.067	0.004	0.897	0.336	0.406	0.781
18S gene	0.196	0.372	0.567	0.486	-0.354	-0.485	-0.39	0.633	0.332	0.388	-0.47	0.380	-0.38	0.405	0.078	-0.56	-0.10	-0.47	0.246	0.202		0.297	0.814	0.218	0.163	0.939	0.042	0.001	0.135	0.017	0.006	0.032	0.190
18S transcript	-0.005	0.468	0.371	0.187	0.264	0.107	0.230	0.183	0.498	0.226	0.150	0.338	-0.14	0.088	0.190	-0.03	0.291	-0.07	0.270	-0.01	0.253		0.845	0.543	0.874	0.711	0.108	0.552	0.002	0.322	0.852	0.235	0.439
nirKF gene	0.152	-0.039	-0.076	0.183	-0.334	-0.340	-0.44	0.387	0.087	0.278	-0.29	0.144	0.209	0.057	0.086	-0.08	-0.37	-0.08	0.549	-0.04	0.058	-0.048		0.904	0.018	0.059	0.405	0.292	0.479	0.132	0.937	0.844	0.579
nirKF trans	**0.624**	0.116	0.558	0.588	-0.359	0.384	-0.13	0.430	0.708	0.506	-0.17	0.035	-0.26	0.095	0.551	-0.38	-0.11	-0.45	0.037	0.028	0.296	0.149	0.030		0.073	0.846	0.810	0.135	0.200	0.618	0.367	0.000	0.008
nosZ-1 gene	-0.201	-0.216	-0.436	-0.150	-0.090	-0.220	-0.12	-0.16	-0.02	-0.151	0.233	-0.01	0.592	-0.01	-0.20	0.494	-0.21	0.472	0.146	-0.04	-0.33	0.039	0.536	-0.421		0.031	0.979	0.343	0.389	0.885	0.114	0.276	0.362
nosZ-1 trans	0.297	0.077	-0.059	-0.100	0.051	0.040	0.003	-0.02	0.217	0.463	0.165	0.539	-0.04	0.593	0.181	0.270	0.149	0.392	0.316	0.474	-0.01	0.091	0.441	-0.048	0.495		0.067	0.411	0.065	0.987	0.465	0.899	0.097
nosZ-2 gene	-0.031	0.336	0.374	0.152	0.291	-0.225	0.169	0.410	0.397	0.337	-0.06	0.651	-0.39	0.664	0.335	-0.08	0.468	0.171	0.314	0.473	0.472	0.380	0.203	0.059	0.007	0.429		0.094	0.006	0.646	0.658	0.491	0.501
Arc 16S gene	-0.432	-0.265	-0.566	-0.492	0.334	0.323	0.545	-0.66	-0.34	-0.503	0.623	-0.48	0.485	-0.53	-0.38	0.536	0.050	0.452	-0.37	-0.42	-0.72	0.146	-0.255	-0.356	0.230	-0.201	-0.395		0.252	0.012	0.003	0.018	0.074
Arc 16S	0.249	0.430	0.511	0.262	0.310	0.139	0.281	0.169	0.611	0.473	0.046	0.696	-0.58	0.676	0.571	-0.10	0.618	-0.00	0.190	0.627	0.356	0.667	-0.173	0.308	-0.210	0.432	0.605	-0.27		0.372	0.425	0.049	0.061
AOA amoA gene	-0.363	0.113	0.020	-0.190	0.824	0.422	0.863	-0.27	0.183	-0.158	0.710	0.078	0.151	0.003	0.289	0.532	0.725	0.637	-0.12	0.032	-0.54	0.240	-0.358	-0.122	0.036	-0.004	0.113	0.562	0.217		0.005	0.472	0.403
AOA amoA trans	-0.405	-0.093	-0.322	-0.224	0.448	0.450	0.529	-0.32	-0.06	-0.322	0.850	-0.13	0.372	-0.23	-0.19	0.646	0.170	0.763	-0.10	-0.23	-0.60	0.046	0.020	-0.219	0.374	0.179	-0.109	0.651	-0.195	0.621		0.166	0.105
AOB amoA gene	0.567	0.401	0.802	0.876	-0.325	0.006	-0.29	0.583	0.857	0.612	-0.20	0.342	-0.28	0.264	0.653	-0.33	-0.01	-0.48	0.298	0.202	0.493	0.286	0.048	0.788	-0.263	0.031	0.168	-0.53	0.457	-0.17	-0.33		0.006
AOB amoA trans	**0.902**	0.337	0.533	0.232	-0.264	0.127	-0.29	0.355	0.485	0.946	-0.27	0.304	-0.18	0.259	0.438	-0.29	-0.12	-0.43	0.368	0.068	0.314	0.189	0.136	0.591	-0.222	0.392	0.165	-0.41	0.438	-0.20	-0.38	0.606	

(a)

(b)

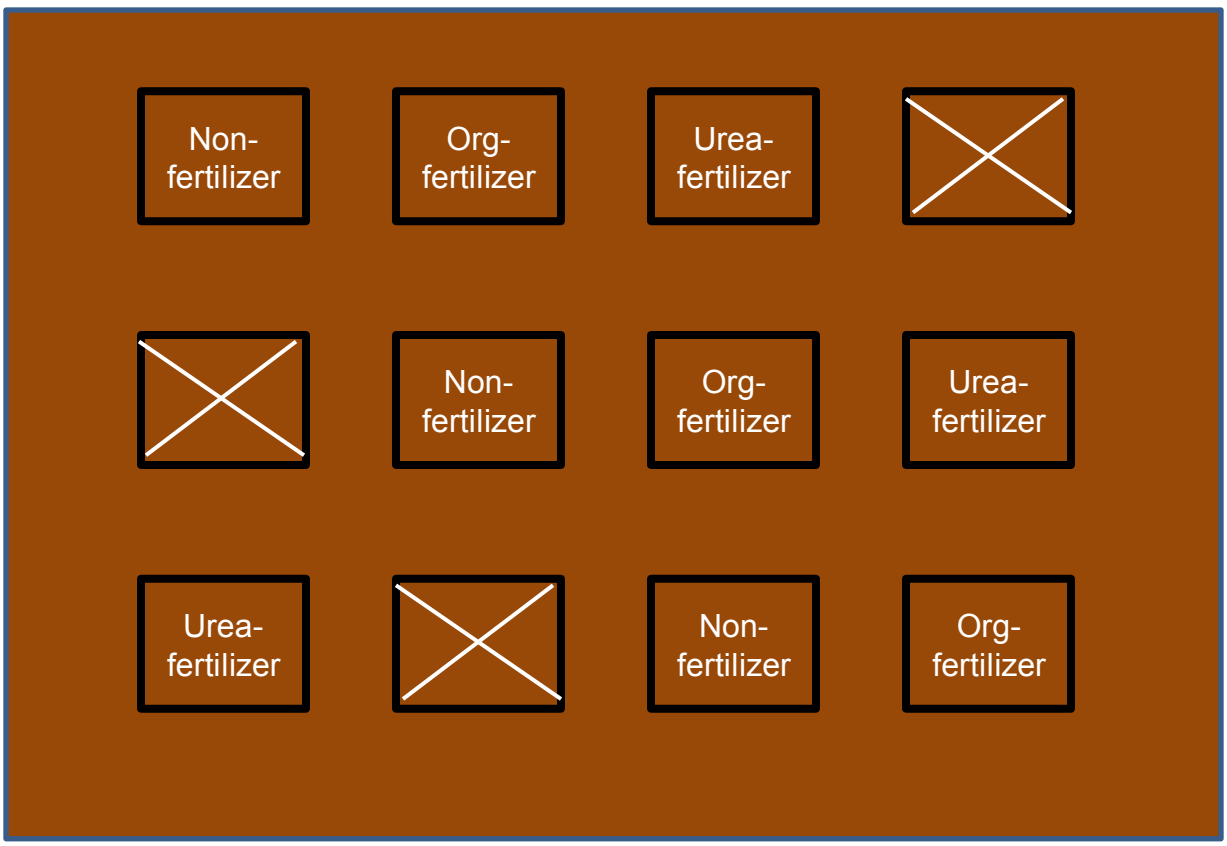

Fig. 5-1 the experimental upland field without cultivation in 2012. (a) the site scene and chamber positions in upland field. (b) the experimental design in the different plots.

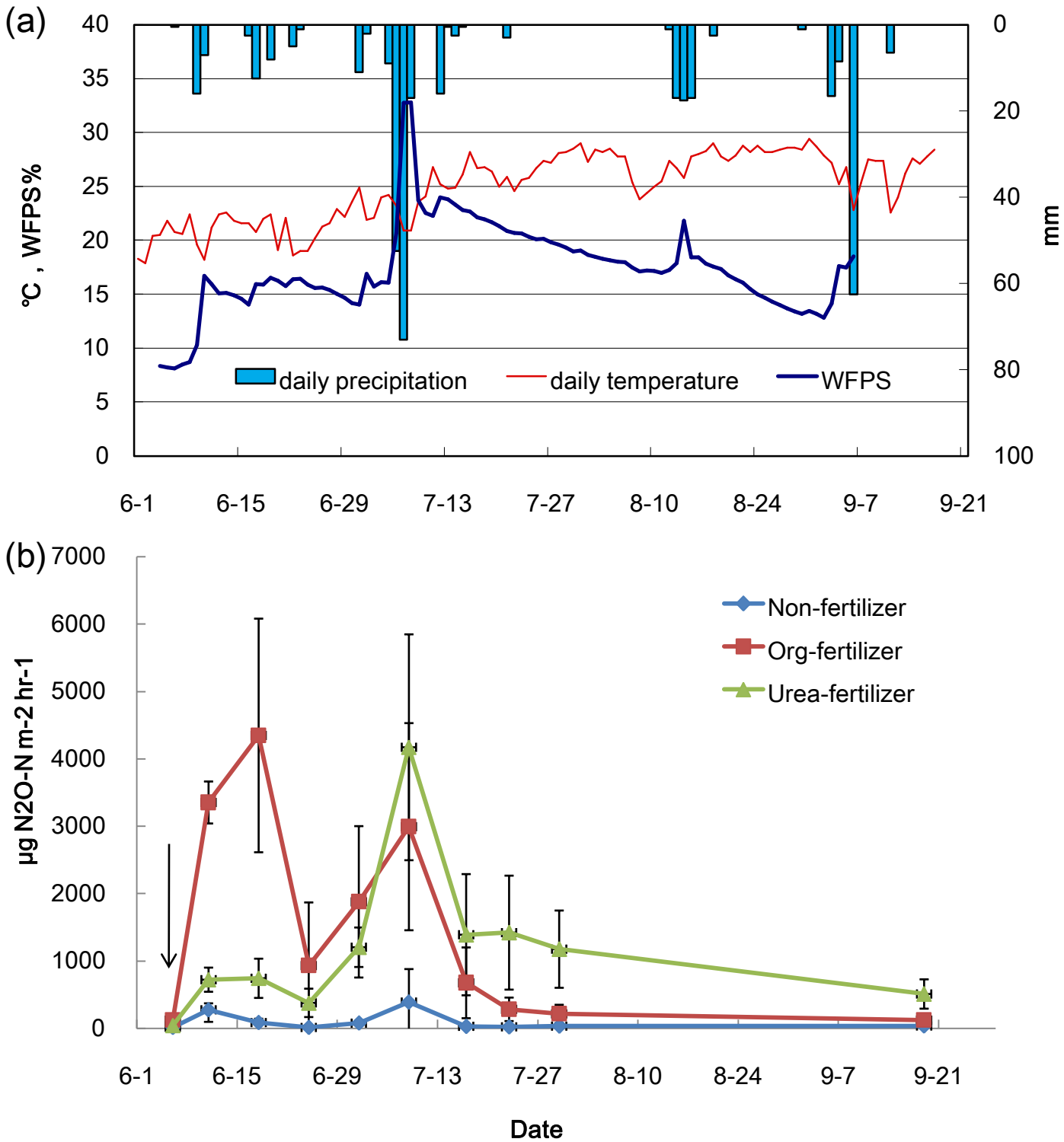

Fig. 5-2 Soil water-filled pore space (WFPS), daily precipitation and daily temperature (a) and N_2O fluxes (b) in an upland field during the cultivation period. The error bars represent the standard deviations (n=3). The arrows indicate the dates of basal fertilizer application

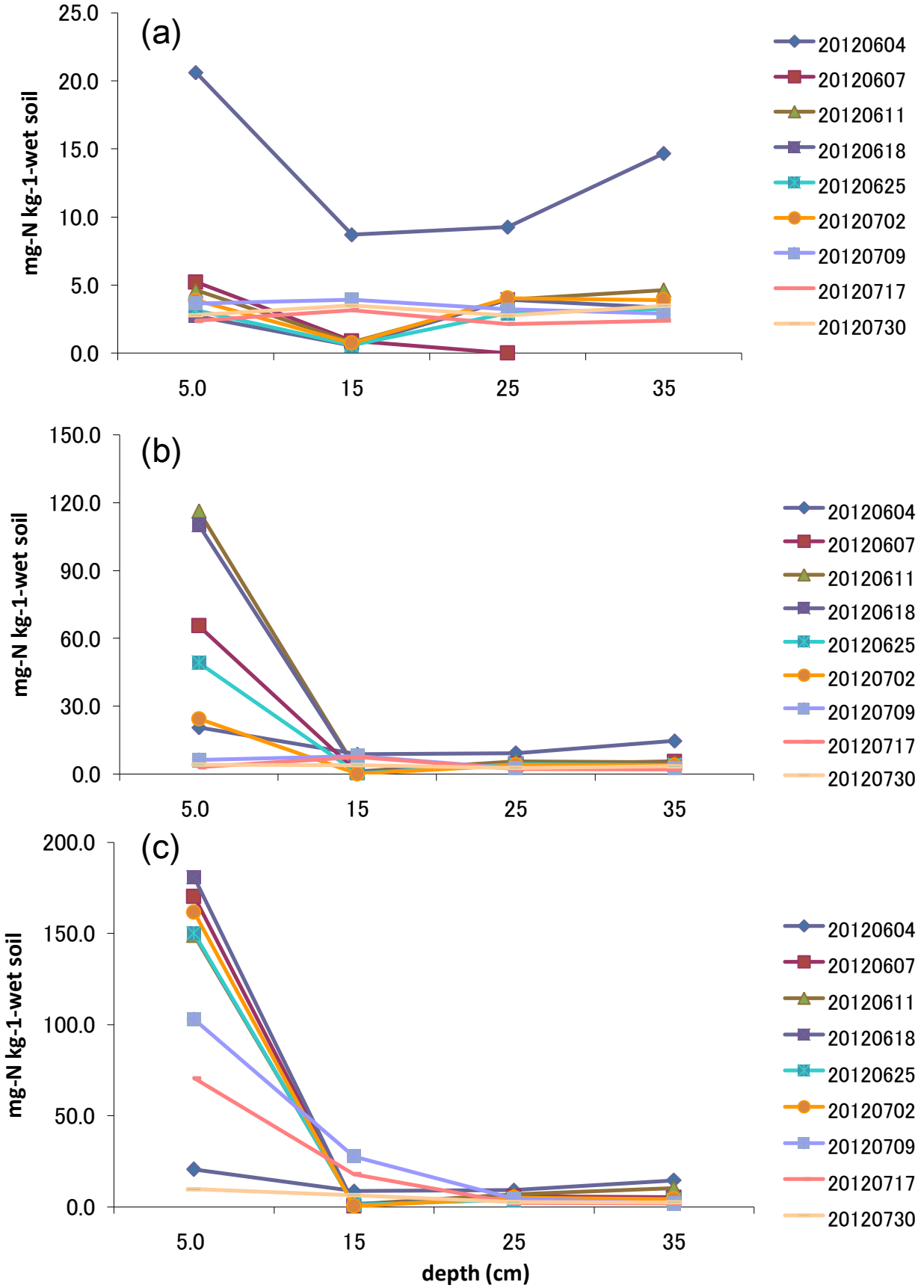

Fig. 5-3 Change of soil NH4+ concentration at different depth in different plots. (a) plots applied with no fertilizer. (b) plots applied with organic fertilizer. (c) plots applied with urea fertilizer

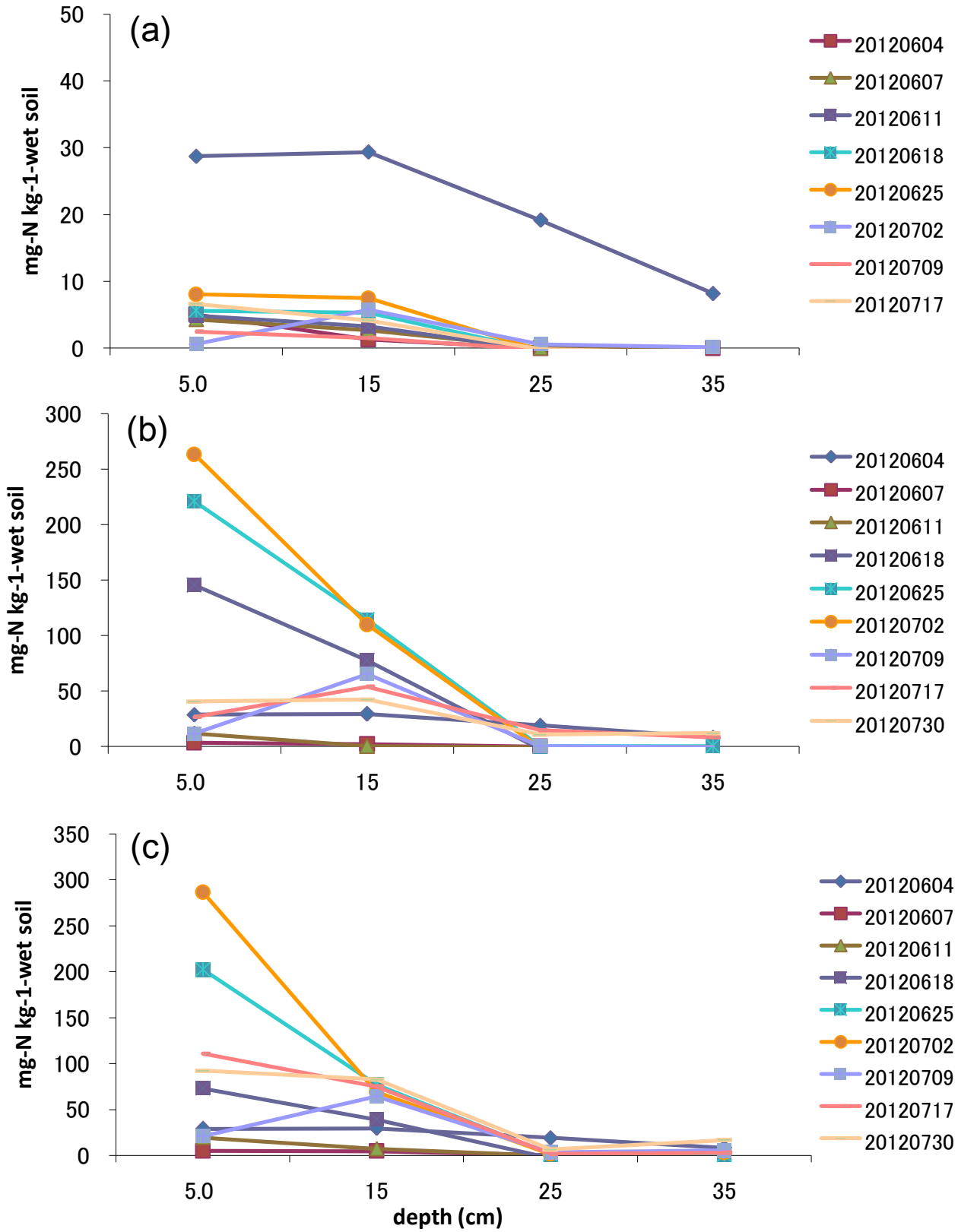

Fig. 5-4 Change of soil NO3- concentration at different depth in different plots. (a) plots applied with no fertilizer. (b) plots applied with organic fertilizer. (c) plots applied with urea fertilizer

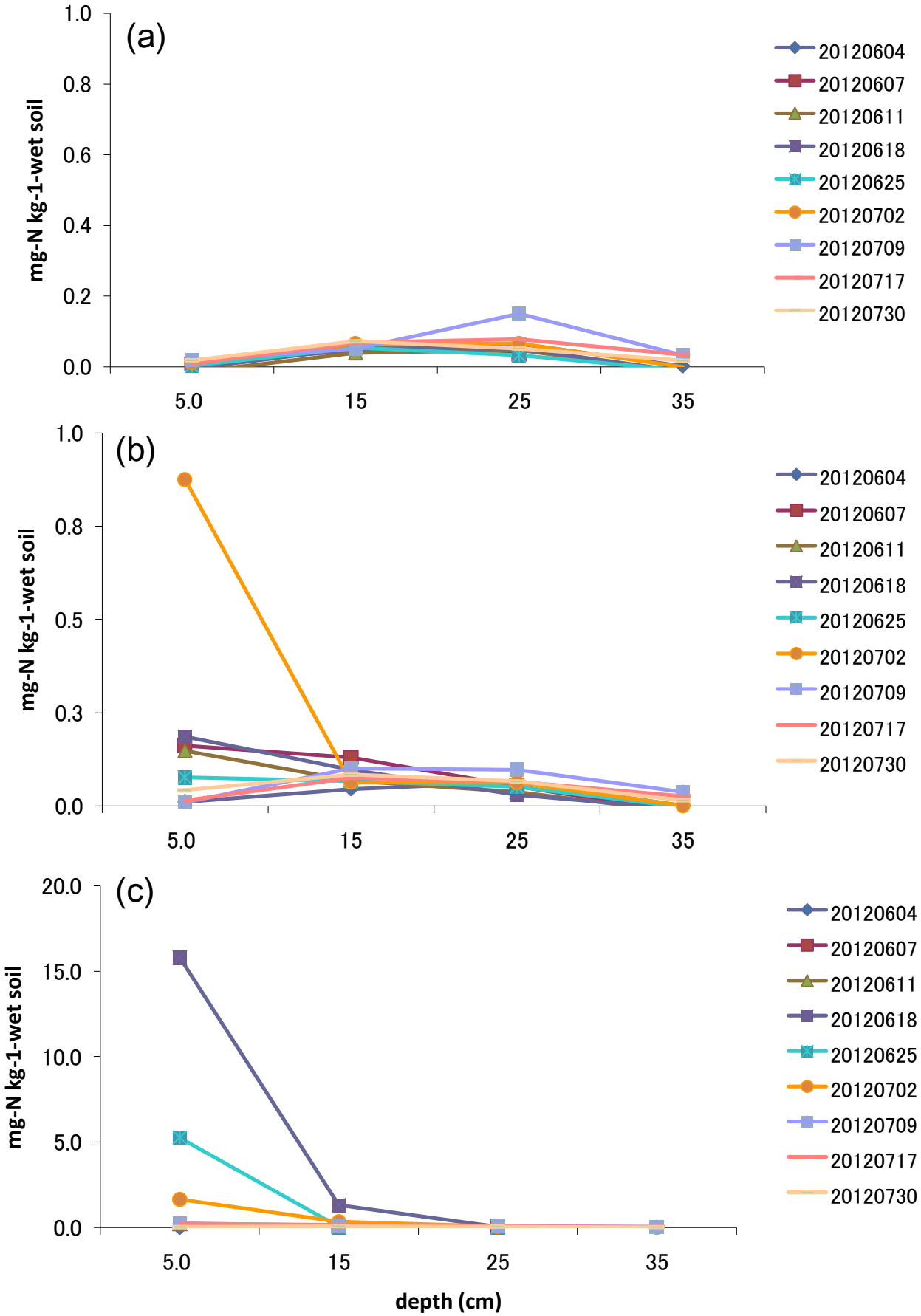

Fig. 5-5 Change of soil NO2- concentration at different depth in different plots. (a) plots applied with no fertilizer. (b) plots applied with organic fertilizer. (c) plots applied with urea fertilizer

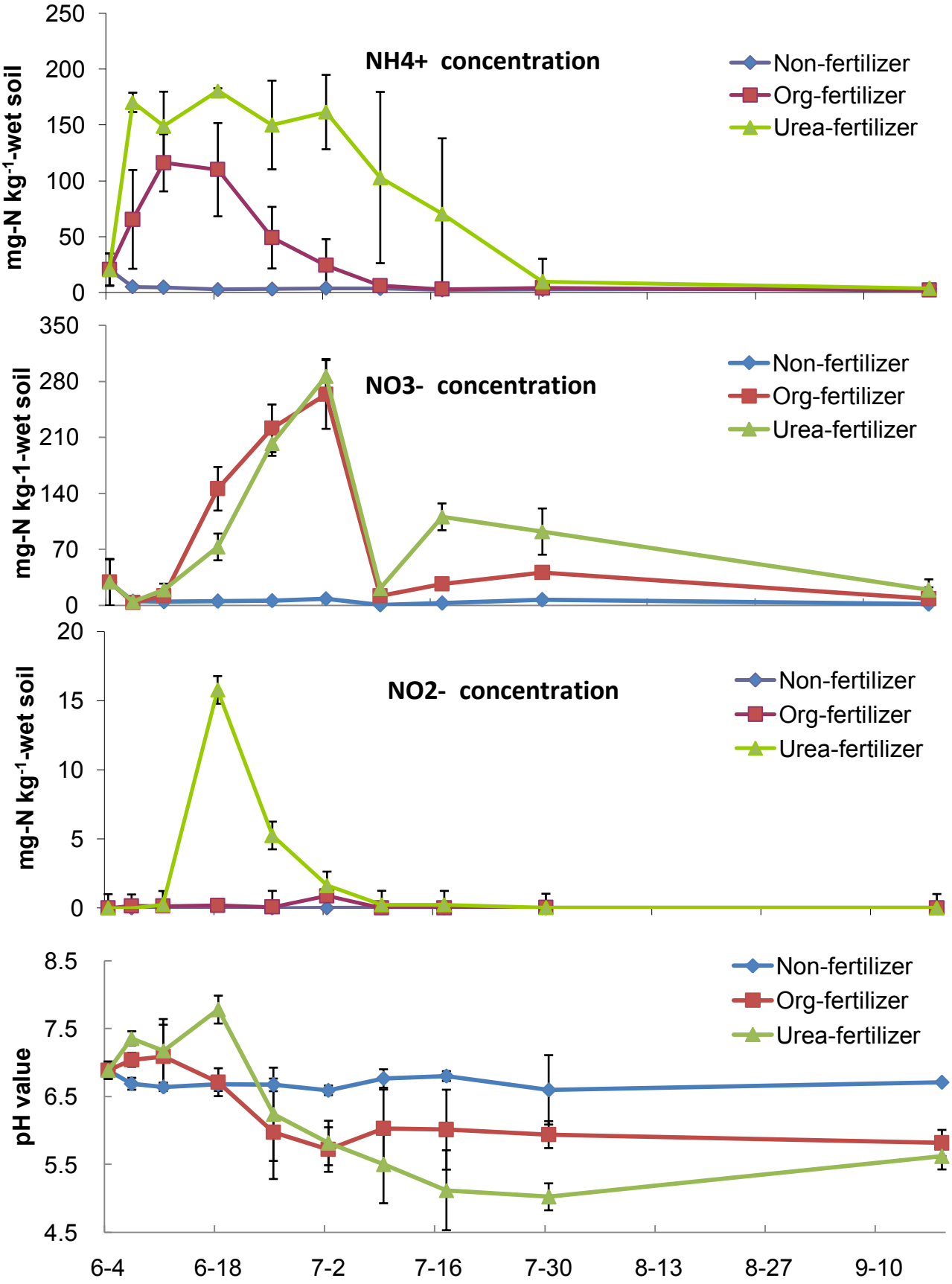

Fig. 5-6 Soil NH_4^+-N, NO_3^--N and NO_3^--N concentrations and soil pH in upland field during the observation period. The error bars represent the standard deviations (n=3).

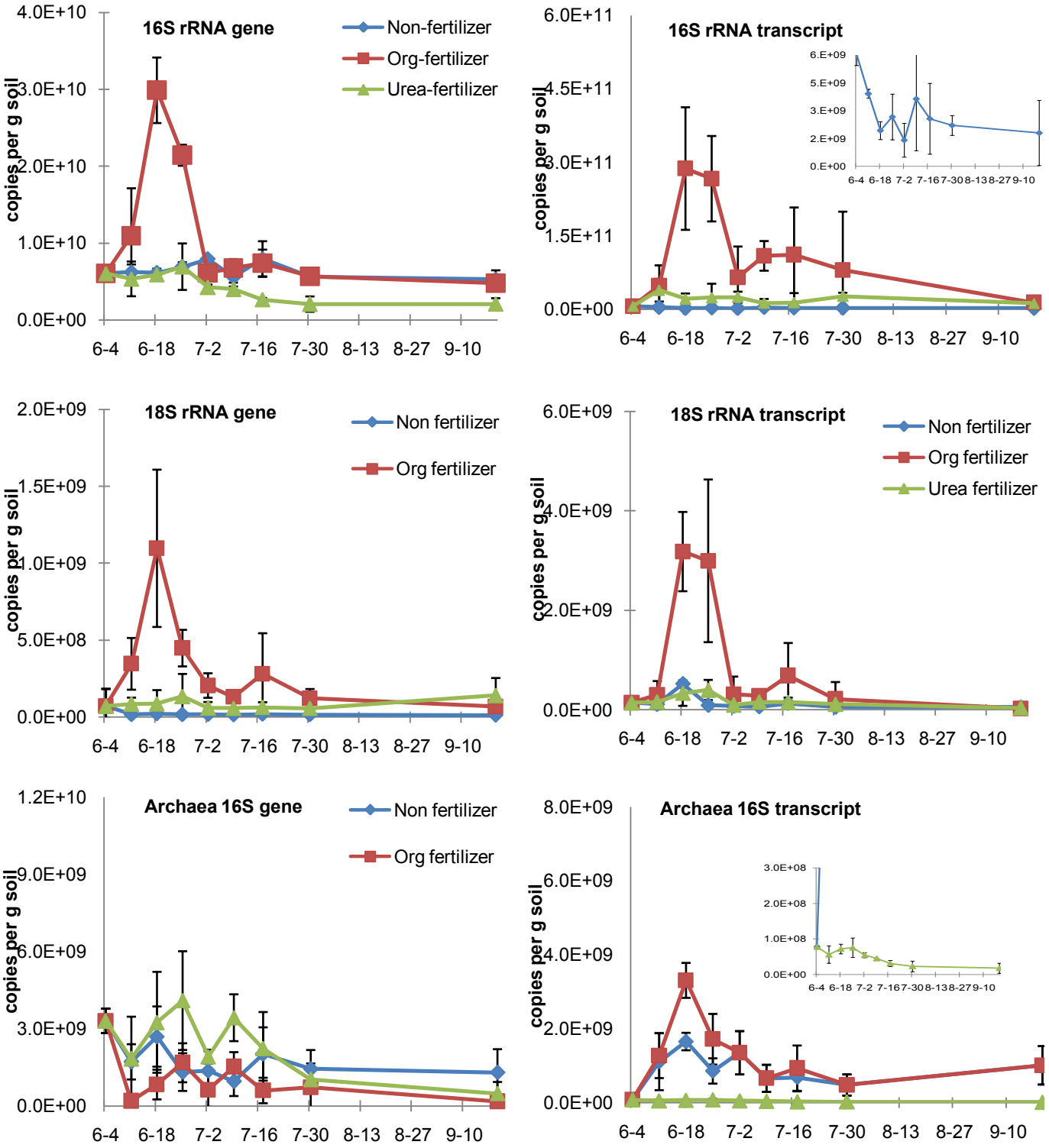

Fig. 5-7 The abundance and expression of bacterial and archaeal 16S rRNA and fungal 18S rRNA gene in upland field after the basal N fertilization. Statistically significant differences (least significant difference, $p<0.05$) between the plots applied with non fertilizers and fertilizers at a certain time point are indicated by small letters above the individual data points (a, between the plots applied with organic fertilizers and no fertilizers; b, between the plots applied with chemical fertilizers and no fertilizers)

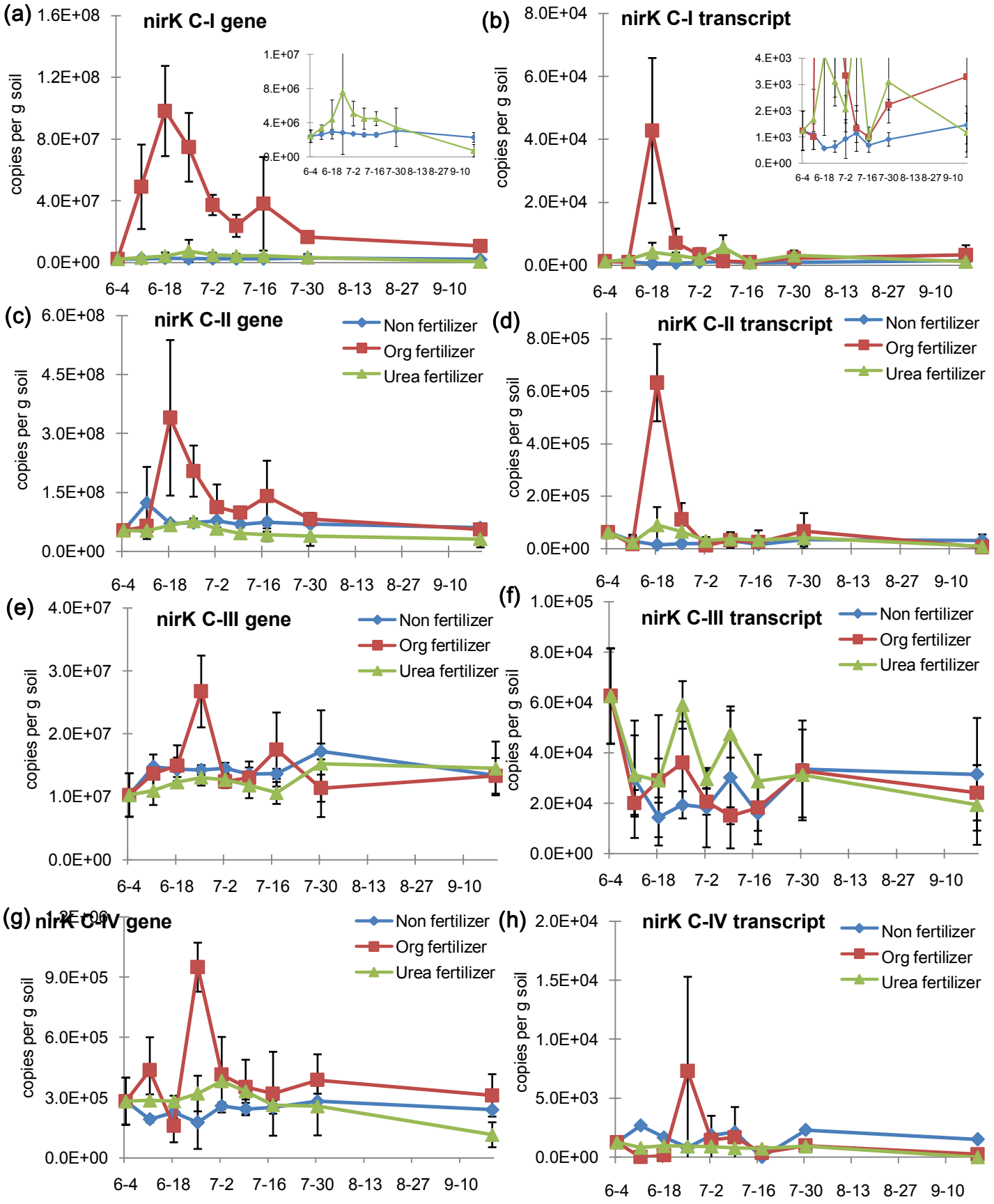

Fig. 5-8 The abundance and expression of prokaryotic *nirK* in upland field after the basal N fertilization. Statistically significant differences (least significant difference, $p<0.05$) between the plots applied with non fertilizers and fertilizers at a certain time point are indicated by small letters above the individual data points (a, between the plots applied with organic fertilizers and no fertilizers; b, between the plots applied with chemical fertilizers and no fertilizers)

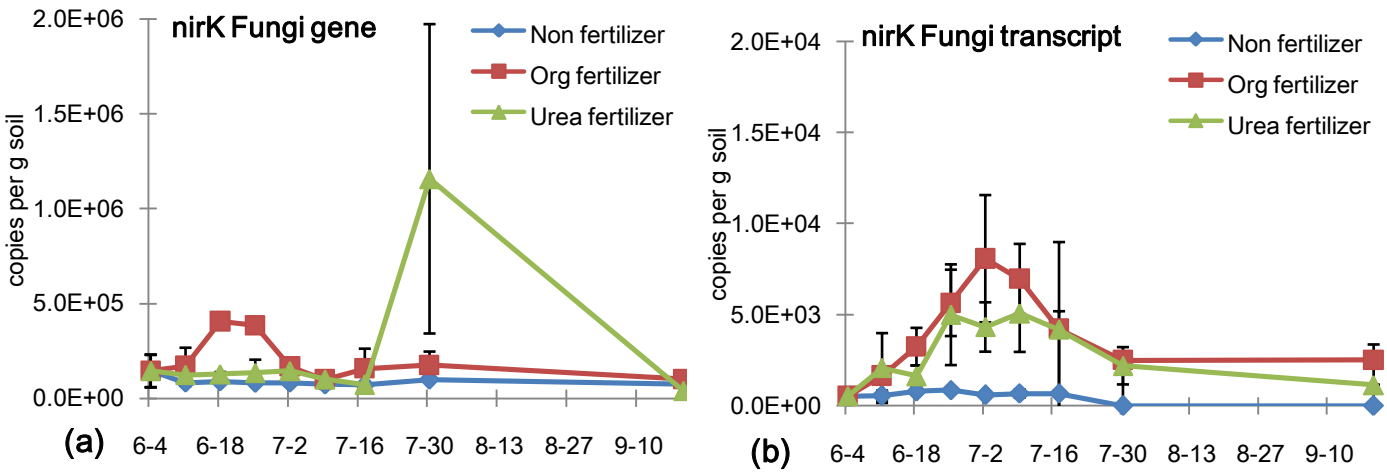

Fig. 5-9 The abundance and expression of fungal *nirK* in upland field after the basal N fertilization. Statistically significant differences (least significant difference, $p<0.05$) between the plots applied with non fertilizers and fertilizers at a certain time point are indicated by small letters above the individual data points (a, between the plots applied with organic fertilizers and no fertilizers; b, between the plots applied with chemical fertilizers and no fertilizers)

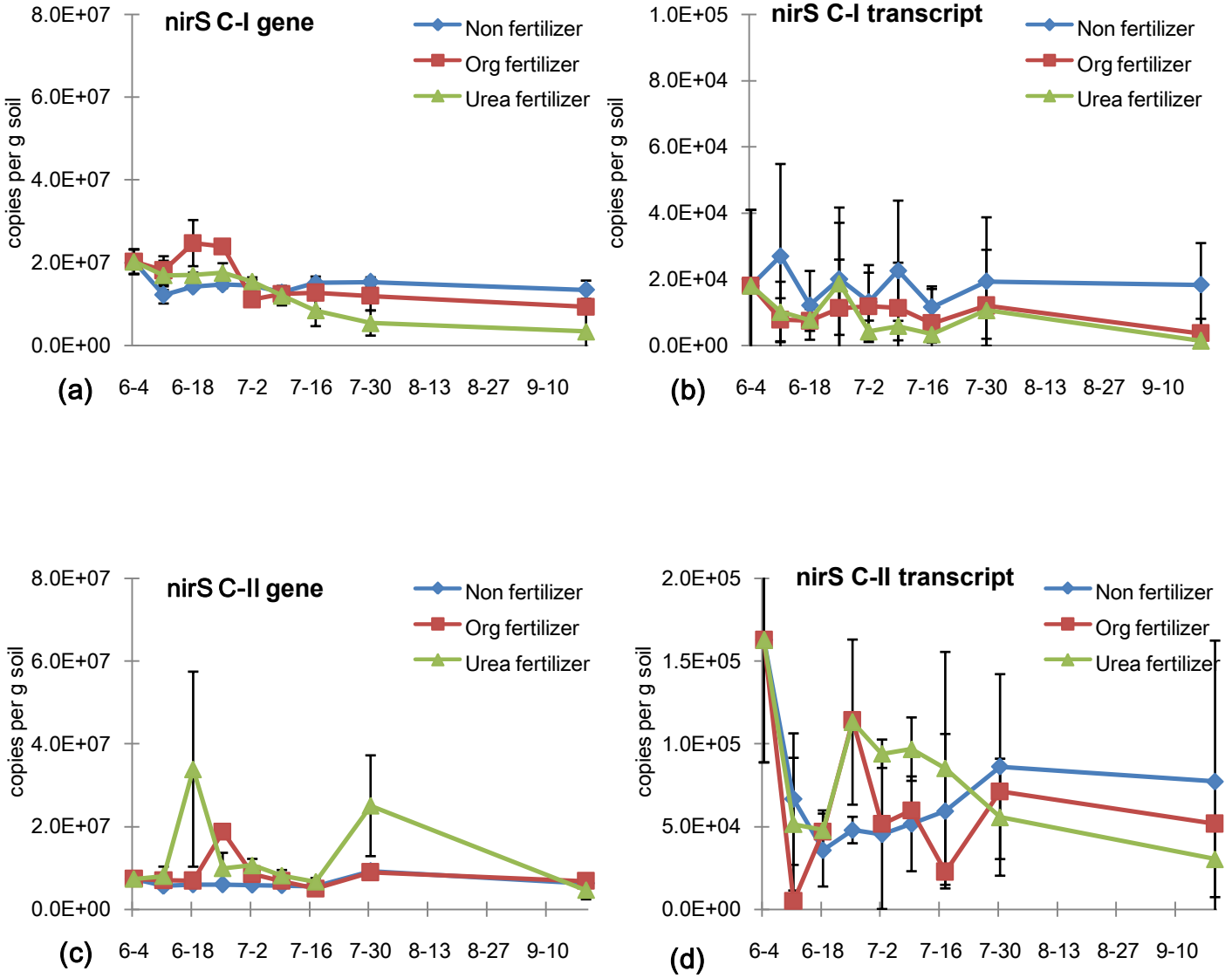

Fig. 5-10 The abundance and expression of prokaryotic *nirS* in upland field after the basal N fertilization. Statistically significant differences (least significant difference, $p<0.05$) between the plots applied with non fertilizers and fertilizers at a certain time point are indicated by small letters above the individual data points (a, between the plots applied with organic fertilizers and no fertilizers; b, between the plots applied with chemical fertilizers and no fertilizers)

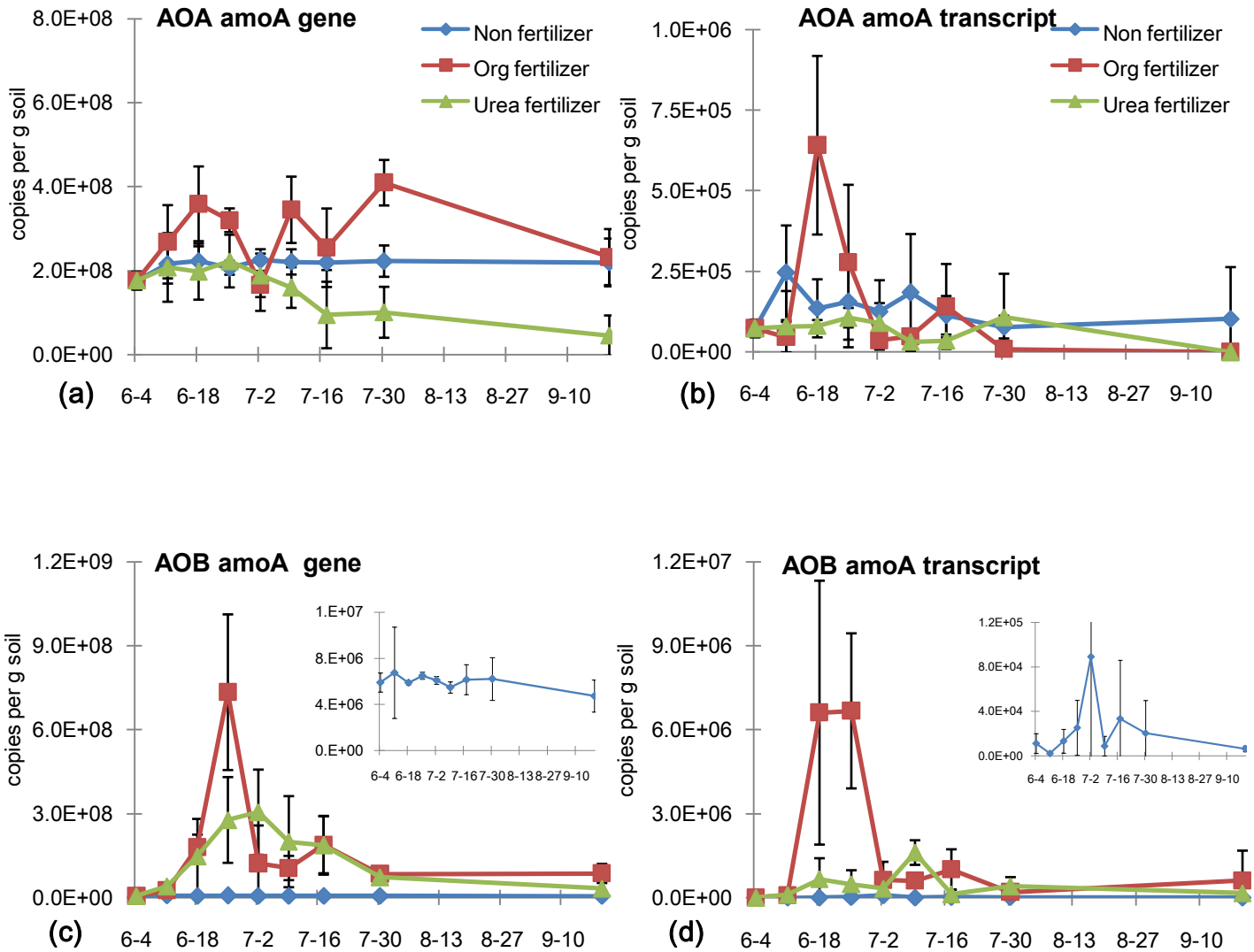

Fig. 5-11 The abundance and expression of bacterial and archaeal *amoA* in upland field after the basal N fertilization. Statistically significant differences (least significant difference, $p<0.05$) between the plots applied with non fertilizers and fertilizers at a certain time point are indicated by small letters above the individual data points (a, between the plots applied with organic fertilizers and no fertilizers; b, between the plots applied with chemical fertilizers and no fertilizers)

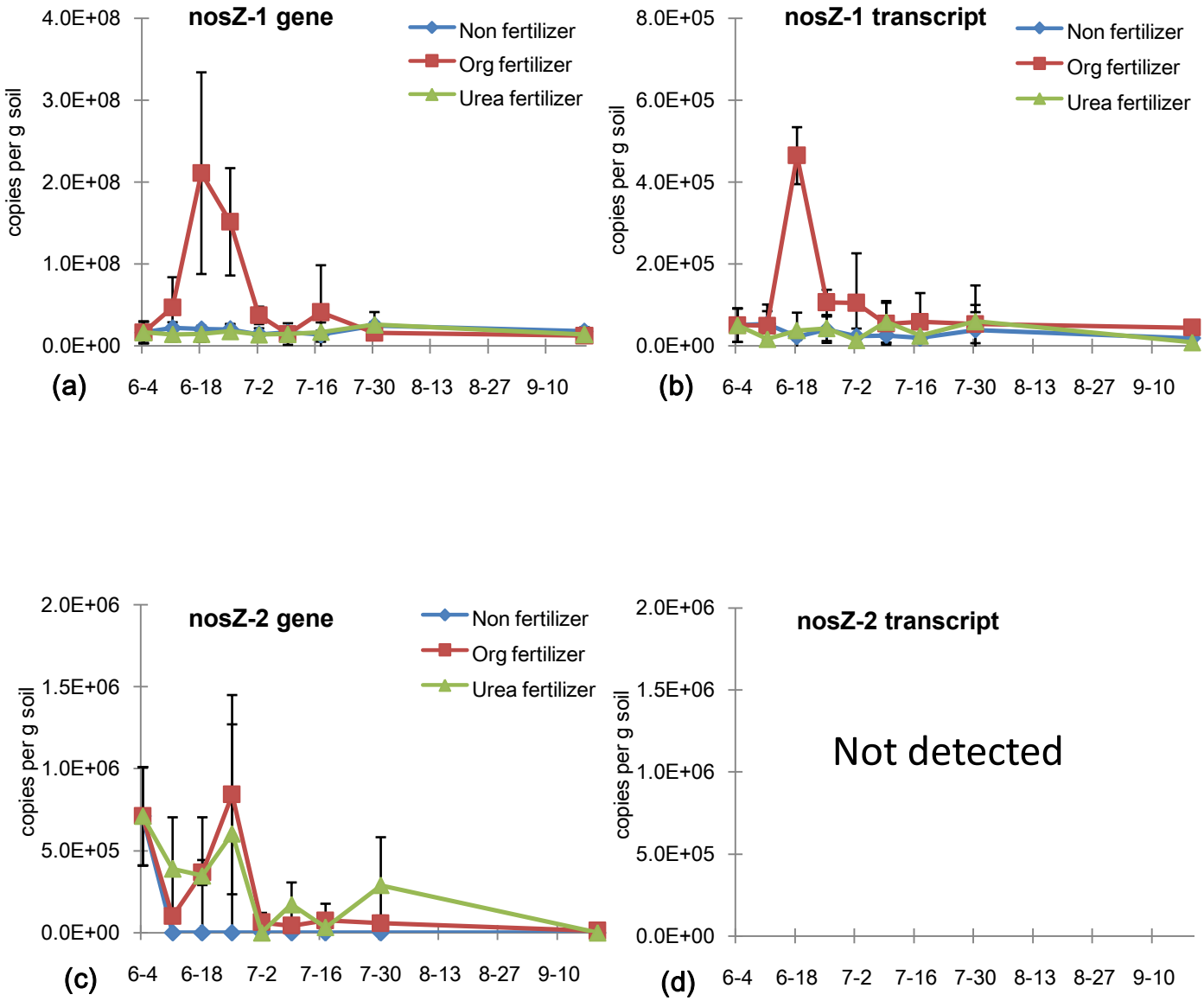

Fig. 5-12 The abundance and expression of prokaryotic *nosZ* in upland field after the basal N fertilization. Statistically significant differences (least significant difference, $p<0.05$) between the plots applied with non fertilizers and fertilizers at a certain time point are indicated by small letters above the individual data points (a, between the plots applied with organic fertilizers and no fertilizers; b, between the plots applied with chemical fertilizers and no fertilizers)

Chapter 6

N_2O emission from upland field soil through fungal denitrification after additional organic fertilization

6.1 Introduction

As described previously, N_2O emissions are greatly stimulated after nitrogen fertilization because N input enhances the microbial N_2O-producing activities in soils.Organic fertilizers are now widely employed instead of chemical fertilizers for the development of sustainable agriculture and the integration of crop nutrition (Inubushi et al., 2000). In particular, the granular organic fertilizers are commonly used due to their ease of transportation, storage and handling. However, the application of organic fertilizers contributes to higher N_2O emission from soils compared with chemical fertilizers (Akiyama and Tsuruta, 2003; Jones et al., 2007; Hayakawa et al., 2009; Toyoda et al., 2011).

N_2O is produced via nitrification and denitrification processes in soils (Davidson, 1991; Conrad, 1996). A wide phylogenetic range of bacteria are involved in denitrification, in which nitrate and nitrite are reduced to gaseous N_2O. Ammonia-oxidizing bacteria (AOB) and archaea (AOA) produce N_2O as a byproduct through the oxidation of ammonia to nitrite via the nitrification process (Shaw et al., 2006; Santoro et al., 2011). Because bacterial nitrification and denitrification process are well known, the emission of N_2O from agricultural soils has been studied mainly by focusing on these contributions (Conrad, 1996; Miller et al., 2008; Hamonts et al., 2013). However, many fungal species (e.g., *Trichoderma hamatum*, *Chaetomium funicola*, *Neocosmospora vasinfecta, Paxillus involutus* and *Penicillium digitatum*) can produce N_2O (Shoun et al., 1992; Yanai et al., 2007; Prendergast-Miller et al., 2011; Jirout et al., 2013); this finding was elucidated after the initial discovery that a hyphomycetes fungus, *Fusarium oxysporum*, has the distinct ability to produce N_2O (Shoun and Tanimoto, 1991). Moreover, some recent studies have demonstrated that fungal contributions to N_2O emissions in terrestrial environments such as grassland fields and forest soils are larger than the contributions of bacterial denitrification and/or nitrification (Laughlin and Stevens, 2002; Spokas et al., 2006; Laughlin et al., 2009; Blagodatskaya et al., 2010). However, despite the importance of agricultural soils as a large N_2O emission source, the extent of fungal contributions to such emissions and the fungal communities that produce this N_2O in upland field soils have not been well characterized.

As soil nutrients are rapidly consumed during crop growth, fertilizer is usually applied several

times per growing season. The first (basal) fertilization is performed by incorporating fertilizer into the plowed layer, and several top-dressings are applied later. In the Chapter 4, we described the fungal denitrification was responsible for N_2O emission in a corn upland field after the additional organic fertilization, according to the isotopomer ratio analysis and gene quantification. This result strongly supported that fungal denitrification play an important role in N_2O emission in upland field induced by additional N fertilization. In another radish-growing field located in Niigata, Japan (described below), we observed a large quantity of N_2O was emitted after the basal organic fertilization. However, substantial quantities of N_2O were also emitted after later surface applications. The fertilizers applied onto the field surface were obviously covered by fungal mycelia (Fig. 6-1). Based on the results in Chapter as described previously, we hypothesized that fungi rather than bacteria were responsible for the N_2O emission after the application of organic fertilizers as top-dressing in the upland field.

To test this hypothesis, we performed experiments (1) to assess the relative contribution of bacteria and fungi to N_2O production using antibiotics in a laboratory-scale soil microcosm system that imitated the field conditions, (2) to examine the difference in population density and community composition of fungi and fungal denitrifiers between additional fertilized and non-fertilized soil in the field, and (3) to isolate the abundant fungi in the additional fertilized soil and analyze their N_2O and N_2 producing activities.

6.2 Materials and methods

6.2.1 Study site and field management

The study field is located at the Niigata Agricultural Research Institute (N37°26′, E138°52′, Nagaoka, Niigata, Japan). Radish (*Raphanus sativus* var. *longipinnatus*) was cultivated in the field from Sep. 8 to Nov. 29 in 2011. The total precipitation and mean daily air temperature during the cultivation period were 672.1 mm and 15.5 °C, respectively. The soil is of an Andisol type, which is widespread in Japan. The physicochemical properties of the soil are as follows: total carbon, 39 g-C/kg-soil; total nitrogen, 2.6 g-N/kg-soil; bulk density, 0.81 g cm^{-3}; solid phase rate, 34.5%; and pH, 6.5. The field experiment was arranged in a randomized block design with three replicate plots per treatment. Each block was 25 m^2 (5 m × 5 m) and comprised two 5-m × 2.5-m plots: one with applied organic fertilizer and one without fertilizer application. We used a commercially available granulated organic fertilizer that is a mixture of food manufacturing residues such as feather meal, fish meal, rapeseed meal, rice bran, oil palm ash and poultry litter ash (Total N: 6%, P_2O_5: 6%, K_2O: 6%). A basal fertilization of granular organic fertilizer at 21 g N m^{-2} was performed on Sep. 7 in 2011 by incorporating the fertilizer into the plowed layer. Seeds were sown in all the plots on Sep. 8. Supplemental top-dressings of granular organic fertilizer at 3 g N m^{-2} were performed on Oct. 7 and 31, respectively. All radishes were harvested on Nov. 29.

6.2.2 Measurements of N_2O flux and soil N concentrations during the cultivation period

N_2O flux in the field was measured every week during the cultivation period using the chamber method. Chambers were set at three locations in each plot. Gas samples (500 ml) were taken from the chambers at 0, 15, and 30 min after closure. The N_2O concentration in the samples was measured using a gas chromatograph equipped with an electron capture detector (GC-ECD; GC-14B, Shimadzu, Kyoto, Japan). The N_2O flux was calculated from the increase in the N_2O concentration of the sample. Soil samples were collected at 0-5 cm depth at three locations in each plot on the same day to measure the nitrate (NO_3^-) and ammonium (NH_4^+) concentrations in the soils. Ten-gram soil samples were extracted with 100 ml of 2 M KCl solution. The NH_4^+ and NO_3^- concentrations in the extract were measured colorimetrically (Akiyama and Tsuruta, 2003).

6.2.3 Establishment of laboratory-scale soil microcosm

A laboratory-scale soil microcosm system was established to imitate the field fertilization conditions. Twenty grams of non-fertilized soil were placed in 80-ml glass bottles and mixed with 0.25 g of granular organic fertilizers as the basal fertilization. The soil water content was adjusted to 50% of maximum water holding capacity (MWHC) by adding distilled water. All bottles were covered with aluminum foil and incubated at 27 °C for 46 days. Soil water content was increased to 70% of MWHC on the 4th day of incubation to imitate a field rain event. A 0.25-g top-dressing of granular organic fertilizer was applied on the 18th day of incubation. Soil water content was again increased to 70% of MWHC on the 24th day of incubation. The N_2O flux was measured every 2 days after sealing and incubating the bottles for 60 min. The N_2O concentration was measured using a GC-ECD instrument (GC-2014, Shimadzu, Kyoto, Japan).

6.2.4 Substrate-induced respiration (SIR) inhibition experiment

The relative contributions of fungal and bacterial activity to N_2O emission were evaluated through the substrate-induced respiration (SIR) inhibition method (Anderson and Domsch, 1975) using the soil of the soil microcosm systems on the 8th and 34th incubation days when N_2O flux peaks were observed after the basal and additional fertilizations, respectively. Optimal inhibitor concentrations (5 mg g^{-1} soil of cycloheximide and 8 mg g^{-1} soil of streptomycin) were determined through preliminary experiments, in which glucose (5.0 mg g^{-1} soil) as a C source, cycloheximide (0, 2.0, 5.0, and 10.0 mg g^{-1} soil) as a fungal inhibitor and streptomycin sulfate (0, 2.0, 5.0, 8.0, and 12.0 mg g^{-1} soil) as a bacterial inhibitor were used according to Laughlin and Stevens (2002). The inhibitors and glucose were dissolved in 5 ml of distilled water and applied to the duplicate soil microcosm system containing 20g of the soils as described above. The bottles containing soil, glucose, and antibiotic solutions were incubated at 27 °C under aerobic conditions for 2 hours on a rotary shaker (150 rpm). The bottles were then sealed and incubated for 4 hours under the same conditions, and gaseous N_2O and CO_2 concentrations were measured every 2 hours using a GC-TCD instrument (GC-14, Shimadzu, Kyoto, Japan).

The contributions of nitrifiers to N_2O emission were determined using 0.01% acetylene (C_2H_2) as a nitrification inhibitor (Schimel et al., 1984). The C_2H_2 was added in the headspace of the soil samples on the 8th and 34th incubation days after sealing the bottles. The bottles were incubated at

27 °C for 4 hours. Gaseous N_2O concentrations were measured every 2 hours using a GC-ECD instrument (GC-2014, Shimadzu, Kyoto, Japan).

6.2.5 Isolation and identification of soil fungi

Samples were collected from the additional fertilized and non-fertilized soils at a depth of 0-5 cm in each plot on 18 Oct., when an increase in the N_2O flux and fungal mycelium around the granular organic fertilizers (Fig. 6-1) were observed after the first surface fertilization. The granular organic fertilizers applied to the additional fertilized soil samples were easily separated from the soil using forceps. Separated fertilizers were termed collected organic fertilizer (COF), and the soils were termed residual soil (RS).

To isolate the fungi in additional fertilized soil (COF and RS) and non-fertilized soil, fungal colonies grown on Rose Bengal chloramphenicol agar (RBCA) medium plates were purified by transferring the mycelia to fresh potato dextrose agar (PDA) medium plates after fungal colony counting (described below). After DNA extraction, endobacterial contamination was tested using PCR with the primer sets 27F/1492R, which target the partial sequence of the bacterial 16S rRNA gene (Lane et al., 1991). The PCR was performed using the following conditions: initial denaturation at 95 °C for 10 min; 30 cycles of 95 °C for 30 s, 55 °C for 45 s, and 72 °C for 90 s; final extension at 72 °C for 5 min. Accordingly, the endobacterial contamination was not detected from any isolates. The isolated fungi were identified at the taxonomic level on the basis of macroscopic and microscopic morphological features and their phylogenetic properties. For the morphological identification, cultures grown on the PDA medium described above were transferred onto specific diagnostic media (CYA-Czapek-Dox yeast extract agar, CLA-carnation leaf-piece agar, SNA-Spezieller Nährstoffarmer agar, MEA-malt extract agar, and BWA-beer wort agar), and the morphological features were examined, including the presence or absence and characteristics of the conidiospore, sporodochia, and ascus, the type and length of sporophores, and aerial mycelium characteristics (Domsch et al., 1980; Leslie and Summerell, 2006). For the phylogenetic identification, the isolates were cultivated for 6 days at 28 °C in the PDB medium, and the mycelia were collected by centrifuging at 10000 rpm for 1 min. DNA was extracted from mycelia using an ISOPLANT kit (Nippon Gene, Toyama, Japan); the DNA was further purified

using a PowerClean DNA clean-up kit (MoBio Laboratories, USA). The partial regions of the 18S rRNA gene and the internal transcribed spacer (ITS) between the 18S and 28S rRNA genes were amplified using the primer sets NS1 (White et al., 1990)/Fung (May et al., 2001) and ITS1/ITS2 (White et al., 1990), respectively. The composition of the reaction mixture has been described previously (Möhlenhoff et al., 2001; Yao et al., 2006). The PCR was performed using the following conditions: initial denaturation at 95 °C for 10 min; 30 cycles of 95 °C for 30 s, 50 °C (55 °C for ITS sequence) for 30 s, and 72 °C for 30 s; final extension at 72 °C for 5 min. The sizes and concentration of the final PCR products were confirmed using agarose gel electrophoresis and a NanoDrop ND-1000 spectrophotometer (Thermo Fisher Scientific, USA). Sequencing and phylogenetic analyses were performed as described elsewhere (Saito et al., 2008).

6.2.6 The N_2O producing activity of fungal isolates

The abilities of the fungal isolates to produce N_2O and N_2 were analyzed. Isolated strains were pre-incubated for 4 days in liquid basal medium containing 1% glucose, 0.2% peptone, and mineral salts (Shoun et al., 1991). The pH was adjusted to 7.5 as described in Shoun et al. (1992). Subsequently, 1-ml aliquots were inoculated into 4 ml of fresh basal medium (pH 7.5) in 25-ml glass serum vials. The medium contained 3.5 mM ^{15}N-labelled $NaNO_2$ (98 atom%-^{15}N, Cambridge Isotope Laboratories, USA) or $NaNO_3$ (99.5 atom%-^{15}N, SI Sciences, Japan). After inoculation, the vials were tightly sealed with rubber stoppers. Fungal isolates were cultured under two conditions: initially aerobic conditions and continuously anaerobic conditions. In the first condition, the vials were sealed without gas replacement under initially aerobic conditions; therefore, the O_2 concentration in the headspace gas gradually changed from ambient levels to a nearly anaerobic environment, which allowed improved initial growth of the fungal mycelia (Bollag and Tung, 1972). In the second condition, the headspace gas in the vials was replaced with purified helium immediately after sealing. The isolates were grown at 27 °C for 1 week on a rotary shaker (150 rpm) in the both condition. The $^{15}N_2O$ and $^{15}N_2$ concentrations in the headspace were determined using a GC-MS system (GCMS-QP2010 Plus, Shimadzu, Kyoto, Japan) equipped with a CP-PoraPLOT Q-HT column (25 m × 0.32 mm; Agilent, Japan) or a CP Molsieve 5 Å column (30 m × 0.32 mm; Agilent, Japan) as described by Isobe et al. (2011). The $^{15}N_2O$ and $^{15}N_2$

concentrations dissolved in the media were calculated as described by Tiedje (1994). Then, the biomass of the fungal strains was determined as described by Bollag and Tung (1972) and $^{15}N_2O$ and $^{15}N_2$ producing activity of the fungal strains was normalized with the biomass.

6.2.7 Analysis of fungal population density and community composition in additional fertilized and non-fertilized soils

The fungal population density in additional fertilized and non-fertilized soils was estimated using the colony counting method. Ten grams of soil from non-fertilized soil or COF and RS obtained from 10 g of additional fertilized soil were added into 100 ml of 0.15% water agar and mixed thoroughly in quadruplicate (Steinkellner and Langer, 2004). A 10-fold dilution series with sterilized H_2O was prepared, and 1 ml of the final dilution (1:10,000, based on preliminary tests) was transferred to a RBCA medium plate (Jarvis et al., 1983; Steinkellner and Langer, 2004). The plates were incubated at 28 °C in the dark for 6 days, and the total number of fungal colonies was recorded as the colony forming units per g (CFU/g) of air-dried soil.

The fungal community composition in additional fertilized and non-fertilized soils was assessed using denaturing gradient gel electrophoresis (DGGE) and subsequent phylogenetic analyses. The DNA of soil microbes was extracted from 1.0 g of COF, RS and non-fertilized soils in triplicate using an ISOIL kit (Nippon Gene, Toyama, Japan). The extracted DNA was further purified using a PowerClean DNA clean-up kit (MoBio Laboratories, USA) to remove PCR inhibitors. A partial region of the 18S rRNA gene and the ITS were amplified using the primer sets Fung-GC/NS1 (Möhlenhoff et al., 2001) and ITS1/ITS2-GC (Yao et al., 2006), respectively. The PCR reaction conditions are described above. The PCR product was further purified using a Gel and PCR clean-up system (Promega corporation, USA). DGGE was performed using 200 ng of the purified PCR products, which were loaded onto a 7% polyacrylamide gel with a 20-45% denaturing gradient (8% polyacrylamide gel; the same denaturing gradient was used for the ITS sequence). Electrophoresis was performed at 60 °C and 75 V for 16 hours, and the resulting bands were excised from the gel. DNA was eluted from the gel and amplified using the primer sets with GC clamp. The PCR products were applied to DGGE and the band mobility was confirmed by comparing the position of the PCR products with the original DGGE banding profiles. After that,

the eluted DNA was amplified using the primer sets without GC clamp for the subsequent procedures. The PCR reaction, cloning, sequencing (five clones per band), and phylogenetic analysis were performed as previously described (Wang et al., 2009). The digitalized DGGE banding profiles were aligned based on relative intensity and position of each band (reflecting the population size and composition, respectively). These normalized data were subsequently subjected to principal component analysis (PCA).

6.2.8 Nucleotide sequence accession numbers

The nucleotide sequences of the partial 18S rRNA gene from fungal isolates and DGGE bands in this study have been submitted to the DDBJ/EMBL/GenBank databases with accession numbers AB831111 to AB831159. The nucleotide sequences of the partial ITS region from fungal isolates and DGGE bands have been submitted to the databases with accession numbers AB831189 to AB831233.

6.2.9 Statistical analysis

Comparisons of the field soil N parameters, the N_2O flux and the CFUs among different soils and treatments were tested using one-way analysis of variance with Tukey's honestly significant difference. A level of 0.05 was considered significant. These statistical analyses were performed using the R software package (R Development Core Team, 2007). The digitalized DGGE banding profiles were aligned using CS analyzer 3.0 software (Marantz Electronics Ltd., Japan). PCAs were performed using Minitab 15 software (Minitab, PA, USA).

6.3 Results

6.3.1 N_2O emission rate and soil N concentrations during the cultivation period

Three N_2O flux peaks were observed during crop cultivation. The first peak occurred on 22 Sep. (2 weeks after basal fertilization), the second peak occurred on 18 Oct. (2 weeks after the first additional fertilization), and the third peak occurred on 5 Nov. (1 weeks after the second additional fertilization) (Fig. 6-2). The first peak was the largest (332 μg N $m^{-2}h^{-1}$) and was observed after heavy rain and the related increase in soil water-filled pore space (WFPS) (Fig. 6-2). The total amount of emitted N_2O derived from the basal fertilization (from 8 Sep. to 29 Sep.) was 64.4 mg N m^{-2}, and the amount derived from the additional top-dressings (from 6 Oct. to 23 Nov.) was 48.6 mg N m^{-2} (Fig. 6-2).

The soil NH_4^+ and NO_3^- concentrations increased after the basal fertilization and decreased and reached the nearly background levels before the first additional fertilization (Fig. 6-2). The soil NH_4^+ and NO_3^- concentrations increased after the first additional fertilization but did not reach the background levels before the second additional fertilization (Fig. 6-2).

6.3.2 Relative fungal contributions to N_2O emission in a laboratory-scaled soil microcosm

N_2O flux peaks were observed after the basal and additional fertilizer applications in the laboratory-scale microcosm experiment, similar to the field monitoring (Fig. 6-3). The N_2O emission rate reached a peak (545 ug N kg^{-1} h^{-1}) and then decreased to approximately zero on 8 and 18 days after the basal fertilization, respectively. The rate increased again after the additional surface application and reached the second highest level (509 ug N kg^{-1} h^{-1}) on 16 days after the additional fertilizer application. The addition of cycloheximide as a fungal inhibitor decreased the N_2O emission rate by 30% during the first peak and by 84% during the second peak (Table 6-1). The addition of streptomycin as a bacterial inhibitor decreased the N_2O emission rate by 59% during the first peak and by 20% during the second peak (Table 6-1). A nitrification inhibitor, 0.01% acetylene, decreased the rate by 10% during the first peak and by almost 0% during the second peak.

6.3.3 Identification and N_2O production of isolated fungi

A total of 32 fungal strains were isolated: 27 strains from additional fertilized soil in the field

(20 from COF, 7 from RS) and 5 strains from non-fertilized soil (Table 6-2). These strains were identified as 16 species from 11 genera based on morphological characteristics (Table 6-2). The identification of all isolates was further supported by phylogenetic trees based on the partial sequence of the 18S rRNA gene and ITS. Twenty isolates belonging to 10 species, *Actinomucor elegans*, *Bionectria ochroleuca*, *Fusarium avenaceum*, *Fusarium equiseti*, *Fusarium oxysporum*, *Fusarium solani*, *Nectria* sp., *Penicillium purpurogenum*, *Pythium ultimum* and *Rhizomucor* sp., exhibited the ability to produce N_2O but did not produce N_2 under the tested conditions (Table 6-2). The N_2O production of these strains, except for an isolate of *F. solani* COF-19, was larger when the N source was nitrite rather than nitrate (Table 6-2). All of these strains exhibited clearly higher N_2O production when the condition was initially aerobic rather than continuously anaerobic, except that the isolates *F. equiseti* COF-5, COF-8, COF-9, *F. avenaceum* RS-8, and NF-4 exhibited similar ability to produce N_2O under both tested conditions.

6.3.4 Fungal population density and community composition in soils after additional fertilizer application

The fungal population densities estimated as CFU obtained on 18 Oct. during the second peak differed between the additional fertilized soil (COF and RS) and non-fertilized soil (p=0.0045): 2.6 × 10^6 CFU/g·soil in the additional fertilized soil (COF: 2.3 × 10^6 CFU/g·soil, RS: 2.9 × 10^5 CFU/g·soil) and 1.0 × 10^5 CFU/g·soil in non-fertilized soil (Fig. 6-4). The abundance of fungal 18S rRNA and *nirK* gene in additional fertilized soil were significantly higher than that in no fertilized soil by an order of magnitude (Table 6-3)

Fungal community compositions, as indicated by DGGE banding profiles targeting the partial region of the 18S rRNA gene (Fig. 6-5A) and ITS (Fig. 6-5C), also differed between the additional fertilized soil (COF and RS) and non-fertilized soil. PCA plots of the two DGGE band profiles (bands from non-fungal organisms were excluded from the analysis) exhibited similar results. Three distant fungal community composition groups were also formed by the first ($PC1_{18S\ rRNA}$=71.9%, $PC1_{ITS}$=76.0%) and second ($PC1_{18S\ rRNA}$=16.4%, $PC1_{ITS}$=13.7%) components (Figs. 6-5B and 4D).

In Fig. 6-5A, 23 bands (from the 10, 13, and 12 bands in the COF, RS, and non-fertilized soil,

respectively, including commonly observed bands among treatments) were intense (bands A to W). Bands B, C, F, and G were commonly detected in COF, RS and non-fertilized soil. Bands A, D, E, H, I, L, and T were commonly detected in additional fertilized soil (COF and RS), and bands J, K, and S were observed only in RS. In contrast, bands M, N, O, P, Q, R, U, V, and W were observed only in the non-fertilized soil. In the phylogenetic tree based on the partial 18S rRNA gene (Fig. 6-6), 17 bands were derived from fungi belonging to the four clusters representing phyla Ascomycota, Basidiomycota, and Zygomycota, as well as Fungi incertae sedis. The remaining bands consisted of sequences from soil fauna (bands I, T, U, V, and W) and Chromalveolata (band N). All of the isolated fungi possessing the ability to produce N_2O were clustered in phyla Ascomycota and Zygomycota exclusively and shared similar sequences with some DGGE bands (Fig. 6-6). The dominant bands A and E in the additional fertilized soil (COF and RS in Fig. 6-5A) shared highly similar sequences with the N_2O-producing isolates RS-8, NF-4 (*F. avenaceum*), and COF-3 (*A. elegans*).

In Fig. 6-5C, 14 bands (from 10, 10, and 7 bands in the COF, RS, and non-fertilized soil, respectively, including commonly observed bands among treatments) were intense (bands a to n). Bands b, c, g, and h were commonly detected among the three treatments. Bands a, d, j, l, m, and n were detected in both additional fertilized soil fractions (COF and RS), and band f was observed only in RS. In contrast, bands e, i, and k were observed only in the non-fertilized soil. In the phylogenetic tree based on the partial ITS sequence (Fig. 6-7), all bands except k (*Cryptococcus* sp.) were derived from fungi belonging to clusters representing phylum Ascomycota and shared similar sequences with isolated N_2O-producing fungi. The dominant bands c, d, g, j, and l in the additional fertilized soil (COF and RS in Fig. 6-5C) shared highly similar sequences with the N_2O-producing isolates COF-2 (*F. oxysporum*), COF-14 (*Nectria* sp.), COF-19 (*F. solani*), COF-8 (*F. equiseti*), and RS-3 (*B. ochroleuca*).

6.3.5 The diversity and phylogeny of fungal *nirK* in soils after additional fertilizer application

We also investigated the diversity and phylogeny of fungal *nirK* in *t*he surface-fertilized cropland soil. In total, 44 and 26 sequences of fungal *nirK* were obtained from COF and RS and classified into six COF and three RS OTUs, respectively, with 3% differences using the Mothur

program (Schloss et al., 2009). From the phylogenetic tree of *nirK* and 18S rRNA gene (Fig. 6-8), the *nirK* clones were expected to be classified into Hypocreales, Sordariales, and Eurotiales of Ascomycota based on the congruence between the two phylogenies. Based on culture-dependent and DGGE analyses, we previously showed that denitrifying fungi closely related to *Fusarium* and *Bionecter* sp. in Hypocreales and to *Chaetomium* sp. in Sordariales are dominant in soils. The results of the clone library analysis using fungal *nirK* strongly show that they are responsible for the N_2O production in the tested surface-fertilized soil. We previously did not detect the presence of fungi of Eurotiales based on their 18S rRNA and ITS genes; however, we obtained the *nirK* clones and denitrifying isolates (*Penicillium purpurogenum* and *Aspergillus niger*) of this order. This shows that the designed primer set can sensitively detect the denitrifying fungi regardless of its lower abundance in soils.

6.4 Discussion

6.4.1 Fungal N_2O production in cropland soil after additional fertilizer application

The N_2O flux derived from additional surface fertilizer applications was not as large as the flux derived from basal fertilization. However, the cumulative amount of emitted N_2O derived from the additional fertilizer applications accounted for 43% of the total amount during crop cultivation. Moreover, the emitted N_2O derived from the additional fertilizer applications accounted for 0.8% of input N, which was 2.7-fold larger than that from basal fertilization. Therefore, N_2O emissions resulting from top-dressing can result in large N loss during the cultivation and result in ineffective fertilization from a sustainable agriculture viewpoint.

In the laboratory-scale soil microcosm experiments, the use of cycloheximide in the SIR inhibition assay reduced the rate of N_2O emission observed after the additional fertilizer application more than that achieved using streptomycin, suggesting that fungal denitrification dominated the N_2O production over bacterial denitrification and nitrification in the examined soil. We also confirmed little N_2O emission via the nitrification by the C_2H_2 inhibition assay. In addition, the population density of fungi and fungal denitrifiers in the additional fertilized soil (COF and RS) was much higher than that in the non-fertilized soil in the field. The community composition of the additional fertilized soil was also significantly different from that of the non-fertilized soil, whereas the compositions of the COF and RS were similar. These differences in biomass and community composition indicate that fertilizer applications affected the fungal community compositions and increased their biomass. In addition, because the N_2O emission after the additional surface fertilization was not observed from the sterilized soils but observed from the non-sterilized soils in the soil microcosm experiments (data not shown), the fertilizer applications could induce the growth of microorganisms indigenous in the soils including denitrifying fungi rather than those indigenous in the fertilizers. Finally, the dominant fungal species in the additional fertilized soil, *A. elegans*, *B. ochroleuca*, *F. avenaceum*, *F. oxysporum*, *F. solani*, *Nectria* sp., and *Rhizomucor* sp., were successfully isolated, and their ability to produce N_2O was confirmed. The clone library further revealed that the fungi belonging to Eurotiales, Hypocreales, and Sordariales were primarily responsible for N_2O emissions in soils.

These field-based and laboratory-scale observations strongly suggest that fungi are more responsible than bacteria for the N_2O emission produced after the additional application of organic fertilizers in the field. The enrichment of N_2O-producing fungi and the high density of nutrient N in the COF suggested that organic fertilizers on the soil surface might be a hot spot for fungal N_2O production. This finding is clearly important because additional top-dressings are conventionally applied to maintain sufficient soil nutrients for crop growth.

6.4.2 N_2O production of isolated fungi

The ability of most fungal isolates to produce N_2O was considerably increased under initially aerobic conditions. Oxygen might be used to activate fungal denitrification, which is different from bacterial denitrification (Zumft, 1997). Fungal denitrification generally requires a minimal oxygen supply as suggested in several studies with *F. oxysporum* (Zhou et al., 2002; Shoun et al., 2012), indicating that fungal denitrification process might be coupled with oxygen respiration process, both of which use the respiratory chain of mitochondria and occur simultaneously under limited oxygen concentration (Takaya et al., 2002; Shoun et al., 2012). These physiological differences might be reflected in the relative contribution of fungi and bacteria to N_2O emission in the field. Fertilizers applied to the field surface can contain many oxidative sites. This could explain the larger contribution of N_2O-producing fungi. In contrast, the contribution of denitrifying bacteria might be larger after the basal fertilization in which fertilizers are incorporated into the soil and oxidative portions should be smaller. In fact, the results of the laboratory-scale microcosm demonstrated that the addition of streptomycin reduced N_2O emission after the basal fertilization more than the addition of cycloheximide, suggesting that bacteria dominated N_2O production within the soil (i.e., not on the surface). A study on N_2O production in redox-controlled wetland sediments supports this idea and demonstrated the dominance of fungal (rather than bacterial) denitrification under weakly oxidizing conditions (Seo and DeLaune, 2010).

All of the fungi isolated in this study, except *F. solani* COF-19, favored nitrite rather than nitrate as a substrate for N_2O production, indicating that nitrite could be the favored N substrate for soil fungi for the production of N_2O. The concentration of nitrite was too low to be detected in this study; nevertheless, due to its rapid turnover (Burns et al., 1995; Isobe et al., 2012), nitrite could

be consistently produced through the reduction of nitrate and the oxidation of ammonia and organic N (Rütting and Müller, 2008).

6.4.3 Implication for fungal N_2O emission from terrestrial soils

Agricultural fields are a major source of N_2O emissions in terrestrial environments. The results of this study suggest that fungal denitrification is the dominant source of N_2O emissions in cropland soils, depending on the fertilizers used and their application regimens. We would like to emphasize the agricultural and environmental importance of fungal denitrification in cropland soils; fungi can cause the direct loss of nitrogen (N) from fertilizers and enhance the emissions of potent greenhouse trace gas because N_2O, but not N_2, is the main end-product of fungal denitrification.

Fungal denitrification in surface soils could also be an important process for N_2O emissions in other terrestrial environments. It has been previously reported that fungal denitrification contributes to greater N_2O emission than bacterial denitrification and ammonia oxidation in the surface soils of grasslands (Laughlin et al., 2009) and forests (Castaldi and Smith, 1998). It has also been reported that a substantial amount of N_2O can be emitted from the topsoil of no-tilled cornfield soils (Parkin, 1987), grassland soils (Laughlin et al., 2009), and peatland soils (Marushchak et al., 2011). The fungal biomass in such surface soils is generally high because of the rich organic matter content and oxic/hypoxia conditions. Physiological analyses of isolates and antibiotics assays of the soil have also demonstrated that fungal denitrification can dominate over bacterial denitrification in such surface soil environments. These observations suggest widespread fungal denitrification in the surface soils of terrestrial environments.

6.5 Conclusion

In our experimental cropland field, the additional surface applications of organic fertilizer as well as the basal application caused the substantial N_2O emission. Fungal denitrification dominated the N_2O production after the additional surface fertilization over bacterial denitrification and nitrification. The dominant fungi in the soil, including *A. elegans*, *B. ochroleuca*, *F. avenaceum*, *F. oxysporum*, *F. solani*, *Nectria* sp., and *Rhizomucor* sp. could be responsible for the N_2O emission, and especially fungi belonging to Eurotiales, Hypocreales, and Sordariales were primarily responsible for N_2O emissions in soils. The physiological features of the denitrifying fungi showed the possibility that fungal denitrification could occur widely in the surface soils of other terrestrial environments.

Table 1. Inhibition rate of N_2O emission after basal and additional fertilization by fungal and bacterial antibiotics in a soil microcosm system.

Inhibitor	After basal fertilization (%)		After additional fertilization (%)	
	N_2O	CO_2	N_2O	CO_2
Fungal antibiotic (cycloheximide)	30±9	42±1	84±1	65±9
Bacterial antibiotic (streptomycin)	59±10	59±2	20±3	21±5

Table 2. N_2O production of isolated fungal strains using $NaNO_2$ or $NaNO_3$ as a substrate in initially aerobic or continuously anaerobic conditions.

Strain number [a]	Taxonomic assignment	N_2O production (μg/ day/ g-biomass)			
		$NaNO_2$		$NaNO_3$	
		initially aerobic	continuously anaerobic	initially aerobic	continuously anaerobic
COF-1	*Penicillium* sp.	—[b]	—	—	—
COF-2	*Fusarium oxysporum*	193	29.6	1.3	0.7
COF-3	*Actinomucor elegans*	85.1	6.5	—	—
COF-4	*Mucor circinelloides*	—	—	—	—
COF-5	*Fusarium equiseti*	14.3	18.1	0.3	0.4
COF-6	*Fusarium solani*	—	—	—	—
COF-7	*Rhizomucor* sp.	109.1	37.2	—	—
COF-8	*Fusarium equiseti*	18.4	26.1	0.4	0.7
COF-9	*Fusarium equiseti*	3.9	3.8	0.4	0.2
COF-10	*Fusarium oxysporum*	263.3	19	1.9	0.3
COF-11	*Fusarium oxysporum*	—	—	—	—
COF-12	*Fusarium equiseti*	29.1	10	1.8	0.3
COF-13	*Fusarium oxysporum*	74.7	20.8	1.2	0.2
COF-14	*Nectria* sp.	7.0	1.5	—	—
COF-15	*Nectria* sp.	—	—	—	—
COF-16	*Bionectria ochroleuca*	—	—	—	—
COF-17	*Fusarium oxysporum*	—	—	—	—
COF-18	*Fusarium oxysporum*	—	—	—	—
COF-19	*Fusarium solani*	142.2	13.4	154.5	2.3
COF-20	*Fusarium solani*	41	35	7.3	0.4
RS-1	*Aspergillus niger*	—	—	—	—
RS-3	*Bionectria ochroleuca*	142.3	9.6	2.8	2.9
RS-5	*Fusarium oxysporum*	400.9	26.5	1.4	11.2
RS-6	*Penicillium purpurogenum*	15	4.8	2.3	0.3
RS-7	*Gibellulopsis* sp.	—	—	—	—
RS-8	*Fusarium avenaceum*	6.3	11.8	0.7	0.5
RS-9	*Fusarium oxysporum*	36.5	8.4	0.4	—
NF-1	*Aspergillus* sp.	—	—	—	—
NF-2	*Cunninghamella* sp.	—	—	—	—
NF-3	*Fusarium oxysporum*	366.1	17.4	2.1	0.8
NF-4	*Fusarium avenaceum*	0.3	5.7	0.1	0.5
NF-5	*Pythium ultimum*	5.6	0.3	0.5	—

[a] Strain names beginning with COF, RS, and NF denote strains isolated from collected organic fertilizer (COF), residual soil (RS), and non-fertilized soil samples, respectively.
[b] The dash symbol "—" denotes not detected.

Table 6-3 the abundance of fungal *nirK* and 18S rRNA gene in additional fertilized and non-fertilized soil.

Treatment	Gene abundance (copies per gram soil)		Relative abundance (%) [a]
	Fungal nirK	Fungal 18S rRNA	
SF (COF+RS)	$1.97\pm0.10 \times 10^5$	$1.50\pm0.25 \times 10^8$	0.13±0.02
NF	$2.03\pm0.51 \times 10^4$	$3.59\pm2.72 \times 10^7$	0.08±0.05

Note: COF, collected organic fertilizer; RS, residual soil; NF, no fertilizer. Different letters indicate significant differences at $P<0.01$.

Fig. 6-1. The additional granular organic fertilizers surrounded with fungal mycelium.

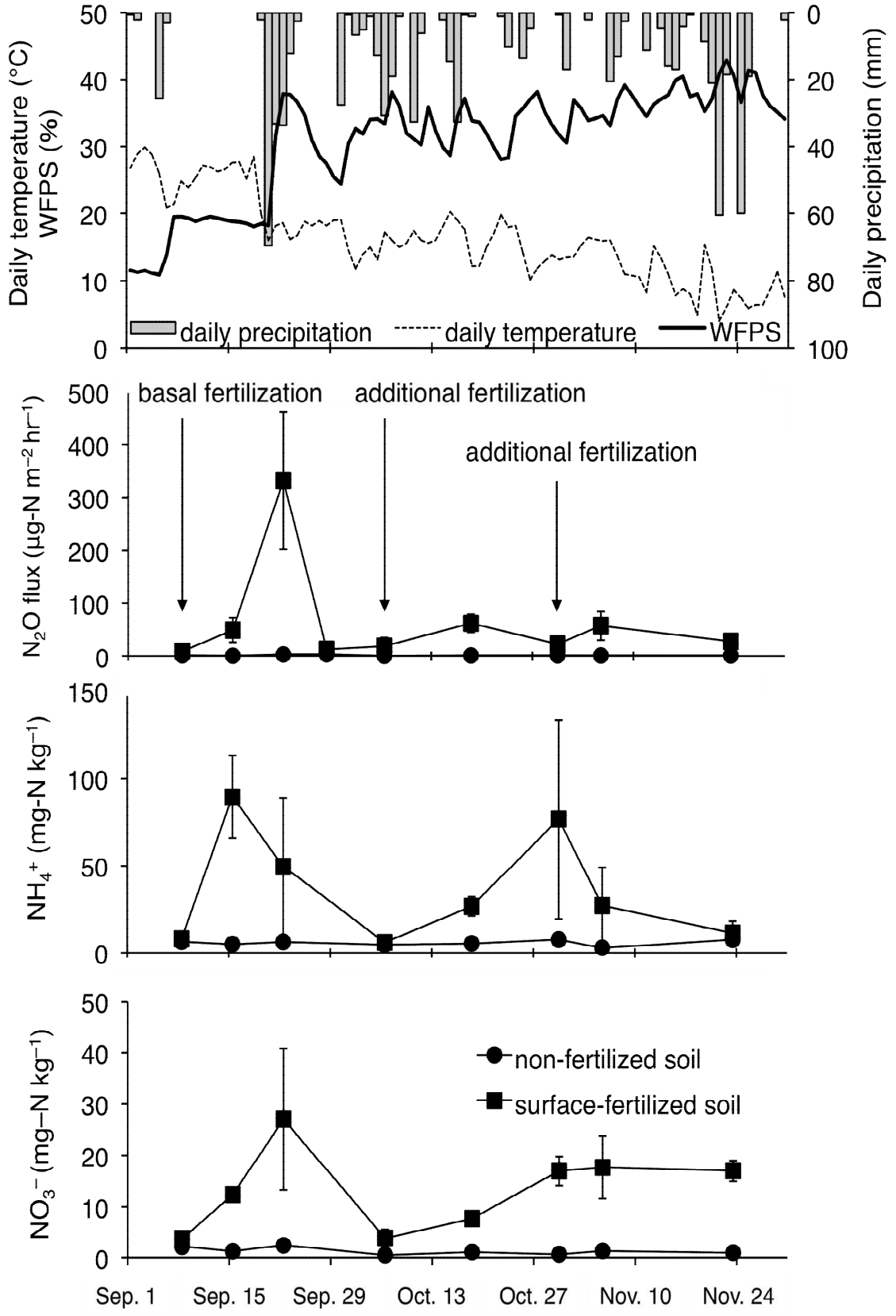

Fig. 6-2. Soil water-filled pore space (WFPS), daily precipitation and daily temperature, N_2O fluxes and soil NH_4^+-N and NO_3^--N concentrations in an experimental Andisol field during the cultivation period. The error bars represent the standard deviations (n=3). The arrows indicate the dates of basal and additional fertilizer applications.

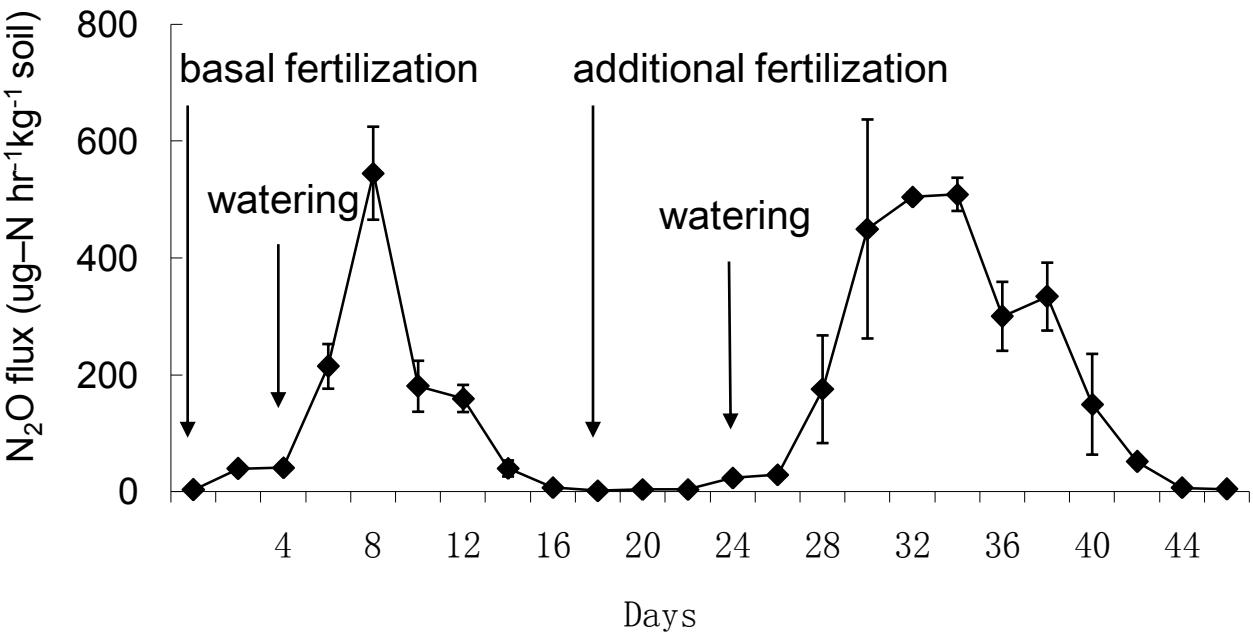

Fig. 6-3. N_2O fluxes in the soil microcosm. The error bars represent standard deviations (n=2). The arrows indicate the days on which granular organic fertilizer was supplied and soil moisture was adjusted, imitating the conditions of the experimental Andisol field.

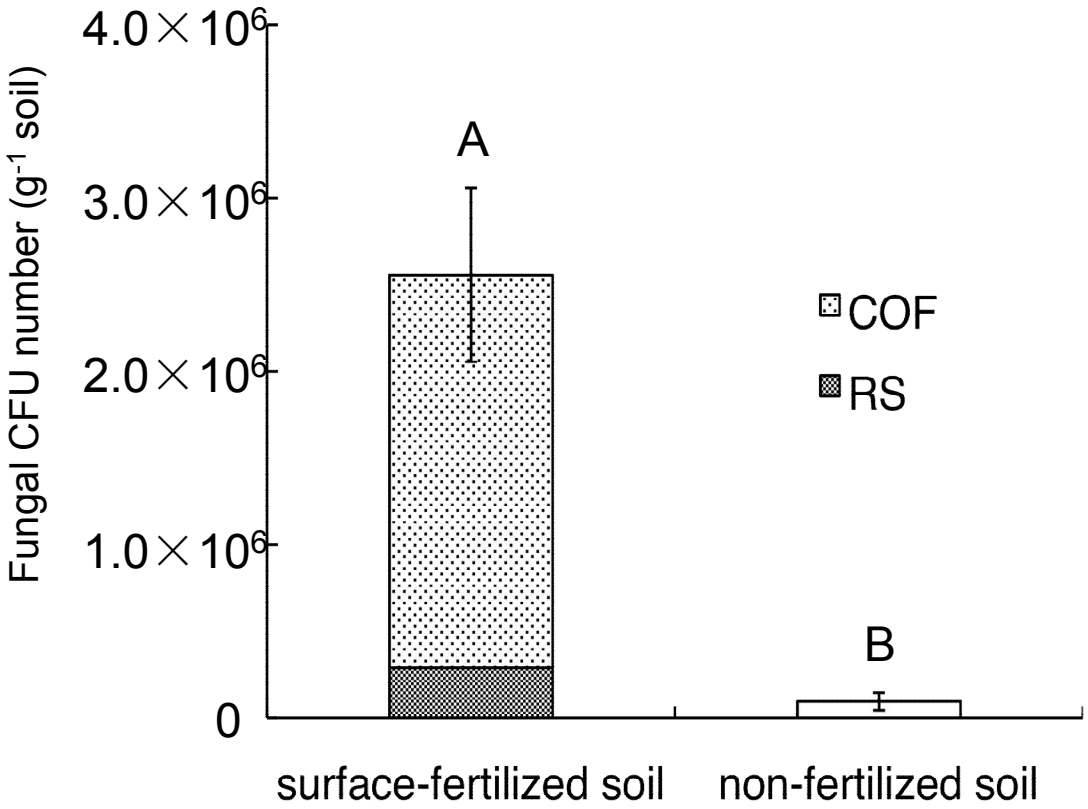

Fig. 6-4. The number of fungal CFU in the surface-fertilized and non-fertilized soils. Note: COF, collected organic fertilizer; RS, residual soil. Different letters indicate significant differences at $P<0.01$.

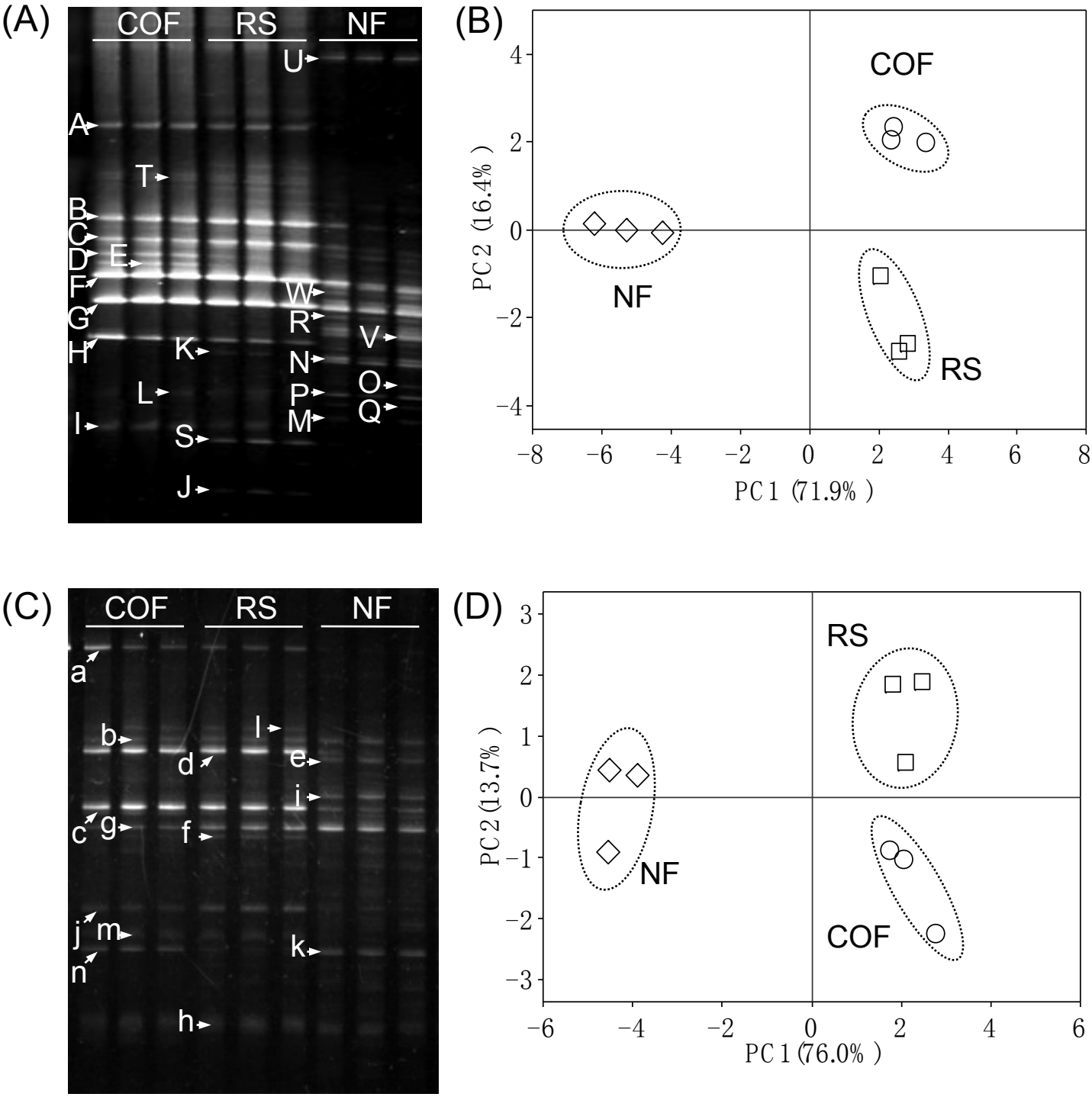

Fig. 6-5. DGGE fingerprints of fungal communities and PCA results based on partial sequences of the 18S rRNA gene (A and B) and the ITS (C and D). Note: COF, collected organic fertilizer; RS, residual soil; NF, non-fertilized soil. In Fig. A, bands M, N, O, P, Q, R, U, V, and W were exclusive in NF, and bands J, K, and S were exclusive to RS; bands A, D, E, H, L, and T were common to COF and RS; bands B, C, F, and G were common to all treatments; I, T, U, V, and W were not of fungal origin. In Fig. C, bands e, i, and k were exclusive to NF, as was band f for RS; bands a, j, l, m, and n were common to COF and RS; bands b, c, d, g, and h were common to all treatments.

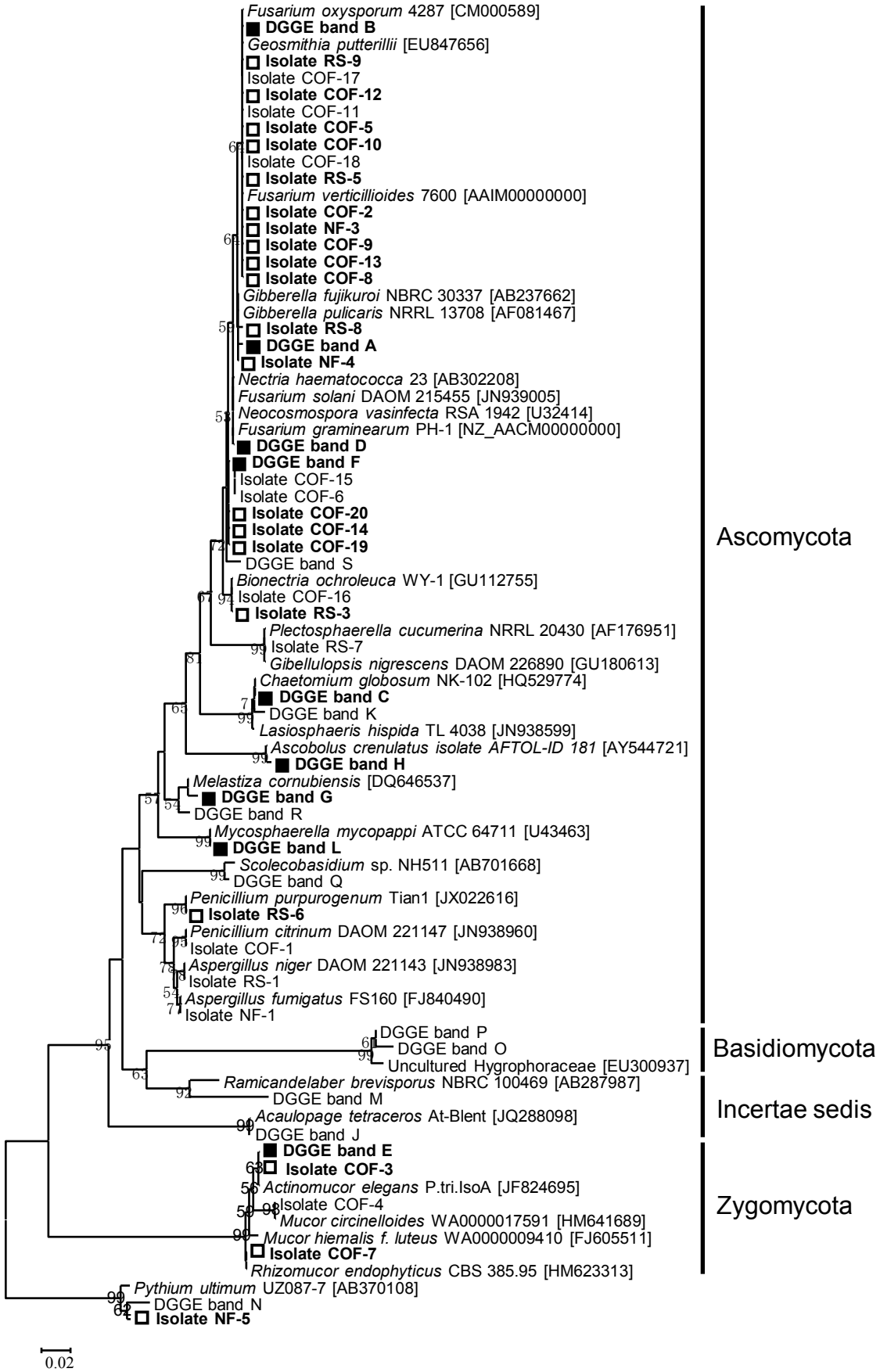

Fig. 6-6. Phylogenetic tree including the excised DGGE bands and isolated strains based on the partial sequence of the 18S rRNA gene. Bootstrap values (1,000 replicates) greater than 50% are indicated above the branches. Branch lengths correspond to sequence differences as indicated by the scale bar. Strains with □ and bold numbering exhibited the ability to produce N_2O, corresponding with that listed in Table 1. DGGE bands with ■ denote the dominant bands in the COF and RS treatments.

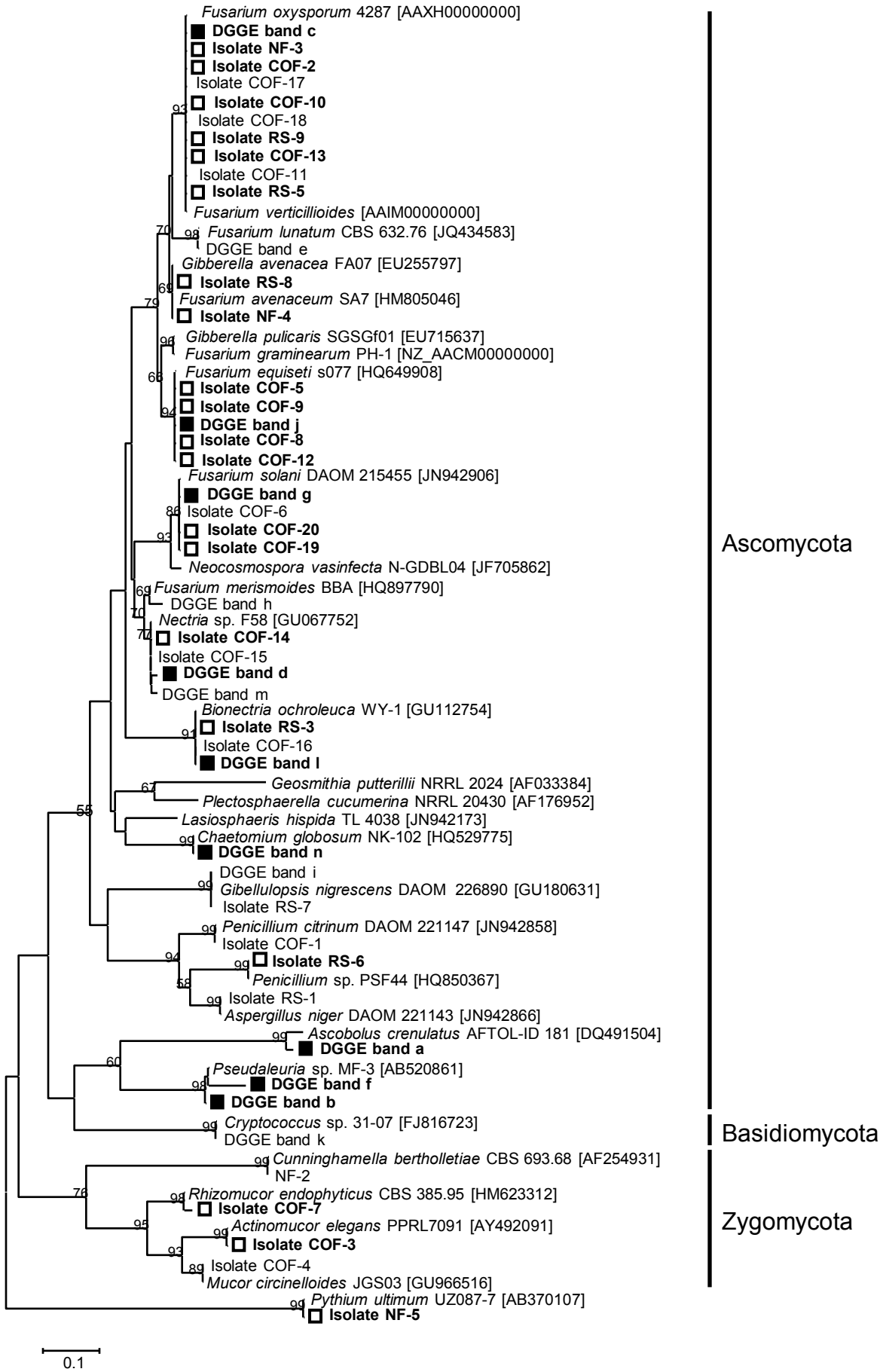

Fig. 6-7. Phylogenetic tree including the excised DGGE bands and isolated strains based on the partial ITS sequence. Bootstrap values (1,000 replicates) greater than 50% are indicated above the branches. Branch lengths correspond to sequence differences as indicated by the scale bar. Strains with □ and bold numbering exhibited the ability to produce N_2O, corresponding with that listed in Table 1. DGGE bands with ■ denote the dominant bands in the COF and RS treatments

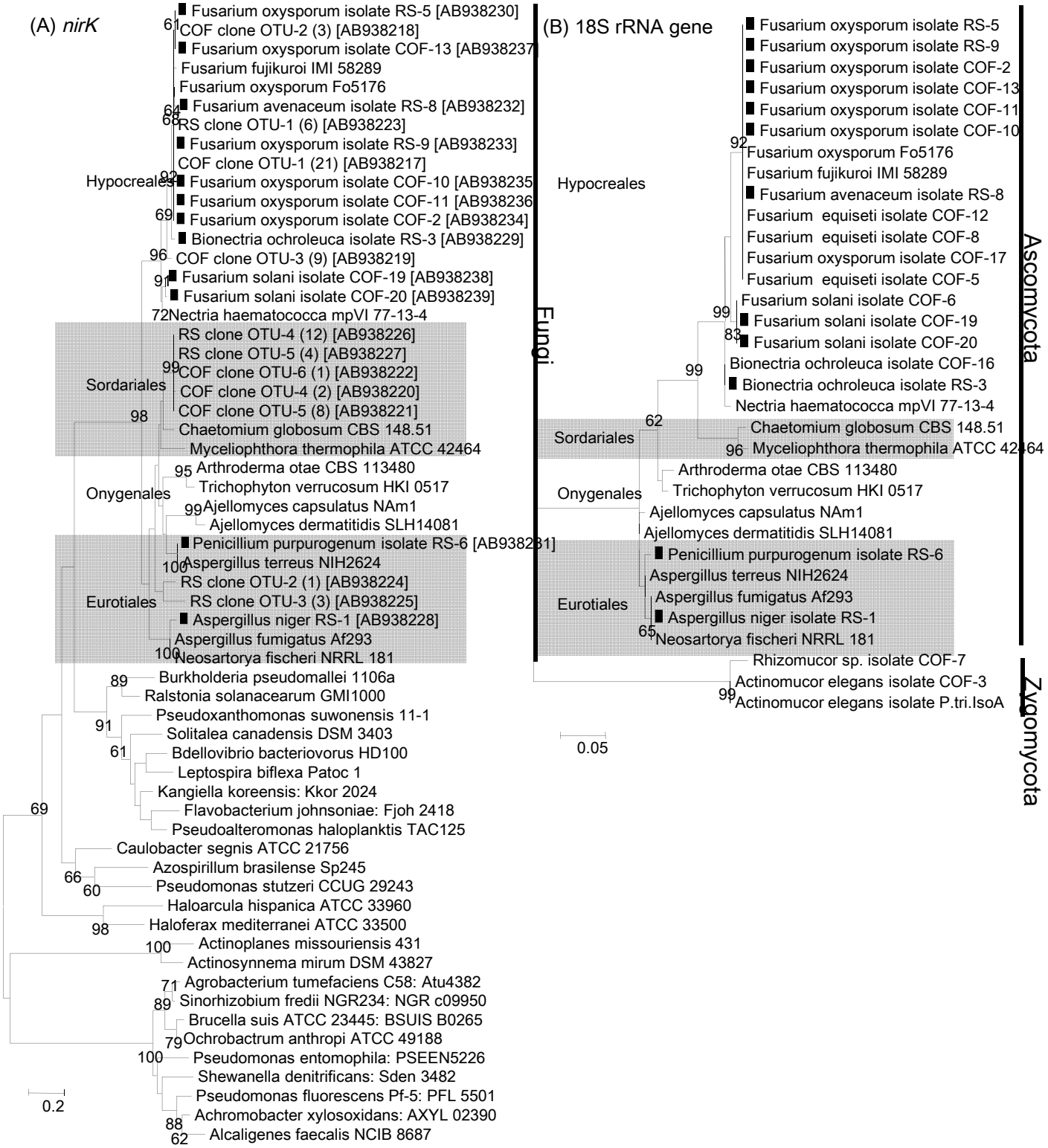

Fig. 6-8. Tree of maximum likelihood phylogeny of (A) *nirK* of clones and fungal isolates obtained from the COF and RS amplified with the designed primer set and (B) the 18S rRNA gene obtained in a previous study. The *nirK* phylogenetic tree includes prokaryotic *nirK*. The 18S rRNA gene and *nirK* of the fungal isolates are highlighted in gray. The numbers in parentheses represent the numbers of fungal *nirK* clones in the operational taxonomic units. The numbers in square brackets represent accession numbers of the nucleotide sequences of partial fungal *nirK* from the environmental samples and isolates deposited in the DDBJ/EMBL/GenBank databases. The bootstrap values (>70%) from 500 replicates are indicated next to the branches.

Chapter 7

General overview

Nitrous oxide (N_2O) is commonly known as a powerful greenhouse gas (GHG), which generates a 298-fold stronger effect on global warming than carbon dioxide (CO_2). N_2O can be photolyzed into nitric oxide (NO) in the stratosphere, which contributes to acid rain and involve in stratospheric ozone depletion. Therefore, N_2O has long drawn substantial attention in field of environmental science. Soil accounts for about 62% of global N_2O emission, and cropland soils applied with N fertilizers contribute mainly of total soil N_2O emissions because of the large enhancement of microbial N_2O-producing activities by N input. In upland field soil, substantial N_2O emission is always observed after the basal and additional organic or chemical N fertilization during the cropping season. Therefore, we suggest that upland field soil applied with different types and management practices of N fertilizers acts as a mainly N_2O source.

N_2O is known to be produced by soil microorganisms via nitrification and denitrification pathway. To clarify the contribution of soil microbial nitrification and denitrification to N_2O emission, many strategies and methods were established and developed to assess the regularity of N_2O in upland field soils, e.g. the observation of the environmental factors controlling N_2O emission; substance-induced respiration inhibition analysis for determining the fungal and bacteria contribution to N_2O emission; acetylene inhibition analysis and isotopomer analysis for assessing the contribution of nitrification and denitrification to N_2O emission; functional gene based quantification and sequencing analysis. However, some limitations of these methods lead us underestimate and misunderstand the regularity of N_2O emission and related controlling

factors in upland field soils. For example, the current *nirK* and *nirS* primers, widely used for detecting the nitrite reductase gene associated with N_2O emission, amplified a limited range of bacterial denitrifiers and mismatch not only substantial bacterial denitrifiers but also archaeal and fungal denitrifiers; isotopomer analysis cannot clearly distinguish the contribution between the nitrification and fungal denitrification. Thus, to obtain a comprehensive and precise understanding of the regularity of N_2O emission in upland field soil, we should improve the methodology (such us primers design for full range of functional gene in N_2O emission) and combine several research strategies into a multiple analysis for clarifying the N_2O emission process.

Thus, Thus, the objective of this thesis was to assess the N_2O emission rate and pathway, and then identify N_2O-generating microorganisms in upland field soil after the basal and additional application with organic or chemical fertilizers, through the multiple analysis methods including the observation of environmental factors, isotopomer ratio, SIR inhibition and acetylene inhibition analysis of N_2O, and abundance and expression of soil microbial genes associated with N_2O emission. The knowledge and methodology obtained and developed in this thesis will lead us to a more comprehensive understanding of microbial communities involved in N_2O generation and consumption in upland field soils.

Greater diversity and abundance of denitrifiers in upland field than previously realized

In the denitrification process, nitrite reduction to nitric oxide (NO) is a crucial step catalyzed

by nitrite reductases (NirK and NirS). The NirK and NirS genes (*nirK* and *nirS*) have been used as marker genes to study the distribution, abundance, diversity and activity of denitrifiers in the environment. However, our phylogenetic analysis of the currently available full-length sequences of prokaryotic *nirK* and *nirS* and fungal *nirK* revealed that conventional PCR primers can detect only a limited variety of the genes only in bacterial phylum Proteobacteria. We therefore designed new primer sets that cover the full diversity of prokaryotic *nirK* (Cluster I to IV) and *nirS* (Cluster I to III) and fungal *nirK*. DNA-based clone library and quantitative PCR analyses that used the newly designed primers revealed that prokaryotic *nirK* and *nirS* and fungal *nirK* sequences distributed in terrestrial environments are more phylogenetically diverse and abundant than previously counted. An RNA-based study that used the newly designed primers combined with culture-based method suggested that prokaryotes carrying the previously unaccounted for *nirK* or *nirS* play an important functional role in denitrification, especially N_2O emission, in upland field soil. In addition, the phylogenies of fungal *nirK* and 18S rRNA gene are congruent at the order level of Ascomycota. These results indicate that we have underestimated the ecological role of prokaryotic and fungal denitrifiers in the environment. Therefore, the knowledge and methodology obtained and developed in the Chapter 2 and 3 will lead us to a more comprehensive understanding of the diversity, abundance and functional importance of prokaryotic and fungal N_2O emitters in upland field soils.

Temporal change of N_2O-generating microorganisms and related environmental factors in

upland field after basal N fertilization

Upland field soils mainly contribute to the total N_2O emissions from soil environments, because substantial microbial N_2O emissions are greatly stimulated by basal and additional organic or chemical N fertilization. In the Chapter 4, we described a lager N_2O emission induced by basal N fertilization than that after the additional N fertilization, and such N_2O emission induced by basal N fertilization were affirmed to be produced mainly by the diverse denitrifiers via denitrification (e.g. prokaryotic denitrifiers having *nirK* in Cluster I and II and *nirS* in Cluster II and fungal denitrifiers), more than that by archaeal nitrifiers via nitrification. In addition, prokaryotic denitrifiers having the *nosZ* in Cluster I reduced the N_2O only in the upland field after the basal organic fertilizers.

To further confirm the temporal change of N_2O-producing microorganisms and related environmental factors induced by basal fertilization in the upland field, We performed a field experiment in upland field to determine the temporal variation of microbial N_2O emission in upland field induced by basal application with organic or chemical fertilizers through the exaggerated application of N fertilizer and the prolonged field-scale and lab-scale observation and investigation. The results based on such improvements showed that the temporal change of diverse N_2O-generating microorganisms and different environmental factors controlling such N_2O emission induced by basal N fertilization. After the basal organic or chemical fertilization, denitrification contributed mainly to N_2O emission more than nitrification. Under the potential

influence of organic carbon supply, prokaryotes having *nirK* in Cluster I to III could be firstly activated by basal N fertilization and produced N_2O via denitrification rapidly at two weeks after the fertilization; then following the decrease of soil pH, the prokaryotes having *nirS* in Cluster II and fungal denitrifiers were most active and produced N_2O via denitrification at three weeks after the basal fertilization. Bacterial nitrifiers, rather than archaeal nitrifiers were mainly responsible for the N_2O produced via nitrification. In addition, under the influence of organic carbon supply and soil pH, denitrifiers having *nosZ* in Cluster I as the N_2O reducers play a role in N_2O sink only in upland field during the early phase after the basal organic fertilization.

N_2O emission from upland field soil through fungal denitrification after additional N fertilization

In the Chapter 4, we also described a N_2O emission induced by additional N fertilization, which was lesser than that after the basal N fertilization. Interestingly, such N_2O emission induced by additional N fertilization were affirmed to be produced mainly by the fungal denitrifiers, which was confirmed by a distinctive *SP* value in the isotopomer analysis and a only active expression of fungal *nirK* in the quantification analysis. The level of O_2 supply was considered as the determinate factors for such N_2O emission.

To further confirm this conclusion, we observed the N_2O emission in an Andisol upland field, in which the organic fertilizers were applied on the soil surface as the additional fertilization and surround by fungal mycelium after a rainfall as described in the Chapter 6. N_2O

emissions following additional organic fertilization accounted for 40% of the total emission amount, and such N_2O emission were suppressed by 84 and 20% after the addition of cycloheximide (a fungal inhibitor) and streptomycin (a bacterial inhibitor) in a soil microcosm, respectively, suggesting that fungi provide the main contribution to the observed N_2O emission. The abundance of fungal population and fungal denitrifiers in the surface-fertilized soil was much higher than that in the non-fertilized soil. In addition, the fungal community compositions of the soils differed. The N_2O producing activities of thirty-four fungal strains isolated from the soils were analyzed, and *Actinomucor elegans*, *Bionectria ochroleuca*, *Fusarium avenaceum*, *Fusarium equiseti*, *Fusarium oxysporum*, *Fusarium solani* and *Nectria* sp. dominated the surface-fertilized soil. These isolates favored the initially aerobic condition to produce N_2O, which strongly supported our hypothesis that the O_2 supply determine the fungal denitrifiers mainly contribute to the N_2O emission after the additional N fertilization. In addition, fungi belonging to Eurotiales and Hypocreales were further confirmed to be primarily responsible for N_2O emissions in soils, based on functional gene markers. These results suggested that N_2O emission in the upland field soil induced by the application with the additional N fertilizers, especially organic fertilizers, were mainly resulted from fungal denitrification.

References

Akiyama, H., Tsuruta H., 2003. Nitrous oxide, nitric oxide, and nitrogen dioxide fluxes from soils after manure and urea application. Journal of Environmental Quality 32, 423-431.

Anderson, I.C., Poth, M., Homstead, J. and Burdige, D. (1993) A comparison of NO and N_2O production by the autotrophic nitrifier Nitrosomonas europaea and the heterotrophic nitrifier Alcaligenes faecalis. Appl. Environ. Microbiol. 59, 3525–3533.

Anderson, J.P.E., Domsch, K.H., 1975. Measurement of bacterial and fungal contributions to respiration of selected agricultural and substrate forest soils. Canadian Journal of Microbiology 21, 314-322.

Arah JRM, Smith KA. 1990. Factors influencing the fraction of the gaseous products of soil denitrification evolved to the atmosphere as nitrous oxide. In: Bouwman AF, editor. Soils and the greenhouse effect: the present status and future trends concerning the effect of soils and their cover on the fluxes of greenhouse gas. John Wiley & Sons, p. 475-480.

Ashida N, et al. (2010) Isolation of functional single cells from environments using a micromanipulator: Application to study denitrifying bacteria. Appl Microbiol Biotechnol 85(4):1211-1217.

Baggs, E. M. et al., 2000. Nitrous oxide emission from soils after incorporating crop residues. Soil Use and Management, 16(2): 82-87.

Bakken LR, Bergaust L, Liu B, Frostegård A. 2012. Regulation of denitrification at the cellular level: a clue to the understanding of N2O emissions from soils. Philos Trans R Soc Lond B Biol Sci. 67(1593):1226-1234.

Balderston WL, Sherr B, Payne WJ. 1976. Blockage by acetylene of nitrous oxide reduction in Pseudomonas perfectomarinus. Appl Environ Microbiol, 31:504-508.

Bartossek R, Nicol GW, Lanzen A, Klenk HP, Schleper C (2010) Homologues of nitrite reductases in ammonia-oxidizing archaea: diversity and genomic context. Environ Microbiol 12(4):1075-1088.

Beauchamp EG, Gale C, Yeomans JC., 1980. Organic matter availability for denitrification in soils of different textures and drainage classes. Commun Soil Sci Plant Anal 11:1221-33.

Bender, M., and R. Conrad. 1995. Effect of methane concentrations and soil conditions on the induction of methane oxidation activity. Soil Biol. Biochem. 27:1517–1527.

Berg, P., Klemedtsson, L., Rosswall, T., 1982. Inhibitory effect of low partial pressures of

acetylene on nitrification. Soil Biology and Biochemistry. 14(3): 301-303.

Bergstrom, D. W. et al., 2001. Nitrous oxide production and flux from soil under sod following application of different nitrogen fertilizers. Communications in Soil Science and Plant Analysis, 32(3-4), 553-570.

Bhandral R, Saggar S, Bolan NS, Hedley MJ. 2007. Transformation of nitrous oxide emission from grassland soils as affected by compaction. Soil Tillage Res, 94:482-492.

Blagodatskaya, E., Dannenmann, M., Gasche, R., Butterbach-Bahl, K., 2010. Microclimate and forest management alter fungal-to-bacterial ratio and N_2O-emission during rewetting in the forest floor and mineral soil of mountainous beech forests. Biogeochemistry 97, 55-70.

Bollag, J.M., Tung, G., 1972. Nitrous oxide release by soil fungi. Soil Biology and Biochemistry 4, 271-276.

Borne, M., H. Dorr, and I. Levin. 1990. Methane consumption in aerated soils of the temperate zone. Tellus 42:2-8.

Bouwman AF, Boumans LJM, Batjes NH (2002) Emissions of N_2O and NO from fertilized fields: Summary of available measurement data. Global Biogeochem Cy 16(4):1058-1071.

Braker, G., Fesefeldt, A., Witzel, K.P., 1998. Development of PCR primer systems for amplification of nitrite reductase genes (nirK and nirS) to detect denitrifying bacteria in environmental samples. Appl. Environ. Microbiol. 64, 3769-3775.

Braker G, et al. (2000) Nitrite Reductase Genes (nirK and nirS) as Functional Markers to Investigate Diversity of Denitrifying Bacteria in Pacific Northwest Marine Sediment Communities. Appl Environ Microbiol 66(5):2096-2104.

Brentrup, F. et al., 2000. Methods to estimate on-field nitrogen emissions from crop production as an input to LCA studies in the agricultural sector. The International Journal of Life Cycle Assessment, 5(6): 349-357.

Burns, L.C., Stevens, R.J., Smith, R.V., Cooper, J.E., 1995. The occurrence and possible sources of nitrite in a grazed, fertilized, grasslands oil. Soil Biology and Biochemistry 2 7, 47-59.

Castaldi, S., Smith, K.A., 1998. Effect of cycloheximide on N_2O and NO_3^- production in a forest and an agricultural soil. Biology and Fertility of Soils 27, 27-34.

Cantera JJ, Stein LY (2007) Molecular diversity of nitrite reductase genes (nirK) in nitrifying bacteria. Environ Microbiol 9(3):765-776.

Chisteroserdova, L. V., Lidstrom, M. E. 1994. Genetics of the serine cycle in Methylobacterium extorquens AM1: identification, sequence, and mutation of three new genes involved in C1 assimilation, orfA, mtkA, and mtkB. J. Bacteriol. 176: 7398-7404.

Conrad, R., 1996. Soil microorganisms as controllers of atmospheric trace gases (H_2, CO, CH_4, OCS, N_2O, and NO). Microbiological Reviews 60, 609-640.

Crutzen, P.J., 1970. The influence of nitrogen oxides on the atmospheric ozone content. Quarterly Journal of the Royal Meteorological Society 96:320-325

Davidson, E.A., 1991. Fluxes of nitrous oxide and nitric oxide from terrestrial ecosystems. In: Rogers, J.E., Whitman, W.B. (Eds.), Microbial production and consumption of greenhouse gases: methane, nitrogen oxides, and halomethanes. Washington, D.C., pp. 219-235.

Davidson, E. A., 2009. The contribution of manure and fertilizer nitrogen to atmospheric nitrous oxide since 1860. Nature Geoscience 2, 659-662.

Davidson, E.A., Swank, W.T., 1986. Environmental parameters regulating gaseous nitrogen losses from 2 forested ecosystems via nitrification and denitrification. Applied and Environmental Microbiology, 52(6): 1287-1292.

Di, H. J., Cameron, K. C., Shen, J. P., He, J. Z., Winefield, C. S., O'Callaghan, M. & Bowatte, S. (2010). Nitrate leaching and nitrous oxide emissions related to bacteria and not to archaea in nitrogen rich grassland soils. In R. J. Gilkes & N. Prakongkep (Eds.) Soil Solutions for a Changing World : Proceedings of the 19th World Congress of Soil Science, Brisbane, Australia, 1-6 August 2010. Symposium 3.5.2, Risk assessment and risk based remediation (pp. 44-47). Brisbane, Australia: IUSS.

Domsch, K.H., Gams, W., Anderson, T.H., 1980. Compendium of Soil Fungi, Academic Press, London.

Dobbie, K.E., Mc Taggart, I.P., Smith, K.A., 1999. Nitrous oxide emissions from intensive agricultural systems: variations between crops and seasons, key driving variables, and mean emission factors. Journal of Geophysical Research 104 (21), 26891-26899.

Drury CF, Myrold DD, Beauchamp EG, Reynolds WD. Denitrification techniques for soils. In: Carter MR, Gregorich EG, editors. Soil sampling and methods of analysis. 2nd edition. Boca Raton, FL (USA): CRC Press Taylor & Francis; 2008. p. 471-493.

Dunfield, P., R. Knowles, R. Dumont, and T. R. Moore. 1993. Methane production and

consumption in temperate and subarctic peat soils: response to temperature and pH. Soil Biol. Biochem. 25:321–326.

Einsle O, Messerschmidt A, Huber R, Kroneck PM, Neese F (2002) Mechanism of the six-electron reduction of nitrite to ammonia by cytochrome c nitrite reductase. J Am Chem Soc 124(39):11737-11745.

Enwall K, Throbäck IN, Stenberg M, Söderström M, Hallin S (2010). Soil resources influence spatial patterns of denitrifying communities at scales compatible with land management. Appl Environ Microbiol 76(7):2243-2250.

Francesca C, et al. (2001) The nitrite reductase from Pseudomonas aeruginosa: Essential role of two active-site histidines in the catalytic and structural properties. P Natl Acad Sci USA 98(5):2232-2237.

Freney, J.R., Randall, P.J., Smith, J.W.B., Hodgkin, J., Harrington, K.J., Morton, T.C., 2000. Slow release sources of acetylene to inhibit nitrification in soil. Nutrient Cycling in Agroecosystems. 56(3): 241-251.

Gillam, K.M., Zebarth, B.J., Burton, D.L., 2008. Nitrous oxide emissions from denitrification and the partitioning of gaseous losses as affected by nitrate and carbon addition and soil aeration. Canadian Journal of Soil Science, 88(2): 133-143.

Goreau, T. J., Kaplan, W. A., Wofsy, S. C., McElroy, M. B., Valois, F. W., Watson, S. W., 1980. Production of NO_2^- and N_2O by nitrifying bacteria at reduced concentrations of oxygen. Appl. Environ. Microb., 40, 526-532.

Groffman, P.M., 1994. Denitrification in freshwater wetlands. Curr. Top. Wetland Biochem. 1, 15-35.

Hamonts, K., Balaine, N., Moltchanova, E., Beare, M., Thomas, S., Wakelin, S.A., O'Callaghan, M., Condron, L.M., Clough T.J., 2013. Influence of soil bulk density and matric potential on microbial dynamics, inorganic N transformations, N_2O and N_2 fluxes following urea deposition. Soil Biology and Biochemistry 65, 1-11.

Hashidoko, Y., Takeda, H., Darung, U., Melling, L., Hatano, R., 2010. Genetic analysis of active N_2O-emitting bacteria from tropical peat soils for their nitrous oxide reductase gene. Proceedings of the 19th World Congress of Soil Science: Soil solutions for a changing world, Brisbane, Australia, Congress Symposium 4: Greenhouse gases from soils 2010 pp. 86-88

Hallam, S.J., Mincer, T.J., Schleper, C., Preston, C.M., Roberts, K., Richardson, P.M. & DeLong, E.F. (2006). Pathways of carbon assimilation and ammonia oxidation suggested by environmental genomic analyses of marine Crenarchaeota. PloS Biology 4, 520-536.

Hallin, S., Lindgren, P.E., 1999. PCR detection of genes encoding nitrite reductase in denitrifying bacteria. Appl. Environ. Microbiol. 65, 1652-1657.

Harter, J., Krause1, H.M., Schuettler, S., et al., 2014. Linking N_2O emissions from biochar-amended soil to the structure and function of the n-cycling microbial community. The ISME Journal, 8, 660-674.

Hatch, D.J., Jarvis, S.C., Philipps, L., 1990. Field measurement of nitrogen mineralization using soil core incubation and acetylene inhibition of nitrificiation. Plant and Soil, 124, 97-107.

Hayakawa, A., Akiyama, H., Sudo, S., Yagi, K., 2009. N_2O and NO emissions from an Andisol field as influenced by pelleted poultry manure. Soil Biology and Biochemistry 41, 521-529.

He, J., Shen, J., Zhang, L., Zhu, Y., Zheng, Y., Xu, M. & Di, H.J. (2007). Quantitative analyses of the abundance and composition of ammonia-oxidizing bacteria and ammonia-oxidizing archaea of a Chinese upland red soil under long-term fertilization practices. Environmental Microbiology 9(9), 2364-2374.

Herrmann, M., Saunders, A.M. & Schramm, A. (2008). Archaea dominate the ammoniaoxidizing community in the rhizosphere of the freshwater macrophyte Littorella uniflora. Applied and Environmental Microbiology 74(10), 3279-3283.

Heylen K, et al. (2006) The incidence of nirS and nirK and their genetic heterogeneity in cultivated denitrifiers. Environ Microbiol 8 (11):2012-2021.

Hochstein LI, Tomlinson GA (1988) The enzymes associated with denitrification. Annu Rev Microbiol 42:231-261.

Hyman, M.R., Wood., P.M., 1985. Suicidal inactivation and labelling of ammonia monooxygenase by acetylene. Biochemical Journal, 227, 719-725.

Inubushi, K., Goyal, S., Sakamoto, K., Wada, Y., Yamakawa, K., Arai, T., 2000. Influences of application of sewage sludge compost on N_2O production in soils. Chemosphere Global Change Science 2, 329-334.

IPCC, 2007. Climate change 2007. In: Mitigation of Climate Changed Contribution of Working Group III to the Fourth Assessment Report of IPCC. Cambridge University Press, Cambridge,

pp. 497-540 (Chapter 8).

Ishii, S., H. Ohno, M. Tsuboi, S. Otsuka, K. Senoo. 2011. Identification and isolation of active N_2O reducers in rice paddy soil. ISME J. 5: 1936-1945.

Ishii, S., Ikeda, S., Minamisawa, K., Senoo, K., 2011. Nitrogen cycling in rice paddy environments: Past achievements and future challenges. Microbes. Environ. 26, 282-292.

Isobe, K., Koba, K., Suwa, Y., Ikutani, J., Kuroiwa, M., Fang, Y., Yoh, M., Mo, J., Otsuka, S., Senoo, K., 2012. Nitrite transformations in an N-saturated forest soil. Soil Biology and Biochemistry 52, 61-63.

Isobe, K., Koba, K., Ueda, S., Senoo, K., Harayama, S., Suwa, Y., 2011. A simple and rapid GC/MS method for the simultaneous determination of gaseous metabolites. J. Microbiol. Meth. 84, 46-51.

Isobe, K., Ohte, N., 2014. Ecological perspectives on microbes involved in N-cycling. Microbes Environ. 29. 4-16.

Jarvis, B., Seiler, D.A.L., Ould, A.J.L., Williams, A.P., 1983. Observations on the enumeration of moulds in food and feedingstuffs. Journal of Applied Bacteriology 55, 325-336.

Jia, Z.J. & Conrad, R. (2009). Bacteria rather than Archaea dominate microbial ammonia oxidation in an agricultural soil. Environmental Microbiology 11(7), 1658-1671.

Jirout, J., Šimek, M., Elhottová, D., 2013. Fungal contribution to nitrous oxide emissions from cattle impacted soils. Chemosphere 90, 565-572.

Jones, C.M., Stres, B., Rosenquist, M., Hallin, S., 2008. Phylogenetic analysis of nitrite, nitric oxide, and nitrous oxide respiratory enzymes reveal a complex evolutionary history for denitrification. Mol. Biol. Evol. 25, 1955-1966.

Jones, S.K., Rees, R.M., Skiba, U.M., Ball, B.C., 2007. Influence of organic and mineral N fertilizer on N_2O fluxes from a temperate grassland. Agriculture Ecosystems and Environment 121, 74-83.

Jones CM, Graf DR, Bru D, Philippot L, Hallin S (2013) The unaccounted yet abundant nitrous oxide-reducing microbial community: a potential nitrous oxide sink. ISME J 7(2):417-26.

Kaya M, Matsumura K, Higashida K, Hata Y, Kawato A, Abe Y, et al. 2004. Cloning and enhanced expression of the cytochrome $P450_{nor}$ gene (nicA; CYP55A5) encoding nitric oxide reductase from Aspergillus oryzae. Biosci Biotechnol Biochem, 68:2040-2049.

Khalil, K., Mary, B., Renault, P., 2004. Nitrous oxide production by nitrification and denitrification in soil aggregates as affected by O_2 concentration. Soil Biology & Biochemistry, 36(4): 687-699.

Kim, S.W., Fushinobu, S., Zhou, S., Wakagi, T., Shoun, H., 2010. The possible involvement of copper-containing nitrite reductase (NirK) and flavohemoglobin in denitrification by the fungus Cylindrocarpon tonkinense. Biosci. Biotechnol. Biochem. 74, 1403-1407.

Knowles R (1982) Denitrification. Microbiol Rev 46:43-70.

Kobayashi, M., Shoun, H., 1995. The copper-containing dissimilatory nitrite reductase involved in the denitrifying system of the fungus Fusarium oxysporum. J. Biol. Chem. 270, 4146-4151.

Koskinen WC, Keeney DR. 1982. Effect of pH on the rate of gaseous products of denitrification in a silt loam soil. Soil Sci Soc Am J, 46:1165-1167.

Kraemer SM (2004) Iron oxide dissolution and solubility in the presence of siderophores. Aquat Sci 66(1):3-18.

Lane, D.J., 1991. 16S/23S rRNA sequencing. In: Stackebrandt, E., Goodfellow, M. (Eds.), Nucleic acid techniques in bacterial systematics. John Wiley and Sons, New York, pp. 115-175.

Laughlin, R.J., Stevens, R.J., 2002. Evidence for fungal dominance of denitrification and codenitrification in a grassland soil. Soil Science Society of America Journal 66, 1540-1548.

Laughlin, R.J., Rütting, T., Müller, C., Watson, C.J., Stevens, R.J., 2009. Effect of acetate on soil respiration, N_2O emissions and gross N transformations related to fungi and bacteria in a grassland soil. Applied Soil Ecology 42, 25-30.

Leahy JG, Olsen RH (1997) Kinetics of toluene degradation by toluene-oxidizing bacteria as a function of oxygen concentration, and the effect of nitrate. FEMS Microbiol Ecol 23(1): 23-30

Leslie, J.F., Summerell, B.A., 2006. The Fusarium Laboratory Manual. Blackwell Publishing Professional, Ames, Iowa, USA.

Lesschen, J.P. Velthof, G.L., de Vries, W. Kros, J., 2011. Differentiation of nitrous oxide emission factors for agricultural soils. Environmental Pollution. 159(11): 3215-3222.

Li, X., Inubushi, K., Sakamoto, K., 2002. Nitrous oxide concentrations in an Andisol profile and emissions to the atmosphere as influenced by the application of nitrogen fertilizers and

manure. Biology and Fertility of Soils 35, 108-113.

Liu B, Mørkved PT, Frostegård A, Bakken LR. 2010. Denitrification gene pools, transcription and kinetics of NO, N_2O and N_2 production as affected by soil pH. FEMS Microbiol Ecol, 72:407-417.

Liu, C. et al., 2011. Effects of irrigation, fertilization and crop straw management on nitrous oxide and nitric oxide emissions from a wheat-maize rotation field in northern China. Agriculture, Ecosystems and Environment, 140, 226-233.

Liu, X.J. et al. 2005. Tillage and nitrogen application effects on nitrous and nitric oxide emissions from irrigated corn fields. Plant and Soil, 276: 235-249.

Liu, X. J. et al., 2006.The impact of nitrogen placement and tillage on NO, N2O, CH4 and CO2 fluxes from a clay loam soil. Plant and Soil, 280: 177-188.

Lloyd D. 1993. Aerobic denitrification in soils and sediments: from fallacies to facts. Trends Ecol Evol, 8:352-356.

Löscher, C.R., Kock, A., Könneke, M., Roche, J. L., Bange, H.W., Schmitz, R.A., 2012. Production of oceanic nitrous oxide by ammonia-oxidizing archaea. Biogeosciences, 9, 2419-2429.

Ma, W.K., Farrell, R.E., Siciliano, S.D., 2008. Soil formate regulates the fungal nitrous oxide emission pathway. Appl Environ Microbiol. 74(21): 6690-6696.

Maag, M., Vinther, F.P., 1996. Nitrous oxide emission by nitrification and denitrification in different soil types and at different soil moisture contents and temperatures. Applied Soil Ecology 4: 5-14.

Marushchak, M.E., Pitkämäki, A., Koponen, H., Biasi, C., Seppälä, M., Martikainen, P.J., 2011. Hot spots for nitrous oxide emissions found in different types of permafrost peatlands. Global Change Biology 17, 2601-2614.

Martin TL, Kaushik NK, Trevors JT, Whiteley HR (1999) Review: Denitrification in temperate climate riparian zones. Water Air Soil Poll 111(1-4):171-186.

May, L.A., Smiley, B., Schmidt, M.G., 2001. Comparative denaturing gradient gel electrophoresis analysis of fungal communities associated with whole plant corn silage. Canadian Journal of Microbiology 47, 829-841.

Michotey V, Mejean V, Bonin P (2000) Comparison of methods for quantification of cytochrome

cd1-denitrifying bacteria in marine samples. Appl Environ Microbiol 66(4), 1564-1571.

Miller, M.N., Zebarth, B.J., Dandie, C.E., Burton, D.L., Goyer, C., Trevors, J.T., 2008. Crop residue influence on denitrification, N_2O emissions and denitrifier community abundance in soil. Soil Biology and Biochemistry 40, 2553-2562.

Minami, K., 1997. Atmospheric methane and nitrous oxide: sources, sinks and strategies for reducing agricultural emissions. Nutrient Cycling in Agroecosystems 49: 203-211.

Möhlenhoff, P., Muller, L., Gorbushina, A.A., Petersen, K., 2001. Molecular approach to the characterization of fungal communities: methods for DNA extraction, PCR amplification and DGGE analysis of painted art objects. FEMS Microbiology Letters 195, 169-173.

Moir JWB (2011) Nitrogen Cycling in Bacteria: Molecular Analysis. 236. Caister Academic Press

Morales1 SE, Cosart T, Holben WE (2010) Bacterial gene abundances as indicators of greenhouse gas emission in soils. ISME J 4:799-808.

Mosier, A., & C. Kroeze. 2000. Potential impact on the global atmospheric N2O budget of the increased nitrogen input required to meet future global food demands. Chemosphere Global Change Sci. 2:465-474.

Myrold DD, Tiedje JM. Diffusional constraints on denitrification in soil. Soil Sci Soc Am J 1985;49:651-7.

Nägele W, Conrad R. 1990. Influence of soil pH on the nitrate-reducing microbial populations and their potential to reduce nitrate to NO and N_2O. FEMS Microbiol Ecol, 74:49-57.

Nakanishi, Y., Zhou, S., Kim, S.W., Fushinobu, S., Maruyama, J., Kitamoto, K., Wakagi, T., Shoun, H., 2010. A eukaryotic copper-containing nitrite reductase derived from a NirK homolog gene of Aspergillus oryzae. Biosci. Biotechnol. Biochem. 74, 984-991.

Nicol, G.W., Leininger, S., Schleper, C. & Prosser, J.I. (2008). The influence of soil pH on the diversity, abundance and transcriptional activity of ammonia oxidizing archaea and bacteria. Environmental Microbiology 10(11), 2966-2978.

Nishimura, S., Sawamoto, T., Akiyama, H., Sudo, S., Cheng, W., Yagi, K., 2005. Continuous, Automated Nitrous Oxide Measurements from Paddy Soils Converted to Upland Crops. Soil Sci. Soc. Am. J. 69:1977-1986 .

Nishizawa T, et al. (2012) Advantages of functional single-cell isolation method over standard agar plate dilution method as a tool for studying denitrifying bacteria in rice paddy soil. AMB

Express 2:50.

Nishizawa T, et al. (2013) Taxonomic composition of denitrifying bacterial isolates is different among three rice paddy field soils in Japan. Soil Sci Plant Nutri 59(3):305-310.

Nolan M, et al. (2009) Complete genome sequence of Rhodothermus marinus type strain (R-10^T). Stand Genomic Sci 1(3):283-290.

Ostrom, N.E., Pitt, A., Sutka, R., Ostrom, P.H., Grandy, A.S., Huizinga, K.M., Robertson, G.P., 2007. Isotopologue effects during N2O reduction in soils and in pure cultures of denitrifiers. Journal of Geophysical Research, 112, G02005.

Palmer K, Biasi C, Horn MA (2012) Contrasting denitrifier communities relate to contrasting N_2O emission patterns from acidic peat soils in arctic tundra. ISME J 6:1058-1077.

Parkin, T.B., 1987. Soil Microsites as a Source of Denitrification Variability. Soil Science Society of America Journal 51, 1194-1199.

Philippot L, Andert J, Jones CM, Bru D & Hallin S (2011). Importance of denitrifiers lacking the genes encoding the nitrous oxide reductase for N_2O emissions from soil. Glob Change Biol 17: 1497-1504.

Philippot L, et al. (2009) Mapping field-scale spatial patterns of size and activity of the denitrifier community. Environ Microbiol 11(6):1518-1526.

Philippot, L., Hallin, S., Schloter, M., 2007. Ecology of Denitrifying Prokaryotes in Agricultural Soil. Advances in Agronomy, 96, 249-305.

Philippot L, Piutti S, Martin-Laurent F, Hallet S, Germon JC. 2002. Molecular analysis of the nitrate-reducing community from unplanted and maize-planted soils. Appl Environ Microbiol, 68:6121-6128.

Phillips, R.L., 2007. Organic agriculture and nitrous oxide emissions at sub-zero soil temperatures. Journal of Environmental Quality, 36(1) :23-30.

Poth, M. and Focht, D. D. 1985. ^{15}N kinetic analysis of N_2O production by Nitrosomas europaea: An examination of nitrifier denitrification, Appl. Environ. Microb., 49, 1134-1141.

Prendergast-Miller, M. T., Baggs, E.M., Johnson, D., 2011. Nitrous oxide production by the ectomycorrhizal fungi Paxillus involutus and Tylospora fibrillosa. FEMS Microbiology Letters 316, 31-35.

Ravishankara, A.R., Daniel, J.S., Portmann, R.W., 2009. Nitrous oxide (N_2O): the dominant ozone-depleting substance emitted in the 21st century. Science 326, 123-125.

Reed DC, Algar CK, Huber JA, Dick GJ (2014) Gene-centric approach to integrating environmental genomics and biogeochemical models. Proc Natl Acad Sci USA 111(5):1879-84.

Richardson DJ. 2000. Bacterial respiration: a flexible process for a changing environment. Microbiology, 146, 551-571.

Robertson, L.A., Cornelisse, R., de Vos, P., Hadioetomo, R. and Kuenen, J.G. (1989) Aerobic denitrification in various heterotrophic nitrifiers. Antonie van Leeuwenhoek 56, 289-299.

Roesch LF, et al. (2007) Pyrosequencing enumerates and contrasts soil microbial diversity. ISME J 1: 283-290.

Rose, T.M., Schultz, E.R., Henikoff, J.G., Pietrokovski, S., McCallum, C.M., Henikoff, S., 1998. Consensus-degenerate hybrid oligonucleotide primers for amplification of distantly related sequences. Nucleic. Acids Res. 26, 1628-1635.

Rotthauwe J, Witzel K, Liesack W (1997) The ammonia monooxygenase structural gene amoA as a functional marker: molecular fine-scale analysis of natural ammonia-oxidizing populations. Appl Environ Microbiol 63: 4704–4712.

Rousk, J., Brookes, P.C., Bååth, E., 2009. Contrasting Soil pH Effects on Fungal and Bacterial Growth Suggest Functional Redundancy in Carbon Mineralization. Appl Environ Microbiol. 75(6): 1589-1596.

Ruser, R. et al., 2006. Emission of N_2O, N_2 and CO_2 from soil fertilized with nitrate: effect of compaction, soil moisture and rewetting. Soil Biology & Biochemistry, 38(2): 263-274.

Rütting, T., Müller, C., 2008. Process-specific analysis of nitrite dynamics in a permanent grassland soil by using a Monte Carlo sampling technique. European Journal of Soil Science 59, 208-215.

Rysgaard S, Risgaard-Petersen N, Nielsen LP, Revsbech NP. 1993. Nitrification and denitrification in lake and estuarine sediments measured by the ^{15}N dilution technique and isotope pairing. Appl Environ Microbiol, 59:2093-2098.

Saari P, Saarnio S, Kukkonen JVK, Akkanen J, Heinonen J, Saari V, et al., 2009. DOC and N2O dynamics in upland and peatland forest soils after clear-cutting and soil preparation.

Biogeochemistry, 94:217-231.

Saggar S, Jha N, Deslippe J, Bolan NS, Luo J, Giltrap DL, Kim DG, Zaman M, Tillman RW, 2013. Denitrification and N2O:N2 production in temperate grasslands: processes, measurements, modelling and mitigating negative impacts. Sci Total Environ, 465:173-195.

Saito, T., Ishii, S., Otsuka, S., Nishiyama, M., Senoo, K., 2008. Identification of Novel Betaproteobacteria in a Succinate-Assimilating Population in Denitrifying Rice Paddy Soil by Using Stable Isotope Probing. Microbes and Environments 23, 192-200.

Sakurai, T., Kataoka, K., 2007. Structure and function of type I copper in multicopper oxidases. Cell. Mol. Life Sci. 64, 2642-2656.

Sánchez-Martín, L., Vallejo, A., Dick, J., Skiba, U.M., 2008. The influence of soluble carbon and fertilizer nitrogen on nitric oxide and nitrous oxide emissions from two contrasting agricultural soils. Soil Biology and Biochemistry 40, 142–151.

Sanford, R.A., Wagner, D.D., Wu, Q., Chee-Sanford, J.C., Thomas, S.H., Cruz-García, C., Rodríguez, G., Massol-Deyá, A., Krishnani, K.K., Ritalahti, K.M., Nissen, S., Konstantinidis, K.T., Löffler, F.E., 2012. Unexpected nondenitrifier nitrous oxide reductase gene diversity and abundance in soils. Proc Natl Acad Sci U S A. 109(48):19709-14.

Santoro, A.E., Buchwald, C., Mcllvin, M.R., Casciotti, K.L., 2011. Isotopic signature of N_2O produced by marine ammonia-oxidizing archaea. Science 333, 1282-1285.

Schils, R. L. M. et al. 2008. Nitrous oxide emissions from multiple combined applications of fertilizer and cattle slurry to grassland. Plant and Soil, 310(1-2): 89-101.

Schimel, J.P., Firestone, M.K., Killham, K.S., 1984. Identification of heterotrophic nitrification in a Sierran forest soil. Applied and Environmental Microbiology 48, 802-806.

Schloss, P.D., Westcott, S.L., Ryabin, T., Hall, J.R., Hartmann, M., Hollister, E.B., Lesniewski, R.A., Oakley, B.B., Parks, D.H., Robinson, C.J., Sahl, J.W., Stres, B., Thallinger, G.G., Van Horn, D.J., Weber, C.F., 2009. Introducing mothur: Open-source platform-independent, community supported software for describing and comparing microbial communities. Appl. Environ. Microbiol. 75, 7537-7541.

Seitzinger SP, Nielsen LP, Caffrey J, Christensen PB, 1993. Denitrification measurements in aquatic sediments: a comparison of three methods. Biogeochemistry, 23: 147-167.

Seo, D.C., DeLaune, R.D., 2010. Fungal and bacterial mediated denitrification in wetlands:

Influence of sediment redox condition. Water Research 44, 2441-2450.

Shaw, L.J., Nicol, G.W., Smith, Z., Fear, J., Prosser J.I., Baggs E.M., 2006. Nitrosospira spp. can produce nitrous oxide via a nitrifier denitrification pathway. Environmental Microbiology 8, 214-222.

Shoun, H., Kim, D.H., Uchiyama, H., 1992. Denitrification by fungi. FEMS Microbiol. Lett. 94, 277-282.

Shoun, H., Tanimoto, T., 1991. Denitrification by the fungus Fusarium oxysporum and involvement of cytochrome P-450 in the respiratory nitrite reduction. The Journal of Biological Chemistry 266, 11078-11082.

Shoun, H., Fushinobu, S., Jiang, L., Kim S.W., Wakagi T., 2012. Fungal denitrification and nitric oxide reductase cytochrome P450nor. Philosophical Transactions of the Royal Society B 367, 1186-1194.

Signor, D., Eduardo C., Cerri P., 2013. Nitrous oxide emissions in agricultural soils: a review. Pesq. Agropec. Trop., 43(3): 322-338.

Skiba, U. & Smith, K. A. 2000. The control of nitrous oxide emissions from agricultural and natural soils. Chemosphere Glob. Change Sci. 2, 379-386.

Smith CJ, Nedwell DB, Dong LF, Osborn AM (2007) Diversity and Abundance of Nitrate Reductase Genes (narG and napA), Nitrite Reductase Genes (nirS and nrfA), and Their Transcripts in Estuarine Sediments. Appl Environ Microbiol 3(11):3612-3622.

Smith MS, Tiedje JM. 1979. Phases of denitrification following oxygen depletion in soil. Soil Biol Biochem, 11:261-267.

Smith, P., et al., 2008. Greenhouse gas mitigation in agriculture. Phil. Trans. R. Soc. B 363, 789-813.

Spokas, K., Wang, D., Venterea, R., Sadowsky, M., 2006. Mechanisms of N_2O production following chloropicrin fumigation. Applied Soil Ecology 31, 101-109.

Steinkellner, S., Langer, I., 2004. Impact of tillage on the incidence of Fusarium spp. in soil. Plant and Soil 267, 13-22.

Stevens, R.J., Laughlin, R.J., Malone, J.P., 1998. Soil pH affects the processes reducing nitrate to nitrous oxide and di-nitrogen. Soil Biology and Biochemistry, 30(8-9), 1119-1126.

Struwe S, Kjøller A. 1994. Potential for N_2O production from beech (Fagus silvatica) forest soils

with varying pH. Soil Biol Biochem 26:1003-1009.

Sutka, R.L., Adams, G.C., Ostrom, N.E., Ostrom, P.H., 2008. Isotopologue fractionation during N_2O production by fungal denitrification, Rapid Commun. Mass Spectrom., 22, 3989-3996.

Sutka, R.L., Ostrom, N.E., Ostrom, P.H., Breznak, J.A., Gandhi, H., Pitt, A.J., Li, F., 2006. Distinguishing nitrous oxide production from nitrification and denitrification on the basis of isotopomer abundances. Appl. Environ. Microbiol. 72: 638-644.

Takai K, et al. (2006) Sulfurimonas paralvinellae sp. nov., a novel mesophilic, hydrogen- and sulfur-oxidizing chemolithoautotroph within the Epsilonproteobacteria isolated from a deep-sea hydrothermal vent polychaete nest, reclassification of Thiomicrospira denitrificans as Sulfurimonas denitrificans comb. nov. and emended description of the genus Sulfurimonas. Int J Syst Evol Microbiol 56(Pt8):1725-1733.

Takaya, N., 2002. Dissimilatory nitrate reduction metabolisms and their control in fungi. Journal of Bioscience and Bioengineering 94, 506-510.

Takeda, H., Takahashi, N., Hatano, R., Hashidoko, Y., 2012. Active N_2O emission from bacterial microbiota of Andisol farmland and characterization of some N_2O emitters. J Basic Microbiol. 2012, 52(4): 477-486.

Thomson AJ, Giannopoulos G, Pretty J, Baggs EM, Richardson DJ. 2012. Biological sources and sinks of nitrous oxide and strategies to mitigate emissions. Philos Trans R Soc Lond B Biol Sci. 367(1593):1157-1168.

Throbäck IN, Enwall K, Jarvis A, Hallin S (2004) Reassessing PCR primers targeting nirS, nirK and nosZ genes for community surveys of denitrifying bacteria with DGGE. FEMS Microbiol Ecol 49(3):401-417.

Tiedje JM (1988) Ecology of denitrification and dissimilatory nitrate reduction to ammonium. Biology of Anaerobic Microorganisms, eds Zehnder AJB (JohnWiley& Sons, New York), pp 179-244.

Tiedje, J.M., 1994. Denitrifiers. In: Bottomley, P.S., Angle, J.S., Weaver, R.W. (Eds.), Methods of Soil Analysis: Part 2-Microbiological and Biochemical Properties. Soil Science Society of America, Madison, pp. 253-254.

Toyoda, S., Mutobe, H., Yamagishi, H., Yoshida, N., Tanji, Y., 2005. Fractionation of N_2O isotopomers during production by denitrifier, Soil Biol. Biochem., 37(8), 1535-1545.

Toyoda, S., Yano, M., Nishimura, S., Akiyama, H., Hayakawa, A., Koba, K., Sudo, S., Yagi, K., Makabe, A., Tobari, Y., Ogawa, N., Ohkouchi, N., Yamada, K., Yoshida, N., 2011. Characterization and production and consumption processes of N_2O emitted from temperate agricultural soils determined via isotopomer ratio analysis. Global Biogeochemical Cycles 25, GB2008.

Toyoda, S., Yoshida. N., 1999. Determination of nitrogen isotopomers of nitrous oxide on a modified isotope ratio mass spectrometer. Anal. Chem. 71:4711-4718.

Toyoda, S., Yoshida, N., Miwa, T., Matsui, Y., Yamagishi, H., Tsunogai, U., Nojiri, Y., Tsurushima. N., 2002. Production mechanism and global budget of N_2O inferred from its isotopomers in the western North Pacific. Geophys. Res. Lett. 29:7-11.

Venterea RT. 2007. Nitrite-driven nitrous oxide production under aerobic soil conditions: kinetics and biochemical controls. Glob Chang Biol,13:1798-1809.

Wang, G., Xu, Y., Jin, J., Liu, J., Zhang, Q., Liu, X., 2009. Effect of soil type and soybean genotype on fungal community in soybean rhizosphere during reproductive growth stages. Plant and Soil 317, 135-144.

Wessén, E., Nyberg, K., Jansson, J.K. and Hallin, S. (2010). Responses of bacterial and archaeal ammonia oxidizers to soil organic and fertilizer amendments under long-term management. Applied Soil Ecology 45(3), 193-200.

White, T.J., Bruns, T., Lee, S., Taylor, J., 1990. Amplification and direct sequencing of fungal ribosomal RNA genes for phylogenetics. In: Innins, M.A., Gelfand, D.H., Sninsky, J.J., White, T.J. (Eds), PCR Protocols. Academic Press, San Diego, pp. 315-322.

Wolf, I., Brumme, R., 2002. Contribution of nitrification and denitrification sources for seasonal N_2O emissions in an acid German forest soil. Soil Biology & Biochemistry, 34(5): 741-744.

Xiong, Z., 2002. Field Study on Nitrous Oxide Emissions from Upland. Soil Science and Plant Nutrition, 48(4), 539-546.

Yamazaki T, Oyanagi H, Fujiwara T, Fukumori Y (1995) Nitrite reductase from the magnetotactic bacterium Magnetospirillum magnetotacticum. A novel cytochrome cd1 with Fe (II): nitrite oxidoreductase activity. Eur J Biochem 233(2):665-671.

Yanai, Y., Toyota, K., Morishita, T., 2007. Fungal N_2O production in an arable peat soil in Central Kalimantan, Indonesia. Soil Science and Plant Nutrition 53, 806-811.

Yao, S., Merwin, I.A., Abawi, G.S., Thies, J.E., 2006. Soil fumigation and compost amendment alter soil microbial community composition but do not improve tree growth or yield in an apple replant site. Soil Biology and Biochemistry 38, 587-599.

Zaman M, Nguyen ML. 2010. Effect of lime or zeolite on N_2O and N_2 emissions from a pastoral soil treated with urine or nitrate-N fertilizer under field conditions. Agric Ecosyst Environ, 136:254-261.

Zhang, J., Han, X., 2008. N_2O emission from the semiarid ecosystem under mineral fertilizer (urea and superphosphate) and increased precipitation in northern China. Atmospheric Environment, 42(2), 291-302.

Zhang, L.M., Hu, H.W., Shen, J.P. He, J.Z., 2012. Ammonia-oxidizing archaea have more important role than ammonia-oxidizing bacteria in ammonia oxidation of strongly acidic soils. The ISME Journal, 6, 1032-1045.

Zhao, X., Min, J., Wang, S., Shi, W., Xing, G., 2011. Further understanding of nitrous oxide emission from paddy fields under rice/wheat rotation in south China. Journal of Geophysical Research, 116, G02016, doi:10.1029/2010JG001528,

Zhou, Z., Takaya, N., Nakamura, A., Yamaguchi, M., Takeo, K., Shoun, H., 2002. Ammonia fermentation, a novel anoxic metabolism of nitrate by fungi. Journal of Biological Chemistry 277, 1892-1896.

Zumft, W.G., 1997. Cell biology and molecular basis of denitrification. Microbiology and Molecular Biology Reviews 61, 533-616.

Abstract

論文の内容の要旨

応用生命化学専攻
平成 23 年度博士課程入学
氏　　名　　魏　　巍
指導教員名　　妹尾　啓史

論文題目

Identification of N_2O-generating microorganisms in upland field after nitrogen fertilization
（窒素施肥畑圃場における一酸化二窒素ガス生成微生物の特定）

Chapter 1. Introduction

Nitrous oxide (N_2O) is commonly known as a powerful greenhouse gas (GHG), which generates a 298-fold stronger effect on global warming than carbon dioxide (CO_2). N_2O can be photolyzed into nitric oxide (NO) in the stratosphere, which contributes to acid rain and involve in stratospheric ozone depletion. Therefore, N_2O has long drawn substantial attention in field of environmental science. Soil accounts for about 62% of global N_2O emission, and upland soils applied with N fertilizers contribute mainly to the total soil N_2O emissions because of the large enhancement of microbial N_2O-producing activities by N input. Therefore, we suggest that upland field soil applied with different types and management practices of N fertilizers acts as a mainly N_2O source.

N_2O is known to be produced by soil microorganisms via nitrification and denitrification pathway. To clarify the emission rate and pathway of N_2O in upland field, many strategies and methods were established and developed. However, some limitations of these methods lead us underestimate and misunderstand the regularity of N_2O emission and related controlling factors in upland field soils. For example, the current *nirK* and *nirS* primers, widely used for detecting the nitrite reductase gene associated with N_2O emission, amplified a limited range of bacterial denitrifiers and mismatch not only substantial bacterial denitrifiers but also archaeal and fungal

denitrifiers; isotopomer analysis cannot clearly distinguish the contribution between the nitrification and fungal denitrification. Thus, to obtain a comprehensive and precise understanding of the regularity of N_2O emission in upland field soil, we should improve the methodology and combine several research strategies into a multiple analysis for clarifying the emission rate and pathway of N_2O in upland field soil.

Thus, the objective of this thesis was to assess the emission rate and pathway of N_2O in upland field soil after the basal and additional application with organic or chemical fertilizers, through the multiple analysis methods including the observation of environmental factors, isotopomer ratio, SIR inhibition and acetylene inhibition analysis of N_2O, and abundance and expression of soil microbial genes associated with N_2O emission. The knowledge and methodology obtained and developed in this thesis will lead us to a more comprehensive understanding of the emission rate and pathway of N_2O in upland field soil.

Chapter 2. Greater diversity and abundance of prokaryotic denitrifiers in upland field soil than previously realized

In the denitrification process, nitrite reduction to nitric oxide (NO) is a crucial step catalyzed by nitrite reductases (NirK and NirS). The NirK and NirS genes (*nirK* and *nirS*) have been used as marker genes to study the distribution, abundance, diversity and activity of denitrifiers in the environment. However, our phylogenetic analysis of the currently available full-length sequences of prokaryotic *nirK* and *nirS* revealed that conventional PCR primers can detect only a limited variety of the genes. We therefore designed new primer sets that cover the full diversity of prokaryotic *nirK* (Cluster I to IV) and *nirS* (Cluster I to III), including sequences that have been unaccounted for to date. DNA-based clone library and quantitative PCR analyses that used the newly designed primers revealed that prokaryotic *nirK* and *nirS* sequences distributed in terrestrial environments are more phylogenetically diverse and 2-6 times more abundant than previously counted. An RNA-based study that used the newly designed primers combined with culture-based

method suggested that prokaryotes carrying the previously unaccounted for *nirK* or *nirS* play an important functional role in denitrification, especially N_2O emitters, in cropland soil. These results indicate that we have underestimated the role of prokaryotic denitrifiers in the environment. The knowledge and methodology obtained and developed in this chapter will lead us to a more comprehensive understanding of the ecology of prokaryotic denitrifiers in environments.

Chapter 3. Unaccounted diversity and abundance of fungal denitrifiers in upland field soil

Fungal denitrification in soils is receiving considerable attention as one of the dominant N_2O production processes, because N_2O, not N_2, is the end product of fungal denitrification. However, because of the lack of a methodology to detect fungal denitrification-related genes, the diversity and ecological behavior of denitrifying fungi in soil remains unknown. Thus, we here designed a primer set to detect the fungal nitrite reductase gene (*nirK*) based on the homologs of the copper center type 1 domain used for the primer design of prokaryotic *nirK* in Chapter 2, which allow us compare fungal *nirK* sequences with the massive store of bacterial *nirK* sequences. We validated the sensitivity and specificity of primers by using fungal and bacterial and archaeal strains having the N_2O producing activity. Then, through clone library analyses, we identified congruence between phylogenies of the fungal 18S rRNA gene and *nirK* of denitrifying fungal isolates, and affirmed the *nirK* of the most dominant denitrifying fungal group in soil (Ascomycota) can be sufficiently detected. The methodology developed here allows to precisely identify denitrifying fungi and to elucidate the importance of fungal N_2O emission in upland field.

Chapter 4. N_2O emission and related controlling factors in upland field soil after N fertilization

Upland field soils mainly contribute to the total N_2O emissions from soil environments, because substantial microbial N_2O emissions are greatly stimulated by basal and additional organic or chemical N fertilization. In this chapter, based on an observation in upland field soil with corn cultivation in 2011, we found substantial N_2O emission was induced by both basal and additional

N fertilization. After basal organic or chemical fertilization, N_2O was produced mainly by denitrification more than nitrification. In such denitrification, the prokaryotic and fungal denitrifiers having *nirK* (Cluster I and II) were mainly responsible for N_2O emission induced by basal organic fertilization, and prokaryotic and fungal denitrifiers respectively having *nirS* (Cluster II) and *nirK* were mainly responsible for N_2O emission induced by basal chemical fertilization. In such nitrification, the nitrifiers having the archaeal *amoA* as the miner N_2O emitters were responsible for organic or chemical fertilizers. In addition, denitrifiers having the *nosZ* in Cluster I as the N_2O reducers in denitrification induced by only organic fertilizers. In contrast, after surface additional organic or chemical fertilization, N_2O was produced dominantly by denitrification and fungal denitrifiers play a dominant active role in N_2O emission and prokaryotes were inactive as the N_2O emitters and reducers because of the O_2 availability.

Chapter 5. The dynamic of N_2O emission and relative controlling factors in upland field soil after basal N fertilization

As described in chapter 4, N_2O emissions induced by basal N fertilization are always concentrated in several weeks after fertilization, and such concentrated N_2O emission performs significantly larger contribution to total N_2O emission than that by additional fertilization. We performed a field experiment in upland field in 2012 with an exaggerated application of N fertilizer and prolonged and frequented field observation, which allow us to determine the comprehensive and precise regularity of N_2O emission and related environmental and microbial controlling factor after the basal organic and chemical fertilization. From the results obtained in this chapter, the regularity of N_2O emission induced by basal N fertilization is proposed as follow, (i) after the basal organic fertilization, firstly emitted N_2O was produced mainly via denitrification more than nitrification. Bacterial denitrification, performed by denitrifiers having the prokaryotic *nirK* in Cluster I, II, III and IV and *nirS* in Cluster II, contributed more to N_2O emission than fungal denitrification. The minor N_2O emission via nitrification was mainly produced by AOB; (ii)

after the firstly emitted N_2O induced by basal organic fertilization, N_2O was still produced mainly via denitrification more than nitrification, but fungal denitrifiers contributed more to N_2O emission than bacterial denitrification; (iii) after the basal chemical fertilization, firstly emitted N_2O was produced slightly and induced mainly via denitrification more than nitrification. Bacterial denitrification, performed by denitrifiers having the prokaryotic *nirK* in Cluster I, II and III and *nirS* in Cluster II, contributed more to N_2O emission than fungal denitrification. The minor N_2O emission via nitrification was mainly produced by AOB; (iv) after the firstly emitted N_2O induced by basal chemical fertilization, N_2O was produced largely mainly via denitrification more than nitrification following a rainstorm, but fungal denitrifiers and bacterial denitrifiers having *nirS* in Cluster II and bacterial nitrifiers having *amoA* contributed equally to N_2O emission; (v) the denitrifiers having *nosZ* in Cluster I as the N_2O reducers play a crucial role in final amount of N_2O emission. The high expression of such denitrifiers only occurred during the first peak period of N_2O emission after the basal organic fertilization because of the sufficient organic carbon and low soil pH level, which lead to an equally released amount of N_2O during the first and second peak period of N_2O emission.

Chapter 6. N_2O emission from upland field soil through fungal denitrification after additional organic fertilization

This chapter focused on the large N_2O emission from upland field soil that occurs after surface additional organic fertilization. N_2O emissions following surface organic fertilization were suppressed by 84 and 20% after the addition of cycloheximide (a fungal inhibitor) and streptomycin (a bacterial inhibitor), respectively, suggesting that fungi provide the main contribution to the observed N_2O emission. Thirty-four fungal strains were isolated from the soils, and their N_2O producing activities were analyzed. The abundance of fungal population and fungal denitrifiers in the surface-fertilized soil was much higher than that in the non-fertilized soil. In addition, the fungal community compositions of the soils differed. *Actinomucor elegans*,

Bionectria ochroleuca, *Fusarium avenaceum*, *Fusarium equiseti*, *Fusarium oxysporum*, *Fusarium solani* and *Nectria* sp. dominated the surface-fertilized soil, and their activity in producing N_2O was confirmed. In addition, based on functional gene markers, fungi belonging to Eurotiales, Hypocreales, and Sordariales were primarily responsible for N_2O emissions in soils. These results suggested that N_2O emission after the surface application of granular organic fertilizers in the cropland field mainly resulted from fungal denitrification.

Conclusion

In the tested upland field soil, substantial N_2O emission was induced by application with fertilization, and the rate and pathway of such N_2O emission were different depending on the types and management practices of fertilizers. During the period of N_2O emission after the basal N fertilization, diverse bacterial denitrifiers in denitrification were dominantly responsible for early N_2O emission, and fungal and bacterial denitrifiers in denitrification and bacterial nitrifiers (in uncultivated soil) or archaeal nitrifiers (in cultivated soil) in nitrification were mainly responsible for latter N_2O emission, because the potential control of soil organic C supply and soil pH level. During the period of N_2O emission after the additional N fertilization, fungal denitrifiers were dominantly responsible for N_2O emission, because the potential control of soil O_2 supply.

Publications

1) Wei, W., Isobe, K., Shiratori, Y., Nishizawa, T., Ohte, N., Otsuka, S., Senoo, K. (2014) N_2O emission from cropland field soil through fungal denitrification after surface applications of organic fertilizer. *Soil Biology and Biochemistry*, 69, 157-167.

Acknowledgments

Firstly，I sincerely want to express my greatest gratitude to my supervisor Professor Keishi Senoo for giving me such a precious opportunity to enter the University of Tokyo and study in the Laboratory of Soil Sciences. By his patient, support and continuous encouragement throughout my work, I harvested so much knowledge of biogeochemistry of N-cycling and enjoyed fruitful life in Japan. I also appreciate Associate Professor Shigeto Otsuka for his attentions and questions which made this work more accurate, and for always being kind. I would like to express my sincerest gratitude to Assistant Professor Kazuo Isobe, who directly guided this work. Thanks for all his guidance and helps in the research strategies and experimental skills of my thesis, and also for his teaching in the writing knowledge and skills, and also for his help in my daily life. I would like to express my thankfulness to the Dr. Tomoyasu Nishizawa, Yutaka Shiratori, Nobuhito Ohte, Keisuke Koba for their kindness and generous help for not only providing soil samplings of this work but also giving the comments and modification as the coauthors of my academic papers.

I would like to thank all members in the Laboratory of Soil Sciences, The University of Tokyo. I will never forget your company during my last four years in Japan, although we could not have so many chances to talk with each other for my poor Japanese, all your kindness and helps warmed me so much. And these beautiful memories will be cherished in my heart eternally.

Finally, I would like to express my greatest and deepest gratitude to my family, for their enormous concerns and powerful encourage. Especially to my wife Lin Zhu, trusting and supporting me so much whatever I do. By surrounded with her loves, I could possess the courage and energy to overcome all the difficulties. I do not how to express my emotional to all the people who helped me, but your kindness I will remember forever.

Wei Wei

2014-06-19